RESISTIVE CRYOGENIC CABLE
PHASE III

EPRI EL-503
(Research Project 7806)
(Contract No. E[49-18]-2104)
(Contract No. EX-77-C-01-2104)

Final Report

October 1977

Prepared by

Cryogenics Branch
Power Generation and Propulsion Laboratory
Corporate Research and Development
GENERAL ELECTRIC COMPANY
Schenectady, New York 12301

Prepared for

Electric Power Research Institute
3412 Hillview Avenue
Palo Alto, California 94304
and
Energy Research and Development Administration
20 Massachusetts Avenue
Washington, D. C. 20545

LEGAL NOTICE

This report was prepared pursuant to an act of Congress. Publication of the findings and recommendations herein should not be construed as representing either the approval or disapproval of the Energy Research and Development Administration. The purpose of this report is to provide information and alternatives for further consideration by the Energy Research and Development Administration and other federal agencies.

Furthermore, this report was prepared by the General Electric Company on account of work sponsored in part by the Electric Power Research Institute, Inc., which does not make any warranty or representation with respect to the accuracy, completeness, or usefulness of the information contained in this report, and does not assume any liabilities with respect to the use of, or for damages resulting from the use of, any information disclosed in this report.

FOREWORD

This final report describes the work performed between April 18, 1974 and March 31, 1977 for the Electric Power Research Institute and the U. S. Energy Research and Development Administration under Contract Nos. E(49-18)-2104 and EX-77-C-01-2104, "Resistive Cryogenic Cable - Phase III". The work was performed and the report was prepared by the Power Generation and Propulsion Laboratory at the Research and Development Center of the General Electric Company in Schenectady, New York. The program is monitored by an EPRI/ERDA Steering Committee consisting of:

W. G. Smith, ERDA, Program Manager
T. J. Rodenbaugh, EPRI
M. Mulcahy, Boston Edison

Dr. M. J. Jefferies, Manager - Cryogenics Branch of the Power Generation and Propulsion Laboratory of General Electric Corporate Research and Development, is the General Electric Company Program Manager. The principal contributors during this Phase III program were:

P. A. Rios, Manager - Cryogenic Engineering Programs
R. Browne
J. S. Hickey
S. S. Kalsi
T. A. Keim
W. J. MacFarland
S. H. Minnich
B. D. Pomeroy
J. P. Retersdorf
K. F. Schoch
C. J. Truax

The following individuals also contributed to various parts of the Phase III program:

E. Eich, Consultant (Power Technologies, Inc.)
J. S. Engelhardt (Underground Systems Inc.)

SPONSOR'S FOREWORD

Results from this and other studies dealing with the cost of cable systems for particular applications have shown that the resistive cryogenic cable system, as configured in this report, is expensive compared to alternative cable systems. The cost of the refrigeration and the system's losses translated into the amount of refrigeration required are the major cost contributors. Based upon the information collected to date, the sponsors have concluded that further development of system components is premature without first initiating material re-evaluation and system characterization activities. Accordingly, introductory tasks are being pursued prior to component development that will address thermal and dielectric insulations, refrigeration and utility costs.

ABSTRACT

The objective of this project was to design, fabricate and test components of an ac resistive cryogenic cable system. Fiber reinforced plastic was considered to be the most promising pipe material. After extensive dielectric tests, cellulose paper was selected for use as the dielectric in the cable samples tested. Instead of the more complex and expensive vacuum multilayered thermal barrier around the liquid nitrogen containment pipe, a closed cell polyurethane foam thermal insulation was chosen as a more desirable envelope. After extensive fabrication and testing efforts, a half-scale sample of pipe with adhesive joints passed all permeation and thermal/pressure cycling tests.

Sections of cable were electrically tested for breakdown stress under step stress testing. Conductors were insulated with a wall of cellulose paper and impregnated with liquid nitrogen (LN_2). The wall thickness on some cables were 550 mils (1.4 cm) and the others were 860 mils (2.2 cm). The breakdown data from the 550-mil cables indicated a breakdown strength greater than 860 Volts/mil (33.9 kV/mm). Designed operating stress of a full scale cable is 400 volts/mil I5.75 kV/mm). The 860-mil insulated cable was not failed electrically; however, due to premature failure which initiated in the capacitor stack of the pothead, further testing of this cable was prevented.

Conventional volt-time dielectric aging studies show that LN_2 impregnated cellulose paper exhibits excellent properties. Step stress tests were conducted using 1/4-, 1-, and 4-hour steps; the voltage was raised in increments of 2.5 kV.

A cable design study was performed in order to characterize the cost of fabricating, installing, and utilizing a resistive cryogenic system of 2000- to 5000-MVA capacity. Based on a 20-mile urban/

suburban scenario used in this study and on the chosen cable parameters of a 500-kV operating voltage, a 3500-MVA capacity, and a fiber reinforced plastic and polyurethane foam insulated envelope, the system costs were between $1,973/MVA-mile and $2,100/MVA-mile, depending on layout and geometry of circuits.

Although this Phase III project was successful in performing the electrical and mechanical tests on subscale samples, G.E. recommends that more confidence is needed before embarking on a development effort for a full-scale system.

OBJECTIVES

As a part of their joint Underground Transmission Research and Development Program, the Electric Power Research Institute and the U.S. Energy Research and Development Administration are providing support for the General Electric Company's investigation of an underground cryogenic power transmission cable.

The general objectives of this contract are to:

- Develop and evaluate the feasibility of a foam-insulated, cryogenic cable envelope.
- Evaluate dielectric materials at cryogenic temperatures and the high-voltage test of flexible cryogenic cable sections of typical EHV dimensions.
- Develop functional specifications for the components and the system required for a demonstration test of a three-phase, cryogenic cable approximately 1000 feet in length.
- Develop and evaluate nonmetallic cylindrical vessels required for the future construction of cryogenic pothead terminations.
- Study the life or aging characteristics of selected cryogenic dielectric systems.
- Conduct a cable system design study to select the cable configurations for capacities ranging from 2000 to 5000 MVA.

TABLE OF CONTENTS

TABLE OF CONTENTS (Cont'd)

TABLE OF CONTENTS (Cont'd)

TABLE OF CONTENTS (Cont'd)

LIST OF ILLUSTRATIONS

LIST OF ILLUSTRATIONS (Cont'd)

LIST OF ILLUSTRATIONS (Cont'd)

LIST OF ILLUSTRATIONS (Cont'd)

LIST OF ILLUSTRATIONS (Cont'd)

LIST OF TABLES

LIST OF TABLES (Cont'd)

Section 1

INTRODUCTION

The difficulties experienced in obtaining overhead transmission line rights-of-way, coupled with more recent concerns of the environmental intrusion of overhead lines, are expected to produce an increasing demand for underground transmission systems. Although the characteristic increase in demand for electrical energy has slackened in recent years, capital expenditures for underground transmission systems expressed as a percentage of the total transmission budget, have increased significantly over the past five years. There is little doubt that the investment in underground transmission systems will increase substantially in the years ahead.

Furthermore, it is necessary to increase the capability of underground transmission systems in an efficient, reliable, economical and environmentally acceptable manner. To a large extent, this increased capability is essential to the realistic and practical development of the nation's overall energy systems of the future. For example, large nuclear generation parks located away from metropolitan load centers require the development of high-capacity, efficient and economical transmission systems. Failure to develop improved underground transmission capability also jeopardizes the ability to exploit advanced energy source technologies. For example, the usefulness of energy generated at locations remote from load centers -- solar, geothermal, liquefied and low Btu gasified coal -- depends upon the availability of high-capacity, efficient and economical electrical energy transmission systems.

Cryogenic cable systems, which take advantage of the increased electrical conductivity of aluminum at liquid nitrogen temperature, represent one of a number of advanced underground transmission systems being developed to address these needs. Such cryogenic cable systems are expected to have single-circuit transmission capacities in the range 2000 to 5000 MVA at a nominal system voltage of 500 kV, significantly enhancing the capabilities of present-day underground transmission systems, in an economical, efficient and environmentally acceptable manner.

A particularly attractive feature of cryogenic cable systems is that the development of such systems can draw heavily on existing well-proven and reliable technologies developed for oil/paper cable systems. The flexible cable itself, which comprises a hollow-bore aluminum conductor taped with cellulose paper insulation, has been manufactured on existing equipment within the cable industry. The development of the cryogenic envelope, which comprises fiber-reinforced plastic (FRP) pipe sections with closed-cell foam thermal insulation, can take advantage of existing liquid natural gas pipeline technology. Cryogenic pothead terminations have been built

and tested which represent a relatively minor adaptation of existing capacitively-graded oil/paper pothead technology.

From April 18, 1974 to March 31, 1977, the General Electric Company conducted a cryogenic cable program (Phase III) that included component development as well as a cable system design study. This effort was carried out under the sponsorship of the Energy Research and Development Administration and the Electric Power Research Institute (Contract No. E(49-18)-2104). Several important accomplishments were achieved under this program, including:

- Development, construction, and test of sections of EHV cryogenic cable. One such cable section impregnated with liquid nitrogen at 80 psig was tested to failure, providing a 60 Hz breakdown strength of 830 V/mil. This stress is greater than twice the operating stress assumed in earlier cable system economic estimates.
- Half-scale sections of FRP pipe, FRP/FRP pipe couplings, and FRP/metal couplings were developed, constructed, and tested. Each component has successfully passed a series of qualification tests involving 50 pressure cycles to 30 atmospheres at 77 K, and 20 thermal cycles to 77 K, and a low-temperature permeation test.
- Cryogenic pothead terminations were designed, built, and tested to a maximum voltage of 430 kV line-to-neutral. These capacitively graded potheads were built to terminate the cable sections described above, and to accommodate the flow of liquid nitrogen to and from the cable bore.
- A study program on the dielectric aging characteristics of cryogenic electrical insulation systems was conducted which indicated that liquid nitrogen impregnated cellulose paper has a conventionally determined aging characteristic superior to that of oil/paper insulation.
- Completion of a cable system design study to select cable and piping configurations for system capacities ranging from 2000 to 5000 MVA. Both performance and cost estimates were obtained to aid in the planning of future demonstration phases.

Section 2

PROGRAM SUMMARY

CRYOGENIC ENVELOPE INVESTIGATION

Previous estimates of cryogenic cable system costs have shown that more than half of the initial system costs may be attributed to the cryogenic envelope and the system installation. These costs were based on the use of a cryogenic envelope with multilayer vacuum insulation. The installation of this pipe requires field welding of each of the vacuum insulated joints with the associated requirements of weld inspection and leak checking. It is also necessary to provide some means of monitoring the condition of the vacuum in each section of pipe, which involves additional instrumentation and control circuit wiring.

In addition to the installation complexities, the application of vacuum insulated pipe as the envelope of a cryogenic cable system raises various questions concerning the reliability of the vacuum insulation. Relatively little reliability data are available to estimate the performance of long lines, but the data that are available do not present an encouraging picture.

In this program, an investigation of alternative envelope configurations was undertaken with the objective of reducing piping and installation costs. Specifically, the work was directed toward a technical evaluation of a cryogenic envelope that utilized fiber-reinforced plastic pressure pipes and rigid foam as the thermal insulation.

As part of the development work, the mechanical properties of a number of fiber-epoxy systems were measured on small samples at low temperature. E-glass and Epon epoxy 826 were selected for the manufacture of the FRP pressure pipe. A number of half-scale FRP pipe spools (1/4-inch wall thickness, 8-inch diameter, and 10-feet long) were manufactured and subjected to a series of tests which were structured to qualify the FRP spools for cryogenic envelope service. These qualification tests comprised the following:

- At least 20 temperature cycles between ambient temperature and liquid nitrogen temperature (77 K). (Cooldown was performed in approximately one hour.)

- At least 50 pressure cycles to 30 atmospheres. This pressure represents 1.5 times rated pressure, and the tests were conducted at liquid nitrogen temperature.

- A final permeation test to measure the permeation rate of nitrogen through the wall of the FRP spool at 77 K. An average permeation

rate less than 7×10^{-9} standard cm^3/cm^2-sec based on the wall area was defined as acceptable.

Permeation rates are of importance from the standpoint of thermal insulation degradation. It is estimated that a nitrogen permeation rate of 7×10^{-9} standard cm^3/cm^2-sec would cause a 15 percent increase in the heat flux through the thermal insulation after 40 years of service. Hence, this value of permeation rate was chosen as a preliminary basis for "qualification" of the trial FRP spools. Figure 2-1 shows one section of half-scale FRP pipe being prepared for the series of qualification tests.

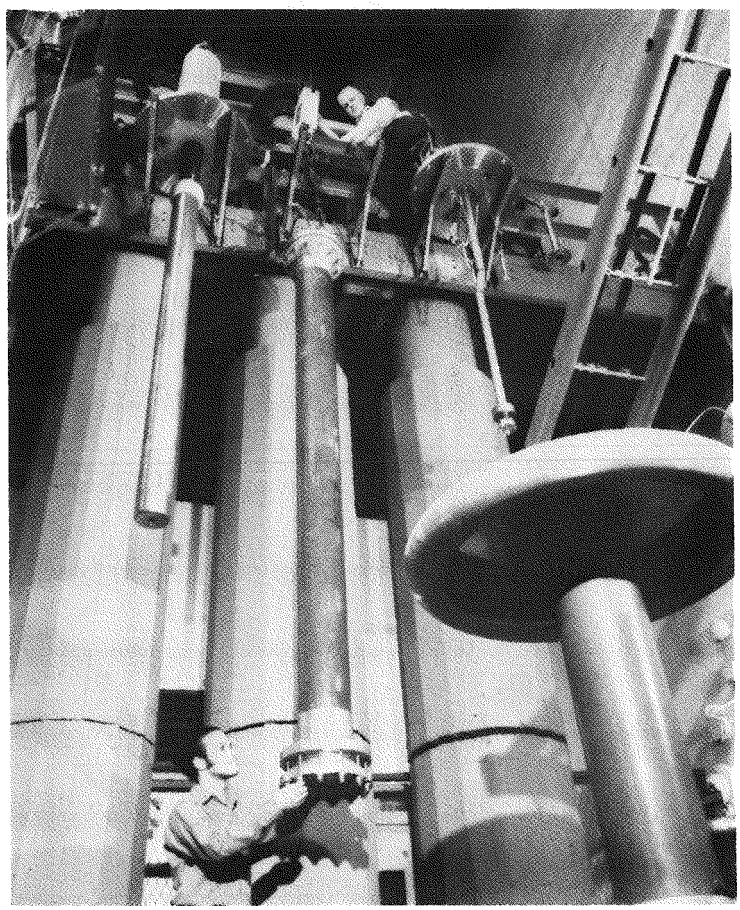

Figure 2-1. Assembled FRP Pipe Section Ready for Testing in Liquid Nitrogen Filled Vessel

A wide range of spool constructions was evaluated before an FRP spool was designed and manufactured which successfully passed the complete series of qualification tests. For the purposes of increasing confidence in the manufacturing process, two additional FRP spools were manufactured in accordance with this design, and they too have passed the complete series of qualification tests.

In addition to the FRP pressure pipe development, two types of joints have been developed for the cryogenic envelope. The first type of joint is required for FRP pipe-to-FRP pipe connection, and the second type is required for FRP pipe-to-metal flange connection. FRP pipe-to-metal flange connections are used at expansion joints, bends, and at terminations. Both types of joints have been developed to the stage whereby they successfully pass the same series of qualification tests described above. Figure 2-2 shows an FRP pipe section with one FRP pipe-to-FRP pipe joint, and two FRP pipe-to-metal flange joints.

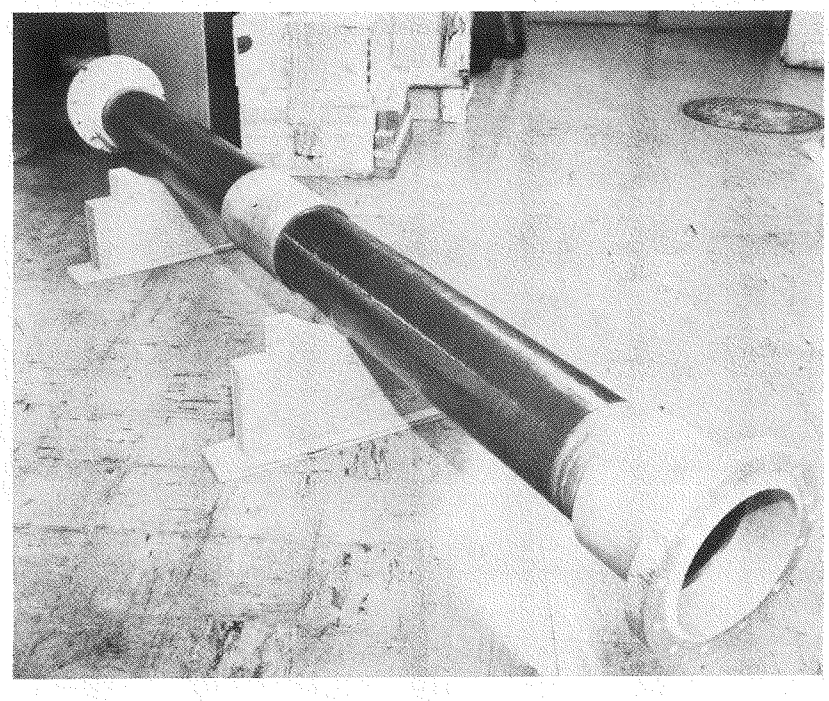

Figure 2-2. Half-Scale Section of FRP Spool, Including FRP/FRP Joint and Two FRP/Metal Joints

In general terms, the results of this development work have been very encouraging and provide a significant step in demonstrating the technical feasibility of this type of envelope configuration for cryogenic cable application. However, it must be added that unexpected difficulties arose in the course of this work in extrapolating high quality manufacturing procedures from small-scale pipes (3-inch diameter) to half-scale pipes (8-inch diameter). Thus, it is reasonable to expect that a considerable development effort will be required to successfully produce the full-scale pipe sections (approximately 17-inch diameter) required for an operational cryogenic cable system.

ELECTRICAL INSULATION EVALUATION

In this task, a wide range of insulation materials was surveyed by comparing measurements of short-term ac breakdown strength and dissipation

factor on small, taped, cylindrical dielectric samples. These samples were tested in liquid nitrogen at 77 K, at a pressure of 80 psig. Tests were conducted at two voltage levels: 50 kV and 200 kV.

On the basis of these tests, a specific cellulose paper insulation was selected for the manufacture of two cryogenic cable sections: one with a nominal insulation thickness of 0.860 inch, the other with a nominal insulation thickness of 0.550 inch. The two cable sections are shown in Figure 2-3.

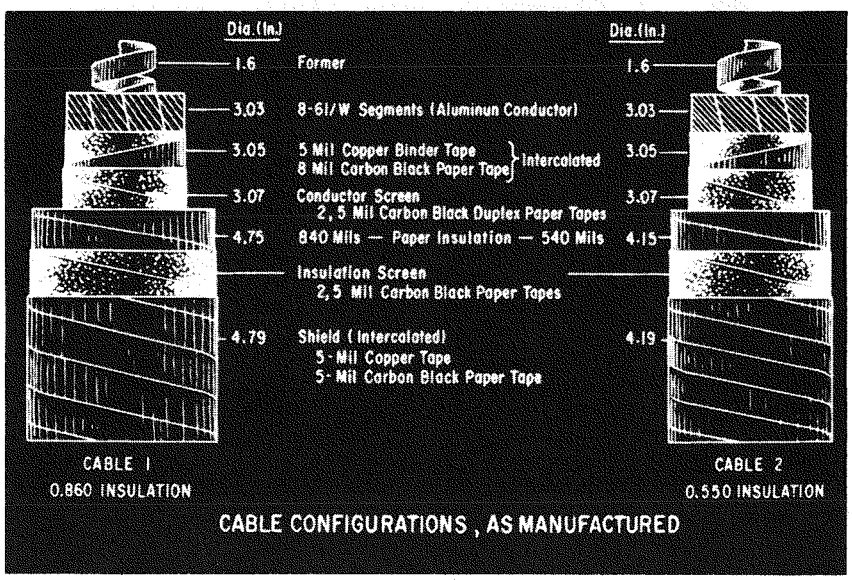

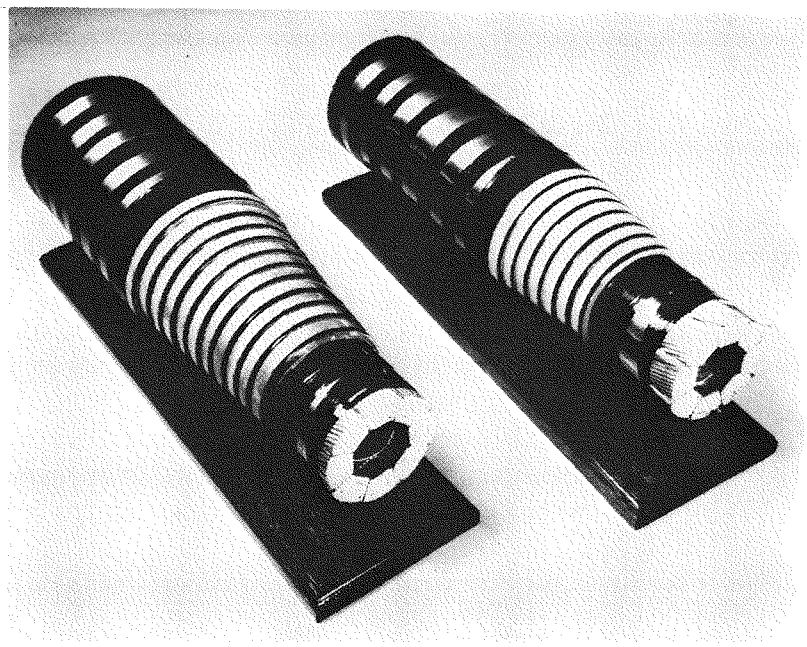

Figure 2-3. Prototype Cryogenic Cable Sections

The principal specifications of the cellulose paper used in each of these cables are:

Type of Pulp	Conventional kraft (CK)
Water treatment	Deionized water
Air resistance (nominal)	2500 Gurley-sec
(minimum)	2000 Gurley-sec
Paper density (nominal)	0.85 gm/cc
Thickness (nominal)	0.005-inch and 0.0065-inch

Short-term ac breakdown strengths of 1481 V/mil and 1334 V/mil were provided by the 0.005-inch and 0.0065-inch papers respectively, in small sample tests. These cylindrical samples had a radial build of insulation of approximately 0.040 inch, and were tested in liquid nitrogen at 77 K at a pressure of 80 psig.

To perform EHV tests on the cryogenic cable sections, the test equipment shown in Figure 2-4 was constructed. This equipment comprises a straight horizontal pipe section, with a 90-degree pipe elbow at each end. The cable is terminated by two capacitively-graded cryogenic pothead structures which also serve to introduce and remove liquid nitrogen from the bore of the cable. Liquid nitrogen, at a temperature of approximately 77 K and at a pressure of 80 psig, is circulated through the cable bore and pipe section, and is cooled externally by a heat exchanger.

A significant problem became evident during the installation of the first cable section. Although the cable had been stored on a "sealed" cable drum, which was purged daily with dry nitrogen gas, it was apparent that the cable paper had absorbed moisture (six to eight percent by weight) during the storage period, compared to a moisture content of approximately one percent by weight, at the time of manufacture. The increased moisture content caused the paper tapes to swell, and prevented uniform bending of the cable. To correct the situation, it was necessary to dry the cable in place on the reel. This was accomplished by evacuating the bore of the cable, heating the conductor to 100 C for a period of six days (refer to Figure 4-7), and sealing the outer periphery of the cable reel in an environment of dry nitrogen gas. On completion of this drying cycle, the cable satisfactorily passed a bend and reverse-bend test, although some evidence of "polygonization" was still present in each of the cable sections.

A total of five cable sections was tested and a summary of the results is presented in Table 2-1. In each case, the voltage applied to the test system was increased until a failure occurred. The voltage steps and the times at each step were different for each of the tests; the values are documented in Section 4, "Electrical Insulation Evaluation," of this report.

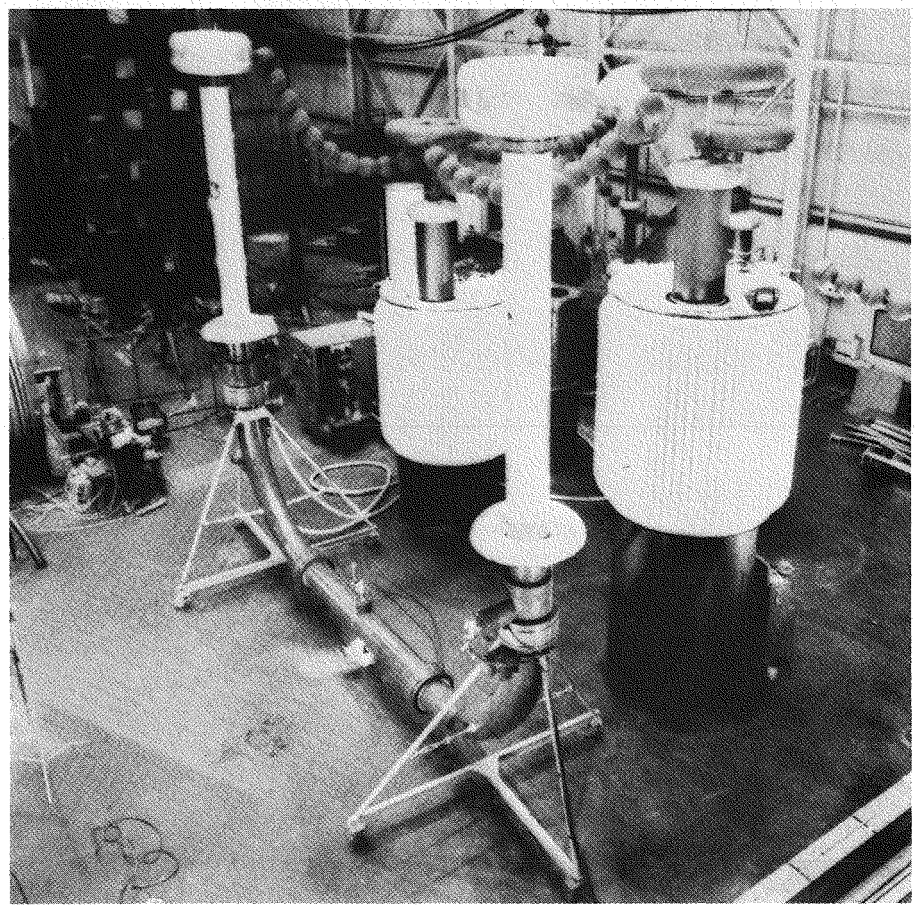

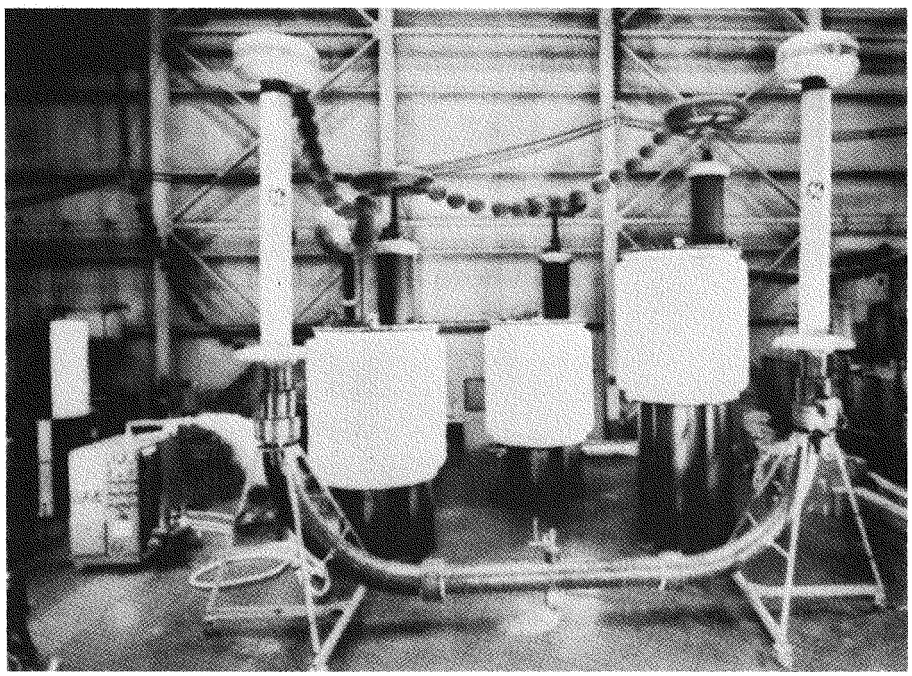

Figure 2-4. Overall Views of the Cryogenic Cable High-Voltage Test Equipment

Table 2-1

SUMMARY OF CRYOGENIC CABLE TESTS

Test No.	Cable Insulation (mils)	Maximum Voltage (kV)	Cable Stresses (V/mil)		Failure Location
			At Conductor Surface	Average	
1	550	386	830	702	East Power Factor Gap
2	860	430	632	500	West Capacitor Stack
3	550	286	615	520	West Stress Cone
4	550	330	710	600	East Stress Cone
5	550	400	860	727	West Stress Cone

Probably the most significant result from this series of tests was that none of the five cable sections failed in the test length. This result is not particularly satisfying to the extent that it was not possible to establish specific breakdown values for each of the cable sections. However, the results are unambiguous in establishing that the breakdown strength of the cable test lengths is greater than 860 V/mil for the cable with an insulation thickness of 0.550 inch. To put this result in perspective, it must be remembered that the operating stress assumed for cryogenic cable systems in the earlier economic studies was 400 V/mil. Thus the tests have demonstrated that the cables are capable of withstanding twice rated stress without failure; an important and encouraging result.

However, the tests do raise the question of why the stress cones failed. It must be remembered that the electric field distribution in the stress cone region is such that an axial component of stress exists in the region. In the cable test length, the theoretical stress distribution is purely radial. In a typical high-pressure, oil-filled (HPOF) cable system the maximum axial stress in the stress cone of a splice is approximately 6 V/mil at rated voltage. In the cryogenic cable tests, the axial stress in the pothead stress cone at failure was in the range 6 to 10 V/mil. It may be speculated that the cause of the stress cone failures was due to one of three factors.

- The intrinsic strength of the cryogenic cable insulation in the axial direction is less than that of oil/paper insulation.
- The construction of the stress cones was defective.
- The high radial stress at the outside diameter of the cryogenic cable prevented the attainment of axial stresses customarily employed.

This third item requires more explanation, since it is believed to be the most likely cause of stress cone failure in the cryogenic cable tests. First

it is necessary to explain that although the maximum radial stresses in conventional and cryogenic cables are similar, the average stresses, and hence the stresses at the outside diameter of the cables, are different. Table 2-2 shows a comparison of the stresses in a typical 500 kV HPOF cable and in the cryogenic test cables.

Table 2-2

COMPARISON OF RADIAL STRESSES
IN HPOF CABLE AND CRYOGENIC TEST CABLES

Cable Type	Radial Stresses (V/mil)		
	Maximum at Conductor Surface	Average	At Outside Diameter of Insulation
HPOF Cable 500/550 kV	425	258	168
Cryogenic Cable (Insulation Thickness 0.550 inch)	425	360	313
Cryogenic Cable (Insulation Thickness 0.860 inch)	425	336	272

Note: The applied voltage has been chosen such that the maximum stress is 425 V/mil in each case

It can be seen that the ratio of average/maximum stress is higher in the cryogenic cables. This ratio is purely a function of the cable geometries, and the difference is readily explained by the larger conductor diameter of the cryogenic cables. Thus, if stress cones are applied to each of these cables such that the axial stress in each stress cone is about 6 V/mil, it is obvious that the cryogenic cable insulation will be exposed to this component of axial stress in conjunction with a relatively high radial stress at the outside diameter of the cable. It is entirely possible that the axial stress capability of any impregnated paper insulation will be a function of the radial stress component. Although the axial stresses in the stress cones of the cryogenic cables were similar to those employed in HPOF cable practice, the stress cone failures may have been caused by the higher radial stresses which existed at the outer diameters of the cables. The above arguments are speculative and it is clear that further work is required in this area to provide a meaningful determination of the cause of the stress cone failures.

In general terms, the performance of the cryogenic potheads was entirely satisfactory. Two capacitively-graded pothead structures were designed and manufactured to terminate each of the above cable sections. The construction of these potheads was somewhat similar to that of conventional oil/paper pothead terminations except that an FRP pressure vessel was used to

contain the liquid nitrogen, and a cylindrical jacket of foam thermal insulation was used to limit the heat leak to the low temperature region. The cryogenic pothead structures also allowed for the introduction and removal of liquid nitrogen from the bore of the cable sections. Figure 2-5 shows an overall view of one of the completed pothead assemblies.

In performing the second cable test, a failure occurred in one of the potheads at an applied voltage of 430 kV. Subsequent dissection of the pothead termination revealed that the failure had occurred between the lower two capacitor elements, with evidence of incipient failure between other capacitor elements. The reason for this failure is understood and is explained in detail in Section 4 of this report. It is believed that minor modification of the end region of the capacitor elements will overcome this problem in future tests. It should be noted that in the other four cable tests involving eight potheads, the capacitor stacks and the build-up rolls performed satisfactorily without failure.

It should also be noted that no problems were encountered with the liquid nitrogen annulus that existed between the capacitor stack and the build-up rolls. This annulus exists as a result of the necessary clearances required to assemble the potheads. In a conventional pothead there is an analogous region where the electric stress is applied to the oil alone, rather than to the impregnated paper insulation. Furthermore it was demonstrated that liquid nitrogen could be transferred to the bores of the cables via the potheads. The liquid nitrogen flow and the temperature distribution in the test system were stable throughout the testing period of several weeks.

TEST SYSTEM SPECIFICATIONS

The electric utility industry's acceptance of the application of any new technology can only come about after a period of demonstrated reliable performance, and some reasonable expectation of economic benefit. Thus it is generally recognized that a developmental, advanced underground transmission system will have to prove itself in some form of demonstration or qualification test before being accepted by the industry. Such tests will necessarily involve a configuration in which all the major system components are brought together and are operated under actual or simulated power system conditions. The precise nature of such a test is often the subject of some debate, and generally involves a trade-off between the overall costs of constructing and testing such a system, and the breadth and depth of the technical information to be derived from such a test.

In the case of cryogenic cable systems, it is proposed that this demonstration test will necessarily involve the design, construction, and test of a representative 500 kV, 3500 MVA three-phase cable system involving pothead terminations and splices. This section is assumed to be on the order of 1000 feet in length and is shown schematically in Figure 2-6.

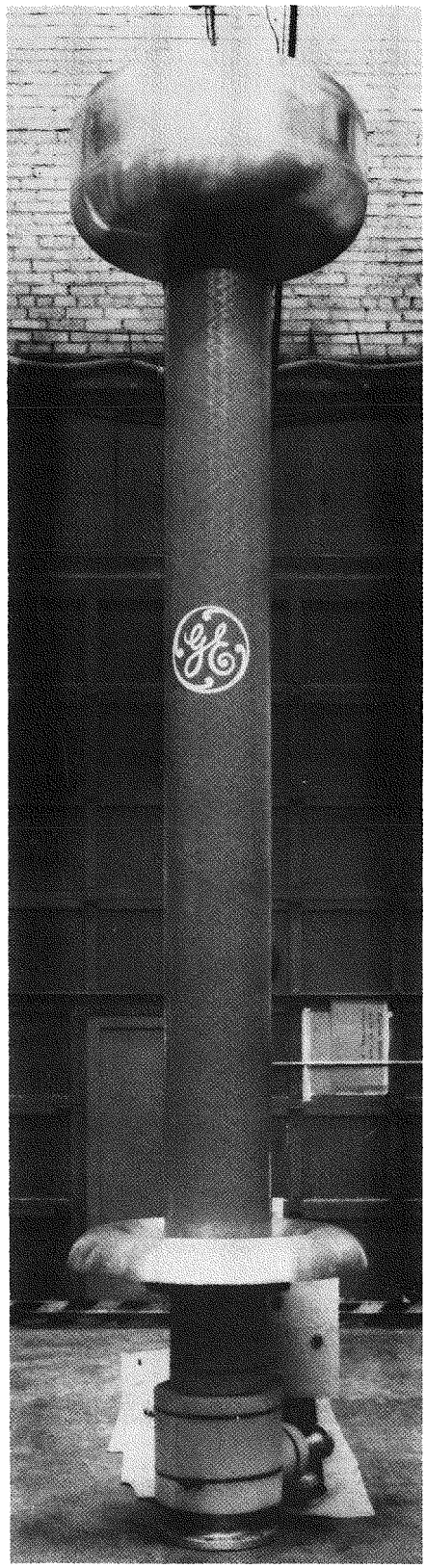

Figure 2-5. Completed Pothead Assembly

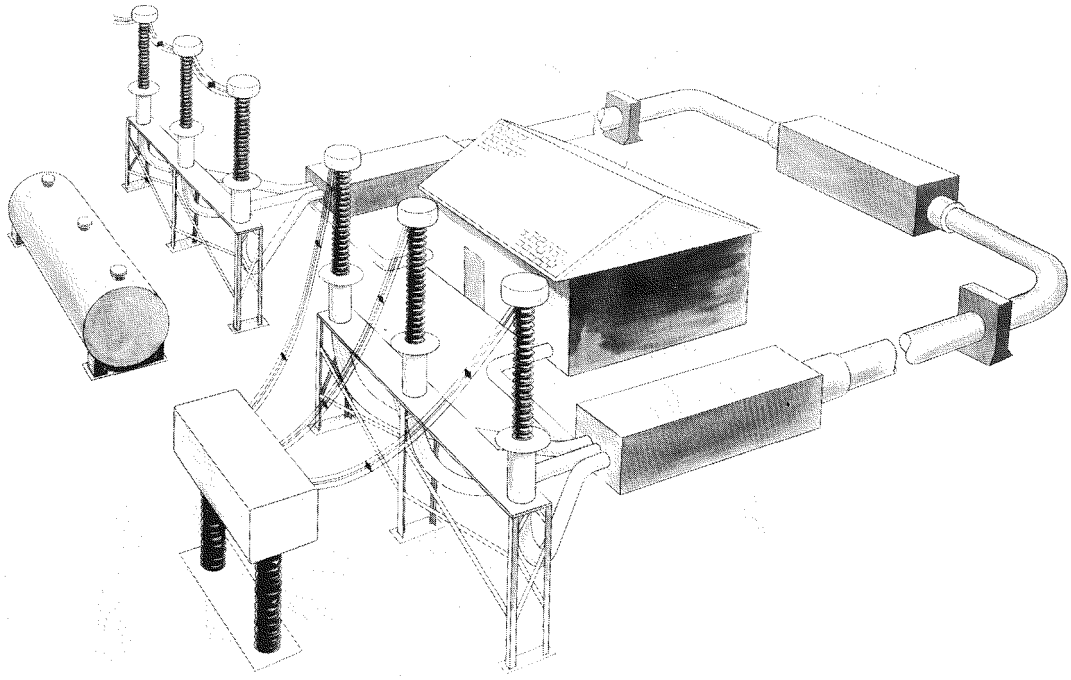

Figure 2-6. 1000-Foot, 500-kV, 3500-MVA Test System

On the basis of the development work conducted in this and prior phases of the cryogenic cable program, best estimates of component specifications for the elements of this test system configuration have been prepared. It is emphasized that the objective of this task was to develop preliminary specifications for the test system, as it is envisaged at the present time. Test system design was not within the scope of this program.

The specifications of the components envisaged for this 500 kV, 3500 MVA, 1000-foot test system are presented in Section 5 of this report.

ELECTRICAL INSULATION AGING STUDY

The objective of this task was to determine basic information on the high-voltage characteristics of cryogenic dielectrics as a function of time. The task was divided into two parts. In the first part, step stress tests of cellulose paper, similar to that used on the cryogenic cable sections, were conducted. In the second part of the task, constant voltage tests were conducted on the same insulation material. All tests were conducted on taped

cylindrical samples, with a radial insulation thickness of approximately 0.040 inch, immersed in liquid nitrogen at 77 K, at a pressure of 80 psig.

Step stress tests were conducted using 1/4, 1, and 4-hour steps; the voltage being raised by 2.5 kV at each step. Constant voltage tests were performed at 41 kV (approximately 1250 V/mil) and at 38.5 kV (approximately 1175 V/mil).

The data obtained from these tests have been combined and entered into a computer program which fits the data to the Weibull distribution with an inverse power law voltage dependence. The resulting mathematical expression for the predicted fraction of samples to survive after time t, at a constant stress E, is given by:

$$S(t) = \exp\left[-\left(\frac{E^n t}{c}\right)^{\beta}\right]$$

Fitting the data derived from the above experiments to this expression yields:

$$S(t) = \exp\left[-\left(\frac{E^{38.39} t}{10.06 \times 10^6}\right)^{0.5462}\right]$$

In this expression, the electric stress is expressed in MV/inch, and the time t is expressed in hours; the constant c is adjusted to provide a consistent fit to the data. The most important parameter derived in this manner is the exponent n. A large value of n indicates that the material has a favorable aging characteristic, typical values for n being in the range 10 to 20 for conventional insulating materials. The value of n equal to 38 derived here for the liquid nitrogen impregnated cellulose paper provides a strong indication of the superior performance of this cryogenic electrical insulation compared to oil/paper. For example, using these data in conjunction with the Weibull relationship, it can be computed that the 99 percent survival time for these samples, at an assumed operating stress of 450 V/mil, is 5.2×10^{12} years, assuming that the aging mechanism can be represented by the inverse power law.

It is obviously unrealistic to attempt to draw conclusions from these limited data as to the precise life characteristic expected in a full-scale cryogenic cable using this insulation material. In fact, it is highly questionable whether it would ever be worthwhile to attempt to expand the data such that precise life characteristics could be derived. However, the data obtained and analyzed to date do provide a strong indication that the life

characteristic of cryogenic insulation will be as good as, or better than, that of conventional oil/paper insulation.

CABLE SYSTEM DESIGN STUDY

A system design study was conducted to determine system performance and to estimate installed costs, based on 1976 prices, for systems ranging in capacity from 2000 to 5000 MVA. Thermal insulation losses were based upon the use of foam thermal insulation for the cable pressure pipe and the liquid nitrogen return pipe. Metallic piping concepts were also examined to determine whether further development of FRP piping is justified by the smaller losses and resulting lower costs obtained with FRP piping. Cable configurations were also studied to identify component dimensions and to evaluate the relative performance of hollow conductor versus solid conductor cables.

The major results obtained from this design study are summarized below:

- A cable with a solid, rather than a hollow, conductor provides significant operational and cost advantages. Figure 2-7 shows dimensions and general design features of a 500-KV cable, rated for 3500 MVA, selected by this study to achieve highest efficiency within limitations imposed by cable manufacture and cable shipment by reels. Dimensions for cables of other capacities are also provided in this report.

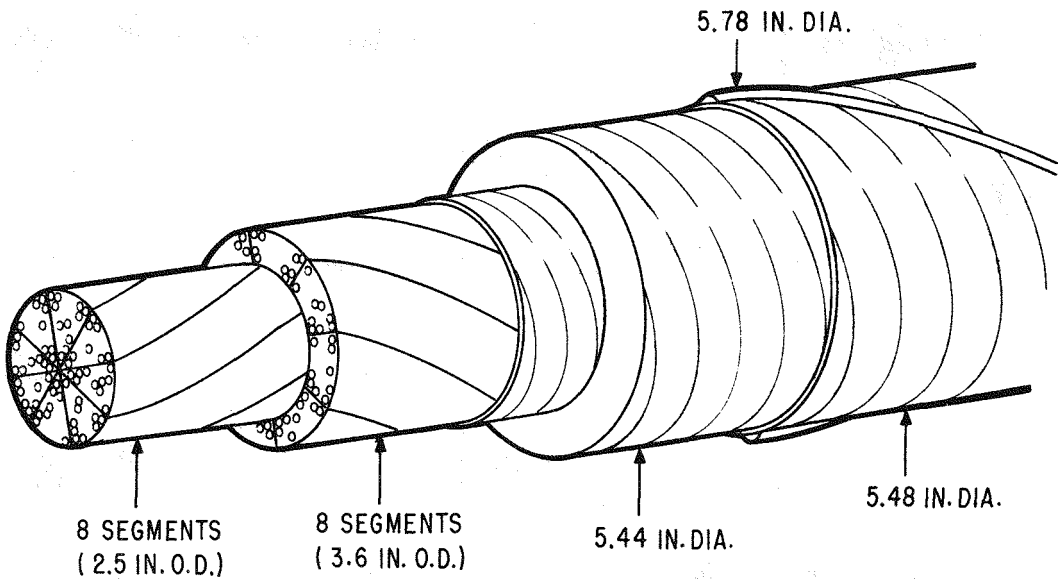

Figure 2-7. Solid-Conductor, Liquid-Nitrogen-Cooled, 500 kV, 3500-MVA Cable

- The use of FRP (nonmetallic) pressure piping results in a significantly lower cost than is possible with any one of several metallic piping concepts considered. This comparison is shown in Figure 2-8.

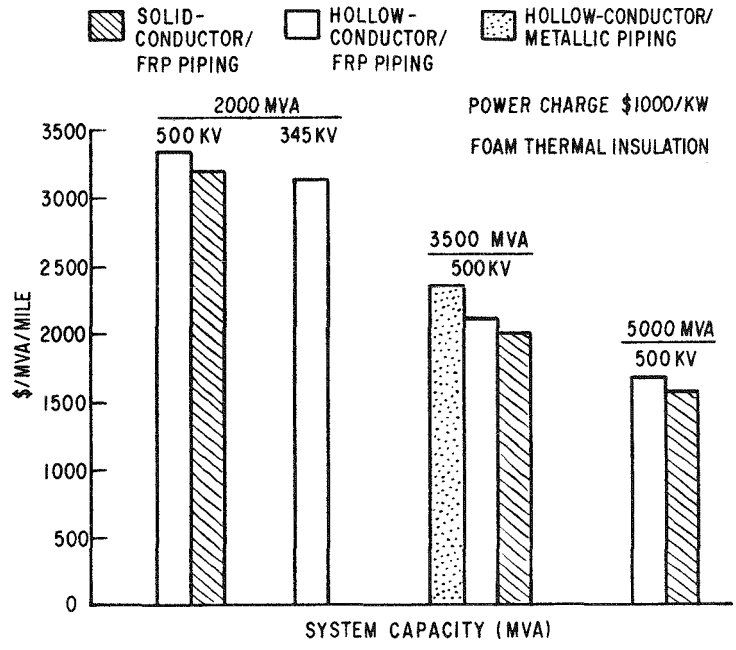

Figure 2-8. Twenty-Mile Owner's System Cost Estimates

- Distances between refrigeration stations can range from 26.4 to 12.6 miles for systems having transmission capacities of 2000 to 5000 MVA.
- Cost estimates show the sum of the installation cost and the cost for power losses to be more than one-half of the total owner's system cost.

SUBJECT INVENTIONS

In the course of this contract, contractor's invention disclosure letters were submitted to the contracting officer in the following areas:

- A novel concept for providing electrical-stress grading in pothead structures. The proposed concept involves a combination of resistive and capacitive grading and is theoretically applicable to both conventional and cryogenic pothead terminations. The proposed configuration eliminates the need for buildup rolls and a stress cone in the termination. Consequently, it has the potential for reducing the overall diameter and cost of the pothead terminations.
- A demountable joint to form a leak-tight connection between a metal flange and an FRP pipe section. The proposed concept avoids the use of metal studs or inserts in the walls of the pipe to obtain the required axial force against the sealing surfaces. Thermal stressing of the pipe during cooldown is reduced and pipe manufacture is simplified.

- A thermal conductivity monitoring sensor. It is envisaged that the proposed sensor could be applied in the foam thermal insulation of the cryogenic cable envelope sections as a means of monitoring the thermal conductivity of the foam insulation. Such a technique could be used for the detection of degradation in the performance of the foam insulation as a function of time.

Section 3

CRYOGENIC ENVELOPE INVESTIGATION

The development of a foam insulated fiber-reinforced plastic (FRP) cryogenic envelope was undertaken in view of the potential reductions in manufacturing and installation costs compared to a vacuum-insulated metallic envelope. The manufacture and installation of the cryogenic envelope represents a major factor in the overall cable system cost. The primary objective of this investigation was to demonstrate the technical feasibility of FRP pressure pipe for cryogenic cable application, both as the cable containment pipe and as the liquid nitrogen return pipe as shown in Figure 3-1. Related to this effort was the development of joints to interconnect separate lengths of FRP pipe and the development of joints to connect FRP pipe sections to metal flanges.*

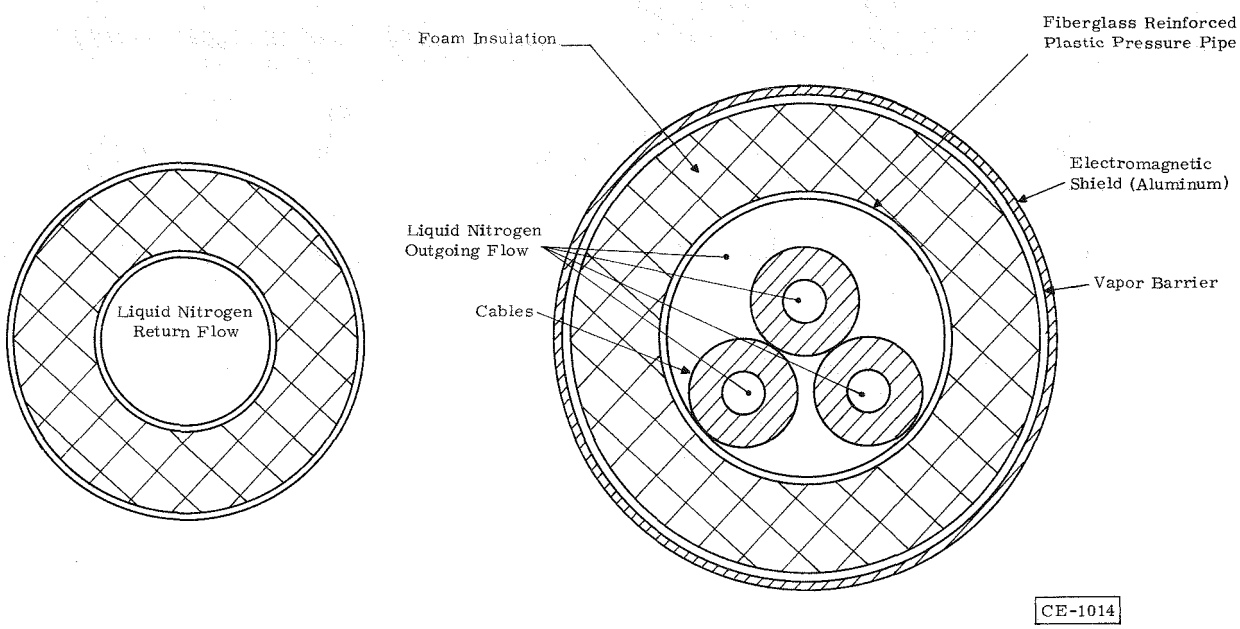

Figure 3-1. Cross Section of Liquid Nitrogen Return and Cable Pipes

Filament wound, E-glass reinforced epoxy systems offer high strength to weight ratios, low refrigeration loads, structural reliability and low fabrication cost. This construction, however, also presents potential problems in that the liquid nitrogen must not be allowed to permeate through the FRP pipe into the foam thermal insulation. Epoxy resins are also subject to thermal and pressure induced stresses that can lead to crazing and cracking, as a result of the increased brittleness and higher modulus of elasticity

*A bibliography for this section is found in Section 8.

at low temperature. Epoxy-glass composite material is also highly anisotropic, and its properties are strongly dependent on the percentage glass content and the quality of manufacture.

Glass cloth epoxy construction was not considered in this program because of the significantly higher cost (four to ten times) compared to filament glass epoxy construction, and because of the significantly higher strengths offered by filament glass epoxy construction.

Detailed consideration of an envelope concept in which a metallic, rather than an FRP, pressure pipe is used, was not included in this program. It is recognized that such a concept requires less development than the FRP pipe concept, but the potential advantage of the FRP concept, in that it removes all electrical pipe losses, is sufficiently important to warrant greater attention. However, the metallic pipe concept is being retained as a possible backup to the FRP system.

In this task, the effort was directed toward the development of 8-inch diameter pipe (approximately half-scale), rather than the larger diameters required for a full-scale installation, to minimize manufacturing and testing costs. Filament winding machines are commercially available and can be adapted to manufacturing FRP pipe sections in 40-foot lengths.

As a result of the work performed during this Phase III program, filament wound FRP pressure pipe and adhesive bonded joints have been successfully developed to meet the stringent requirements imposed by the cryogenic temperatures and high operating pressures encountered in this cryogenic cable application (see Tables 3-1 and 3-2). Although the development has been performed on half-scale components, the manufacturing technology appears to be capable of extrapolation to full-scale components. However, experience gained in the course of this development has shown that

Table 3-1

FRP PRESSURE PIPE REQUIREMENTS

Operating pressure: approximately 20 atm
Maximum pressure (proof test): 30 atm
Operating temperature range (^{o}K): 65 to 97
Maximum temperature (^{o}K): 305
Permeation into foam insulation: less than 7×10^{-9} std cm^3/cm^2-sec
Design life: 40 years

Table 3-2

QUALIFICATION TESTS

Thermal cycling	
300 K to 77 K	20 Cycles*
Pressure cycling	
1 to 30 atm	50 Cycles†
Maximum permeation	7×10^{-9} cm^3/cm^2-sec

* Warm-up periods were occasionally limited to eight hours to avoid lengthy testing periods. Pipe temperature approached but did not always reach outdoor ambient before the next cooldown.

† Pressure cycling was accelerated by pressurizing the liquid nitrogen filled pipe with helium gas from a high-pressure source. To conserve helium gas, the pressure was reduced to approximately 13 atmospheres before repressurization to 30 atmospheres for some cycles.

manufacture of the FRP pressure pipe requires that void-free, high glass content structures (72 percent by weight) be produced, with a high degree of manufacturing quality control throughout the filament winding and resin curing operations.

As far as FRP/metal joints are concerned, FRP/aluminum bond strengths have been shown to be adequate for the axial loads imposed by a full-diameter joint of this type, when a polyurethane adhesive with glass mat reinforcement is used.

Features of the envelope components developed in the Phase III program are summarized below. Photographs of FRP pipe spools as well as FRP/FRP and FRP/aluminum flanged joints appear in Figures 3-2, 3-3, and 3-4.

FRP pipe

Dimensions	8-inch ID, 1/4-inch wall, 10 feet long
Winding pattern*	o-xx-o-xx-o----xx inner surface outer surface
Glass	"E" glass, Owens-Corning type 410AA675
Resin system	Epon 826/Vandride 2/DMP-30 accelerator, heat cured
Surface treatment	Glass veil covered inner surface

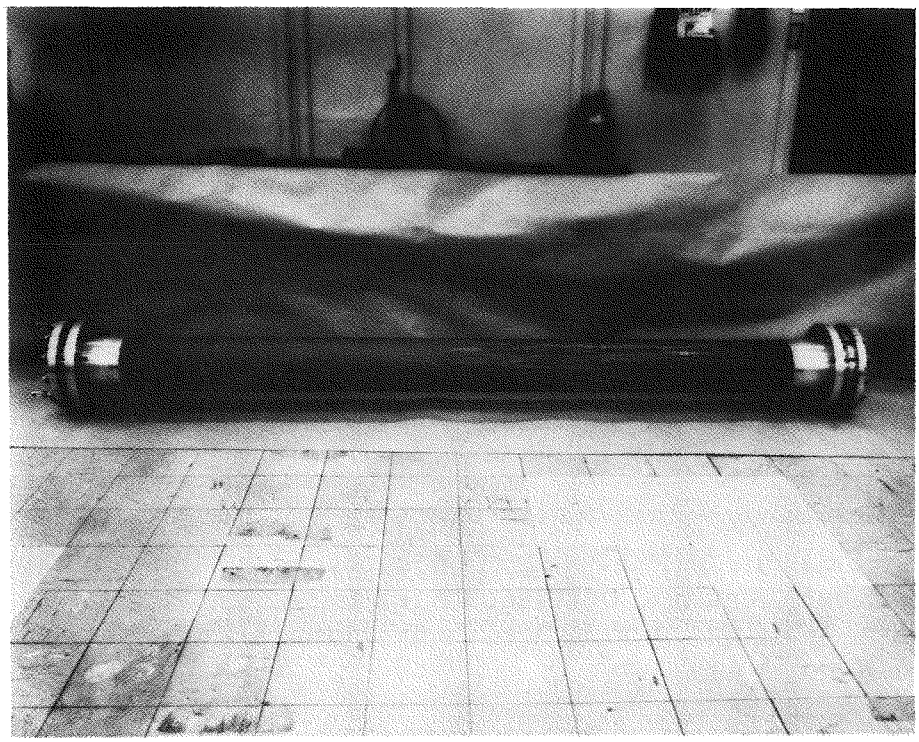

Figure 3-2. FRP Spool (F-14) Following Qualification Tests

*o represents a circumferential winding (88° to 89°)
x represents a helical winding (44° to 46°)

FRP/FRP couplings

Dimensions	8 1/4-inch ID (1 1/2° taper), length 12 inches
Winding pattern	o-xx-o-xx....xx
Glass/resin	Same as FRP pipe
Adhesive	3M Company, modified epoxy #2216 B/A
Adhesive curing	150 F, one hour

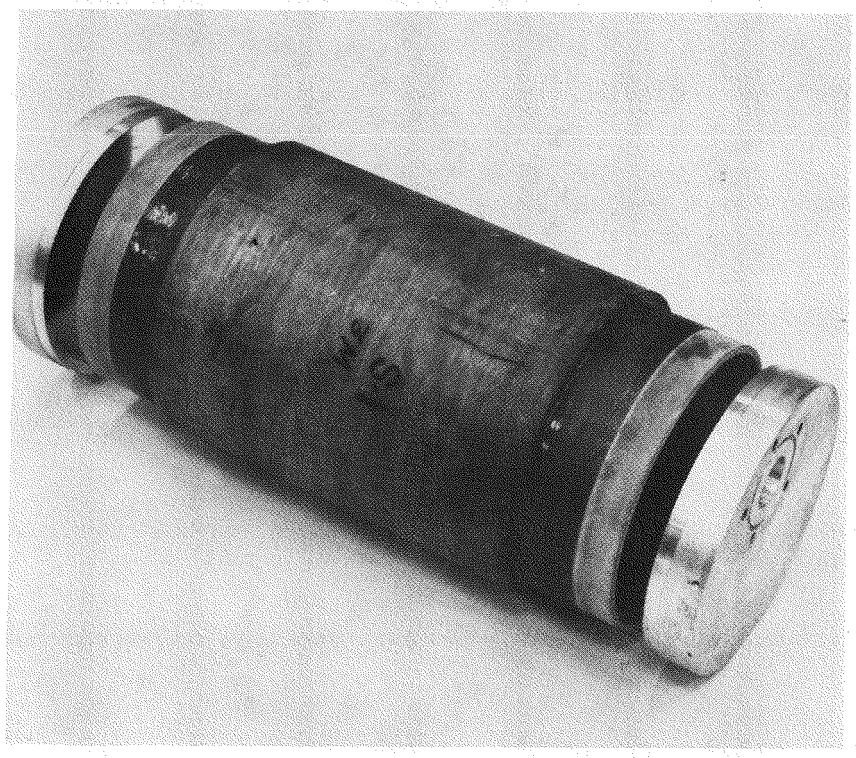

Figure 3-3. FRP Coupling Partially Assembled for Permeation Test

FRP/aluminum flange assembly

Aluminum stub end	Flowline Corporation 8-inch diameter nominal, Part S-4 6061-T6 aluminum

Lap joint flange	Flowline Corporation 8-inch diameter nominal, Part FC-150 6061-T6 aluminum
Seal ring (flange to flange)	Creavy Seal Company AS400-8.875
Adhesive	Amicon Corp. Polyurethane TU 902
Adhesive cure	176 F, two hours

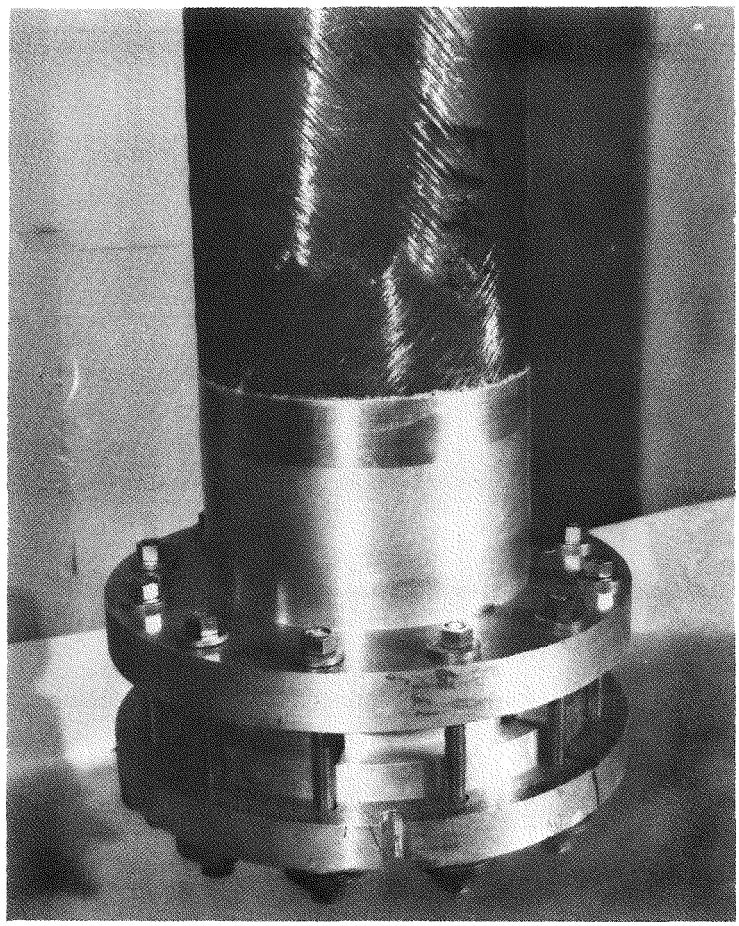

Figure 3-4. FRP Pipe/Metal Flange Joint Using Urethane Adhesive

Foam thermal insulation	
Density	2.5 lbs/ft^3
Protective jacket	1/8-inch polyester glass
Source	Factory applied to FRP Cosmodyne, Torrance, CA

STATUS OF THE FRP PRESSURE PIPE AND JOINT DEVELOPMENT

This summary reviews the status of the cable envelope development at the completion of this Phase III program:

- The development of filament-wound FRP pressure pipe and pipe joints for application to the envelope of cryogenic cable systems has been shown to be technically feasible, based upon the test criteria presented earlier.
- Craze marks that occasionally appear on the surfaces of the FRP spools have shallow depths that are limited to the thickness of the one winding layer in which they are formed. Builtup ends were not used because they delaminated during cooldown.
- Filament-wound FRP pressure pipe is exceedingly strong. Should failure occur in an FRP pipe due to some unforeseen occurrence, it is most unlikely that a sudden destructive rupture would result. Cracks or delamination may develop, but these tend to produce liquid nitrogen seepage, rather than a sudden release of liquid.
- The technical feasibility of adhesive bonded joints has permitted the use of FRP pipe sections having a uniform wall thickness. Specially prepared, built-up end-bells are not required on the FRP pipe sections. Thus, the adhesive bonded joints developed in this program promise a significantly lower envelope cost.
- It is expected that the application of adhesive bonded joints will be viewed with some skepticism, since bonded assemblies generally fail suddenly. In addition, such joints cannot be readily inspected, and some of the joints (approximately 40 percent) have to be prepared in the field. With proper design of the envelope supports, axial movement of the joints can be prevented to ensure a gradual, rather than a sudden, loss of liquid nitrogen pressure in the event of an adhesive joint failure. Good reproducibility of adhesive bonds was obtained with 8-inch diameter joints, as well as with small lap-shear samples, after proper adherend surface preparation and bond-line reinforcement techniques were developed.
- Scale-up to full size components is required before performance can be assured.

FRP PIPE DEVELOPMENT

The development of half-scale FRP pipe sections was initiated with the preparation of small rectangular, uniaxial epoxy-glass samples which were approximately 1 1/2 inches long. Later in the program, 2-inch diameter cylindrical samples were used to screen epoxy-resins, and study the effects of fiber content and void volume on the allowable stress and elastic modulus of the samples. An investigation of the low-temperature sealing capabilities and thermal shock capabilities of these samples was also undertaken. Results of this early work appear in the First and Second Quarterly Reports, pages 6-9 and pages 4-5, 13-15, respectively. The results indicate that small diameter glass-reinforced epoxy tubes can be subjected to thermal cycling from ambient temperature to 77 K while sealed with commercially available sealing rings.

The ends of the first 2-inch diameter spool were sealed with commercially available sealing rings supplied by Pressure Science, Inc. These rings were used to form a seal between the ends of the FRP pipe section and the metal flanges. This configuration is shown in the Third and Fourth Quarterly Reports, Figure 4 and Figures 1, 2 and 8 respectively.

While this technique proved successful in sealing 2-inch diameter pipe sections, it proved to be unsatisfactory when applied to larger assemblies. In the case of the 8-inch diameter FRP pipe sections, it was necessary to increase the wall thickness at the ends of the pipe, from 1/4 inch to 3/4 inch, to provide sufficient room for the sealing ring and the pipe studs. The joint design was then modified to that shown in Figure 3-5. This design also proved to be unsuccessful, despite the elimination of the studs and the use of the larger cross section "C" rings. Further discussion of this design is presented in the "FRP/Metal Joint Development" section of this report.

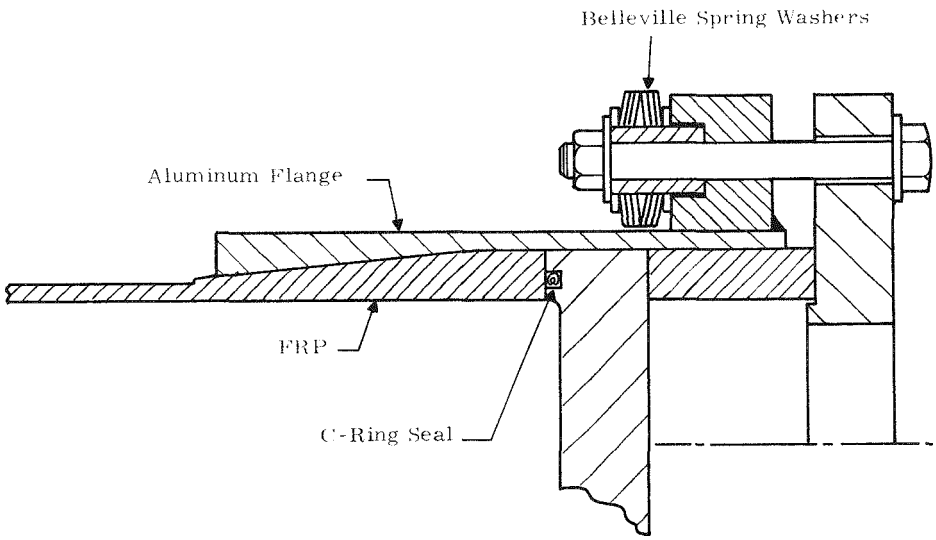

Figure 3-5. FRP Pipe/Metal Flange Joint Using A Tapered Sleeve

FRP pipe spools that were manufactured with heavy-wall end sections, as required by these early FRP/metal joint designs, developed cylindrical cracks in the heavy-wall region during low-temperature testing. These cracks were attributed to differential thermal contraction between the inner layer of circumferentially-wound glass, and the adjacent layer of helically-wound glass. Spools were then manufactured in which the helically-wound layers were more uniformly distributed in both the thin-wall and thick-wall sections of the FRP pipe. This construction is described in the Fourth Quarterly Report, pages 11-13. These and other manufacturing improvements were made with a resulting increase in the glass content of the spools (from 52 to 72% by weight). The winding pattern in the center section of the spool was changed as follows:

from:	o-xxxx-o-xxxx-o....o	(Spools F-1 to F-5)
to:	o-xx-o-xx-o....o	(Spools F-6 to F-12)
to:	o-xx-o-xx-o....xx	(Spools F-13, F-14)

The results of these and other manufacturing modifications are apparent from an examination of Figure 3-6, comparing samples of the first (Sample F-1) and modified (Sample F-6) winding patterns, following the series of pressure cycling and temperature cycling qualification tests described earlier.

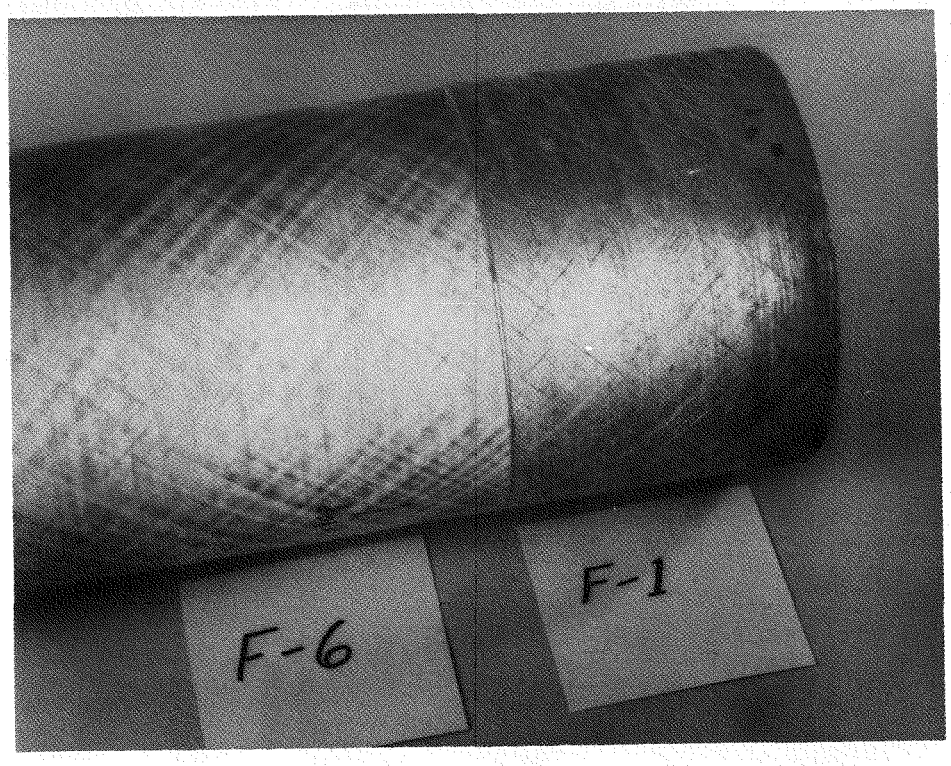

Figure 3-6. Comparison of First (F-1) and Modified (F-6) FRP Spools After Cryogenic Testing

No major additional FRP pipe development was undertaken following the successful tests of the winding pattern used in the modified FRP spool (Sample F-6). This spool successfully withstood 29 thermal cycles, from ambient temperature to 77 K and 84 pressure cycles to 30 atmospheres, at low temperature. On completion of this temperature and pressure cycling, the nitrogen permeation rate through the wall of the FRP spool was measured to be 3×10^{-10} std cm^3/cm^2-sec, based on the overall surface area of the spool. This value is well below the "acceptance" rate of 7×10^{-9} std cm^3/cm^2-sec, estimated to cause a 15 percent increase in the heat flux through the thermal insulation, after a period of 40 years. Permeation rates are discussed in more detail in the First and Fifth Quarterly Reports, pages 11 and 4 respectively.

Table 3-3 lists all FRP spools manufactured in the Phase III program with brief remarks describing the manufacturing features and the results of cryogenic testing. Of particular interest is the successful development of spools F-13 and F-14 described in further detail in the next portion of this report. Details of earlier spools are provided in Quarterly Reports.

HALF-SCALE FRP SPOOL TESTS

Two identical half-scale, 8-inch diameter, 10-foot long, FRP spools were manufactured near the close of the Phase III program to verify the reproducibility of the manufacturing process used for the F-6 spool. Each of these FRP spools, F-13 and F-14, was manufactured with a helical layer, rather than a hoop layer, on the outer surface. This was done in an attempt to remove a few shallow cracks that were observed along the inside and outside surfaces of the F-6 spool, following cryogenic testing. These cracks or craze marks were of a "cosmetic" nature in so far that they did not interfere with the successful completion of the full series of qualification tests.

A summary of the qualification test results for these two FRP spools, F-13 and F-14, together with the test results for spool F-6 are presented in Table 3-4. It should be noted that spools F-13 and F-14 also included identical adhesive bonded FRP/aluminum flange joints, whereas testing of the F-6 spool had been conducted by epoxy-bonding an aluminum cap over the ends of a short section of the spool. The F-6 FRP spool is shown in Figure 3-7, following the complete series of qualification tests.

Spool F-13 is shown before assembly and after testing in Figures 3-8 and 3-9, respectively. Spool F-14 is shown in Figure 3-2, following the complete series of cryogenic qualification tests.

Table 3-3

SUMMARY OF FRP SPOOL RESULTS

Spool Number	Remarks	Results
F-1	Commercial manufacture, built-up ends	Extensive cracking throughout
F-2	Commercial manufacture, built-up ends	Room temperature pressure cycling OK, ID surface shows light cracks
F-4*	Commercial manufacture, built-up ends	Delaminated at built-up ends, not tested
S-1	Utilize sections of F-3, F-5, uses four joints	Passed thermal and pressure cycling. Unable to test permeation due to leaks at seal rings on built-up ends
F-6	Modified winding pattern, tested straight section with adhesive bonded caps.	Passed all pressure cycling, thermal cycling, and permeation tests
F-7	Same pattern as F-6	Built-up ends cracked on cooldown
F-8	Same pattern as F-6 with high-yield glass	Tested with tapered demountable joint. Failed permeation test
F-10**	Same as F-8	Delamination at built-up end, not tested
F-12	Same as F-8	Delamination at built-up end, not tested
F-13	Straight spool, helical winding on OD	Passed all qualification tests
F-14	Straight spool, helical winding on OD. Veil on half of OD	Passed all qualification tests

*Note: F-3 and F-5 are similar to F-1.
**Note: F-9 and F-11 are oversize for use as couplings.

Table 3-4

SUMMARY OF QUALIFICATION TESTS
OF FINAL FRP SPOOLS

FRP Spool	Number of Thermal Cycles	Number of Pressure Cycles	Permeation Rate (std cm^3/cm^2-sec)
F-6	29	84	3.0×10^{-10}
F-13 FRP pipe*	32	61	1.4×10^{-10}
adhesive joints	20	61	
F-14	20	51	5.9×10^{-9}

*This FRP pipe received additional thermal cycling as part of the testing of epoxy bonded joints that were later remanufactured using urethane adhesive TU-902.

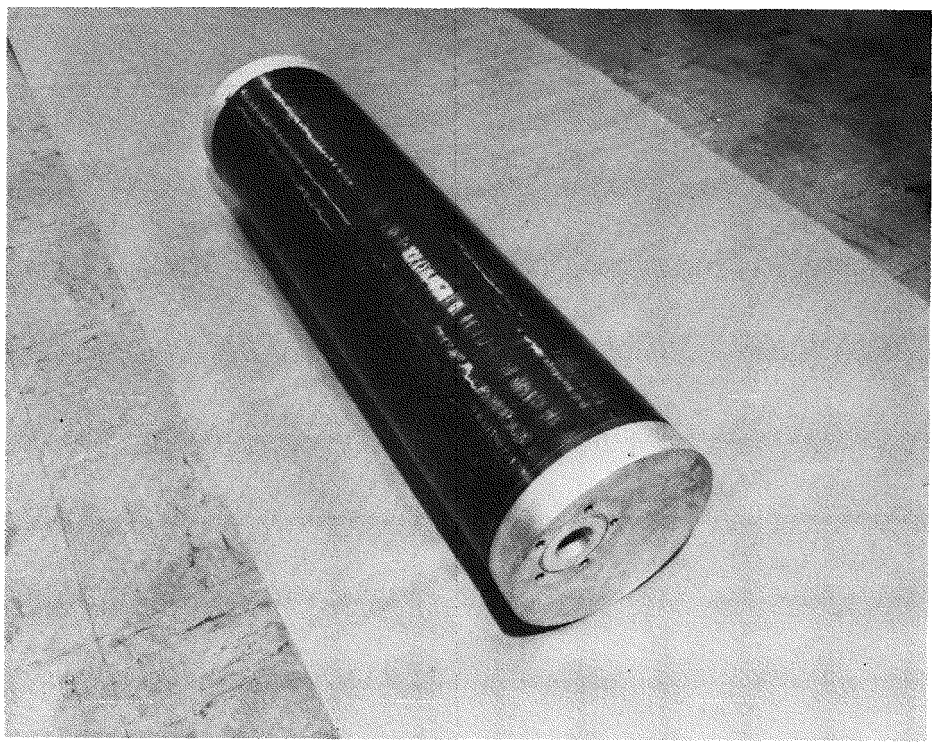

Figure 3-7. Section of FRP Spool (F-6) Following Qualification Tests

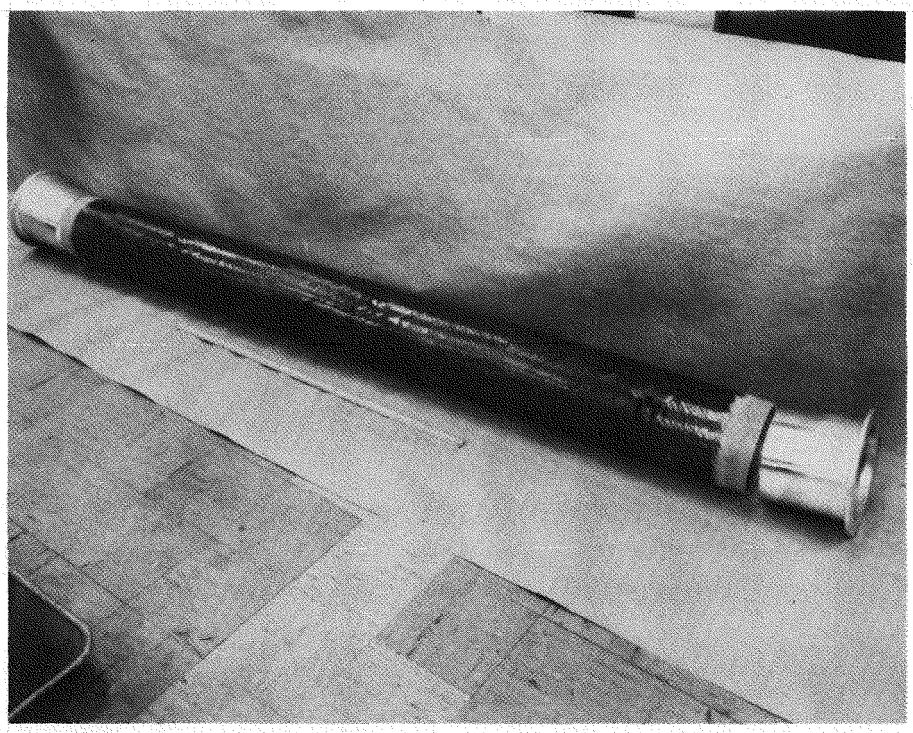

Figure 3-8. FRP Spool (F-13) Prior to Adhesive Bonding of Metal Flanges

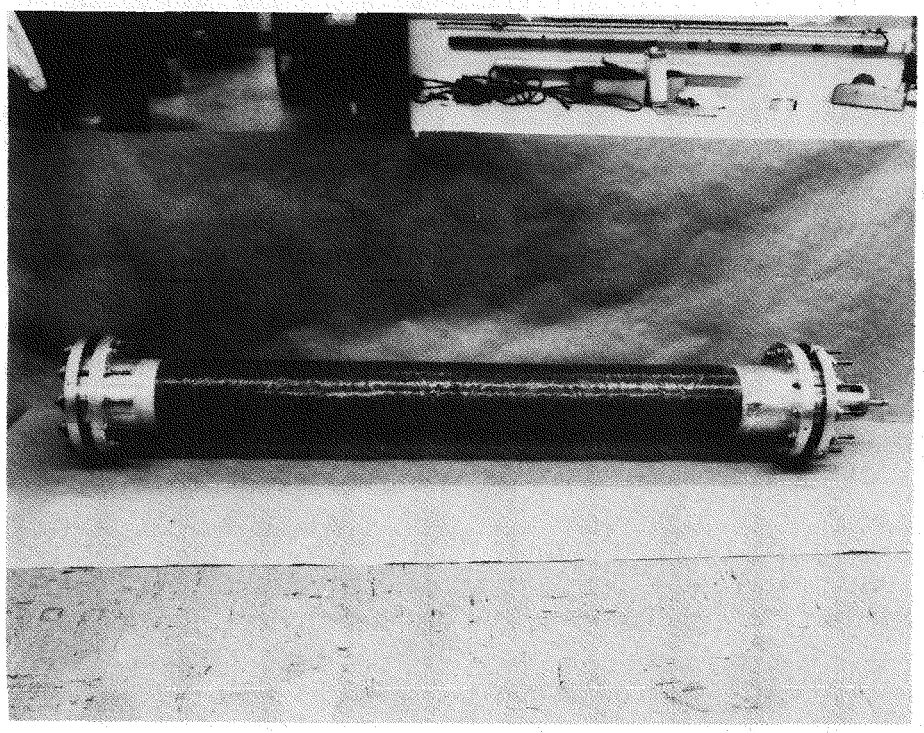

Figure 3-9. FRP Spool (F-13) Following Qualification Tests

In a further attempt to strengthen the outer surface of the FRP pipe, a glass veil (surfacing mat)* was applied to the wet resin of spool F-14, immediately after filament winding was completed. This veil was already being applied on the inner surface of the FRP pipe as part of the standard manufacturing procedure.

To evaluate the effectiveness of the mat, only one-half of the outer surface of spool F-14 was covered. The difference in surface appearance due to the mat is visible in Figure 3-2. The left half of the pipe has the mat applied in this photograph. Examination of spool F-14 following completion of cryogenic testing indicated that this veil did not prevent formation of surface crazing at some locations. This may be attributed to the resin-rich surface beneath wrinkles that developed in the veil as it was applied.

The permeation rate for spool F-14 was found to have changed from 3×10^{-10} to 5.9×10^{-9} std cm^3/cm^2-sec. The final permeation rate, measured at the completion of all thermal cycling tests, remained below the desired limit of 7×10^{-9} std cm^3/cm^2-sec.

Photographs of spool F-14 after successful completion of all testing are shown in Figures 3-10 (a), (b) and (c). Dye penetrant was applied to portions of the outer surface of the FRP pipe to make superficial craze marks more visible. From Figures 3-10 (a) and (b), it may be seen that the craze marks appear only on those surfaces that were covered with the glass veil. Surfaces which were not covered (Figure 3-10(c)), show no evidence of craze marks.

FRP PRESSURE PIPE MANUFACTURE

During the Phase III program, a total of 14 FRP pipe spools were manufactured for cryogenic testing. A few additional samples were rejected as a result of improper epoxy curing or the presence of delaminated areas. All 8-inch diameter spools were manufactured at the Pittsfield, Massachusetts, General Electric Plant (Insulation Systems Laboratory Operation). Figure 3-11 shows the manufacture of a 10-foot spool as glass roving is being fed to a rotating mandrel during filament winding. A McClean-Anderson filament winding machine was used for spool manufacture.

Initially, all spools were manufactured with 3/4-inch thick built-up end sections as shown in Figure 3-12. The heavy walled section was required for the particular FRP/metal joint design then under investigation.

*Owens-Corning Fiberglas Corporation, type M-514, finish #236, 0.010-inch thick

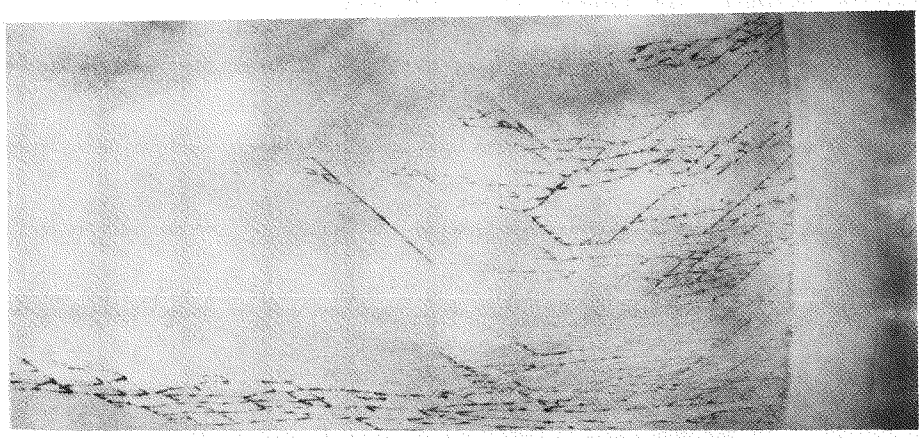

a) Crazing at the Joint, Where Surface Mat Applied

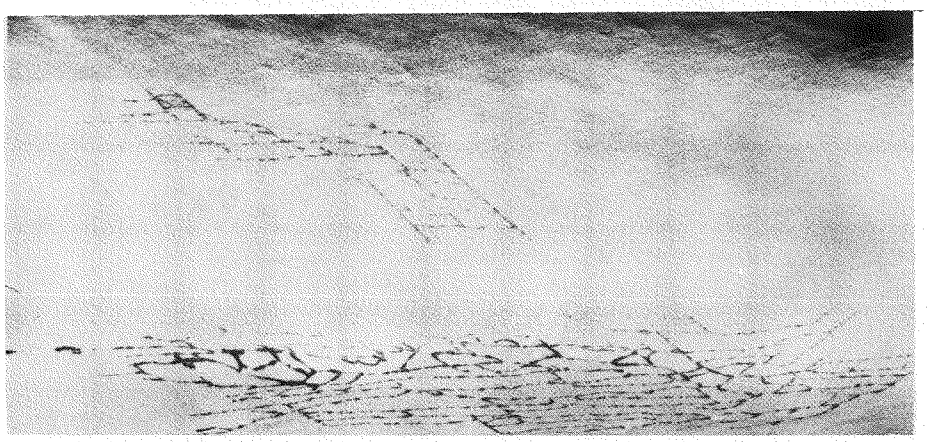

b) Crazing in the Straight Section, Where Surface Mat Applied

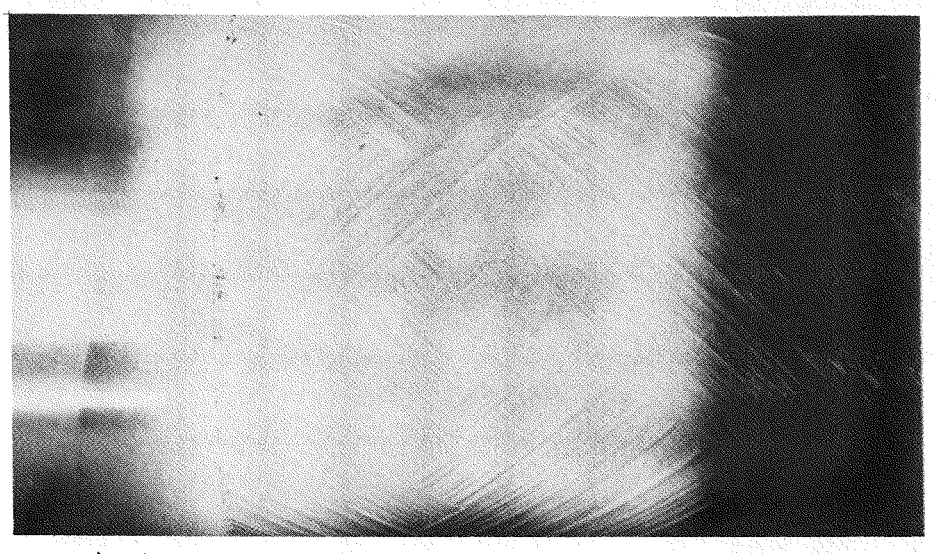

c) At the Joint, Where No Surface Mat Applied

Figure 3-10. FRP Spool (F-14) Following Qualification Tests

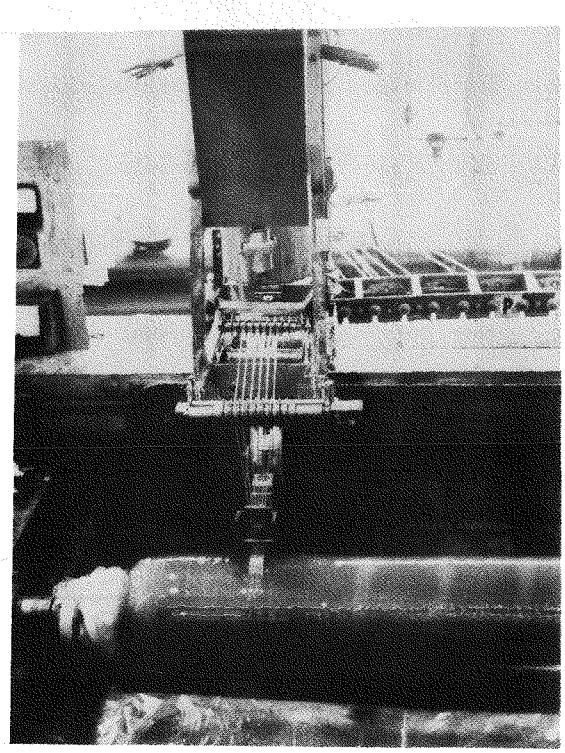

(a) Hoop Winding

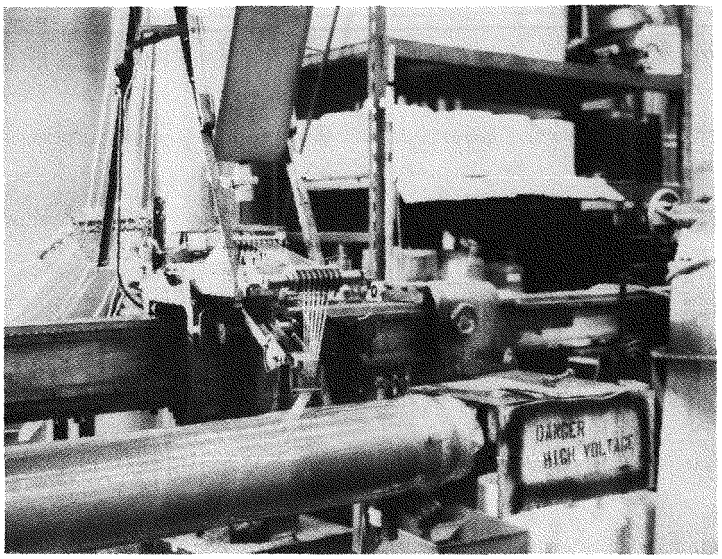

(b) Helical Winding

Figure 3-11. FRP Spool, Filament Winding Operation

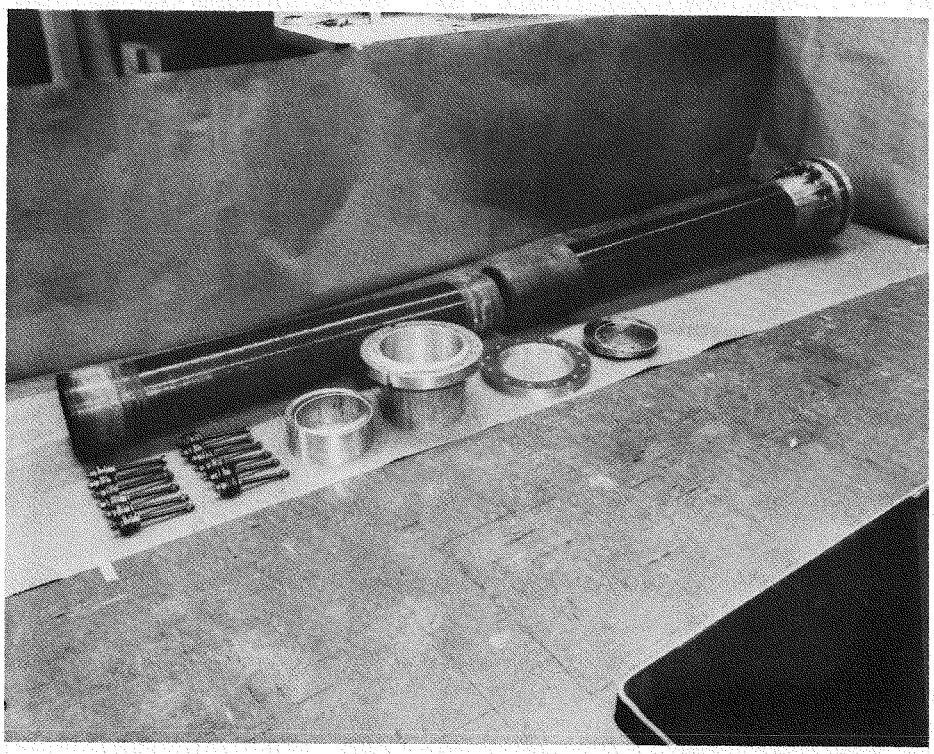

Figure 3-12. FRP Spool (F-8) With Built-up Ends

Two types of delamination were observed during the manufacture of the first spools, which necessitated modification of the joint design. The two types of delamination were:

- Planar delamination. This was observed in the 3/4-inch-thick built-up section of the spool. The planar delamination generally occurs in thick walled cylinders when the curing rate is too rapid, or when the outer portion of the tube gels while the inside remains ungelled. The delamination was prevented on subsequent samples by reducing the heat applied to the outside surface of the spool during gel.

- Crosshatch delamination. This delamination occurred in the portion of the spool where the conical insert to form the bell section joined the mandrel. At this point the shape of the winding changes from a cylinder to a cone. The principal cause of this delamination appeared to be axial shrinkage during polymerization. In addition, expansion of the gas in the annular space between the cylindrical mandrel and the conical insert, as well as motion of the core retainer relative to the mandrel, aggravated the problem.

Although the cross-hatch delamination could probably have been prevented by experimenting with winding, curing and stripping techniques, it

was decided to change the joint design to permit the use of pipe sections having a uniform wall-thickness. In turn, this permits a constant winding pattern to be used over the complete pipe length, during manufacture, effectively reducing the cost of the manufacturing operation. Subsequent testing showed that this modification successfully overcame the delamination problem.

FRP PRESSURE PIPE TESTING

Facilities were constructed by General Electric to conduct cryogenic testing of 10-foot long, half-scale pipe sections. An outdoor facility shown in Figure 3-13 was used to conduct thermal and high-pressure cycling tests of the samples. Measurement for possible permeation of liquid nitrogen through the FRP pipe wall or for leakage at pipe joints was measured in a second facility shown schematically in Figure 3-14. Detailed descriptions of test procedures and facilities are provided in the First and Second Quarterly Reports, pages 12-16 and pages 8-12, respectively.

The first 8-inch diameter test spool was instrumented with strain gauges and temperature sensors to monitor its behavior during thermal cycling and pressure testing. A photograph taken when this spool (F-1) was partially

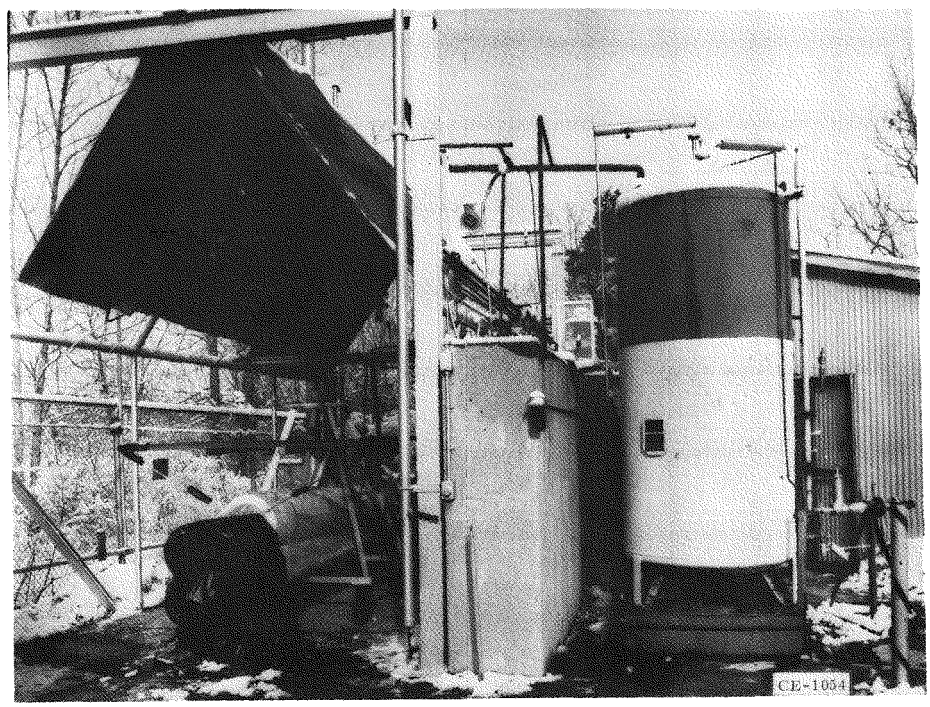

Figure 3-13. Low-temperature, Pressure and Thermal Cycling Test Facility

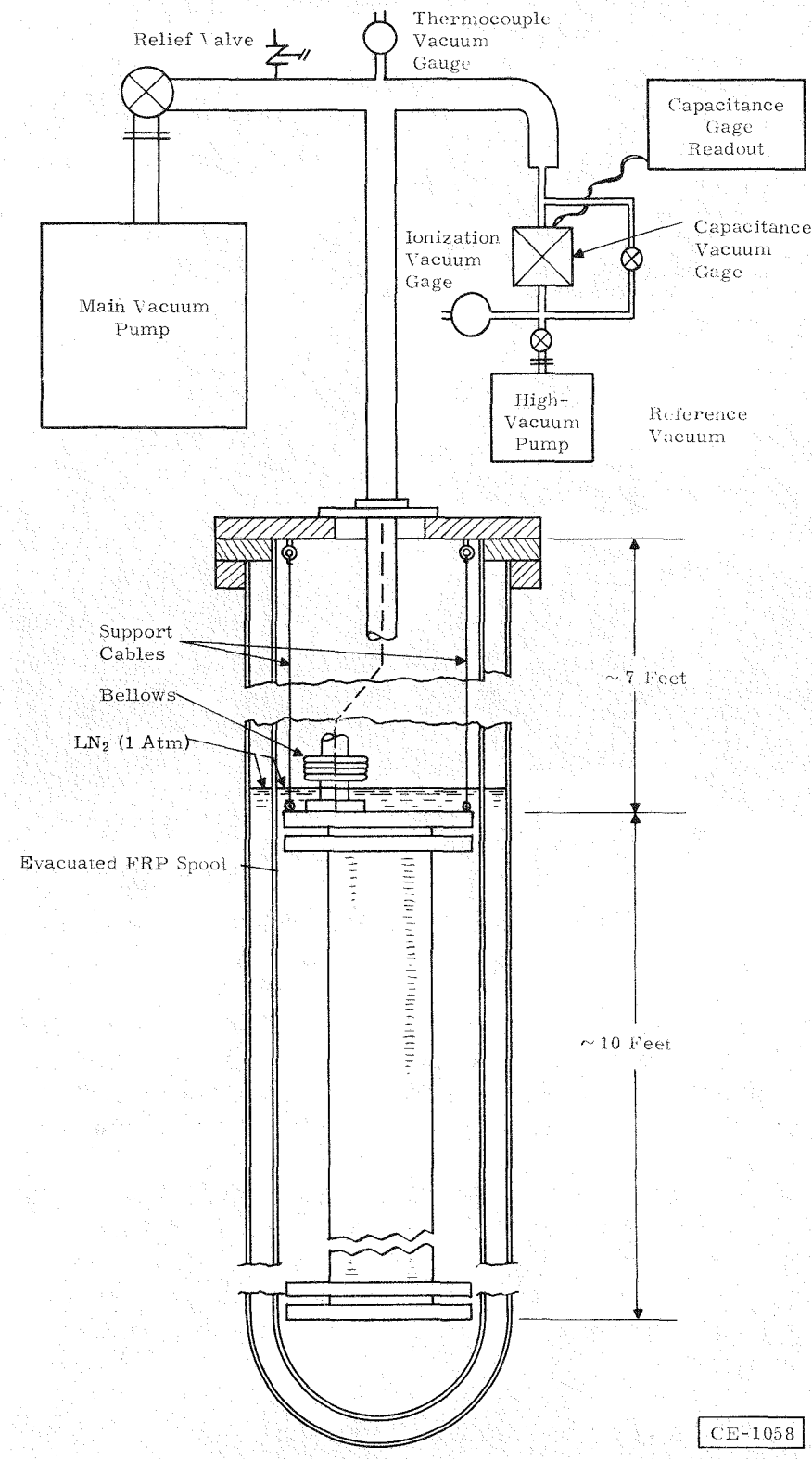

Figure 3-14. Schematic of the Low Temperature, Permeation Test Facility

assembled on a movable test stand is shown in Figure 3-15. Details regarding instrumentation applied to this spool are given in the Third Quarterly Report, pages 8-10. Axial and circumferential strain measurements obtained during tests of FRP spools F-1 and F-2 are described in the Fourth Quarterly Report, pages 5-11.

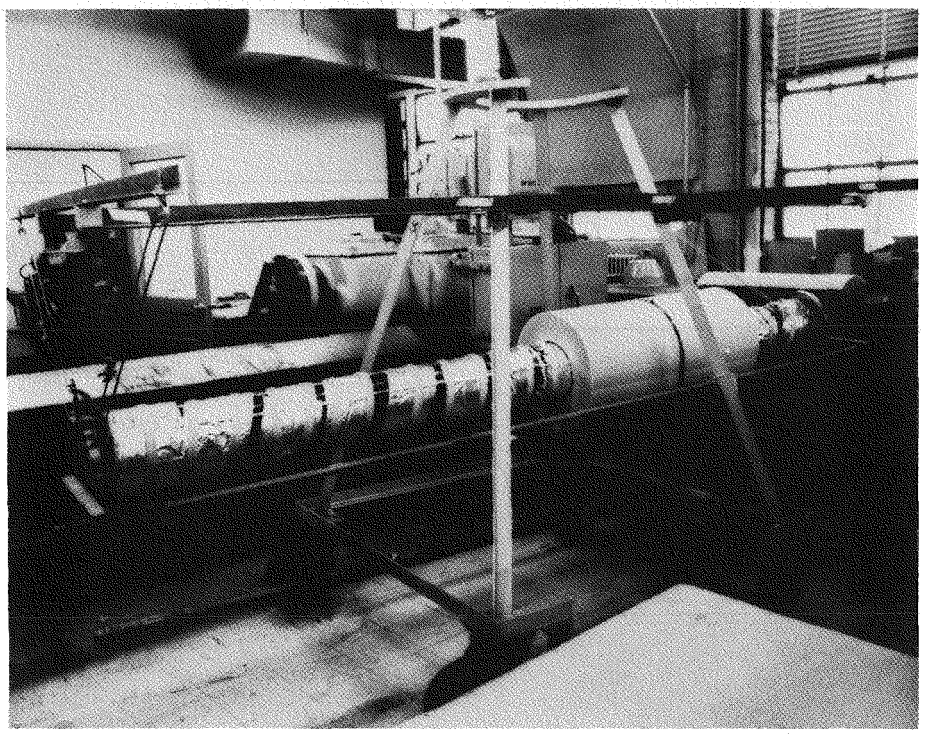

Figure 3-15. Instrumented Section of FRP Spool (F-1)

These measurements indicated that the residual strain, after the pressure and liquid nitrogen were removed from the pipe, continued to increase as the number of pressure cycles increased. This would have led to structural failure of the spool had testing continued (see Figure 3-16).

An analysis of pipe wall stresses using a General Electric stress analysis computer program, was then conducted to evaluate possible modifications that would improve winding patterns. This program computes stresses, strains, and displacements in anisotropic materials and permits the calculation of stresses and strains for loads imposed by thermal gradients, pressures, and body forces.

The program was used to compare pipe-wall stresses caused by cooldown, as well as those caused by pressurization, for a number of different winding patterns with helical and circumferentially wound filaments. This analysis aided the design of samples F-6 and others following it. Predicted

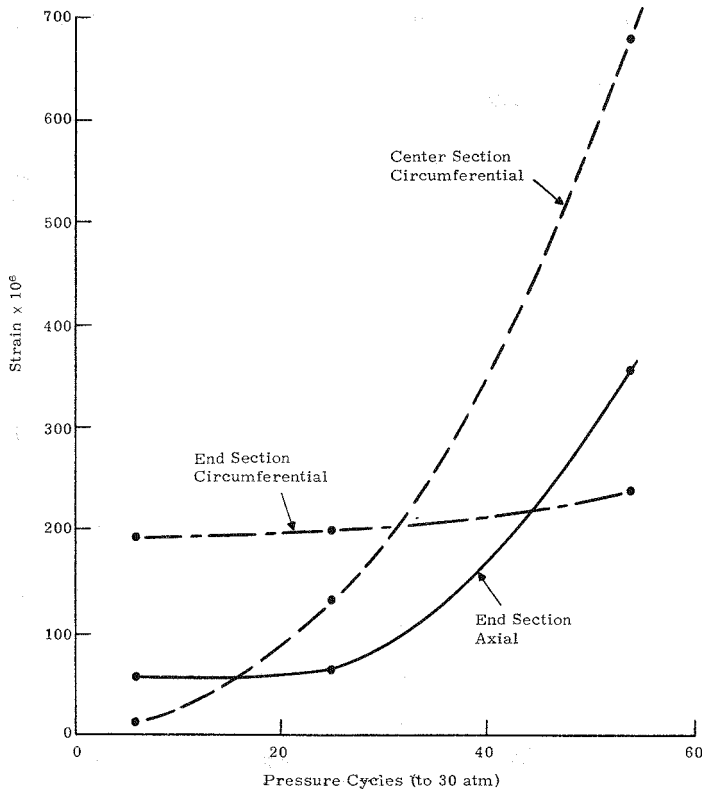

Figure 3-16. Residual Strain Versus Number of Pressure Cycles for FRP Spool (F-1)

stresses as a function of the filament winding pattern are presented in Table 3-5.

Spool F-6 and those manufactured after it did not develop the structural defects observed in the first few samples.

FRP/FRP JOINT DEVELOPMENT

Glass-epoxy piping can be made in lengths limited only by the deflection that can be tolerated in the mandrel on which the glass filaments are wound. Although half-scale spools were manufactured in lengths of 10 feet, it is expected that full-diameter spools will be made 40 feet long.

The manufacture of spools with a bell and spigot joint was attempted early in the program. The bell end of the spool was formed by a sleeve placed over a cylindrical mandrel. The winding pattern was extended over the sleeve to produce a nearly uniform wall thickness throughout the pipe length. However, as noted in the previous section of this report, this concept resulted in delaminations in the bell area of the pipe.

Table 3-5

COMPUTED STRESSES IN 8-INCH SPOOL

(a) After Cooldown and Prior to Pressurization

Section	Radial Stress (psi)	Axial Stress (psi)	Hoop Stress (psi)	Maximum Shear (psi)
F-1 Center Section (O-xxxx-O-xxxx-O)				
Near inner surface	0	2430	1340	1210
Center of pipe wall	10	-1360	-470	690
Near outer surface	0	2360	40	1180
F-1 End Section (OO-xx-OOOO-xx-OO)				
Near inner surface	0	1230	2130	610
Center of pipe wall	80	-7740	-2090	3910
Near outer surface	0	870	-1550	430
All Helical Winding Center Section (xxxxxxxxxxx)				
Near inner surface	0	110	430	50
Center of pipe wall	10	-10	-20	10
Near outer surface	0	-110	-390	50

(b) After Cooldown, Pressurized to 30 Atmospheres

Section	Radial Stress (psi)	Axial Stress (psi)	Hoop Stress (psi)	Maximum Shear (psi)
F-1 Center Section (O-xxxx-O-xxxx-O)*				
Near inner surface	0	3290	8750	1840
Center of pipe wall	-170	3380	5100	1780
Near outer surface	-20	3320	6770	1670
All Helical Winding Center Section (xxxxxxxxxxx)				
Near inner surface	-410	3500	6740	1950
Center of pipe wall	-180	3350	6020	1770
Near outer surface	-10	3240	5470	1630
F-6 Center Section (O-xx-O-xx-O-xx-O)				
Near inner surface	0	3490	9790	1950
Center of pipe wall	-220	4470	6200	2350
Near outer surface	-10	3540	7980	1780
F-7 End Section (OOOOOOOOO-xx-OOOOO-xx-OOOOO-xx-OOOOO)				
Near inner surface	-380	2360	4650	1370
Center of pipe wall	-130	-1910	600	890
Near outer surface	-310	2070	400	1040

To overcome this defect, a sleeve coupling shown in Figure 3-17 was subsequently developed for connecting straight FRP pipe sections using a modified structural epoxy adhesive, #2216 B/A, manufactured by the 3M Company. The coupling contains the identical winding pattern (o-xx-o-xx...) as the FRP pipe, except that more layers are applied to obtain a 1/2-inch wall thickness at the coupling.

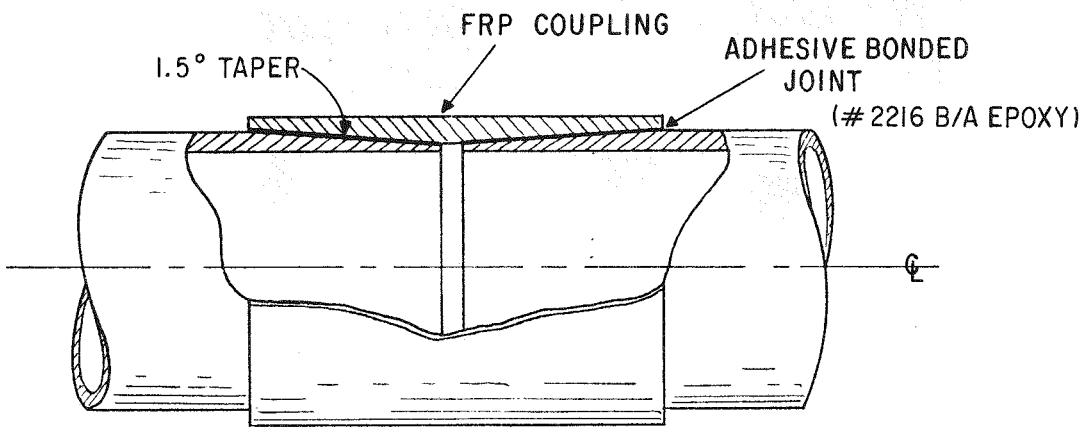

Figure 3-17. FRP Pipe/FRP Pipe, Adhesive Bonded Joint Concept

Three such couplings were assembled and tested at cryogenic temperature and were shown to meet all cryogenic test requirements. One coupling, shown in Figure 3-3, was sealed with aluminum caps and was found to meet permeation requirements while immersed in liquid nitrogen at atmospheric pressure. The permeation rate was measured to be 3.0×10^{-10} std cm^3/cm^2-sec, after the assembled coupling had completed all cryogenic thermal cycling and pressure testing. A representative joint was also subjected to an axial load of 55,000 pounds at liquid nitrogen temperature, with no apparent damage. (See the section on FRP/Metal Joint Development.) Figure 3-18 shows one such coupling, prior to adhesive bonding to straight lengths of 8-inch FRP pipe.

Additional details of the FRP/FRP joint are provided in the Third and Fourth Quarterly Reports, page 6, and pages 15-16, respectively.

The majority of the FRP pressure pipe joints in a cryogenic cable system will use adhesively bonded FRP couplings to join straight lengths of FRP pressure pipe. Each length will contain a factory preassembled coupling at one end and a mating tapered end at the other. It is expected that these pipes will be shipped to the installation site with the foam insulation and vapor tight jacket already assembled around the pressure pipe. One adhesive bonded joint will have to be made at the installation site for each length of pressure pipe. The joining concept is shown in Figure 3-19.

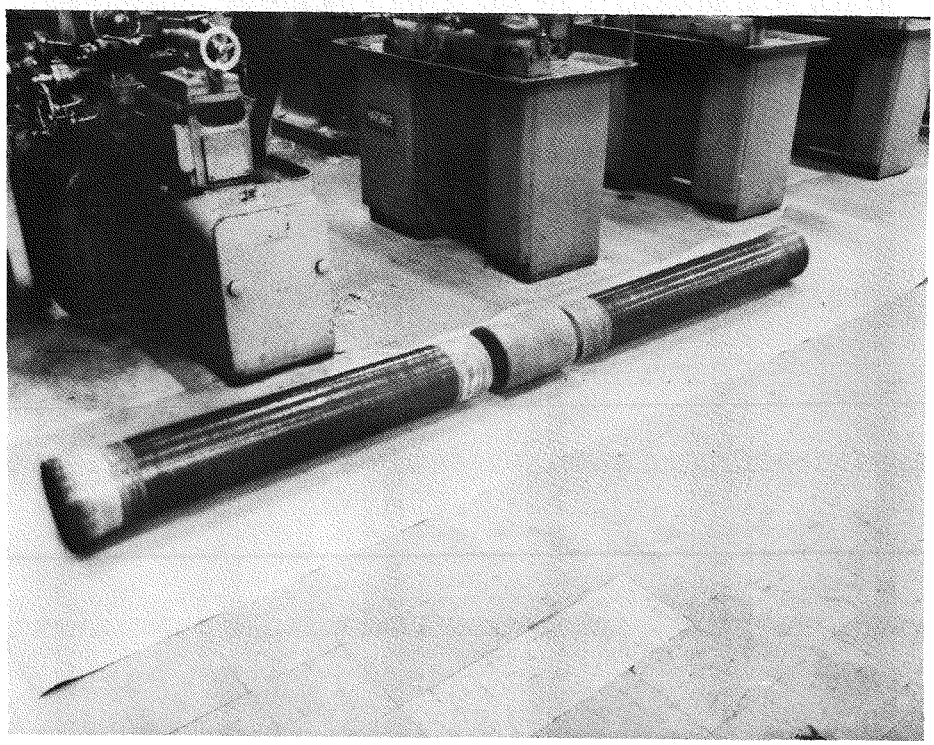

Figure 3-18. FRP Coupling Prior to Adhesive Bonding to FRP Spool

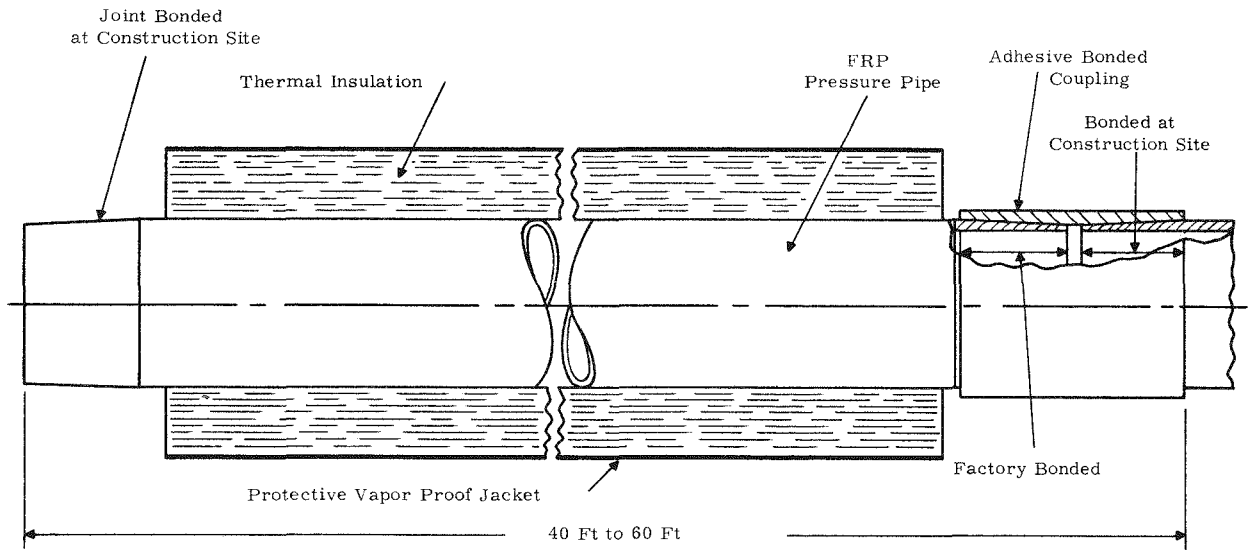

Figure 3-19. Schematic of Spool Assembly With Coupling Attached

Discussions have been held with 3M Company representatives regarding the recommended procedure for using Scotch-Weld® structural adhesive #2216 B/A in making these field joints. This adhesive is a two-part epoxy system that would be supplied to the construction site in "premeasured" cartridges. A single cartridge contains the proper amount of adhesive and curing agent to complete one joint. Cartridges are designed for simple puncturing of internal compartments and mixing immediately before field assembly. A wide range of curing time/temperature options is available. Curing can be achieved in one hour at a temperature of 150 F.

FRP/METAL JOINT DEVELOPMENT

Cryogenic cable installations will include expansion joints, cable splice and splitter boxes that are likely to be fabricated from stainless steel. These metal components will be designed to use standard flanges for bolted connections to the FRP pressure pipe. This application has required the development of an FRP/metal joint to enable metal flange assemblies to be attached to the FRP pipe sections. Locations for this type of joint are illustrated schematically in Figure 3-20. It is expected that many more FRP/FRP joints will be required in a cable installation than FRP/metal joints.

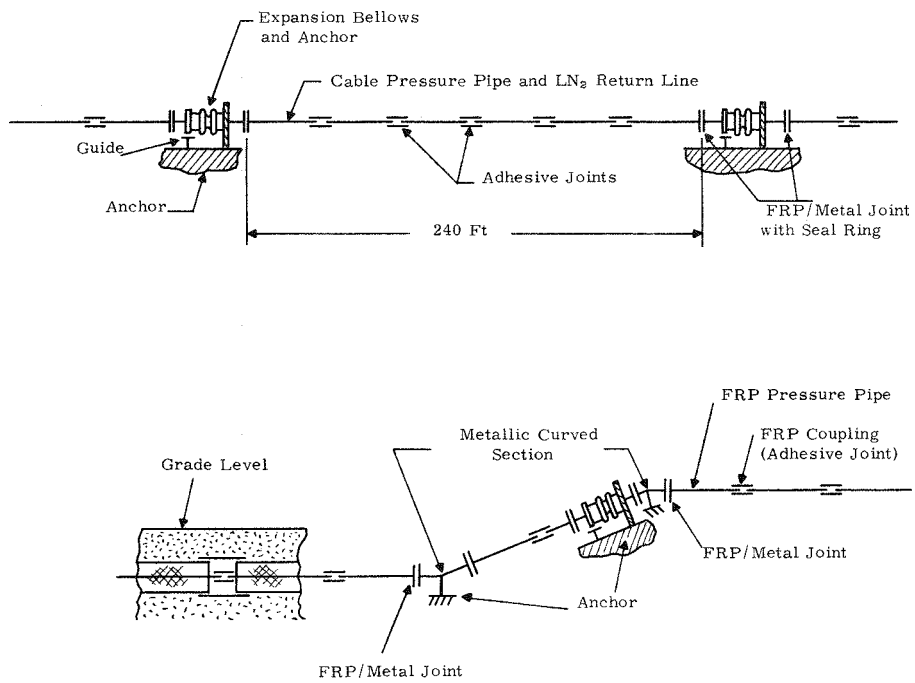

Figure 3-20. Types of Joint Required in a Typical Installation

® Registered trademark of 3M Company.

The use of metal flange joints that are factory mounted will permit rapid assembly during installation and provide high reliability, simple maintenance and fast repair. Commercial sealing rings have been shown to seal the metallic flange faces at 77 K. Pipe spools containing the FRP/metal joint will be supplied to the construction site with the flange assembly already attached, as illustrated in Figure 3-21.

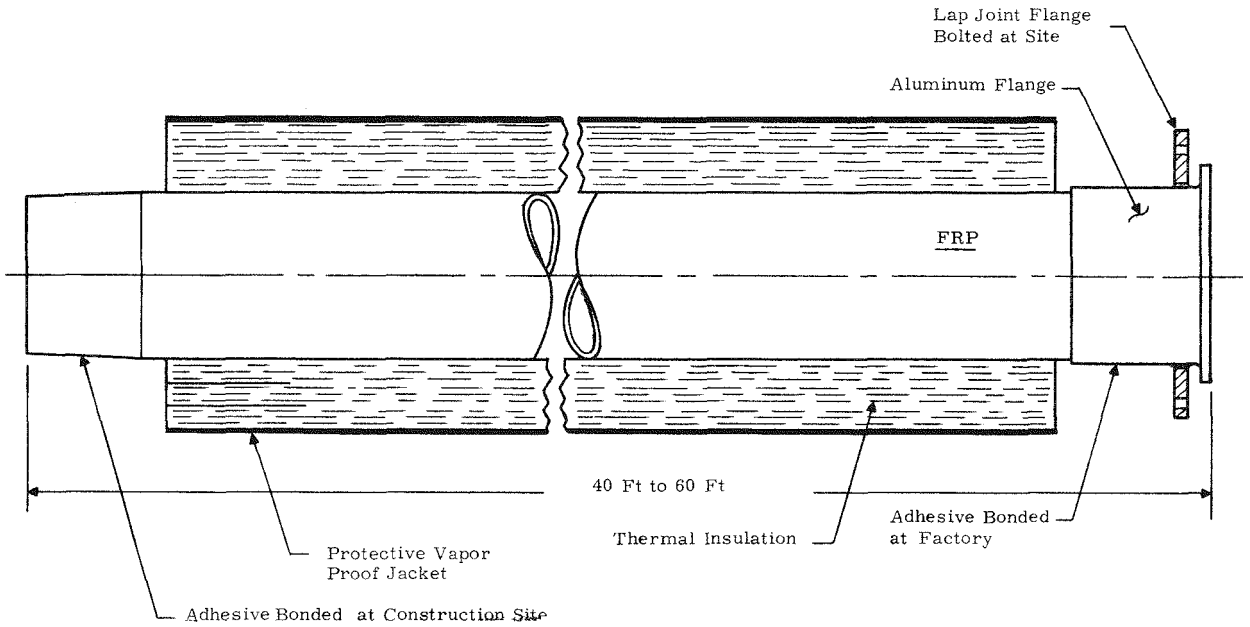

Figure 3-21. Schematic Of Spool Assembly With Metal Flange Attached

Approximately ten commercial sealing rings of two types have been demonstrated to meet the envelope flange joint requirements. They have been supplied by the Creavey Seal Company, Olyphant, Pennsylvania and by Pressure Science, Inc., Beltsville, Maryland. Additional information on sealing rings is contained in the Sixth Quarterly Report, pages 7 and 9.

Several different approaches were pursued in the development of the FRP/metal joint during the Phase III program. A polyurethane adhesive bonded FRP-pipe-to-aluminum joint was shown to meet both the structural and leak rate requirements. Other concepts failed to meet the full range of conditions imposed by thermal and pressure cycling with liquid nitrogen.

Results of FRP/metal development efforts are summarized in Tables 3-6 and 3-7. Detailed discussion of progress during development of the FRP/metal joints is provided in each of the Quarterly Reports.

Table 3-6

SUMMARY OF FRP PIPE/METAL FLANGE JOINT TESTS

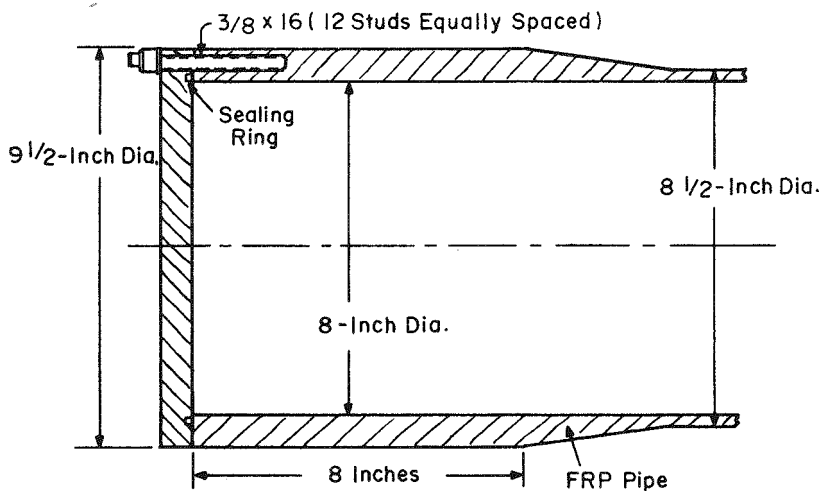

Structural

Adequate for pressure cycling

Sealing

Delamination in FRP near studs caused seal leakage at 77°K

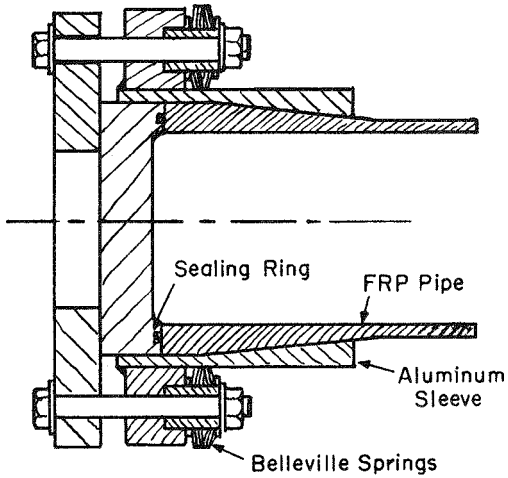

Structural

Not evaluated for pressure cycling with liquid nitrogen

Sealing

Delamination of FRP near seal rings caused leakage at seals

Table 3-7

SUMMARY OF ADHESIVE BONDED FRP/METAL JOINT TESTS

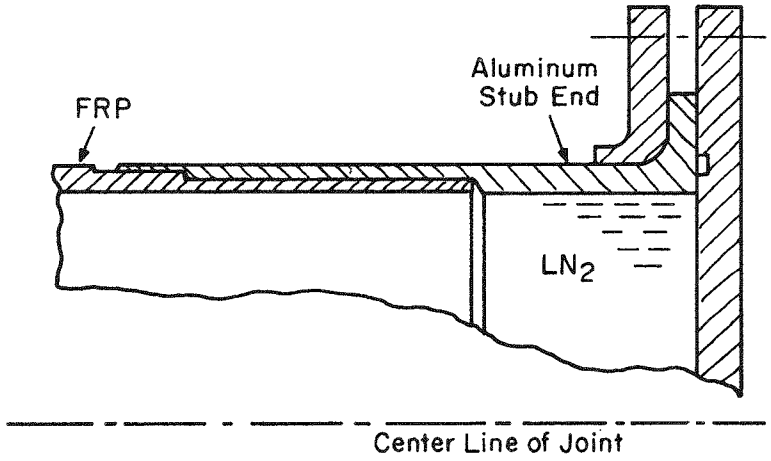

Structural	Sealing
Adequate for thermal cycling and design pressures Inadequate for proof pressures	Met permeation requirements following 20 thermal cycles

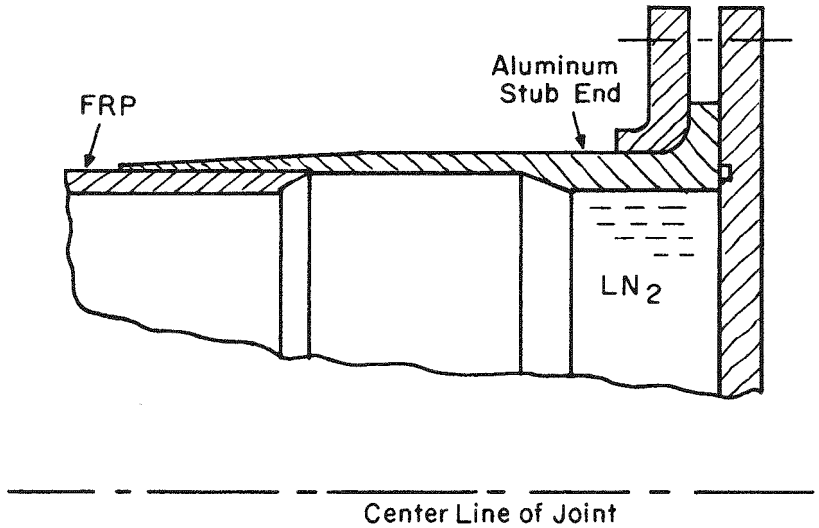

Structural	Sealing
Met all thermal and pressure cycling requirements Some shallow surface craze marks noted on inner and outer surfaces following thermal cycling	Met permeation requirements at completion of liquid nitrogen cycling tests

The polyurethane bonded FRP/metal joint is discussed in more detail in this report since its development took place during the final quarter of this program.

POLYURETHANE BONDED FRP/METAL JOINT

The Seventh Quarterly Report, pages 8-22, describes an investigation conducted with 1-inch wide FRP/aluminum lap-shear samples bonded with a number of epoxy and urethane adhesives. This investigation was undertaken to evaluate the effects of surface preparation techniques, glass mat and glass cloth reinforcement of bond lines, and lap lengths for nine different adhesives supplied by four manufacturers. The objective was to obtain higher strength joints at liquid nitrogen temperature than were obtained with the 2216 B/A epoxy adhesive used for the cylindrical joint, shown in Table 3-7.

As discussed in the Seventh Quarterly Report, three different urethane adhesives were found to have less strength than modified epoxy #3135/7111 supplied by the Crest Products Company of Santa Ana, California. The Crest epoxy adhesive was found to be stronger when reinforced with 0.010-inch thick glass surfacing mat, than the #2216 B/A adhesive used in the original FRP/aluminum bonded joint. The glass surfacing mat used, known as "Modiglass", is a product of Reichold Chemicals, Inc.

A single FRP/aluminum joint using the #3135 epoxy adhesive was then constructed, thermally cycled 20 times to 77 K, and tested to failure at 77 K, in a tensile test machine. The FRP pipe assembly was not pressurized during this test sequence. Failure occurred at the adhesive joint between the FRP and the aluminum at an axial tensile load of 25,400 pounds. This confirmed that strengths obtained with narrow lap-shear specimens could also be obtained with tubular joints. Joint design details are described in the Seventh Quarterly Report, pages 20, 21, 22. Figure 3-22 shows the bonded surfaces after failure. Small cracks in the FRP surface can be seen to extend in the hoop direction. The bond failure was of the desired cohesive nature and not an adhesive type.

This joint was then remanufactured to enable testing under internal proof pressures following thermal cycling from ambient temperature to 77 K. The joint was successfully pressurized to 30 atmospheres at 77 K after the first and tenth thermal cycle, but failed at an internal pressure of 30 atmospheres following the twentieth thermal cycle. As a result of this failure, it was apparent that this adhesive system was marginal for half-scale pipe, and therefore was not adequate for consideration for the full-scale joints that will be required in the future.

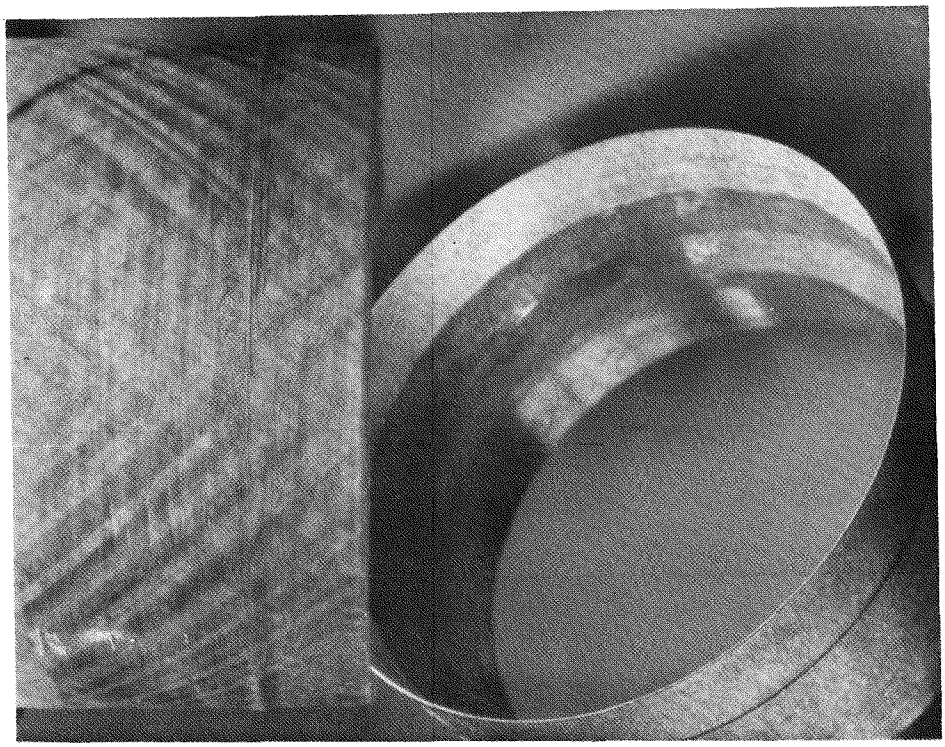

Figure 3-22. FRP Pipe/Metal Flange Joint Following Destructive Tests at 77 K (#3135 Adhesive With Glass Reinforcement)

ADDITIONAL INVESTIGATION OF URETHANE ADHESIVES

The marginal performance of the amine modified epoxy, #3135/7111, at proof pressure, led to the investigation of an additional urethane adhesive. FRP to aluminum lap-shear samples were prepared using urethane adhesive TU-902 supplied by the Amicon Corporation, Lexington, Massachusetts. Dimensions of the samples and test procedures are contained in the Seventh Quarterly Report, pages 10 to 13.

Samples prepared with this adhesive, also reinforced with glass surfacing mat, produced considerably higher failure loads at 77 K than any previously tested adhesive. As shown in Figure 3-23, TU-902 samples have strengths of the order of 2000 pounds per inch of width for lap lengths of 1 1/2 to 2 inches. Full diameter joints will require strengths of this magnitude to withstand axial tensile forces produced during pressure proof testing. Figure 3-24 shows urethane lap-shear samples after testing to failure in liquid nitrogen.

A single 8-inch diameter FRP/aluminum joint was then prepared using the TU-902 adhesive. This joint was successfully subjected to a complete series of thermal and pressure cycling tests with liquid nitrogen. The joint

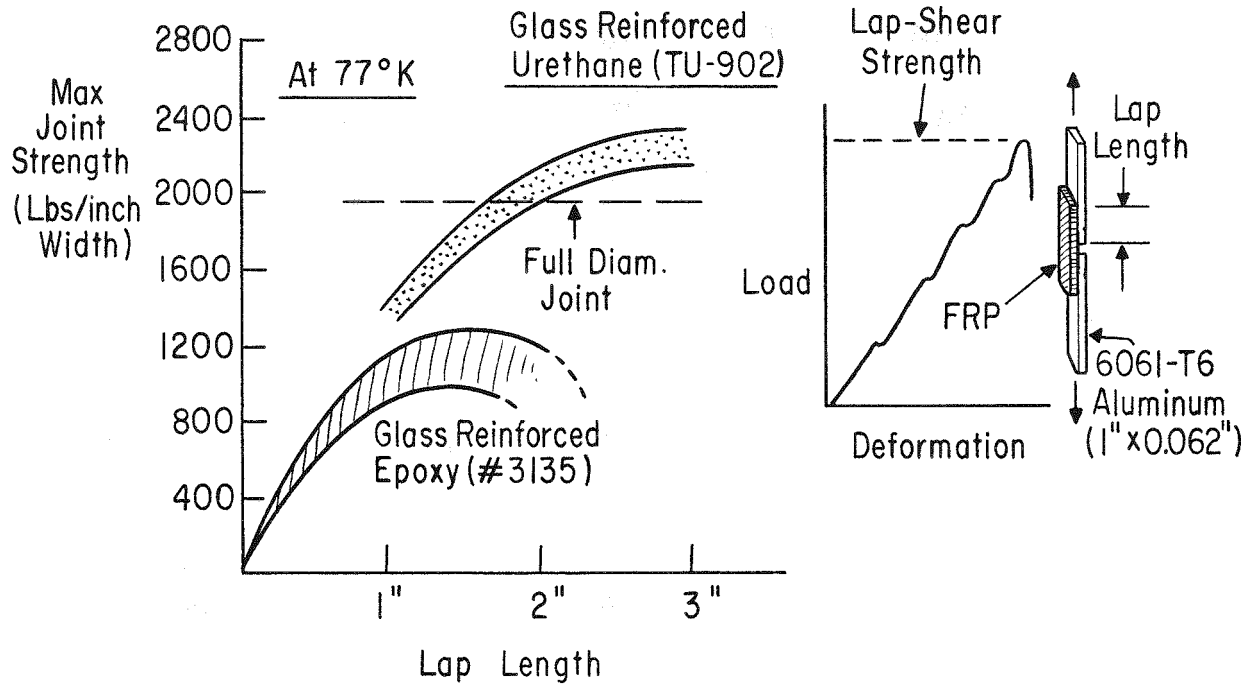

Figure 3-23. Lap Shear Strengths of FRP/Aluminum Lap Joint Samples at 77 K

is shown in Figure 3-25 after testing. The joint was then cooled to 77 K and tested to destruction in a tensile test machine, as shown in Figure 3-26. The urethane adhesive bond failed at an axial load of 55,000 pounds, equivalent to an internal pressure of 64 atmospheres. Figure 3-27 shows the cohesive bond failure surfaces after this destructive test.

A modified scarf joint, having an adhesive joint axial length of 1 1/2 inches was used for this successful joint. The design of this joint is shown in Figure 3-28.

Spools F-13 and F-14 were assembled using this identical urethane bonded joint at the end of each spool. All four of these joints passed the series of thermal and pressure cycling tests with liquid nitrogen. Further discussion of test results with these spools is contained in the "FRP Pipe Development" section of this report.

THERMAL INSULATION

Existing applications of foam thermal insulation to liquefied natural gas (LNG) pipelines were examined to determine whether this technology is also suitable for cryogenic cable application. The cryogenic cable application will involve temperatures lower than the 110 K reached in liquefied natural gas

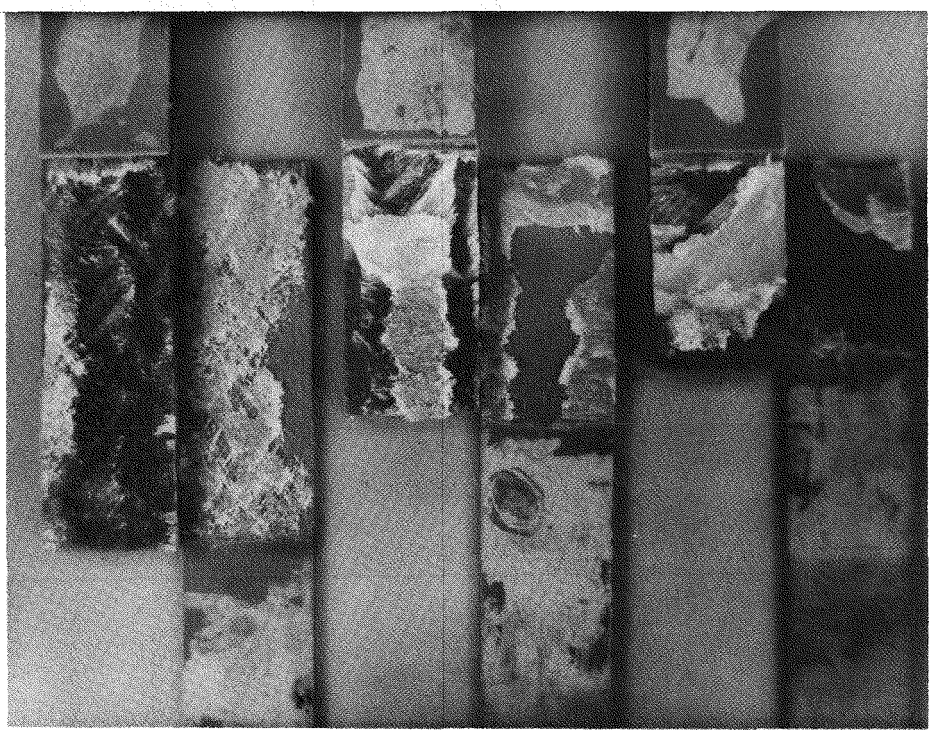

Figure 3-24. Lap Shear Samples With Glass Mat Reinforcement, After Failure at 77 K (TU 902 Urethane On FRP/Aluminum)

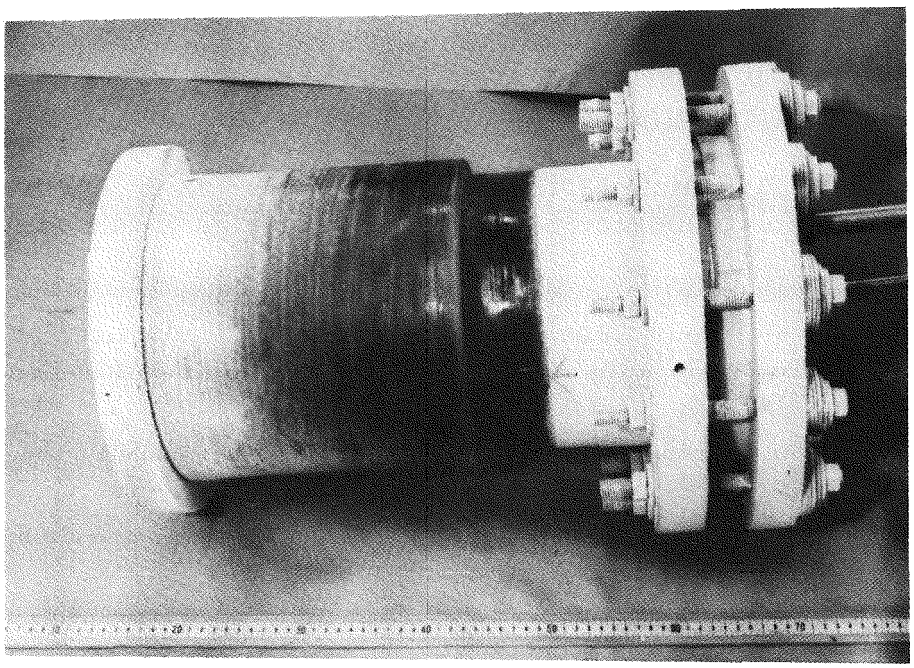

Figure 3-25. Sample FRP Pipe/Metal Flange Joint Bonded With Urethane Adhesive, After Qualification Tests

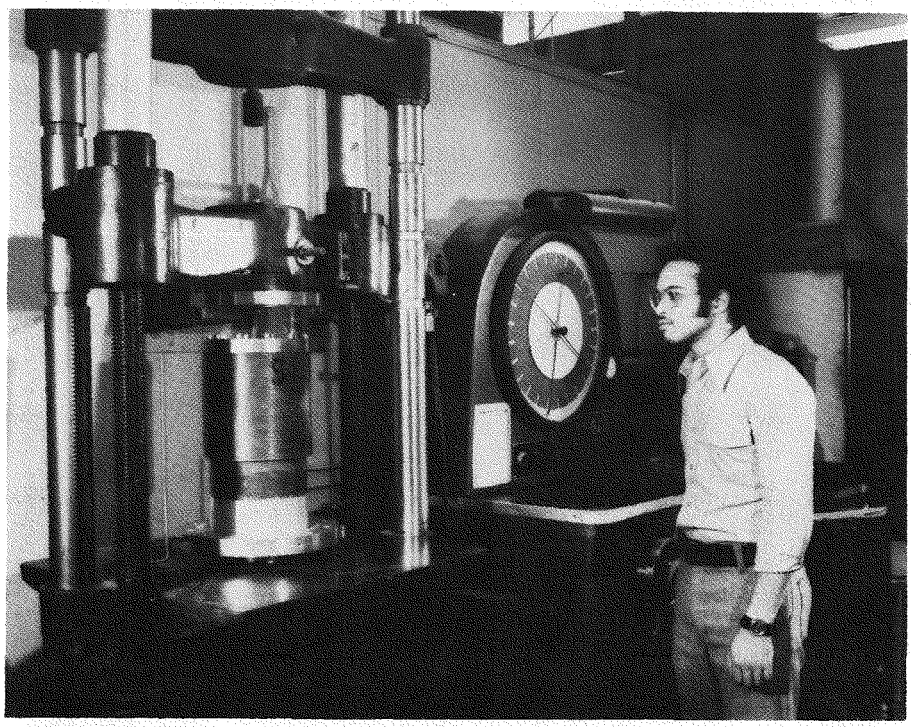

Figure 3-26. Tensile Testing of the FRP Pipe/Metal Flange Joint

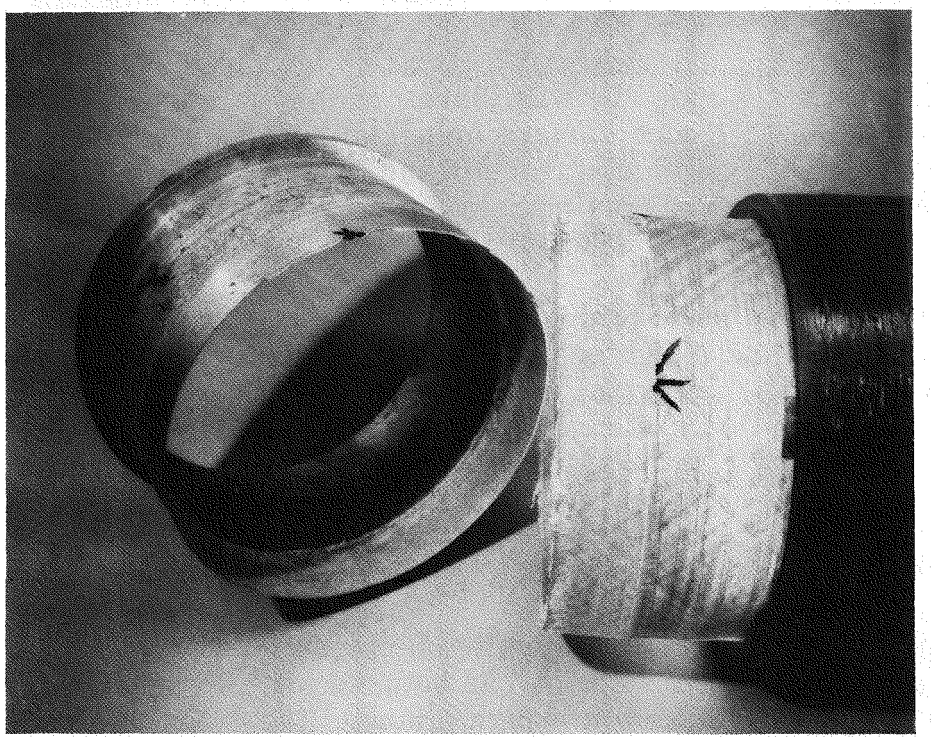

Figure 3-27. Cohesive Failure of FRP Pipe/Metal Flange Joint Using Urethane Adhesive, After Destructive Testing

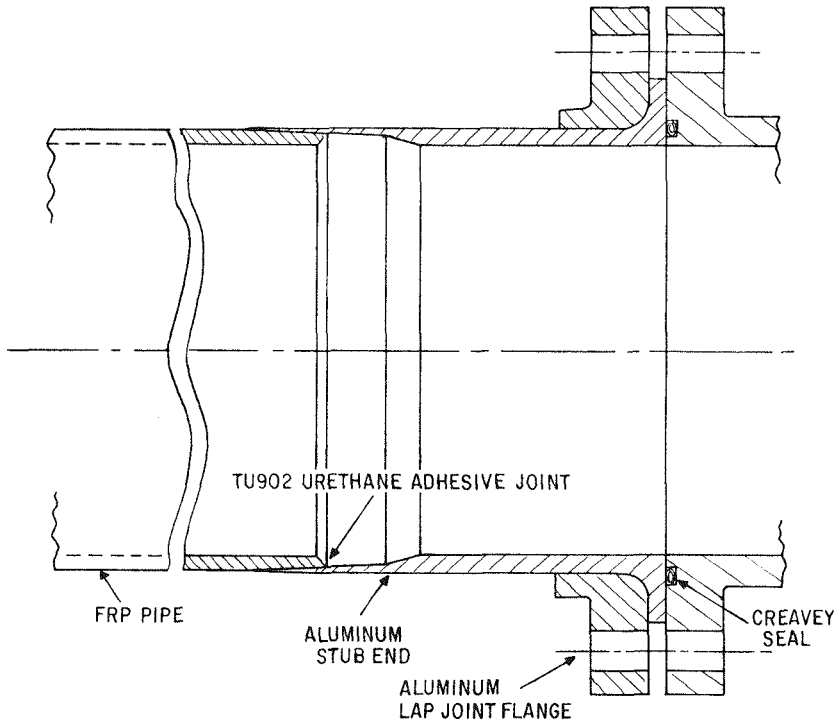

Figure 3-28. Schematic Of Modified FRP Pipe/Metal Flange, Adhesive Bonded Joint

piping and storage systems and will therefore tend to condense both oxygen and nitrogen at the FRP pipe surface unless an adequate vapor tight enclosure is provided at the outside surface of the foam insulation. A polyester glass jacket is used in LNG piping as a moisture vapor barrier and a protective cover for the foam insulation.

Discussions have been held with representatives of Cosmodyne, Torrance, California, and the Owens-Corning Fiberglas Corporation, Toledo, Ohio, manufacturers of thermal insulation for cryogenic piping systems. Cosmodyne has supplied urethane insulated piping for LNG plants that has provided satisfactory operation for several years. Cosmodyne has a plant in operation for spray application of foam to 18-inch and 24-inch diameter stainless steel piping. Figure 3-29 shows Cosmodyne insulated LNG piping installed at a ship loading terminal.

On the basis of information supplied by these manufacturers, it was concluded that this same insulation can be used for the cryogenic cable envelope and the liquid nitrogen return piping. The Owens-Corning insulation system, known as the LTS (low temperature service) type differs from that proposed by Cosmodyne in that it is designed for installation at the construction site and consists of preformed inner layers of high-density

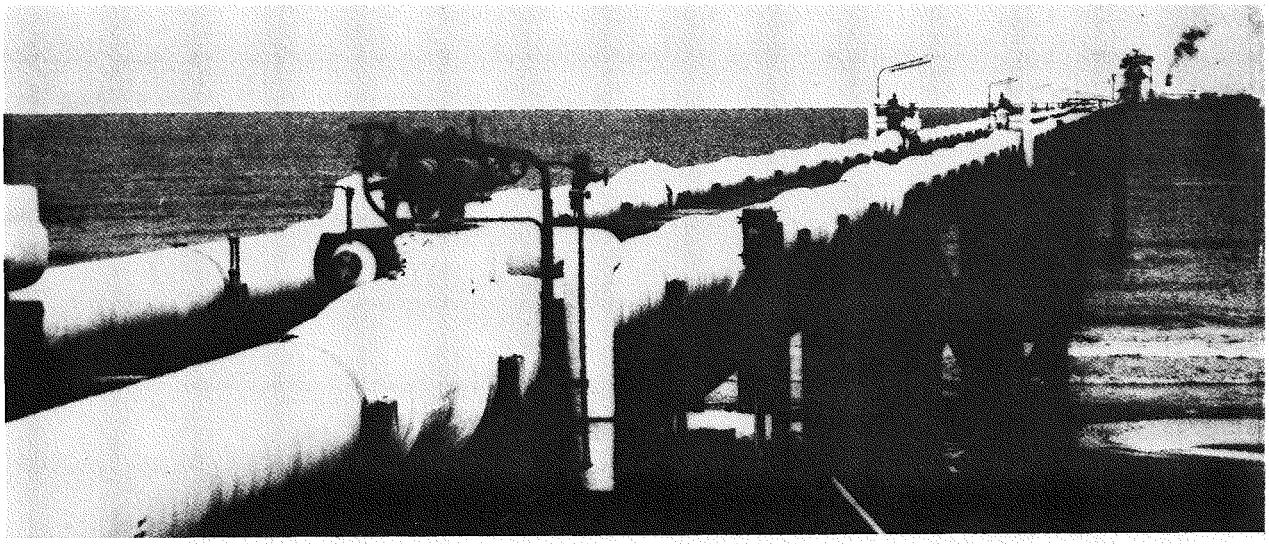

Figure 3-29. Polyurethane Foam Insulated, Stainless Steel Pipeline For Loading Of LNG Tankers. Stainless Pipeline Supplied By Cosmodyne. (18-Inch ID)

fiberglass surrounded by secondary layers of urethane insulation. This assembly is enclosed by a combination vapor and weather barrier (Perm-Guard) consisting of a fiberglass-reinforced plastic approximately 0.100-inch thick.

The Cosmodyne concept was judged to be better suited to cryogenic cable application, since less site labor is required for assembly and installation. A final selection of the foam insulation concept, however, must await a detailed comparison of costs.

Figure 3-30 shows how factory insulated pipe spools would be pre-assembled, prior to shipment to construction sites. Two different types of spool assemblies are shown since some FRP pressure pipe lengths must be supplied with FRP/metal flange joints. As indicated in Figure 3-31, the Cosmodyne concept uses three separate layers of polyurethane foam separated by an open weave glass cloth. These glass cloth layers prevent radial cracks from propagating from the cold FRP pipe surface to the outer protective cover of the cable envelope.

Although not shown in Figure 3-30, an electromagnetic shield may be required to prevent interference with adjacent communication circuits. This shield would be placed over the foam thermal insulation. A loose glass fiber mat

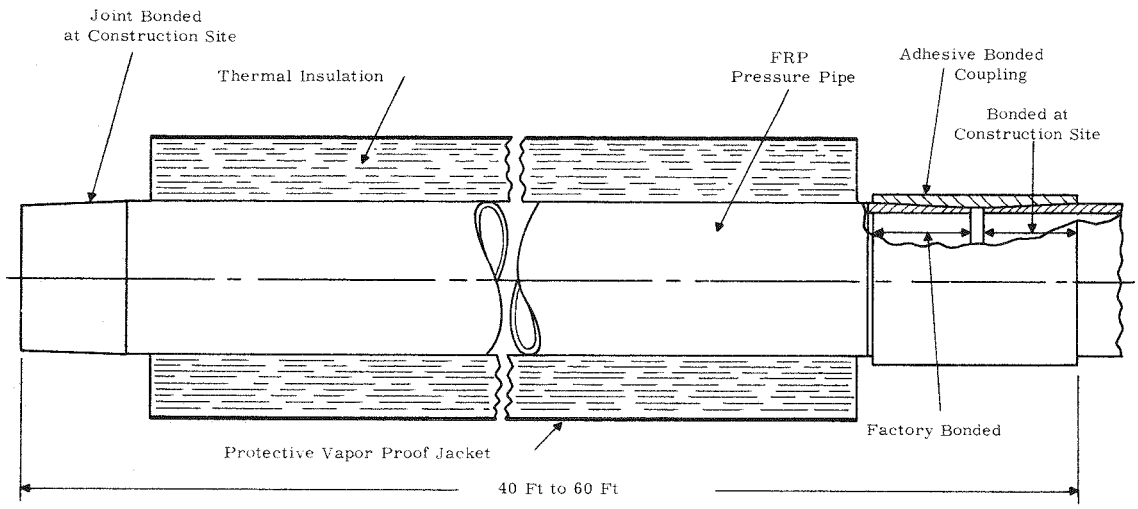

a) FRP Pipe/FRP Pipe Joint

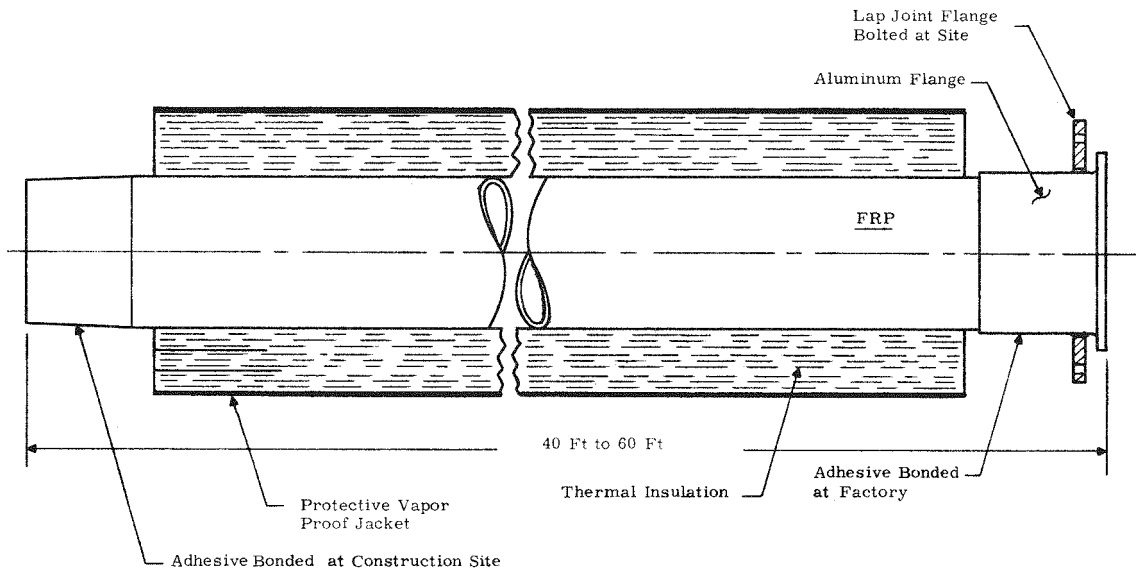

b) FRP Pipe/Metal Flange Joint

Figure 3-30. Thermal Insulation Of FRP Pipe With Preassembled Joints

separates the FRP pressure pipe from the first layer of foam insulation to permit free axial expansion and contraction of the FRP pipe within the thermal insulation. Polyurethane foam would also be used to insulate FRP pipe joints after assembly in the field. An advantage of isocyanate based polyurethane foams is that they can be sprayed, poured or frothed, and therefore joints can readily be insulated after installation. Pipe sections

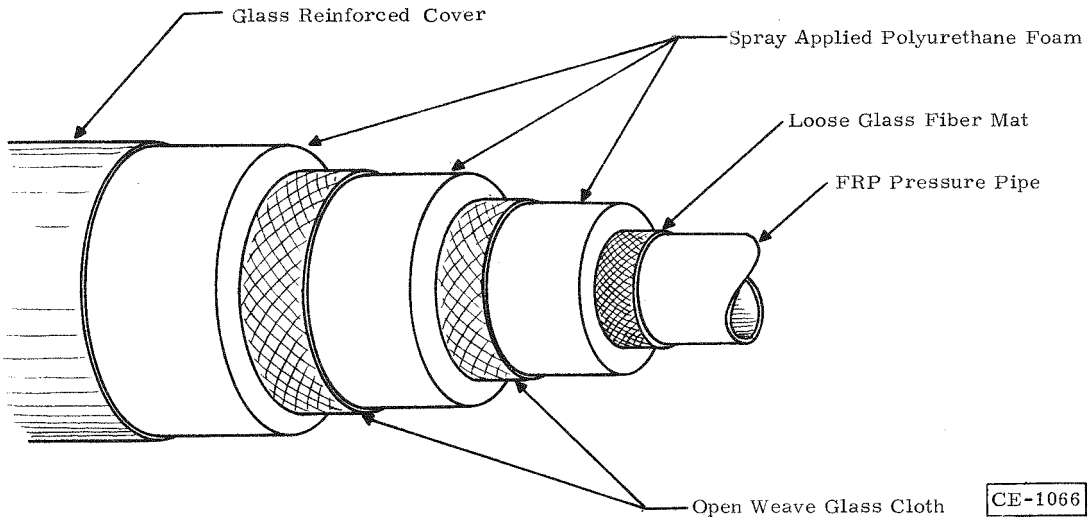

Figure 3-31. Thermal Insulation Of The Cable Envelope

containing damaged insulation can also be readily repaired. Figure 3-32 shows how joints might be insulated using the Cosmodyne concept.

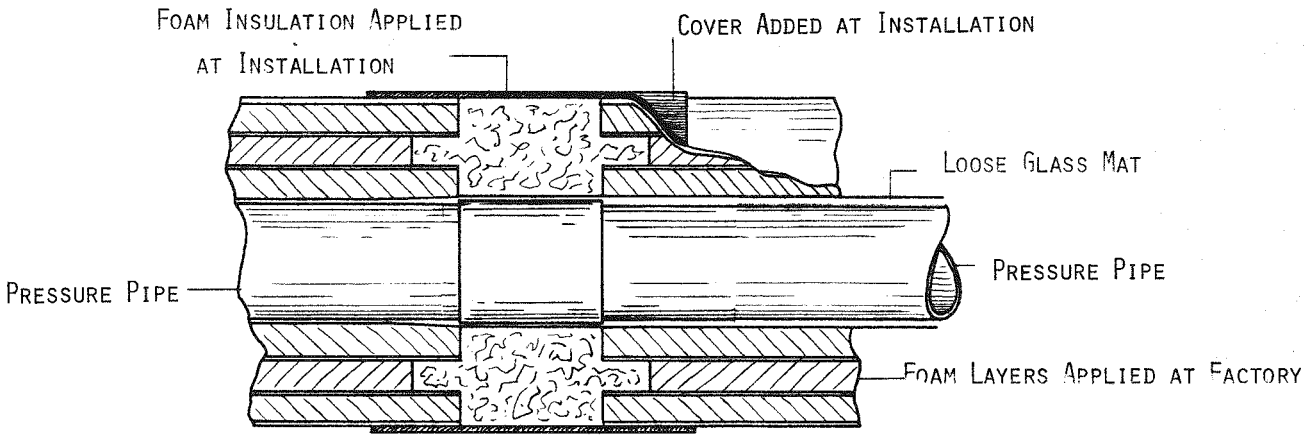

Figure 3-32. Thermal Insulation Of The Pipe Joints

Fluorocarbon-filled closed-cell urethane foam has been used for many cryogenic piping applications because of its low thermal conductivity and good compressive strength. This foam structure continues to provide an effective insulation, even under conditions where the vapor barrier has been damaged, since the foam has a low water vapor permeation rate.

Table 3-8 provides a comparison of ambient temperature thermal conductivity values for a number of potential insulations. Additional properties are listed in Table 3-9. Urethane foam is noted to have the lowest conductivity. As shown in Figure 3-33, this conductivity decreases as the tem-

Table 3-8

COMPARISON OF THERMAL INSULATIONS FOR FRP PIPE SECTIONS

	Mean Thermal Conductivity 75 F
Cellular glass (9#/ft^3)	0.40 Btu in/ft^2-hr-^{o}F
Polystyrene foam (2#/ft^3)	0.26
Glass fiber (3.6#/ft^3)	0.25
Urethane foam (2#/ft^3)	0.14
Cork (6.5#/ft^3)	0.31

Table 3-9

APPROXIMATE PROPERTIES OF SPRAY APPLIED URETHANE FOAM INSULATION

Density	2.0 lbs/ft^3
Compressive strength	25 psi (5% deflection rise direction)
Cell size	4 - 8 mils
Closed cells	90%
Coefficient of thermal expansion	2 - 3.5 $\times$ 10^{-5} in/in-^{o}F
Compressive modulus	700 psi (rise direction)

perature decreases except in a small temperature range near 260 K. This plot also shows thermal conductivity values for glass fiber. Aging of the urethane insulation will tend to raise the thermal conductivity slightly.

An insulation thickness of approximately 6 inches is required to prevent moisture condensation on the outer surface of the pipe, should the soil temperature reach 80 F. Final selection of the foam insulation cannot be made until an overall system study has been performed when system refrigeration characteristics and component cost data are available for trade-off purposes. The maximum heat flux through the insulation has been estimated to be less than 10 Btu/hour/ft^2 of envelope outside surface area. Cosmodyne has completed thermal tests of 18-inch diameter pipe filled with liquid methane that has confirmed this heat flux estimate.

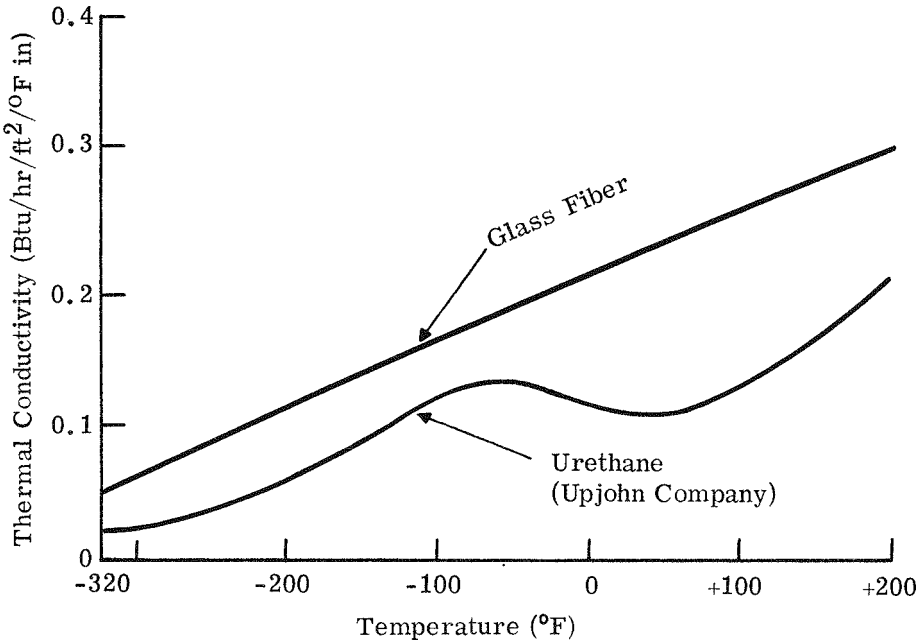

Figure 3-33. Thermal Conductivity Values For Glass Fiber Insulation And Foam Insulation

Further discussion of the foam thermal insulation and a heat transfer analysis appear in Appendix IV of the Phase II Final Report.

With the use of a 0.100-inch thick protective glass polyester cover over the foam, it is estimated that 10.5 pounds of moisture vapor will accumulate inside a one-foot length of 28-inch diameter pipe over a 40-year period. This has been based upon a permeation rate of 0.02 perms for the outer jacket and a 90 F, 100 percent relative humidity ambient condition.

Note:

$$1 \text{ perm} = \frac{1 \text{ grain } H_2O}{ft^2\text{-hr-in Hg}}$$

Section 4

ELECTRICAL INSULATION EVALUATION

ELECTRICAL INSULATION MATERIAL SELECTION

On the basis of dielectric tests performed on small cylindrical specimens at low temperature in the Phase II Cryogenic Cable Program, three electrical insulation materials were identified as potential candidates for cryogenic cable application. These materials were:

- Cellulose paper
- Cellulose paper/polypropylene film, laminate
- Calendered polyethylene paper (Tyvek)

As part of the Phase II program, a number of tests were conducted on representative samples of each of these materials at 60 Hz voltages up to 200 kV. Figure 4-1 shows the measured short-term breakdown strength of each of these materials, impregnated with liquid nitrogen, as a function of

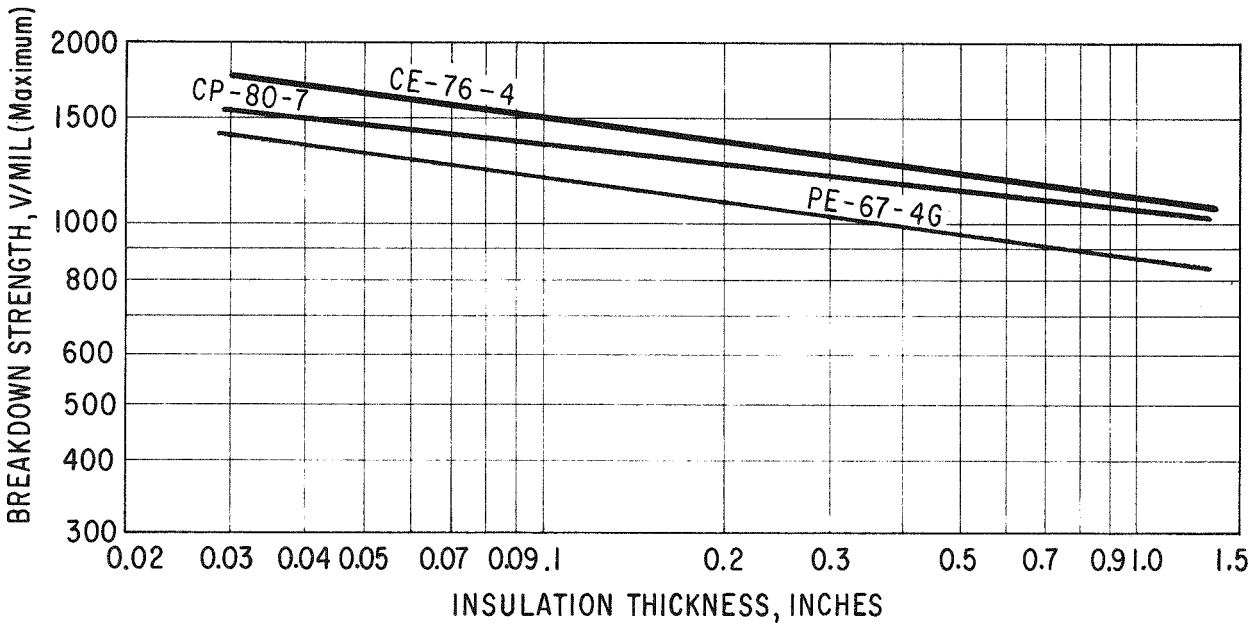

CE-76-4 HIGH ALPHA CELLULOSE PAPER
CP-80-7 CELLULOSE-POLYPROPYLENE LAMINATE
PE-67-4G POLYETHYLENE PAPER

Figure 4-1. Short-term Breakdown Strengths of Candidate Insulation Materials

insulation thickness. However, it is obvious that the selection of an insulation material for this application cannot be made solely on the basis of electrical breakdown strength. Other selection criteria, such as the dissipation factor and the mechanical properties of the material, must also be taken into account. The dissipation factor will impact the cable system dielectric losses, and the mechanical properties of the insulation will influence the taping operation, and hence, the quality of the cable insulation during cable manufacture. Table 4-1 summarizes a number of the more important selection criteria, and compares the properties of each of the above materials in a qualitative manner.

Table 4-1

INSULATION MATERIAL SELECTION CRITERIA

Selection Criterion	Polyethylene	Cellulose	Cellulose/ Polypropylene
AC Breakdown Strength	Medium	High	High
Dissipation Factor	Low	High	Medium
Taping Properties	Poor	Good	Medium
Quality Control	Poor	Good	Good
Cost	Low	Medium	High

The polyethylene paper is an attractive candidate from the standpoint of the low dissipation factor (less than 5×10^{-6}), but the quality control of the material, as it is now manufactured, is unsuitable for high-grade electrical insulation application. It must be emphasized, however, that there is every reason to expect that such a material could be manufactured with the required degree of quality control, if there were sufficient economic justification to do so. The moderate breakdown strength values measured on polyethylene paper impregnated with liquid nitrogen were not so low as to rule out this material for cryogenic cable application. The material also has a low Youngs modulus and a low coefficient of friction which complicates the cable taping operation. Relatively low taping tensions must be used, which tend to yield a "soft" cable, and control of the butt gaps between adjacent tapes is more difficult because the tapes tend to slide. These rather poor mechanical properties, and their impact on the cable taping operation, immediately raise the question of what the "realization coefficient" might be on a full-scale cable; that is, what percentage of the breakdown strength (V/mil) measured on small samples will be achievable in a full-scale cable?

Cellulose paper has the advantage that it is readily available as a high-grade electrical insulation material. Present day cable taping equipment is obviously matched to the relatively good mechanical properties of cellulose paper, and it is to be expected that the "realization coefficient" for a liquid nitrogen impregnated cellulose paper cable will be high. This material also provides a relatively high breakdown strength. The sole disadvantage of cellulose paper is its relatively high dissipation factor; typically, 1250×10^{-6} when impregnated with liquid nitrogen. Although the additional dielectric loss provided by the application of this material to a cryogenic cable system will be undesirable, it is by no means prohibitive.

To some extent, cellulose paper/polypropylene film laminate would be expected to combine the advantages of each of the above materials. It provides reasonable breakdown strength, and the dissipation factor (850×10^{-6}) is less than that provided by cellulose paper alone, reflecting the lower volume of cellulose paper present in the laminate. Mechanical properties of the laminate are acceptable, but are not as good as those of cellulose paper alone. The major drawback to the development of cellulose paper/polypropylene laminate for cryogenic cable application is that of procuring the laminate in the required form. It must be remembered that this material was originally developed for oil/paper application, and the laminate properties (cellulose/polypropylene ratio, cellulose paper density, cellulose paper air resistance, laminate thickness, etc.) were tailored for that application. Thus, off-the-shelf laminates are not ideally suited for cryogenic application when impregnated with liquid nitrogen. The costs of procuring production runs of laminate, with different parameters in each run, for the purposes of thorough evaluation were prohibitively high. In summary, it is believed that this material may well prove to be the "best" for cryogenic cable application in the future, but the development effort required to produce this material for liquid nitrogen impregnation was outside the scope of this Phase III program.

On the basis of the above discussion, cellulose paper was selected as the insulation material to be used on the cryogenic cable sections manufactured as part of this program. This is not to imply that cellulose paper is envisaged as being the best possible insulation material for cryogenic cable application in the future. Rather, cellulose paper was judged to be the most attractive material from the standpoint of successfully demonstrating the technical feasibility of prototype cryogenic cable sections as part of this Phase III program.

CHARACTERIZATION OF CELLULOSE PAPER INSULATION

In selecting a cellulose paper for cryogenic cable application, it is necessary to identify the major effects, if any, of the individual cellulose paper parameters on the breakdown strength of the paper when impregnated

with liquid nitrogen. To define a particular cellulose paper for any cable application requires the specification of many parameters. In particular, the following must be specified:

- Type of pulp
- Paper density
- Paper air resistance
- Water treatment (deionized or regular water)
- Paper thickness

Although the effects of these parameters on the breakdown strength and dissipation factor of oil/paper insulation systems have been examined, little is known on the effects of these parameters in liquid nitrogen impregnated systems. Some general comments on the effects of cellulose paper parameters are given below.

Density: In oil-paper insulation systems, it is generally accepted that the higher the paper density, the higher the dissipation factor will be. The effect of density on breakdown strength is somewhat more nebulous. Certain advocates (Refs. 4-1 and 4-2) have recommended the use of low-density paper in cable manufacture to achieve high breakdown strength, on the basis that high-density papers, with high dielectric constants, tend to overstress the oil in the butt gaps and, hence, initiate cable failure at a lower voltage. Advocates of high-density paper (Ref. 4-3), although agreeing with this argument, insist that a cable made with high-density paper, which also has a high breakdown strength and superior mechanical properties, has a higher voltage withstand capability.

In view of these conflicts of opinion, it is desirable, in studying the effects of paper density in cryogenic insulation systems, to use taped cylindrical samples which have butt gaps included in the structure.

Air Resistance: In general, high-density papers have a high air resistance, and special techniques must be adopted in the manufacture of the paper to realize a low density and high air resistance.

According to one report (Ref. 4-4), certain papers were handmade with different air resistances but with similar densities (0.77 g/cm^3) for the purposes of separating the two effects in oil/paper systems. Higher breakdown strengths were obtained on papers with high air resistance. However, Figure 1 of Reference 4-1 indicates that a low air resistance paper could have higher breakdown strength. Again, in view of these conflicts of opinion, it was appropriate to evaluate the effects of air resistance in cryogenic insulation systems by procuring and testing

a set of papers in which only the air resistance was a variable parameter.

Paper Thickness: In at least one experimental evaluation (Ref. 4-5), an oil/paper cable insulated with thin tapes provided a higher breakdown strength and higher dissipation factor than a cable employing thick tapes. In practice, however, the minimum tape thickness is usually governed by the mechanical constraints of taping and bending the finished cable.

Since the cable designer is not free to choose the tape thickness on the basis of breakdown strength alone, this particular parameter assumes less importance in an evaluation of paper parameters which is directed toward achieving high breakdown strength.

Pulp and Processing Water: In conventional oil/paper insulation systems, the use of conventional and modified kraft papers is observed to produce different breakdown strengths and dissipation factors. In addition, deionized water is often used in processing the pulp, to reduce the dissipation factor and to avoid the inclusion of acids or acid salts in the finished paper that could otherwise damage (Ref. 4-4) the paper at elevated temperatures.

On the basis of the above considerations, an attempt was made to identify those cellulose paper parameters that were critical to the performance of the paper when impregnated with liquid nitrogen. From an ideal standpoint, it would have been desirable to conduct a sufficient number of tests on a wide range of cellulose papers, wherein each paper had only one variable parameter, such that the cellulose paper specifications could have been optimized for cryogenic cable application. From a more practical standpoint, tests were conducted to determine which of the principal cellulose paper parameters, if any, were critical to the short-term ac breakdown strength and dissipation factor of the paper.

To accomplish this objective, sets of cellulose paper were procured from a number of vendors wherein all the paper parameters, except one, were similar. To measure the breakdown strengths and dissipation factors of these papers, taped cylindrical samples were manufactured and tested in liquid nitrogen at 77 K and at a pressure of 80 psig. The results of these tests are presented in Table 4-2.

The data do not permit any rigorous conclusions to be drawn with respect to the effects of the cellulose paper parameters on the breakdown strength in liquid nitrogen. On the basis of a more or less intuitive examination of the data, it can be suggested that the principal variable promoting high breakdown strength is high air resistance. Air resistance did not appear to provide a strong influence on the measured dissipation factor of

Table 4-2

CELLULOSE PAPER BREAKDOWN STRENGTH AND DISSIPATION FACTOR (Both Electrodes Screened with CB-97-C Paper)

Material Code	Lot No.	Density (g/cm^3)	Air Resistance (Gurley sec/100 cm^3)	Pulp	Paper Thickness (mils)	Dielectric Constant	Sample Thickness (mils)	Brekadown Voltage (kV)	Breakdown Stress (V/mil)	Dissipation Factor (μrad) at Stress of (V/mil)			
										300	600	900	1200
CE-84-3	4220	0.84	794	MK	3.00	1.94	36	50	1389	--	--	--	--
						2.05	36	50	1389	--	--	--	--
						2.01	36	50	1389	--	--	--	--
						1.99	37	50	1351	1320	1630	2110	--
						1.98	39	60	1538	1320	1500	1760	2200
						1.98	37	55	1486	1280	1530	1870	2570
						2.05	100	>60	--	1370	1400	--	--
CE-75-4	7155	0.75	758	CK	4.20	2.08	38	50	1316	1370	1590	1890	2730
						2.05	36	50	1389	1430	1640	1850	2250
						2.06	37	55	1486	1430	1530	1720	2210
						1.95	32	50	1562	1410	1520	1790	2150
						2.06	33	50	1515	1460	1540	1720	1940
						2.03	33	50	1515	1480	1600	1860	2200
						2.22	200	>50	--	1360	--	--	--
CE-84-5	4441	0.84	3,811	CK	4.75	1.89	32	50	1562	1320	1500	1990	2830
						1.82	32	50	1562	1310	1446	1800	2250
						2.04	34	50	1471	1330	1430	1590	1870
						2.13	33	45	1364	1440	1500	1650	1880
						2.09	34	50	1471	1400	1480	1640	1880
						2.08	200	>50	--	1320	--	--	--
CE-84-4	6757	0.84	1,990	MK	4.12	1.87	32	50	1562	1300	1420	1740	2250
						1.67	30	50	1666	1230	1430	1870	2660
						1.86	31	45	1451	1330	1450	1780	2290
						2.08	32	45	1406	1430	1490	1630	1800
						2.13	33	50	1515	1460	1520	1700	2020
						2.05	32	50	1562	1380	1450	1590	1790
						2.16	200	>50	--	1250	--	--	--
CE-81-5	4444	0.81	515	MK	5.00	1.94	35	48	1371	1240	1360	2130	2040
						1.91	34	45	1323	1270	1440	2250	2290
						1.92	35	45	1286	1240	1350	2100	2000
						1.87	33	40	1212	1320	1480	1770	--
						2.05	33	45	1364	1420	1500	1640	1800
						2.09	34	45	1324	1400	1490	1630	1840
						2.22	200	>50	--	1250	--	--	--
CE-109-3	K-200	1.09	18,630	CK	3.00	2.34	34	51	1500	1950	2100	2420	3050
						2.27	35	54	1543	1820	2080	2560	3600
						2.31	35	55	1571	1870	2120	2590	3500
						2.44	33	55	1667	2030	2160	2450	2820
						2.44	34	55	1618	1960	2070	2280	2530
						2.65	200	>50	--	2070	--	--	--

the paper. Some effect of the density on the dissipation factor is also suggested; higher density papers appear to have higher dissipation factors. In general, no major effects were observed due to changes in pulp (conventional kraft or modified kraft) or water treatment.

CELLULOSE PAPER SPECIFICATION FOR THE PROTOTYPE CRYOGENIC CABLE

On the basis of the above tests, the cellulose paper specifications were selected as follows:

Type of pulp	Conventional kraft (CK)
Water treatment	Deionized water

Air resistance	(nominal)	2500 Gurley-sec
	(minimum)	2000 Gurley-sec
Paper density	(nominal)	0.85 g/cc
Thickness	(nominal)	0.005 inch and 0.0065 inch

Since no strong effects had been observed on the breakdown strength or dissipation factor between papers manufactured with conventional kraft (CK) pulp and modified kraft (MK) pulp, and since future supplies of modified kraft pulp were expected to be limited or nonexistent, it was judged desirable to use conventional kraft pulp on the prototype cable sections.

A relatively high air resistance was specified with a view to obtaining a high breakdown strength, and a relatively low density was specified with a view to obtaining a low dissipation factor. A deionized water treatment was specified as being preferred. Tape thicknesses of 0.005 inch and 0.0065 inch were specified on the basis of cable geometry and taping considerations only.

Samples of these papers, as manufactured by Crocker Technical Papers, were tested for the purposes of verifying that the expected dielectric properties had been obtained. Six samples each of the 0.005- and 0.0065-inch paper were tested; the average breakdown strengths obtained for each group of samples are shown in the boxes of Table 4-3. Table 4-3 also summarizes the results obtained on the cellulose paper tests described in the previous section. The various papers are ranked according to the breakdown strength, and in Table 4-3, the vertical spacing is approximately to scale. The results show that the two papers adequately fit within the family of high air-resistance papers.

Of additional concern is the fact that the measured dissipation factor on these two papers was on the order of 150×10^{-4}, a value which is approximately ten times higher than those measured on other representative cellulose papers. The duplex carbon-black screen was immediately suspect in this regard, since it was the first time that this screen material had been used, and surface loss effects caused by screen materials are well known.

To verify that the increased dissipation factor was substantially caused by the duplex screen, several cellulose paper samples of different thickness were tested with the identical measuring circuitry. These included two samples of the manufactured cables; one with an insulation thickness of 0.550 inch and the other with an insulation thickness of 0.860 inch. Table 4-4 presents the results of these dissipation factor measurements. The values measured on Samples 6, 9, and 5 lend credence to the hypothesis that the increased dissipation factor in the small samples (4) was entirely

Table 4-3

BREAKDOWN STRENGTH RANKING OF CELLULOSE PAPERS

Paper Number	Thickness (mils)	Density (g/cc)	Pulp*	Air Resistance (Gurley-sec)	E_B Avg (V/mil)	Number of Samples	Standard Deviation (V/mil)
CE-76-4	5	0.81	MK	2060	1593	5	27.5
CE-109-3	3.0	1.09	CK	18630	1580	5	64.9
CE-84-4	4.12	0.84	MK	1990	1527	6	92.0
ANA-50	5.12	0.84	CK	5100	1481	6	56.8
CE-84-5	4.75	0.84	CK	3811	1486	5	82.0
CE-75-4	4.2	0.75	CK	758	1464	6	91.2
CE-84-3	3	0.84	MK	794	1441	4	86.1
ANA-65	6.65	0.84	CK	3300	1334	6	111.3
81-5	5.0	0.81	MK	537	1313	6	58.5

*CK: Conventional Kraft pulp
MK: Modified Kraft pulp

attributable to the losses generated in the duplex screen. Comparison shows that Samples 6 and 9, which are different papers with the same screen, have nearly identical, low dissipation factors. Comparison of Samples 9 and 5, which are of the same paper with different screens, shows a larger dissipation factor for Sample 5, with the duplex screen. Comparing Samples 9 and 5, and assuming that the dissipation factor for Sample 9 is the true dissipation factor of the sample, a corrected value for the dissipation factors of the other sample with a duplex screen can be calculated. These "corrected" values appear in the last column of Table 4-4, and the general trend appears to confirm the hypothesis that the true dissipation factor of the cable paper is around 1300×10^{-6} and that higher values, as measured, are due to surface loss effects caused by the presence of the duplex carbon-black screen.

CRYOGENIC CABLE DESIGN AND MANUFACTURE

Cross sections of each of the two prototype cryogenic cables manufactured for EHV tests are shown in Figure 4-2. The geometry of the larger cable section was chosen on the basis of existing manufacturing equipment limitations, and with a view to producing a maximum electric stress of 430 V/mil at the conductor surface, at rated voltage, 500 kV (290 kV line-to-neutral). This maximum stress was selected to simulate the operating stress of 400 V/mil which had been assumed for full-scale cables in earlier cryogenic cable system studies.

Table 4-4

DISSIPATION FACTORS OF CELLULOSE PAPERS

Sample Number	Paper	Screen	Outside Radius (inches)	Inside Radius (inches)	Thickness (inches)	Tan δ* Measured (μrad)	Tan δ Extrapolated (μrad)
6	CE76-4	CB-97-C	0.450	0.254	0.196	1,440	--
9	CEC-84-5**	CB-97-C	0.453	0.254	0.199	1,340	--
5	CEC-84-5**	Duplex	0.456	0.248	0.208	5,900	--
4	CEC-84-5**	Duplex	0.287	0.251	0.036	17,800	26,300
7	Cable	Duplex	2.35	1.5	0.850	3,030	2,430
8	Cable	Duplex	2.05	1.5	0.550	3,500	2,430

*Applied voltage was 2 kV rms.
**Samples of paper used in cable.

The geometry of the smaller cable was selected such that it could reasonably be assured that the cable could be failed, taking into account the test voltage and charging current limitations of the EHV test equipment. In this manner, it was anticipated that the EHV tests would serve to demonstrate the withstand capability of the larger cable section, and would provide a breakdown strength value for the smaller cable. This breakdown strength value would represent an important data point in predicting the breakdown strength values of full-scale cryogenic cables, and could also provide a guide as to the "realization coefficient" of this type of cable insulation. Such information would not have been provided by a withstand test on the larger cable alone.

The same conductor configuration was used in each cable; only the insulation thicknesses were different. To produce these two cables, 1000 feet of aluminum conductor were manufactured. The conductor comprises eight 45-degree segments wrapped around a helical former. The inside and outside diameters of this conductor are 1.6 and 3.03 inches, respectively. Each conductor segment comprises 91 strands, 97 mils in diameter; the cross-sectional area of each segment is approximately 579,000 circular mils.

The conductor was covered with a binder of 1.25×0.005-inch copper tape intercalated with a 1.25×0.008-inch carbon-black paper tape. The conductor screen comprises two additional carbon-black paper tapes and two duplex tapes.

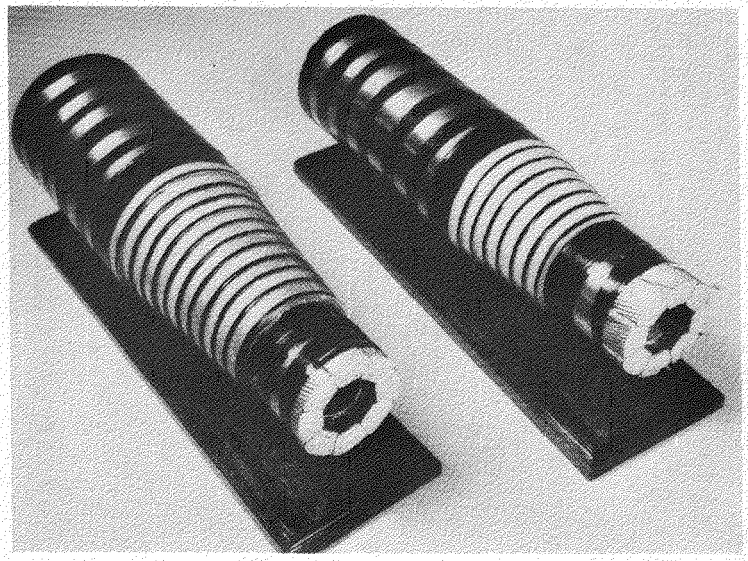

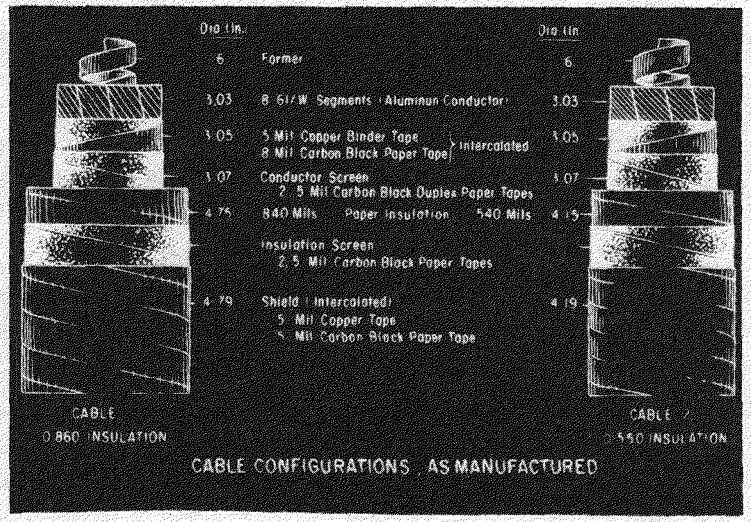

Figure 4-2. Prototype Cryogenic Cable Sections

For the prototype cable with 0.860-inch insulation, the taping machine was loaded with 102 tapes that were 0.005-inch thick and 54 tapes that were 0.0065-inch thick. With this construction, the transition from 0.005 to 0.0065-inch tapes occurred at a diameter of 3.99 inches.

To manufacture the prototype cable with 0.550 inch of insulation, 0.005-inch tapes were used throughout. A total of 110 tapes were applied to the cable; binders and screens similar to those described for the 0.860-inch cable were also used in this cable.

Figure 4-3 shows one of the sixteen taping heads used in the construction of the cable.

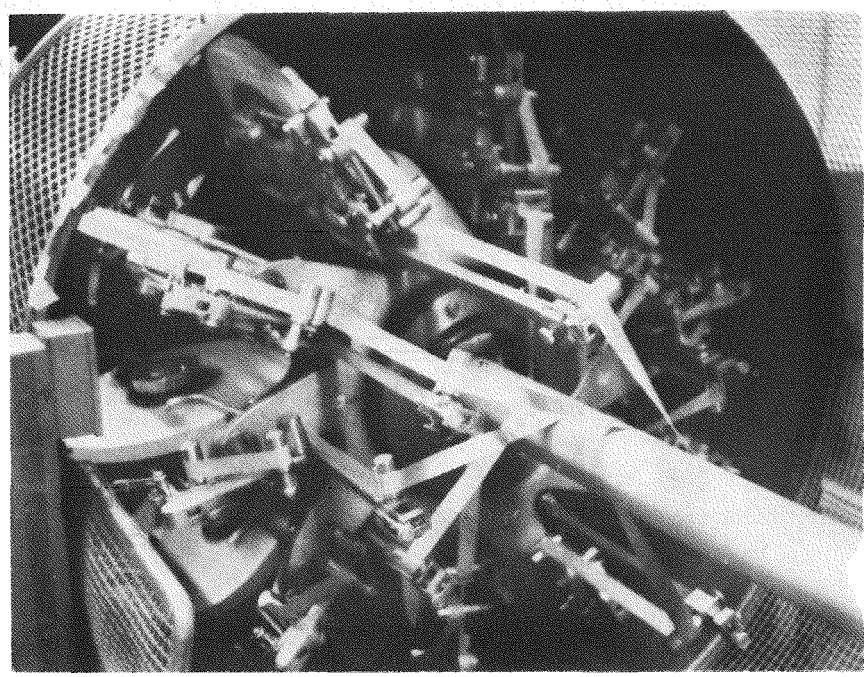

Figure 4-3. One of the Heads of the Taping Machine

BEND TESTS

In addition to the electrical requirements, a cable must satisfy a number of mechanical requirements to survive the rigors of installation in the containment pipe. To this end, all commercial cable is subjected to some form of bend test.

In the manufacture of conventional oil/paper cables, the cable is bent onto an impregnating reel as it comes off the taping machine, and is not straightened again until it has passed through the drying and impregnation cycles. At this time, the paper insulation has shrunk slightly and has been

lubricated with the oil impregnant. It is at this stage that the certification bend tests are normally performed, rather than before oil impregnation.

During the manufacture of each of the cryogenic cable sections, bend tests were performed on samples of cable taken directly from the taping machine, to provide guidance on taping tension and butt gap width adjustments. These tests comprised simple bends on a 100-inch diameter wooden form as shown in Figure 4-4. Each cable section was dissected, before it

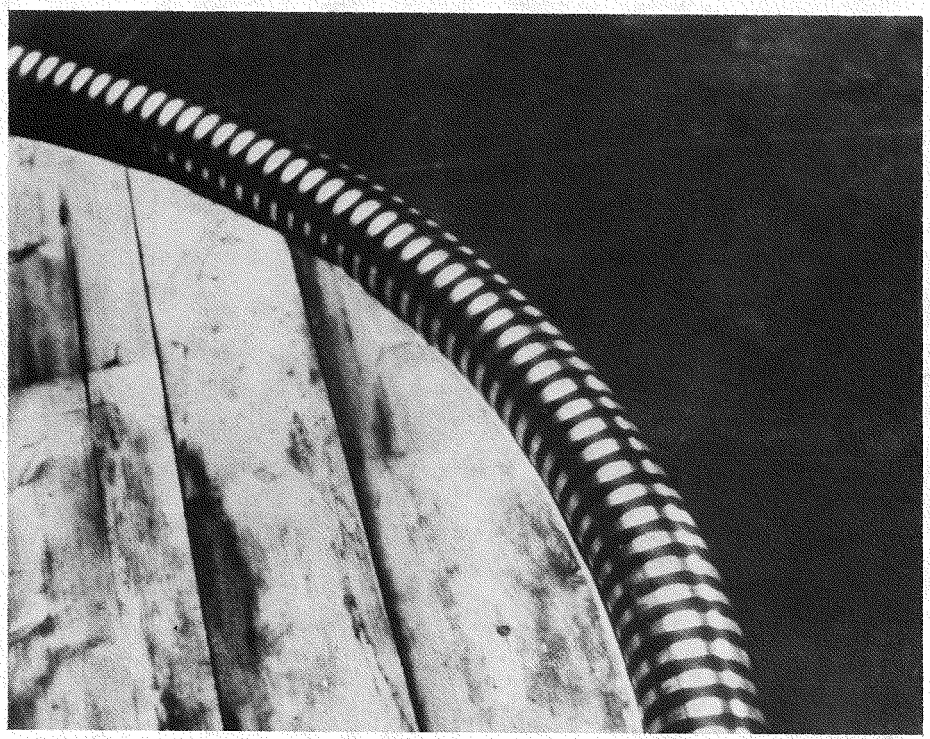

Figure 4-4. Cable Bend Test Around 100-Inch Diameter Form

was straightened, to look for evidence of tape wrinkling or buckling. In the early stages of manufacture, these tests did reveal tape wrinkling that necessitated adjustment of the butt gap width. When each of the cables had been manufactured, a final set of bend tests showed no evidence of damage, the cable sections being free of wrinkles and soft spots.

CABLE DRYING PROCEDURE

Following the manufacture of the cable sections, each of the cables was stored on a blanketed cable reel in the laboratory, and the individual cable reels were purged daily with dry nitrogen gas.

When each of the reels was unwrapped, some two months later, evidence of "polygonization" was observed on each of the cables. Polygonization is a term used to describe a particular form of nonuniform bending of the cable; an exaggerated description of this effect is shown in Figure 4-5. The effect had not been observed when the cables were manufactured, and was not apparent when the bend tests were conducted on the cables after manufacture. However, it is unlikely that this effect could have developed on the cable reel, even with an ingress of moisture.

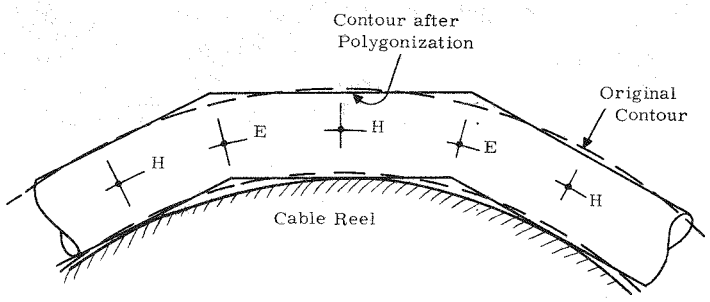

E -- Easy Bend Axis Parallel to Reel Axis
H -- Hard Bend Axis Parallel to Reel Axis

a) Cable on Reel

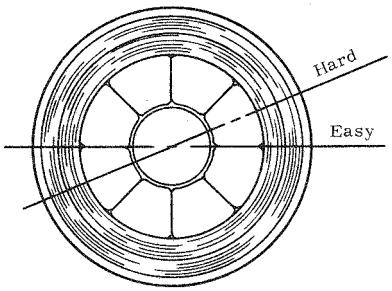

b) Cross Section of Cable

Figure 4-5. Schematic Of Cable Polygonization

As the cables were pulled from the reel and straightened, the effect of the polygonization became more pronounced, causing considerable distortion of the cable. Subsequent dissection of the straightened lengths revealed that the tapes had become severely wrinkled and folded. No such wrinkling or folding had been observed during the cable bend tests immediately after manufacture.

Further examination and evaluation of short lengths of the cable in the laboratory showed that the paper insulation on the cables had a measured moisture content of seven to eight percent by weight, whereas the cables had been manufactured under controlled humidity conditions (ten percent

relative humidity), implying a moisture content of approximately one percent by weight in the paper insulation at the time of manufacture. The paper tapes swell when they absorb moisture, and subject the insulation and conductor to compressive forces which inhibit sliding of the tapes as the cable is bent or straightened. Therefore, it is hypothesized that the forces applied to the cable as it was removed from the reel and straightened caused wrinkling and folding of the tapes.

In view of the poor condition of the cables as initial lengths were removed from the reels, it was judged to be entirely inappropriate to test the cables in that state. Before an attempt was made to dry the cables on the reels, a number of arcs of the cable approximately eight feet long were removed from the reel without straightening. These sections were subjected to a number of different drying cycles to determine which procedure should be adopted to restore the cables on the reel.

The following drying procedure was finally adopted. The bore of the cable was connected to a high-capacity vacuum pump so that the diffusion of gas and water vapor was from the outside to the inside of the cable. The cable reel was enclosed in a blanket of polyethylene, and dry nitrogen gas was introduced under the blanket at a pressure slightly above one atmosphere. This dry gas collected the water vapor as it diffused through the cable insulation to the bore of the cable. At the same time, the cable was heated to a temperature of 100 C by passing direct current through the cable conductor. The temperature rise through the cable insulation was minimized by surrounding the cable with a blanket of thermal insulation. Fifteen thermocouples were distributed along the outer ground shield of the cable at regular intervals, and 15 more were inserted into the cable bore.

The arrangement of the cable reel during this drying operation is shown in Figure 4-6. The instruments shown in the foreground are two 16-point temperature recorders and a Schering bridge. The bridge was used to measure the cable capacitance and dissipation factor, and the recorders were used to provide continuous monitoring of cable temperatures. The heater shown at the right of the figure was used to preheat the dry nitrogen gas before it was fed around the outside of the cable.

The data recorded during the drying process are shown in Figure 4-7. The capacitance and dissipation factor values are necessarily average values for the complete cable length. The temperature values shown in Figure 4-7 are the average values of the conductor temperatures along the cable length. The conductor current which heated the cable was controlled to limit the rate of conductor temperature rise to less than 3 C per hour. This was done to prevent the formation of a steep temperature gradient within the electrical insulation, possibly causing a buildup of moisture in the "cold" regions. Also, the conductor current was controlled so that the maximum temperature reading of any one thermocouple was limited to less than 100 C.

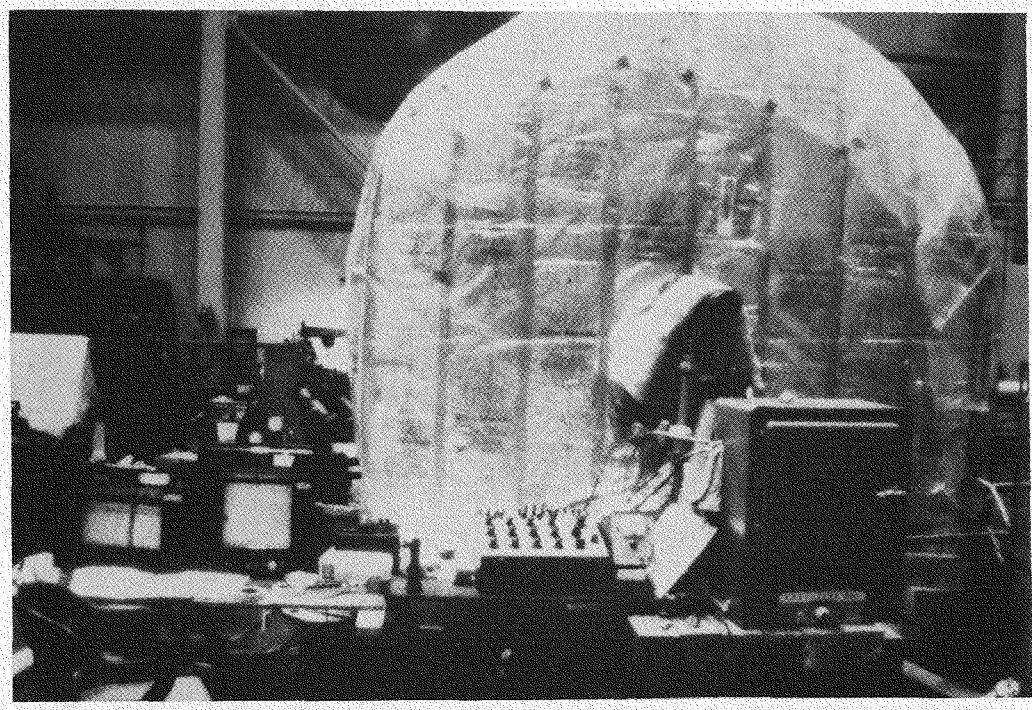

Figure 4-6. Cable Drying Arrangement

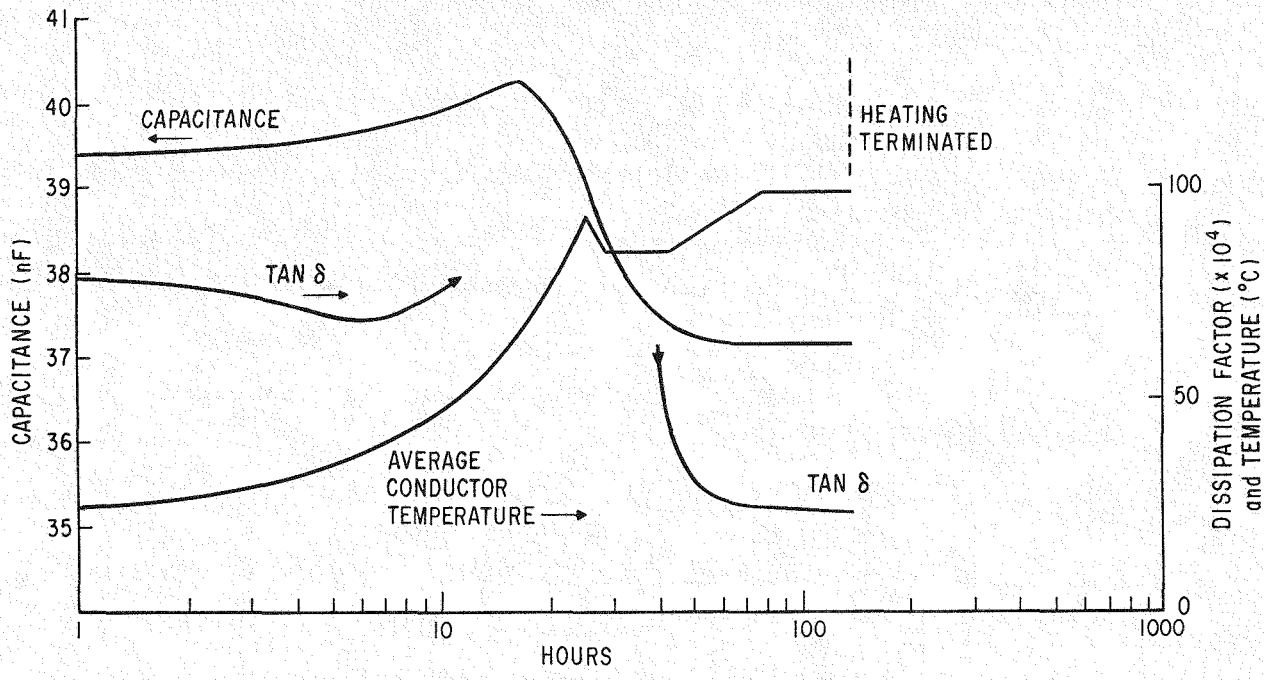

Figure 4-7. Cable Drying Record

Once an equilibrium condition had been established, the vacuum level achieved in the cable bore was 20 inches of mercury, and the flow of dry nitrogen gas through the cable wall was measured to be approximately 10 ft^3/min. This flow rate corresponds to a computed flow velocity of 2.5 ft/sec, assuming a uniform flow through the cable insulation. The capacitance and dissipation factor measurements indicated that the cable had reached an equilibrium condition after about three days, but the drying process was continued for an additional seven days to ensure thorough drying.

Following the completion of the drying process, a short section of cable was cut from the reel and this section was straightened, bent, and dissected. Some minor buckling of the tapes was noted, but the extent of the buckling was judged to be similar to that observed due to the polygonization of the cable on the reel. In other words, the condition of the cable section following bending was judged to be similar to the condition of the cable on the reel. Although the cable could not be described as 'ideal', its condition was such that it was worth testing.

CRYOGENIC POTHEAD TERMINATION DESIGN AND CONSTRUCTION

In testing or installing any cable system, it is necessary to include some form of termination at the ends of the cable which provides the following functions:

- A means of containing the cable impregnant
- A means of controlling the electric field distribution where the ground shield is terminated
- A means of carrying the high-voltage cable conductor through the wall of the containment pipe

In a cryogenic cable system, it is desirable that the termination provides the following additional functions:

- A means of removing the liquid nitrogen from the bore of the cable
- A means of thermally grading the conductor from the low-temperature region to the ambient temperature region

Although many different means of grading and shielding potheads exist, capacitive grading offers the most economical method at high voltages. A full description of a capacitively-graded pothead for a 500 kV, 3500 MVA cryogenic cable system is presented in Reference 4-6, page 79.

Since sections of cryogenic cable were to be tested as part of this program, it appeared logical to gain preliminary experience in the design, construction and test of prototype cryogenic pothead structures at the same time. Thus, it was planned that the cable sections would be tested in a U-shaped configuration, terminated at each end by cryogenic pothead structures. This arrangement permits the demonstration of the electrical, mechanical and thermal performance of the pothead structures, which are also capable of removing liquid nitrogen from the bore of the cable.

Prior to the design of the potheads for the cable tests, considerable experience had been gained in designing and testing capacitively graded terminations for dielectric samples which were tested in liquid nitrogen at voltages up to 50 kV and 200 kV (Ref. 4-6, page 99). In addition, sets of capacitors, designed for 345 kV oil/paper pothead service, were obtained from the Ohio Brass Company and were tested to failure when impregnated with liquid nitrogen. The conditions of these tests approximated the conditions expected in the cable terminations (see the Third Quarterly Report, page 39). The measured breakdown strength of this set of capacitors impregnated with liquid nitrogen was essentially the same as that when impregnated with oil. In conjunction with the personnel of the Ohio Brass Company, Mansfield, Ohio, a cryogenic pothead structure design was prepared for terminating the cryogenic cable sections to be tested as part of this program.

The principal dimensions of the capacitively-graded pothead are shown in Figure 4-8. During assembly, the cable is cut to length and the shielding tape is removed from the section of cable above the baseplate. Cylindrical build-up rolls of cellulose paper insulation are applied in sections over the cable insulation, the tapered spaces between the rolls being filled with crepe paper. The lower build-up roll contains a ground shield which is contoured to form a log-log profile and is connected to the cable ground shield at the lower end.

Ring-shaped capacitors are fitted over a support tube immediately surrounding the build-up rolls, providing a means of longitudinal voltage grading along the build-up roll surface. The diameter of the build-up rolls is chosen such that the radial electric stress in the liquid nitrogen annulus is reduced to an acceptably low value. The capacitor elements are connected in series, the top capacitor being connected to the cable conductor, and the bottom capacitor to the ground shield of the stress cone. An epoxy-fiber glass cylinder is mounted around the capacitors to provide an insulating pressure vessel to contain the liquid nitrogen. Thermal insulation is provided by closed-cell foam, housed in a cylindrical vapor-barrier of epoxy-fiber glass.

Table 4-5 shows the principal stresses within the pothead termination, assuming an applied voltage of 290 kV line-to-neutral, and assuming that the larger of the two cryogenic cables is being terminated. A similar termination is used for the smaller cable, but minor adjustments are made to the build-up roll dimensions.

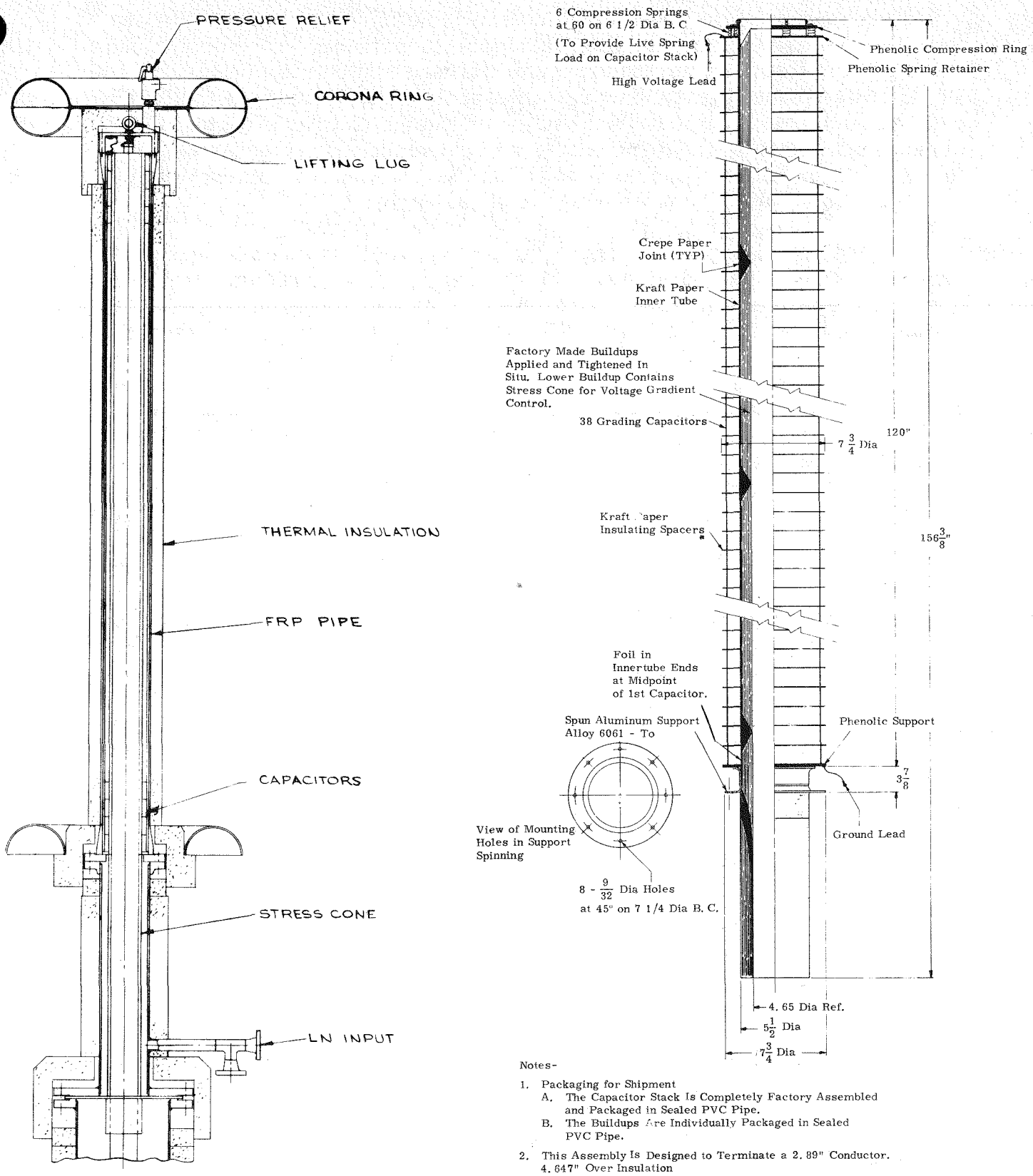

Notes-

1. Packaging for Shipment
   A. The Capacitor Stack Is Completely Factory Assembled and Packaged in Sealed PVC Pipe.
   B. The Buildups Are Individually Packaged in Sealed PVC Pipe.
2. This Assembly Is Designed to Terminate a 2. 89" Conductor. 4. 647" Over Insulation

Figure 4-8. Cryogenic Pothead Configuration

Table 4-5

PRINCIPAL STRESSES IN THE POTHEAD TERMINATION
(APPLIED VOLTAGE 290 kV. L-N)

Characteristic	Parameter
Maximum unit capacitor voltage	8.5 kV
Average stress in capacitor paper	340 V/mil
Axial stress at surface of cable insulation	2.4 V/mil
Axial stress in stress cone	2.55 V/mil
Radial stress at outside surface of cable insulation	185 V/mil
Radial stress in LN annulus under capacitor stack	156 V/mil
Radial stress in buildup roll	
Maximum	185 V/mil
Minimum	156 V/mil
Radial stress at conductor surface	300 V/mil

Figure 4-9 shows an end view of the pothead components, and Figure 4-10 shows the completed pothead assembly.

HIGH-VOLTAGE TEST FACILITY DESIGN AND CONSTRUCTION

The high-voltage cable test facility configuration is shown schematically in Figure 4-11, and comprises a straight horizontal pipe section, with a 90-degree pipe elbow at each end. The cable is pulled into the pipe and is terminated in two cryogenic pothead structures, which also provide a means of introducing and removing liquid nitrogen from the bore of the cable. The liquid nitrogen flow circuit for this configuration is shown schematically in Figure 4-12, and it can be seen that the liquid nitrogen which impregnates the cable insulation is at a temperature of approximately 79 to 80 K, at a pressure of approximately 80 psig. This test configuration offers the following advantages:

- The test configuration provides an opportunity to evaluate the performance of the cryogenic pothead structures, in addition to the performance of the cryogenic cable.
- The test configuration is somewhat representative of a practical installation in that the cable must be bent during installation.

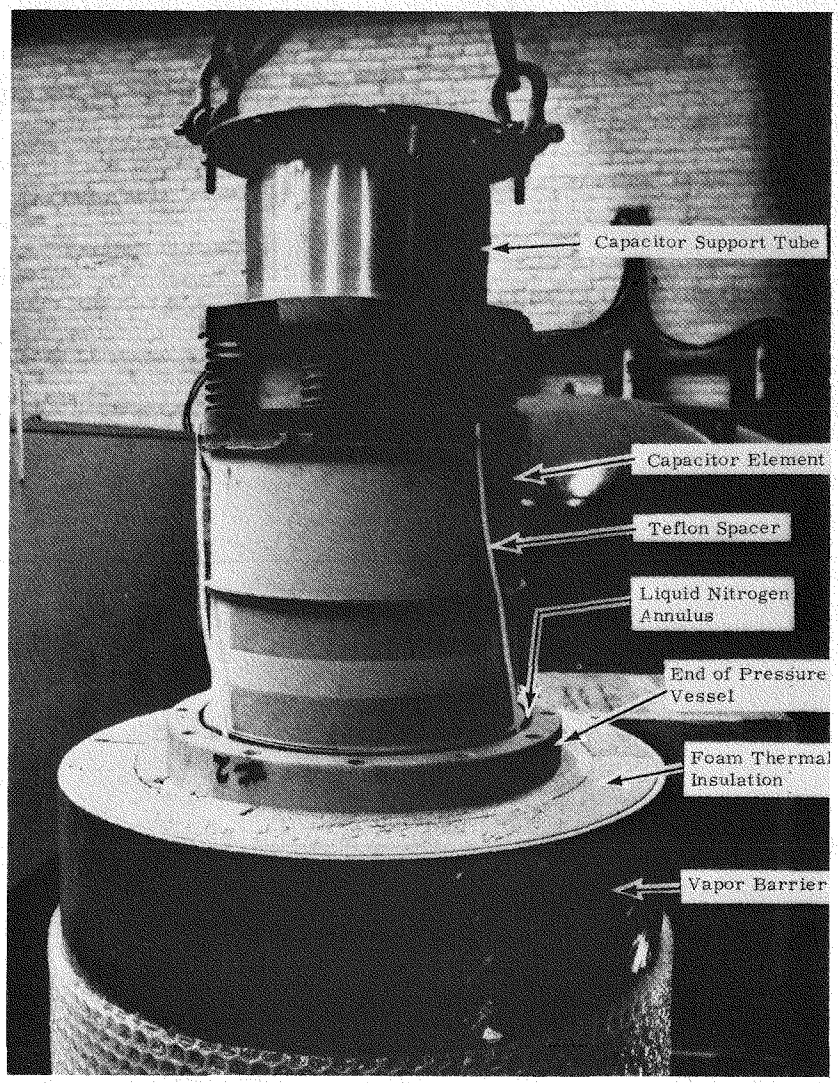

Figure 4-9. End View Of Pothead Components

- The cryogenic pothead configuration is representative of that proposed for an operational system in that it simulates the principal electrical, mechanical and fluid flow requirements.

Two overall views of the completed test facility in the high-voltage laboratory of Anaconda Wire and Cable Company, Hastings-on-Hudson, New York, are presented in Figure 4-13.

CABLE AND POTHEAD INSTALLATION

The installation procedure for the cryogenic cable and potheads is similar to that employed for the installation of conventional oil/paper cable components. With the horizontal pipe section connected to one pipe elbow,

Figure 4-10. Completed Pothead Assembly

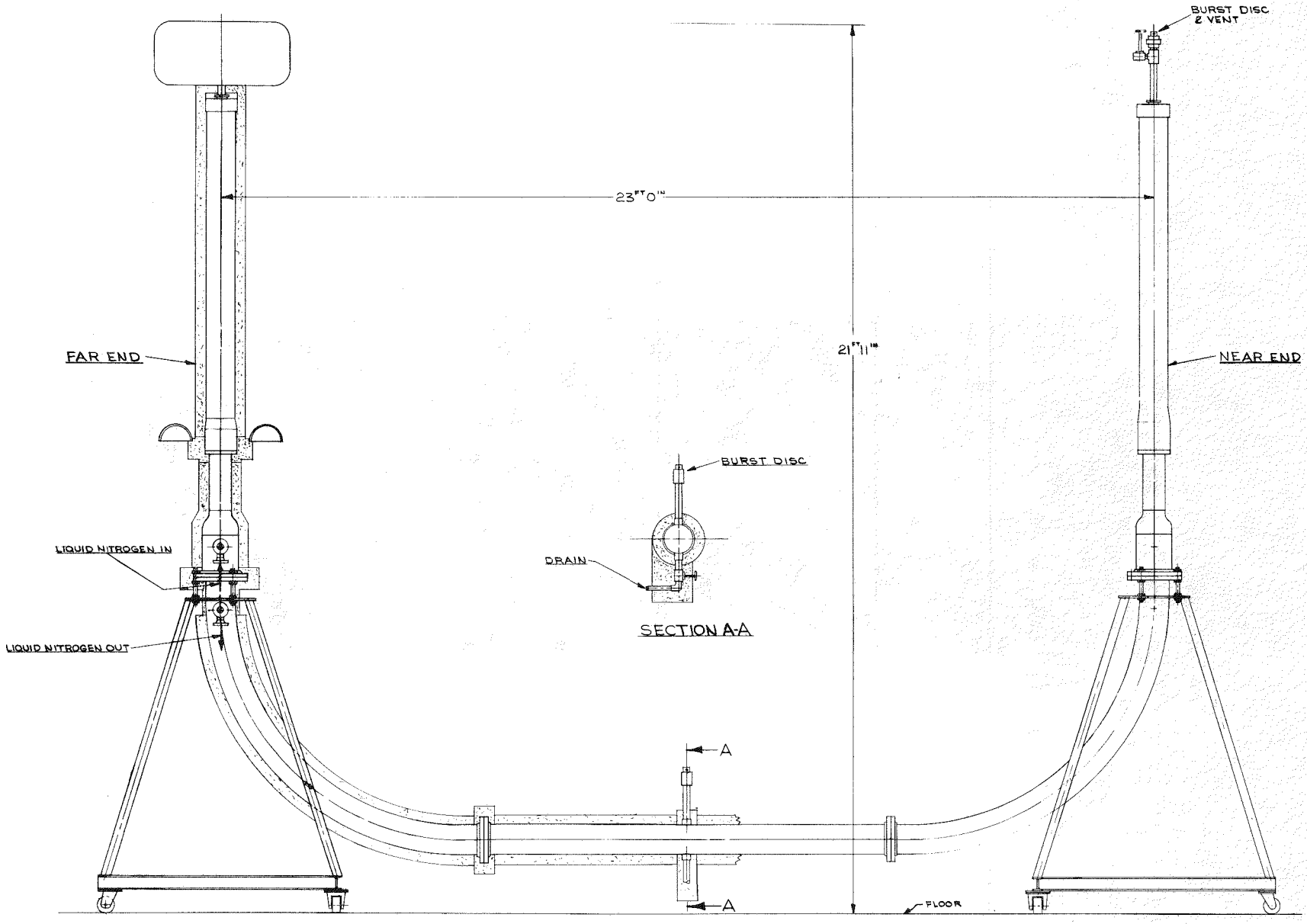

Figure 4-11. High-voltage, Cryogenic Cable And Pothead Test Configuration

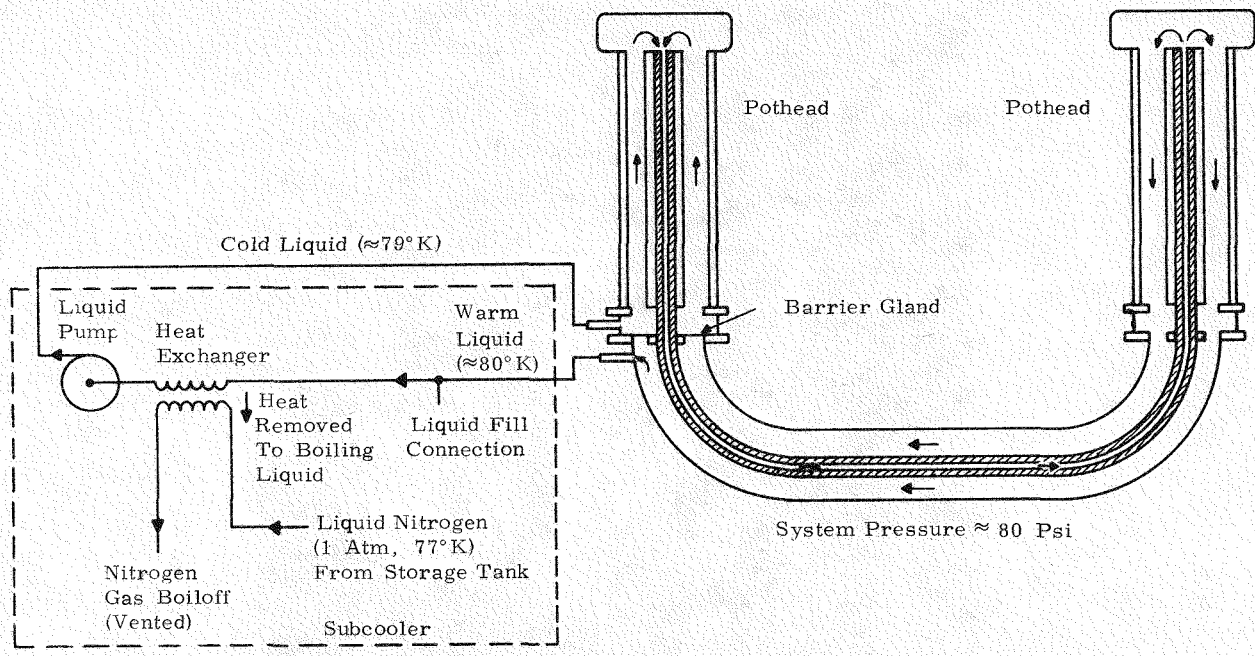

Figure 4-12. Liquid Nitrogen Flow Circuit Schematic

the cable was pulled from the cable reel into the pipe. To perform this operation, it was most convenient to use the available laboratory crane to pull the cable vertically above the pipe elbow. Sufficient cable is pulled through the elbow to allow for assembly of the pothead termination and to allow for a residual length of cable for the purposes of conducting a bend test. With this operation completed, the cable is cut from the reel such that the other end can be installed through the remaining pipe elbow in a similar manner.

To install the potheads, the cable is first clamped with a centering plate located at the top of the pipe elbow, one end of the cable being fitted with a semistop joint to control the flow of liquid nitrogen. The vertical section of the cable is straightened, and the shielding tapes are removed before the stress cone and build-up rolls are applied. The build-up rolls allow the cable insulation diameter to be increased to match the inside diameter of the capacitor stack support tube. The complete capacitor stack, which is housed around a support tube, is then lowered over the build-up rolls. This portion of the assembly procedure is directly comparable to that used for conventional pothead assembly. The fiber-reinforced plastic, pressure vessel, including the foam thermal insulation and vapor barrier, is then lowered over the capacitor stack. To complete the assembly, corona rings are mounted at the top and bottom of the pothead.

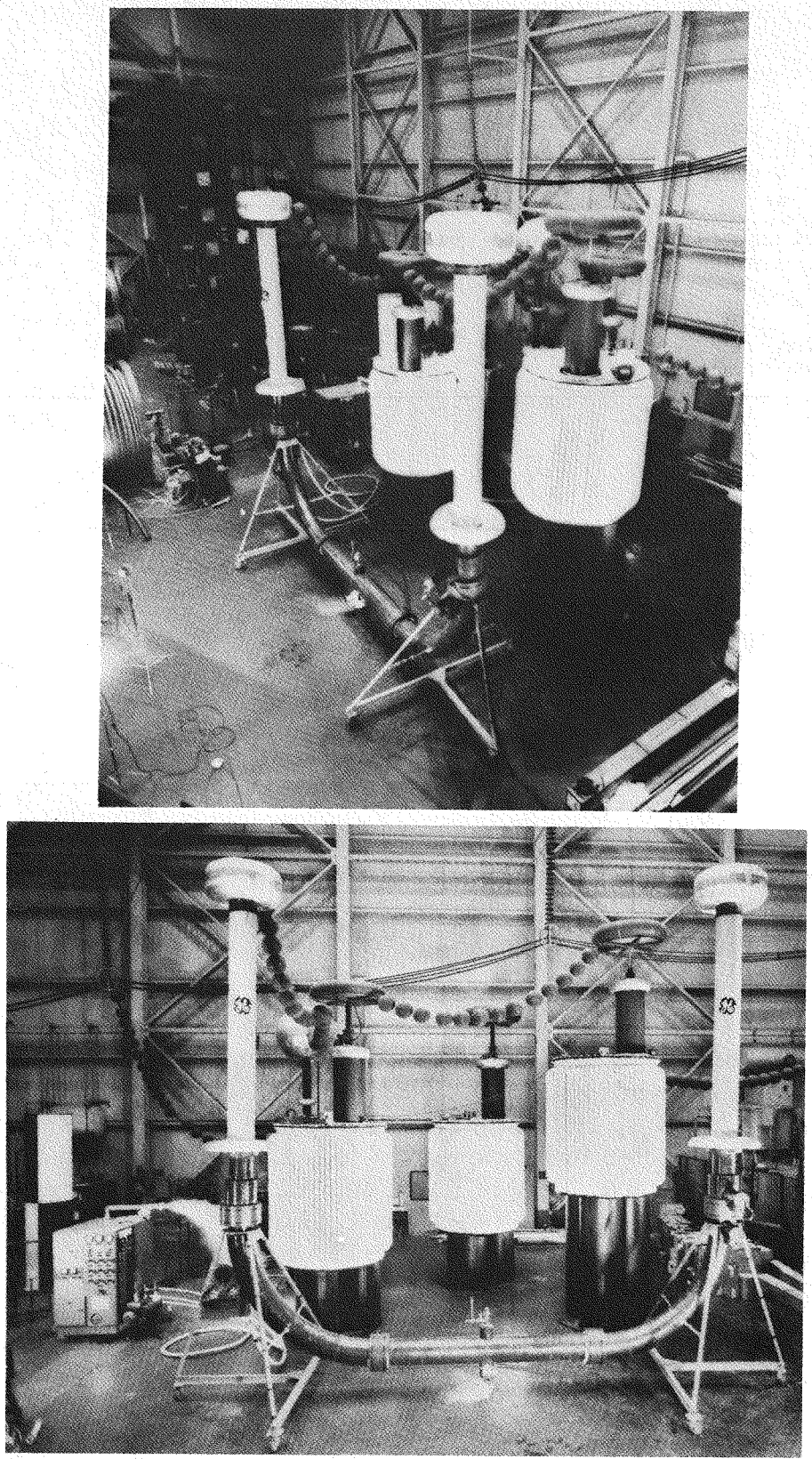

Figure 4-13. Overall Views Of The Cryogenic Cable High-voltage Test Equipment

COOLDOWN PROCEDURE

Prior to cooldown, the completed assembly is purged with dry nitrogen gas and is then evacuated with a mechanical vacuum pump to a pressure of approximately 100 microns for a period of approximately 24 hours. Before liquid nitrogen is introduced into the system, the system pressure is restored to one atmosphere with dry nitrogen gas.

The cooldown procedure may be completed in about ten hours from room temperature. Liquid nitrogen is allowed to fill the test equipment and the heat exchanger, gaseous nitrogen being vented from open valves at the top of each of the pothead structures. When liquid nitrogen is vented from the pothead valves, the valves are closed, and the pump is started to circulate liquid nitrogen through the system. This liquid nitrogen is cooled as it passes through the heat exchanger, and the system pressure rises slowly to 80 psig. A pressure relief valve mounted on the storage tank controls this pressure.

During cooldown, measurements of cable capacitance and dissipation factor were recorded with 25 kV applied to the cable conductor. Interpretation of these measurements indicated that the liquid nitrogen impregnation of the electrical insulation was complete after about six hours, but the system was maintained at low temperature and under pressure for an additional 12 hours before high-voltage tests were initiated.

In this series of cable tests, the cryogenic system components operated in a stable and reliable manner. Initial cooldown from room temperature (300 K) to liquid nitrogen (77 K) was accomplished by feeding liquid nitrogen to the test vessel and venting gaseous nitrogen from the potheads. Once the vessel was cool, flow was initiated by starting a liquid nitrogen pump. Because the pothead top is twenty feet above the pump level, no difficulties in starting the flow were encountered. After flow initiation, the system reached complete thermal equilibrium in a few hours, and was ready for test.

Steady-state flow conditions were reached almost immediately upon pump start-up. At no time was any flow instability, such as surging, evident. During the entire test sequence, the only system maintenance performed was the routine replacement of a worn pump shaft seal. Seal failure was gradual; the leakage of liquid nitrogen had increased to the point where the maintenance effort was justified. Dual pumps had been installed so that this maintenance could be performed without disturbing the test in progress.

Other system components, such as the heat exchanger and its level control, operated satisfactorily for the entire test period.

CRYOGENIC CABLE AND POTHEAD HIGH-VOLTAGE TESTS

The high-voltage tests were conducted at the Anaconda Wire and Cable Company laboratory. The laboratory is equipped with a series resonant set of test transformers, and standard capacitors, as required to conduct the tests described below. In the following descriptions of the five tests that were performed and the descriptions of the failure paths, it will be helpful to refer to the schematic diagram of the failure paths presented in Figure 4-14.

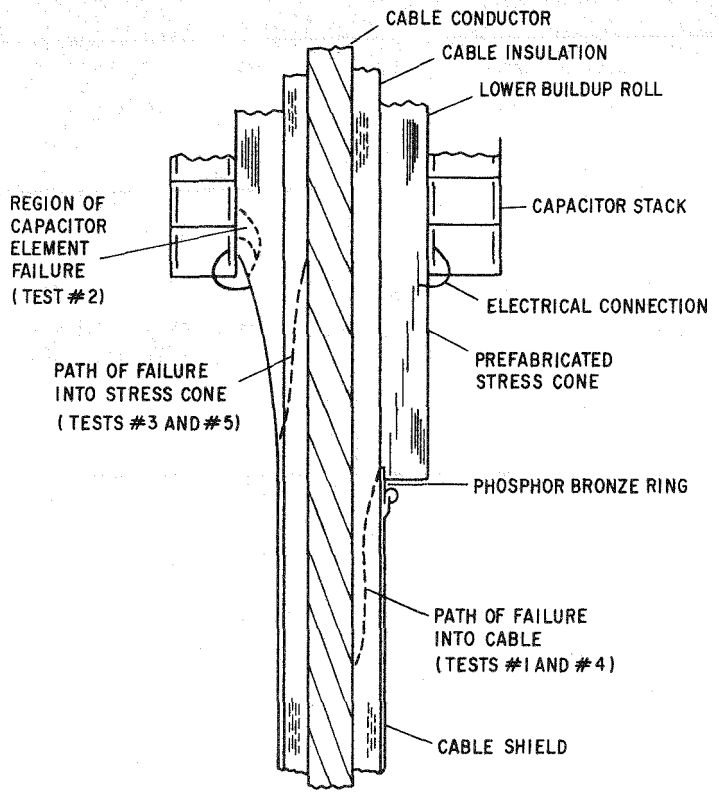

Figure 4-14. Schematic of Failure Paths at the Pothead Terminations

CABLE AND POTHEAD TEST #1

The first cable to be tested was the cable with a nominal insulation thickness of 0.550 inch. Power factor gaps were included at each end of the cable to permit separate measurements of dissipation factor on the cable, the two stress cones and the two capacitor stacks within the potheads.

A record of the cable test log for Cable #1 is shown in Figure 4-15. The measured dissipation factor at 25 kV was 0.0035, in accordance with the data presented in the Sixth Quarterly Report for a short length of this cable. Since the dissipation factor was dependent on the applied voltage,

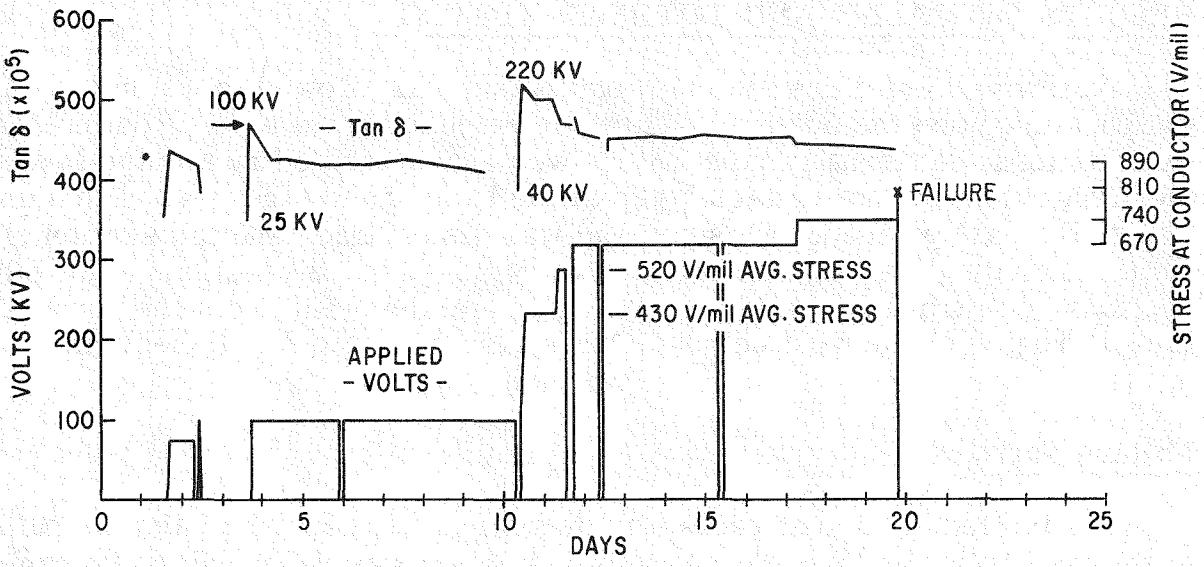

Figure 4-15. Cable Test Log (0.550-Inch Insulation)

the applied voltage was held constant at 100 kV for a period of one week. During this time, the dissipation factor decreased markedly. This conditioning phenomenon is well known in conventional cables, which use carbon-black screens, and has been observed in earlier work on cryogenic dielectric materials.

The voltage on the cable was increased to 236 kV and was held constant for a period of six hours. This voltage, which is an AEIC (Association of Edison Illuminating Companies) standard (Ref. 4-7) test, produced an equivalent average stress in the cable insulation of 430 V/mil. The voltage was then raised to 290 kV, the second part of the AEIC standard test, producing an average stress in the cable insulation of 520 V/mil. Again the dissipation factor was observed to decrease as a function of time, at constant voltage. The voltage was then increased from 290 kV in 10 percent voltage increments until a failure occurred as the voltage was being raised to 386 kV.

Two comments must be made concerning this breakdown. First, dissection of the failed region showed that the failure had occurred at the power factor gap between the cable and the stress cone of the east pothead termination. Thus, it can be argued that the intrinsic breakdown strength of the cable section was greater than the breakdown voltage applied in this test. Second, the breakdown was accompanied by a discharge in the standard capacitor connected to the high-voltage line for measurement purposes. This raises the question of whether or not the capacitor failed first, initiating a surge voltage across the cable power-factor gap, subsequently triggering the cable failure. This hypothesis is substantiated to some extent by a series of breakdown tests which were performed on the standard capacitor following the cable failure. In these tests, the standard capacitor failed in the range 350 to 400 kV; the nominal rating of the capacitor being 550 kV.

RESULTS OF CABLE AND POTHEAD TEST #1

Following the failure, the test equipment was allowed to warm to room temperature, and the outer vessels were removed from each of the pothead terminations. Externally, the failure was characterized by a bulge in the mesh shielding the power factor gap at the base of the stress-cone termination of the east pothead. This pothead was dismantled, and the section of cable, including the faulted region, was removed for dissection. Two other sections, one from the middle of the cable and the other from the power factor gap region of the west pothead, were also removed for dissection.

Failure Path

The faulted section of cable was dissected, tape by tape, and the path of the fault followed through the cable insulation was recorded. Diagrams of the fault path are shown in Figures 4-14, 4-16 and 4-17. In Figure 4-17, the zero reference points for the coordinate system are based on the external point of failure, at the power factor gap.

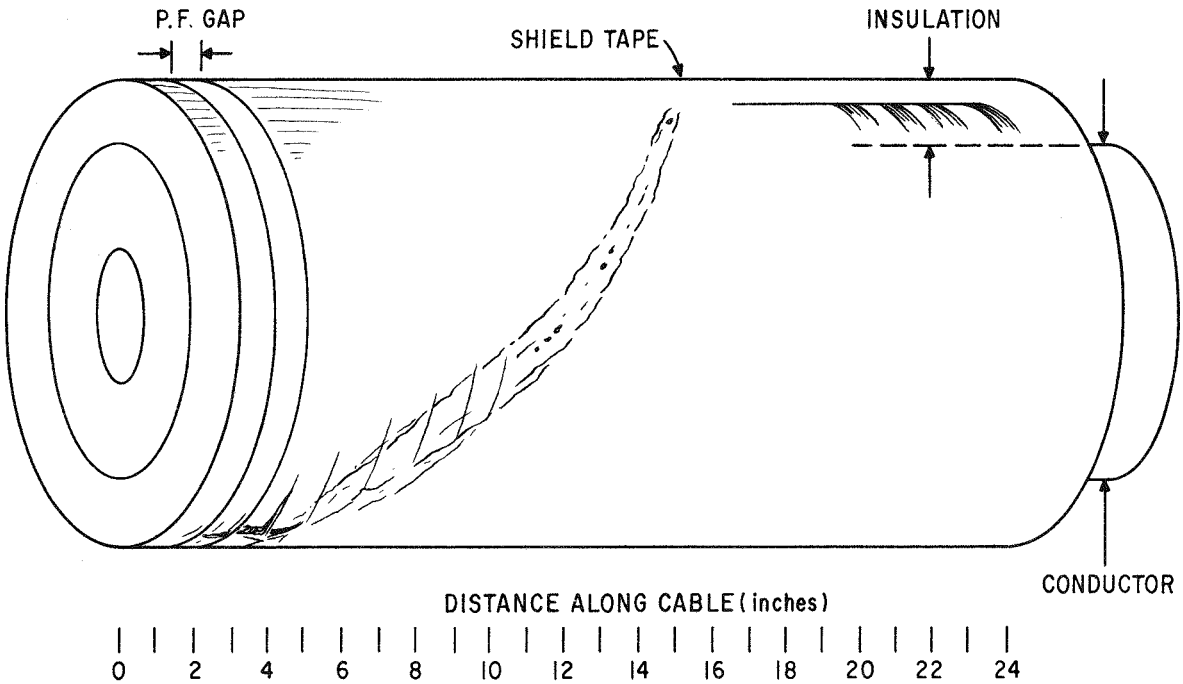

Figure 4-16. Isometric Diagram of Failure Path

The fault was found to progress in a spiral path from the power factor gap, turning approximately 180 degrees over a 15-inch length. The remainder of the fault path progressed axially from this 180 degree location for an additional length of approximately 9 inches. Along the complete length of this path, the fault moved radially inward toward the conductor.

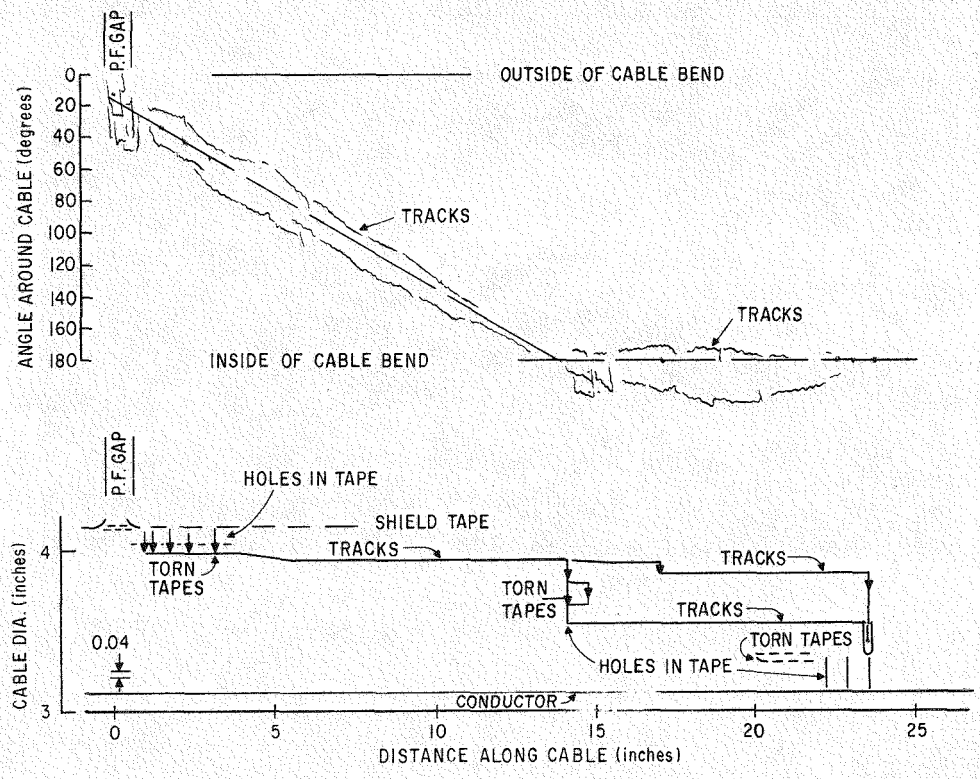

Figure 4-17. Cable Failure Path

That is to say, only the outer tapes were damaged near the power factor gap, and only the inner tapes were damaged near the conductor surface. The pitch of the spiral path bore no relationship to any pitch parameters involved in the cable construction, but the straight section of the fault path did follow a series of minor buckles in the cable tapes, at the inner radius of the cable.

Starting at the power factor gap, the path of the fault comprised a series of holes, radially, through the ten outer paper tapes. The fault then progressed radially inward along a spiral path, moving axially for 15 inches and moving circumferentially for 180 degrees. This path can be best described as a spiral path along the surface of a cone. The fault path then moved axially along the cable, working its way to the conductor surface in a series of radial punctures spaced in the axial direction.

At the conductor shielding tapes, a fibrous material (Figure 4-18) was intercalated with the carbon-black shielding tape. When magnified, this material appeared to be a shredded composition of cellulose paper. A more detailed examination by means of x-ray diffraction analysis and optical microscopy verified this conclusion. This material appeared to have been forced under the shielding tape by the arc. It comprised particles of cellulose paper and carbon-black tape and was not judged to be responsible for initiating the cable failure.

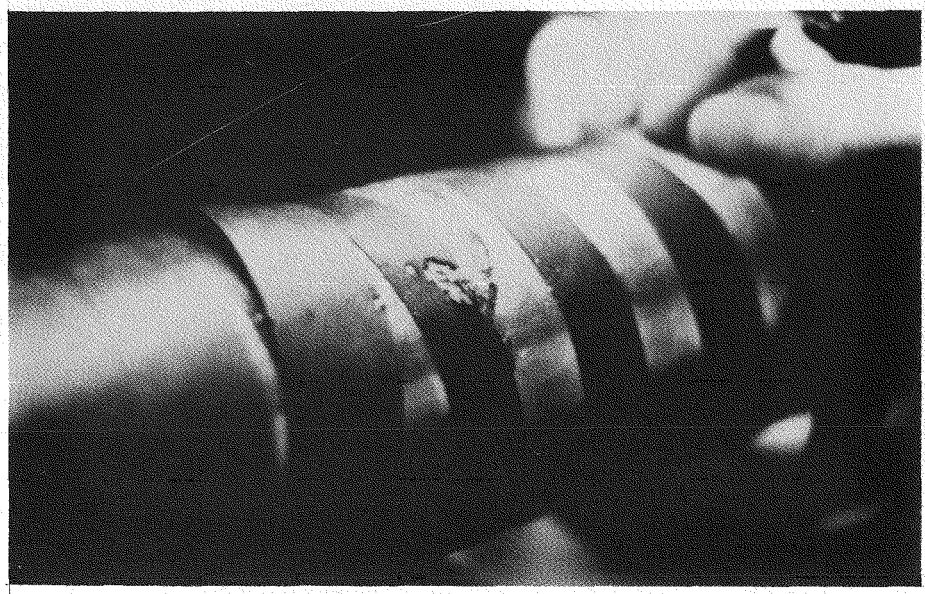

Figure 4-18. Intercalation of Fibrous Material with Shielding Tape

Cable Dissipation Factor

The dissipation factor values measured on the test cable were higher than desirable for an operational cable. However, it is almost certain that these values have resulted from the presence of the carbon-black (duplex) screens on the inside and outside surfaces of the electrical insulation.

In the Fifth Quarterly Report, breakdown strength and dissipation factor measurements were presented for two small samples (0.2-inch insulation thickness) with the same paper type as that used in the prototype cable. One of these samples used duplex screens; the other used a conventional carbon-black screen (CB-97-C). In summary, these measurements showed dissipation factor values of approximately 1340 microradians for the sample that used the conventional carbon-black screen, and 5900 microradians for the sample using the duplex screen, a fourfold increase in the dissipation factor directly attributable to the duplex screen. Dissipation factor values are also discussed under the "Characterization of Cellulose Paper Insulation" section of this report.

In view of this experience, it is clear that consideration should be given to removing or modifying this screen in future prototype cable development.

CABLE AND POTHEAD TEST #2

The second cable to be tested was the cable with a nominal insulation thickness of 0.860 inch. Power factor gaps were not included at the transitions between the cable shield and the stress cone shields in view of the experience obtained in testing the first cable section.

A record of the test history for this second cable section is presented in Figure 4-19. No problems were encountered in raising the voltage on this second cable until a discharge occurred on the west pothead measurement leads, when the voltage applied to the cable was 430 kV line-to-neutral. One end of this measurement lead was connected to the lowest element of the capacitor stack, and the other end was connected to ground, just outside the west pothead. The discharge was observed at the point where this measurement lead exited from the pothead feedthrough. The test system was warmed to ambient temperature to permit examination of the pothead capacitor stack. However, removal of the pothead pressure vessel revealed no evidence of capacitor damage.

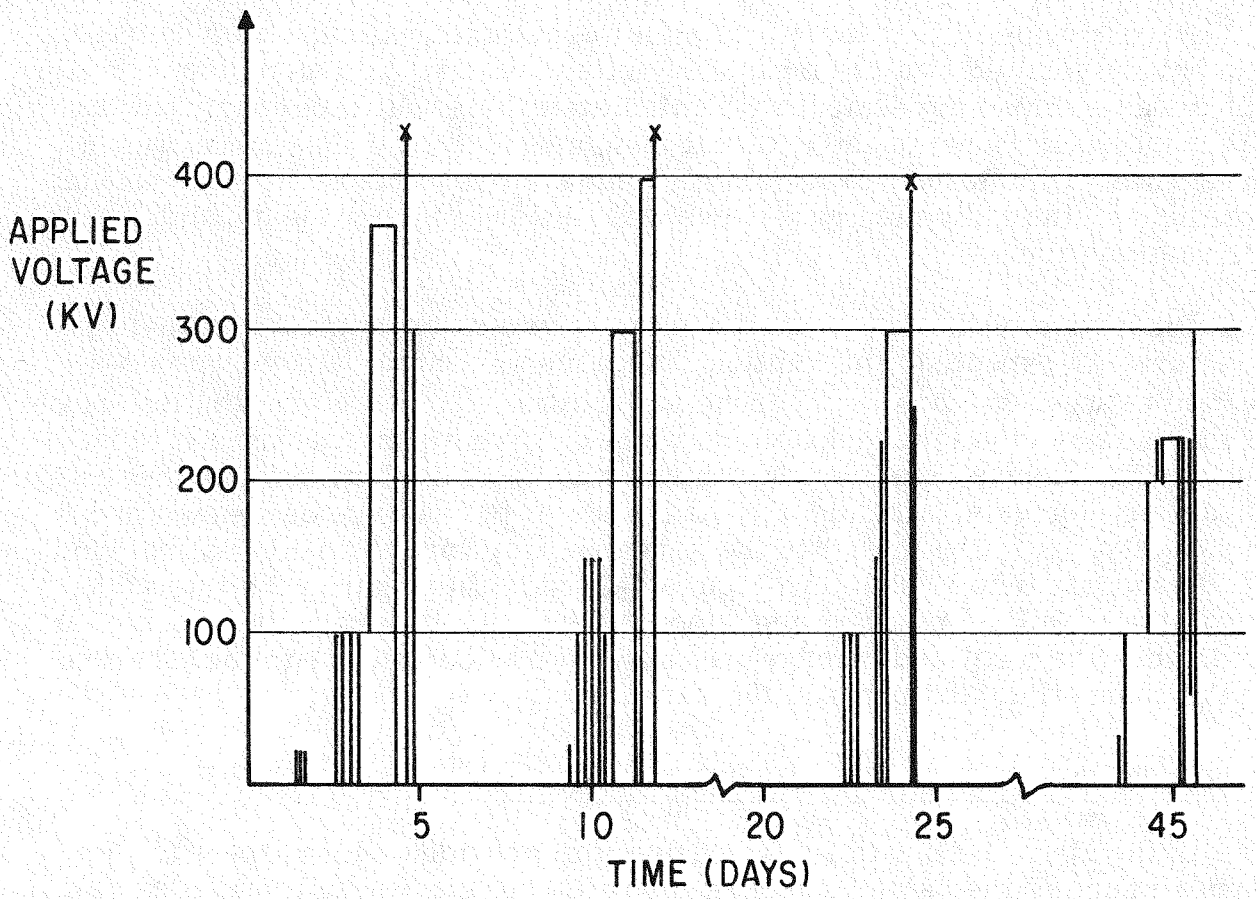

Figure 4-19. Cable Test Log #2 (0.860-Inch Insulation)

A second set of backup capacitors was installed to resume the tests. The system was recooled to low temperature and voltage was applied to the system in steps up to 430 kV. At this stage, it was necessary to shut down the test equipment to make adjustments to the measurement circuitry. The test equipment was not warmed to ambient temperature while these adjustments were made.

As the voltage was raised for the third time, a discharge occurred on the west pothead measurement lead at an applied voltage of 400 kV, similar to the discharge observed in the first test of this cable section. In this case, the system was allowed to warm to ambient temperature, and both pothead pressure vessels were removed to allow inspection of the terminations. With the system warmed to ambient temperature, the voltage distribution along the capacitor stack was measured with an electrostatic voltmeter. These measurements indicated that the ratio of maximum to average voltage across any one capacitor was less than 1.4:1. This measured value was in close agreement with the calculated values of 1.3:1 and 1.6:1, depending on the assumptions of stray capacitance values. Thus, there was no evidence of poor voltage distribution along the capacitor stack.

Having verified that there was no apparent external capacitor damage, and having verified that the measured voltage distribution along the capacitor stack was in close agreement with calculated values, it was concluded that the most likely cause of the external measurement lead discharge was a breakdown of the lowest capacitor element at high voltage. To confirm this conclusion, the individual capacitors were removed from the capacitor stack for examination.

Dissection of the lowest capacitor in the stack revealed a foil-to-foil puncture, as expected. In addition, evidence of corona damage was observed between the first and second capacitors. To determine the full extent of the damage, the other capacitors were removed from the support tube, and it was observed that corona damage was apparent between the next seven capacitor elements, although the magnitude of the damage decreased progressively, from the lowest to the seventh capacitor. The corona marking of the support tube is shown in Figure 4-20. In this figure, the lowest capacitor is still in place on the support tube. At each capacitor/capacitor interface, the localized damage was observed to coincide with the location of the connecting tabs between the capacitors.

RESULTS OF CABLE AND POTHEAD TEST #2

In the above test, little information was provided with respect to the performance of the cable, although the cable did successfully withstand an applied voltage of 430 kV without failure.

However, the test did provide valuable information on the performance of the pothead termination. The question that must be answered is why did the capacitor elements fail at approximately 430 kV (equivalent to a capacitor voltage of 15 kV) when individual capacitor breakdown voltages had been measured at 27 kV in earlier tests.

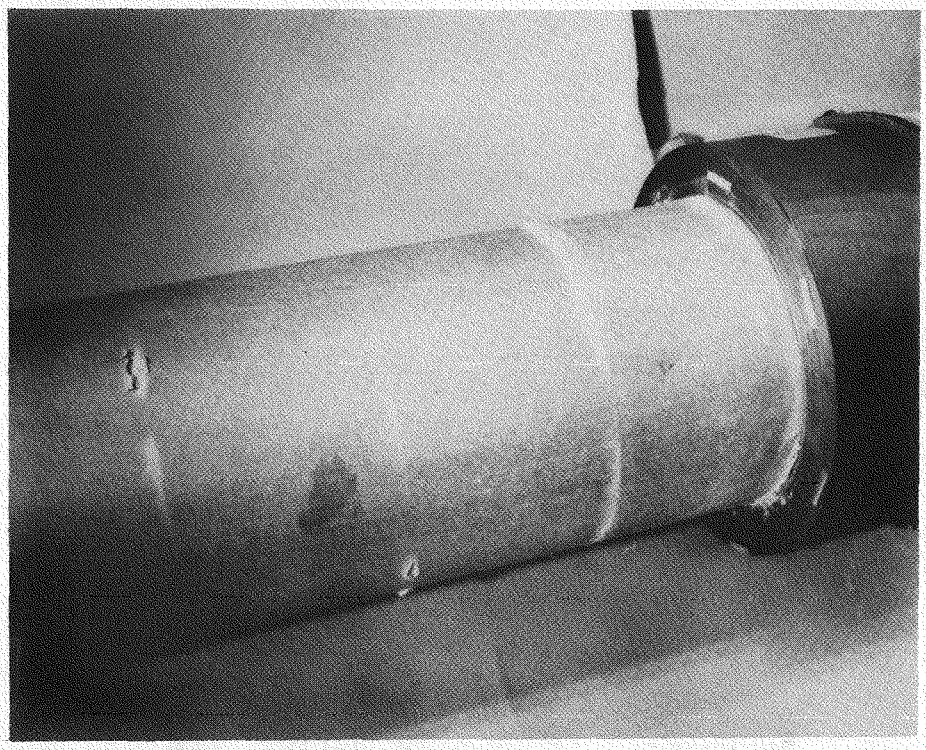

Figure 4-20. Corona Marking of Capacitor Support Tube

To answer this question, it is necessary to refer to Figure 4-21. This figure shows a schematic of the lower two capacitor elements in the capacitor stack, and is approximately to scale. In the following text, the electrical stresses in regions 1 through 6 will be discussed, and these regions are shown in the figure. In region 1, the electric stress between the foils of two adjacent capacitor elements is essentially axial, although a small radial component exists due to the presence of the cable conductor. In region 2, the electric stress between the adjacent foils of one capacitor element is purely radial. In region 3, the stress in the liquid nitrogen interface beneath the capacitor foils is purely radial. This stress is a maximum under the lowest capacitor, and is progressively reduced to zero under the uppermost capacitor element. In region 4, the stress is also radial, and is similar to that in region 3. In region 5, the stress at the conductor surface is purely radial. In region 6, the stress is primarily radial, with a small component of axial stress (approximately 10 percent of the radial stress). The stress distribution in region 6 is not intuitively obvious, and has been derived for this particular geometry by analog computer and analytical techniques. It is in region 6 that the damage was observed in Test #2.

In the Third Quarterly Report, pages 39 to 42, a description of the tests that were conducted on identical capacitor elements prior to the design of the pothead termination is presented. In these tests, six capacitor elements were tested -- two sets of three, series-connected capacitors, back-to-back. This test was designed to simulate the stresses that would occur in regions

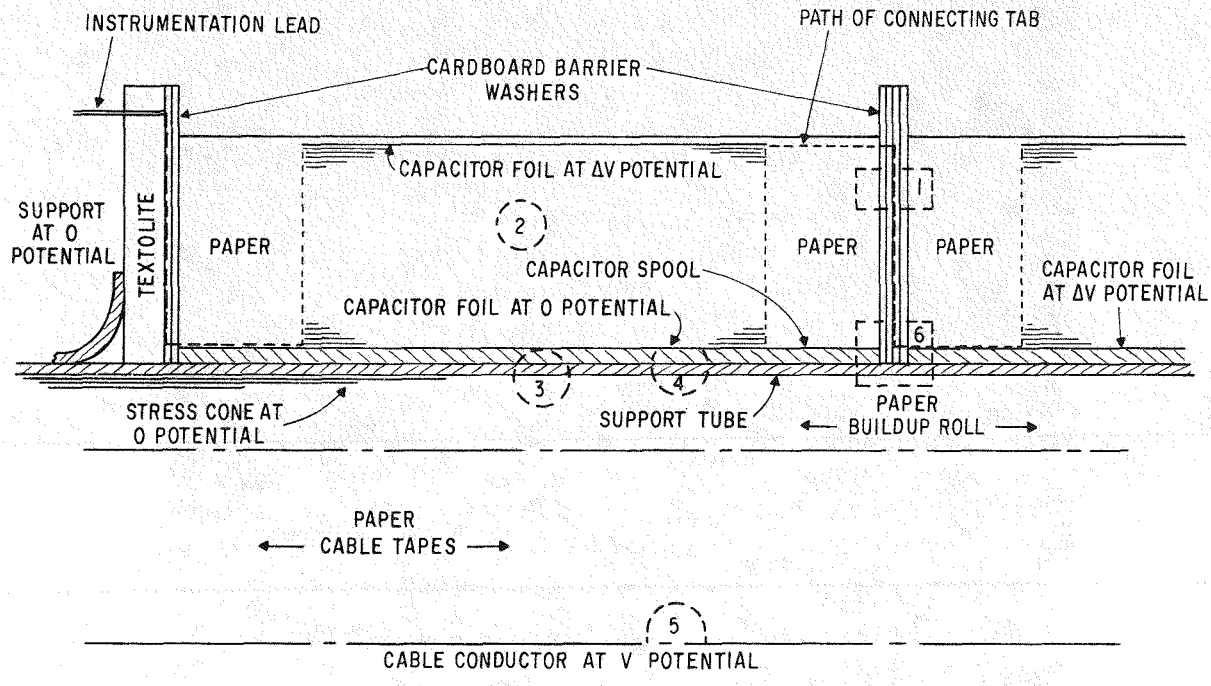

Figure 4-21. Pothead Capacitor Detail

2 and 3 (refer to Figure 4-21) of the final pothead assembly. These regions were believed to be particularly critical to the pothead design, and it was the objective of this simulated test to determine the limiting stresses in region 2, between capacitor foils, and in region 3, in the liquid nitrogen interface beneath the capacitor elements. To accomplish this objective, it was necessary to adjust the conductor diameter in this simulated test, such that the ratio of stresses in regions 2 and 3 of the simulated test was identical to the ratio of stresses in regions 2 and 3 in the final pothead. To accomplish this modeling similarity, it was necessary to increase the diameter of the cable conductor, but doing so reduced both the axial and radial stresses in region 6. This situation is summarized in Table 4-6 below:

Table 4-6

COMPARISON OF STRESSES IN SIMULATED AND FINAL POTHEAD TESTS

Test	Electrical Stress (V/mil)			
	Region 1	Region 2	Region 3	Region 6
Simulated Test (Two sets of 3 Capacitors)	47	667	428	65.0 – Radial 3.9 – Axial
Pothead Test (38 Capacitors)	27.5	391	290	129.0 – Radial 15.7 – Axial

The data in this table provide an explanation of why the capacitors failed in the pothead tests, but did not fail in the simulated test; clearly, they were overstressed in region 6.

In retrospect, it is not obvious that simple simulated tests could have been performed to evaluate the performance of the pothead in this region 6. In any model simulation, it is rarely possible that parameters can be accurately simulated in all regions.

In the future, it is believed that some simple steps can be taken to reduce the stress in this region. One obvious approach is to increase the overall diameter and length of the pothead to reduce the stresses. However, this would require a complete redesign and reconstruction of the pothead components. To avoid a complete redesign, it was believed that modification of the end region of the capacitor elements would permit the attainment of higher voltages, although this approach is not regarded to be as reliable as increasing the pothead diameter by one or two inches.

CABLE AND POTHEAD TEST #3

In view of the potential limitations to testing at higher voltages presented by the pothead terminations, it was decided to use the remaining cable sections for longer term tests at lower voltages. In this third test, the objective was to monitor the performance of the cable section with an insulation thickness of 0.550 inch at 1.5 times rated stress (1.5 x 400 V/mil) over a period of two weeks. This required a maximum test voltage of about 286 kV. The test configuration was the same as that for Test #1, except that the capacitor elements in the two pothead terminations were graded to provide a more uniform voltage distribution along the length of the pothead. Before the pothead pressure vessel was installed, the voltage distribution along the capacitor stack was measured at room temperature by means of an electrostatic voltmeter to verify that the voltage distribution was uniform. The ratio of the maximum to average voltage was improved from approximately 1.4:1 to approximately 1.08:1. The pothead assembly was completed and the test system was cooled to liquid nitrogen temperature.

The voltage was applied to the cable section in increments as shown in Figure 4-22. After $1\frac{1}{2}$ hours at 286 kV, a failure occurred. The failure was unexpected since the first cable section had successfully withstood a higher voltage (290 kV) for a period of approximately eight days.

RESULTS OF CABLE AND POTHEAD TEST #3

The pothead terminations were disassembled and evidence of the failure was apparent at the base of the stress cone termination of the west pothead. Sections of the stress cone were removed from each end of the cable, and the center section of the cable was also removed for dissection and examination.

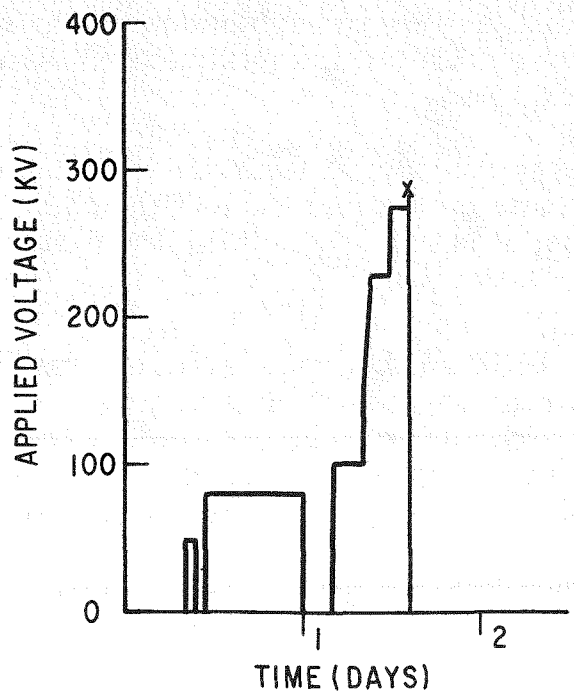

Figure 4-22. Cable Test Log #3 (0.550-Inch Insulation)

Failure Path

One end of the failure path originated at the upper edge of the phosphor-bronze strip (~10 mils thick) used as an anchoring point for the ground shield of the stress cone. The failure region is shown in Figure 4-23 where typical corona damage is observed to extend for approximately 80 degrees around the edge of the phosphor-bronze strip.

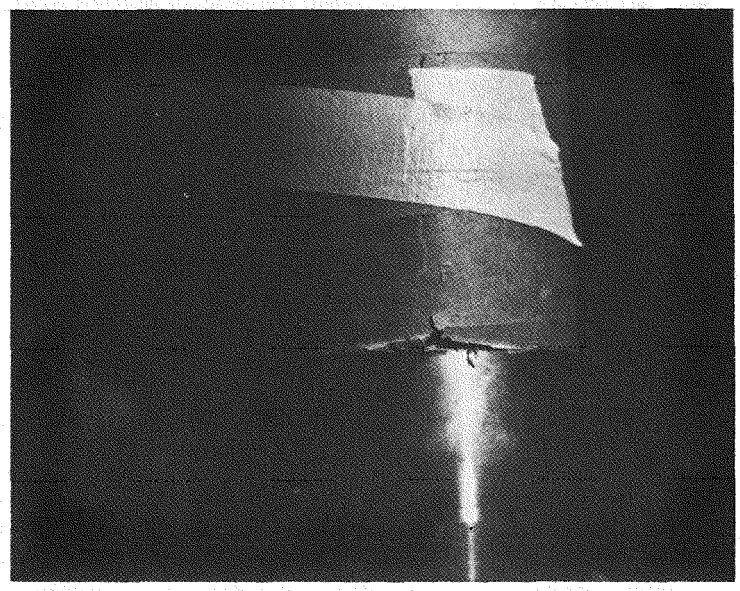

Figure 4-23. Failure Corona Damage

At the center of this region, the failure path extends inward toward the cable conductor for ten tape thicknesses and then moves axially along the cable insulation. The failure path is shown schematically in Figure 4-24. The path of failure was similar to that shown in Figure 4-17, but was approximately 39 inches long. In the case of Test #1, the failure path progressed along a spiral path toward the cable test length whereas the failure path in this third test progressed upward toward the stress cone, showing little circumferential deviation. Furthermore, only 10 to 12 tapes were punctured in this third test; the failure path progressed axially by penetrating the butt gaps. The point of termination of the failure path at the conductor surface was not associated with any discernible imperfection in the conductor or shield geometry.

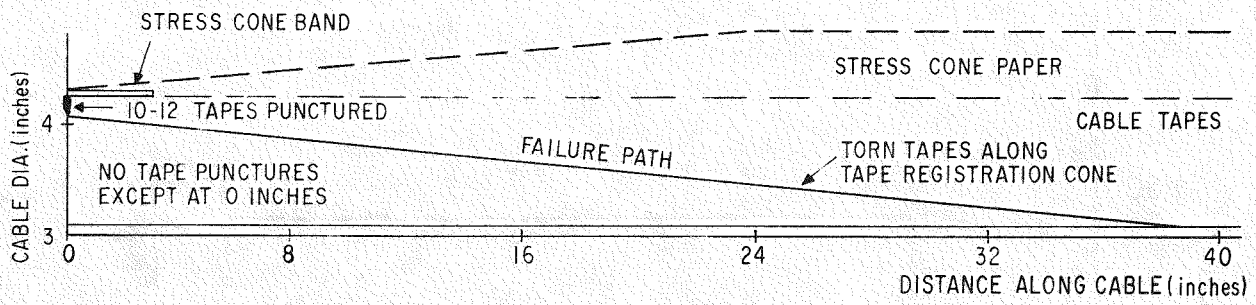

Figure 4-24. Test #3 Failure Path - West End

Although the phosphor-bronze strip had been in close contact with the stress cone on assembly, there was an apparent clearance between the strip and the stress cone when the failure region was disassembled. The clearance at the edge of the strip was approximately 0.030 inch. The results from this test were somewhat ambiguous. No clear explanation for the low breakdown voltage was ascertained, although the phosphor-bronze strip clearly contributed to the failure. No evidence of damage or corona action was apparent in the cable test length or in the east pothead termination.

CABLE AND POTHEAD TEST #4

The unsatisfactory performance of the test system in Test #3 clearly indicated that greater attention had to be paid to the construction or configuration of the stress cones at the ends of the cable test length. The objective of Test #4 was the same as the objective of Test #3: to monitor a section of the cable with an insulation thickness of 0.550 inch at 1.5 times rated stress for a period of two weeks. The component configurations were the same as those used for Test #3 with particular attention paid to the construction of the stress cone terminations. The prefabricated stress cones applied for this Test #4 were "tighter" than the stress cones used in Test #3. Within the same inside and outside diameter limits, more turns were applied to the stress cone roll. It was concluded that the final termination and stress cone

configuration was probably the best that could be accomplished using the standard stress cone rolls; no other obvious improvement being possible with this combination of components.

The voltage was applied to the cable section in increments as shown in Figure 4-25. After reaching 286 kV (600 V/mil maximum stress) the voltage was maintained constant for a period of 20 days. At the end of the 20-day period, the voltage was raised to 315 kV for a period of four days, and a failure occurred as the voltage was raised to 330 kV. Although this test was completely successful in demonstrating the stable operation of the cable test length and potheads at 1.5 times rated stress for a period of 20 days, the ultimate breakdown voltage was lower than anticipated.

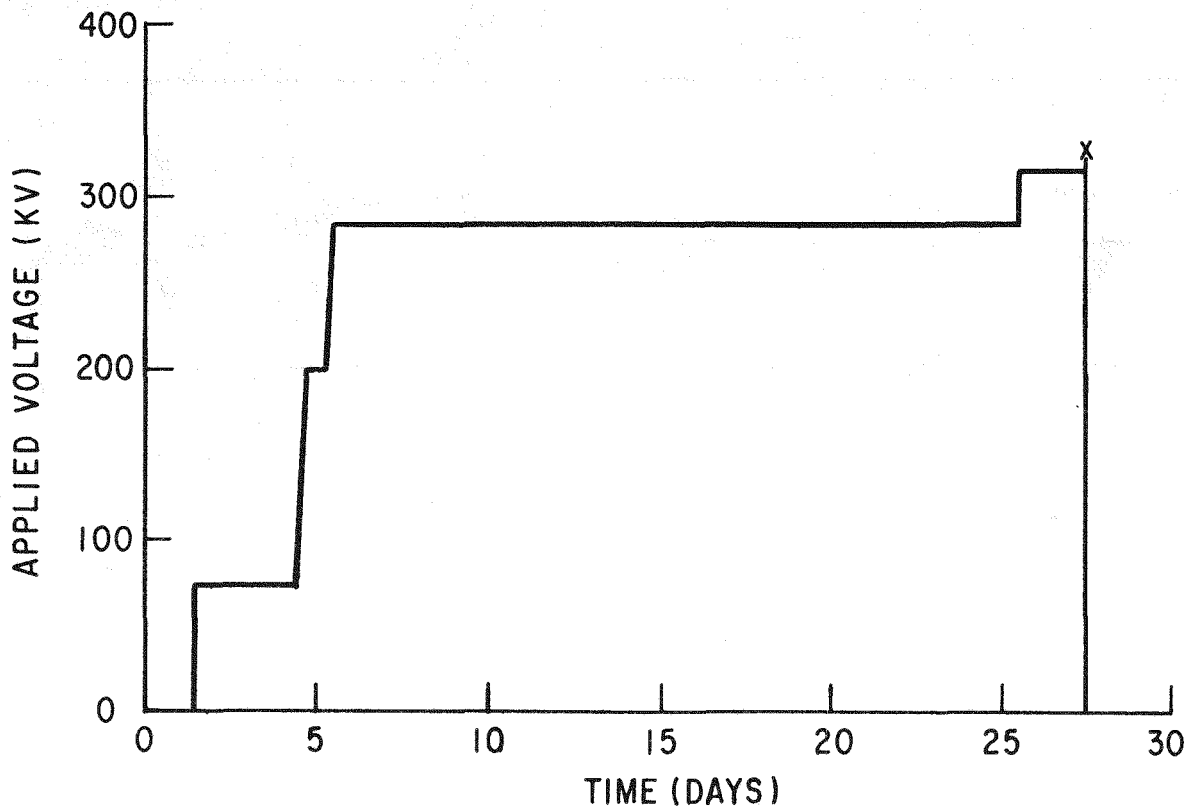

Figure 4-25. Cable Test Log #4 (0.550-Inch Insulation)

RESULTS OF CABLE AND POTHEAD TEST #4

As the test equipment was disassembled, it was apparent that the failure had again occurred at the phosphor-bronze strip of the east pothead and had progressed downward into the cable. The failure path, shown in Figure 4-26 was approximately 26 inches long in the axial direction and was similar in character to the failures observed in Tests #1 and 3 with the exception that the failure path was radially directed after it had progressed 26 inches

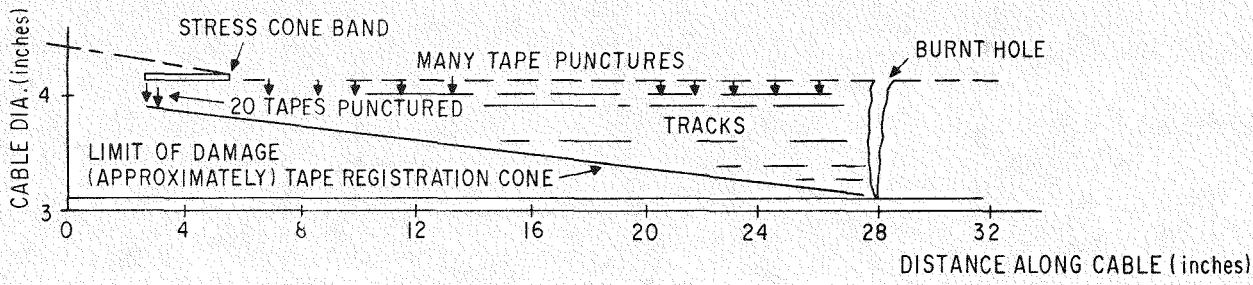

Figure 4-26. Test #4 Failure Path - East End

axially. In Test #3, the failure path at the west pothead had progressed upward into the stress cone and cable. In Test #4, the failure path occurred at the east pothead and progressed downward along and through the cable insulation. No evidence of corona damage was apparent in the cable test length.

CABLE AND POTHEAD TEST #5

In an attempt to overcome the termination limitations that had arisen in the other tests, it was decided to discard the prefabricated stress cone rolls in favor of a hand constructed stress cone. This permitted the application of a carbon-black screen and a ground screen over the entire length of the stress cone log-log profile. It was also possible to increase the length of the stress cone from 24 to 30 inches, reducing the axial stress in the region from approximately 10 V/mil to 8 V/mil at 400 kV. In all other respects, the test configuration and cooldown procedure were identical to those used in Tests #1, 3 and 4. This stress cone construction is shown schematically on the left-hand side of Figure 4-14.

The objective of Test #5 was to establish the breakdown strength of the cable section with an insulation thickness of 0.550 inch. No attempt was made to repeat the time at voltage test conducted in Test #3. The voltage was raised to 286 kV in accordance with the plot shown in Figure 4-27. The voltage was maintained constant at 286 kV (600 V/mil) for a period of approximately two days and was then raised in 10 percent increments. A failure occurred as the voltage was being raised from 381 to 400 kV.

RESULTS OF CABLE AND POTHEAD TEST #5

The failure occurred at the west pothead, and was initiated at the cable end of the stress cone. There was no apparent defect at the outside surface of the stress cone that caused the failure. Again, the failure path progressed along the cable insulation as it moved upward under the stress cone toward the cable conductor. The path is shown in Figure 4-28. The test was unsuccessful in determining the breakdown strength of the cable test length, no evidence of corona damage being apparent in the test length.

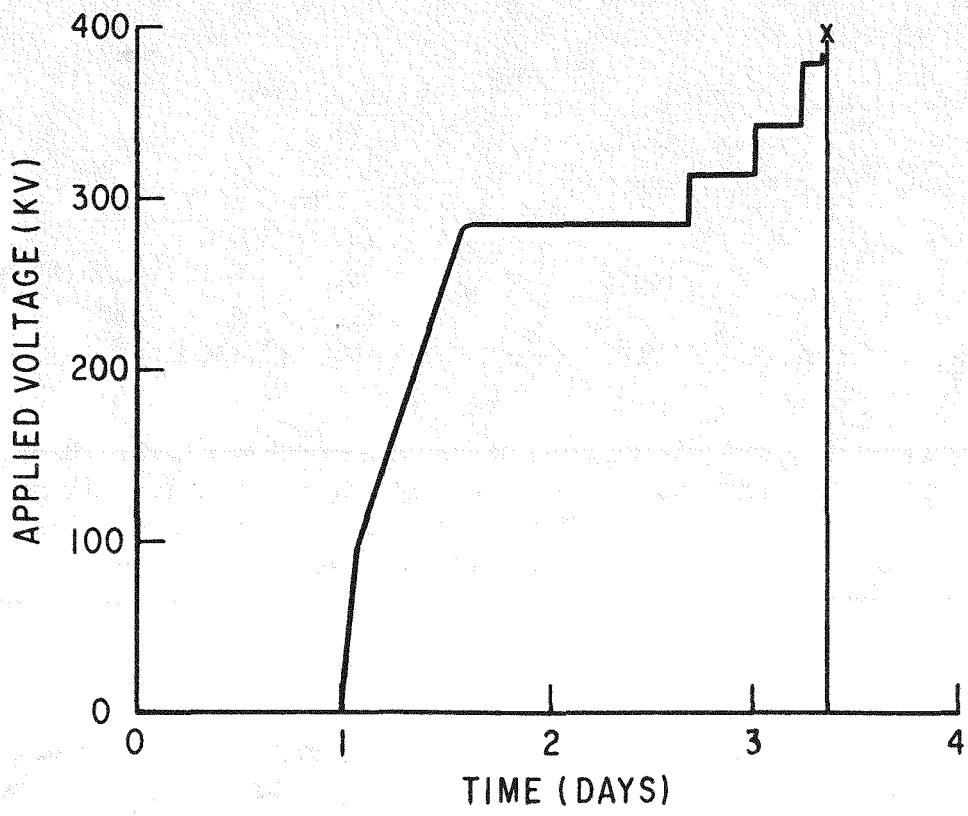

Figure 4.27. Cable Test Log #5 (0.550-Inch Insulation)

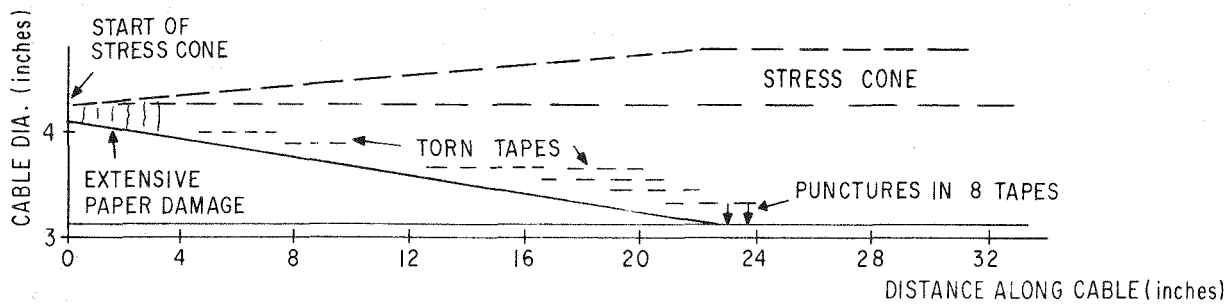

Figure 4-28. Test #5 Failure Path - West End

Examination of the capacitor elements at the conclusion of this test showed some minor evidence of corona damage close to the lowest capacitor element; this element being the most highly stressed element. Apparently, the steps taken to provide a more uniform stress distribution along the length of the capacitor stack had been successful.

CONCLUSIONS

The results of the five cable tests are summarized in Table 4-7.

Table 4-7

SUMMARY OF CABLE TEST RESULTS

Test No.	Cable Insulation (mils)	Maximum Voltage (kV)	Cable Stresses (V/mil)		Failure Location
			At Conductor Surface	Average	
1	550	386	830	702	East Power Factor Gap
2	860	430	632	500	West Capacitor Stack
3	550	286	615	520	West Stress Cone
4	550	330	710	600	East Stress Cone
5	550	400	860	727	West Stress Cone

The results of Test #2 are unique in that a pothead capacitor stack was involved in the failure, and there was no apparent damage to any part of the cable. In the remaining four tests, some form of cable damage was involved immediately adjacent to the stress cone termination, but no evidence of any failures existed in any part of the cable test lengths. In each of these four failures, the failure path was associated with the discontinuity that occurs as the outer cable ground screen is transitioned to the outer ground screen of the stress cone termination. The following conclusions are drawn from the aggregate of the experience gained in obtaining these test results:

- The intrinsic breakdown strength of the cable test length was not reached in any one of these tests. In two tests (Tests #1 and #5), stresses greater than twice the assumed operating stress (400 V/mil) were achieved. In one test (Test #4), the cable test length successfully withstood 1.5 times rated stress (600 V/mil) without failure for 20 days. In summary, these results indicate that the basic cryogenic cable insulation concept is technically sound. The intrinsic strength of the cable insulation is still a matter of some speculation.

- The physical parameters of the cable relating to moisture content and bending must be reexamined. As stored, the present cable sections were shown to have absorbed moisture which resulted in objectionable bending characteristics. Just what impact these mechanical imperfections had on the breakdown strength of the stress cone terminations is unknown, but the irregular cable geometry certainly had an impact on the ability to construct uniform and high-quality stress cone terminations and build-up rolls. This could well be a factor in explaining the low breakdown strength of the stress cone terminations. In the future, however, it will be necessary to either keep the cable dry as it is installed or manufacture the cable with

paper equilibrated to ambient humidity. Since moisture has never been shown to have a detrimental effect on the electrical properties of the cable insulation, the latter approach is a distinct possibility.

- There is every indication that the time-at-voltage performance of the cryogenic cable insulation will be entirely satisfactory. In the small sample aging tests that were performed as a part of this program, the voltage exponent in the Weibull voltage-time relationship was shown to be approximately 38. Thus a cable which successfully withstands 1.5 times rated stress for a period of two days would be equivalent to a cable at rated stress for a period of 27,000 years. Cable #4 withstood 1.5 times rated stress for 20 days without failure and cable #5 withstood 1.5 times rated stress for two days without failure.

- If the intrinsic breakdown strength of the cryogenic cable sections is to be measured in the future, it will be necessary to improve the stress cone termination configuration. It should be noted that the stress cones used in the present tests were designed according to the best state-of-the-art in oil/paper cable technology. A further post-facto observation, however, is that the radial stress at the outer surface of the cable insulation is approximately twice that in the 500/550 kV Waltz Mill cables when both cables are operating at the same maximum stress at the conductor surface. Thus, in designing the stress cones, it may not be appropriate to consider the maximum axial stress alone -- a commonly used criterion. Rather, it may be necessary to consider the combination of radial and axial stresses in the stress cone. This argument is supported to some extent by the diagnosis of the failures in the stress cone region described in the text.

- It is anticipated that some redesign of the pothead terminations will be desirable to permit testing at higher voltages. More attention should be given to grading the capacitors to provide a more uniform axial stress distribution. An on-site modification of the capacitor elements to achieve some partial grading was certainly beneficial in improving pothead performance. Before the potheads were modified, some evidence of corona action was apparent between capacitor elements at a voltage of 300 kV, whereas test voltages of 400 kV were achieved after the modification without producing any significant corona damage. As evidenced by the results of Test #2, it is probably desirable to increase the pothead diameter to reduce the radial stress at the inside diameter of the capacitor elements.

- With respect to the above two comments, it should be noted that in each of the five tests the minimum stress achieved in the cable test lengths was 1.5 times rated stress. Thus, in considering the steps necessary for the pothead and stress cone redesign, the differences between designing for operating conditions and designing for test conditions must be kept in mind.

- While the cable dissipation factor measured in these tests was undesirably high, the analysis presented in the Fifth Quarterly Report shows that this anomaly is entirely attributable to the particular carbon-black screens that were used in the test cable. More care in the selection of the carbon-black tape, or consideration of removing the tape, should be given in future cable designs.
- Comparison of this series of cable tests to the tests performed in 1970 on cryogenic polyethylene paper cable shows a marked improvement in estimated breakdown strength. The polyethylene cable failed in the test length at a maximum stress of 640 V/mil. No failures were observed in the test lengths of the cable in the present series of tests at stresses up to 860 V/mil.
- It should be noted that the direction of the failure path in each of the tests was apparently governed by the registration of the tapes within the cable. Using the phosphor bronze strip at the outside surface of the stress cones as a reference point, all failures at the east pothead progressed downward toward the cable conductor, and all failures at the west pothead progressed upward under the stress cone toward the cable conductor. Since the cable was always installed in the test equipment in the same direction, the failures always progressed from the outside of the cable insulation toward the conductor along the same "steps" of the 35/65 registration. This does indicate that some improvement might be realized in the breakdown strength of the stress cone region by changing the registration of the cable tapes. However, the selection of tape registration is not solely dependent on electrical effects but must also weigh the mechanical parameters of the cable.

Section 5

TEST SYSTEM SPECIFICATIONS

The electric utility industry's acceptance of the application of any new technology can only come about after a period of demonstrated reliable performance, and some reasonable expectation of economic benefit. Thus, it is generally recognized that any of the advanced underground transmission systems presently being developed will have to prove themselves in some form of demonstration or qualification test before they will be accepted by the industry. Such tests will necessarily involve a configuration in which all of the major system components are brought together and are operated under actual or simulated power system conditions. The precise nature of such a test is often the subject of some debate which generally centers on the important trade-off between the overall costs of constructing and testing such a system, and the breadth and depth of the technical information to be drived from such a test.

Clearly, a test system configuration which is designed to demonstrate every facet of a full-scale cryogenic cable system will be more expensive than a test system which demonstrates one component or one parameter only. Thus, it is believed to be desirable to build a test system which is capable of demonstrating the key technical features of the prototype system in a cost effective and timely manner. On this basis, it is recommended that the future test system demonstration for a cryogenic cable system incorporate the following components:

- Three-phase, cryogenic cable sections
- Foam-insulated, FRP cable envelope, including expansion bellows and anchors
- Cryogenic pothead terminations
- Cable splices

The above list includes the major components of a cryogenic cable system, with the exception of the cryogenic refrigerator, which is absent from this list; the refrigerator is discussed later in this section. What are believed to be the key technical features to be demonstrated for each of these major components are listed below:

Cryogenic Cable

- The manufacture of a significant cable length (approximately 3000 feet) with dimensions which are representative of those required for an operational system

- The application of installation and cable-pulling techniques for three-phase cable sections of significant length (approximately 500 feet) in the field, including straight lengths and bends

- The application of rated voltage to all three cable phases

- The circulation of full-load current through all three cable phases

- The measurement of cable dissipation factor and corona level

- The qualification of the cable sections for system BIL ratings

- The measurement of conductor losses at full load. This measurement will necessarily be combined with the pipe loss measurement

- The measurement of fluid pressure drop and temperature rise in the bores of the cable sections

- The ability of the cable sections to accommodate thermal contraction and expansion

Foam-Insulated, FRP Envelope

- The manufacture of significant lengths of cable envelope (approximately 1000 feet) with dimensions which are representative of those required for an operational system

- The application of installation and joining techniques in the field, including the following components:

  - Straight FRP and curved metallic pipe sections
  - FRP/FRP pipe couplings
  - FRP/metal flange couplings
  - Thermal insulation
  - Pipe anchors and expansion bellows

- The measurement of pipe losses under full-load conditions

- The ability of the envelope sections to accommodate thermal contraction and expansion

- The measurement of the combination heat leak of pipe and joint sections

- The measurement of fluid pressure drop and temperature rise

Cryogenic Pothead Terminations and Cable Splices

- The manufacture of full-scale pothead and splice components
- The application of installation and assembly techniques for the pothead and splice components in the field, including conductor welding techniques
- The application of rated voltage to the potheads and splices
- The qualification of the potheads and splices for the system BIL rating
- The circulation of full-load current through the potheads and splices, including the low-temperature to ambient temperature transition joint of the pothead, and the conductor/conductor joint of the splice
- The measurement of pothead and splice dissipation factor and corona levels
- The measurement of fluid pressure drop and temperature rise
- The ability of the potheads and splices to accommodate the forces imposed by thermal contraction and expansion

On the basis of the above requirements, it is recommended that the test system be designed and constructed as a three-phase system. The accurate simulation of eddy currents in the cable conductors and in the electromagnetic shield of the envelope cannot be accomplished in a single-cable or two-cable configuration, and the interpretation of ac loss measurements in such configurations is always open to question.

At the present time, a nominal test system rating of 500 kV, 3500 MVA is recommended. This rating is in the middle of the range of ratings, 2000 to 5000 MVA, over which cryogenic cable systems are believed to be economically attractive. The overall length of the test system is more difficult to select. For a full-scale system simulation, the test system would have to be five to ten miles long, to be representative of the length of one "module" of the cable system. That is the distance between adjacent refrigeration stations which is expected to be in the range five to ten miles. However, the construction of a five- or ten-mile test system would provide little additional technical information for the cable, envelope, potheads and splices, compared to a much shorter length. Extrapolation of data derived from a shorter length would appear to be directly applicable to longer lengths without ambiguity, but, the shorter length should not be so short that the problems and solutions associated with thermal contraction and expansion are not adequately demonstrated. It is impossible to use this

reasoning to establish a specific length for the test system, but the length should be greater than a hundred feet or so, to adequately demonstrate the solution to thermal contraction and cable-pulling problems. In view of these considerations, a test system length of approximately 1000 feet is recommended as being a realistic goal.

Further, it is recommended that a refrigerator not be developed for this system which attempts to model the refrigerator required for an operational system. For a 500 kV, 3500 MVA 1000-foot test system, it is estimated that the total cooling capacity will have to be about 50 kW at 77 K, and the construction of a refrigerator of this rating would provide little information or experience for the future construction of 1000 to 2000 kW refrigerators required for operational systems. This does not mean that a refrigerator will not be included as part of the test system equipment. The question of batch cooling or refrigerator cooling is an economic question, and the selection will depend on the final design of the system, the duration of the test program and the location of the test equipment. It should also be recognized that the development of the refrigerator for a cryogenic cable system can be accomplished separately from the development of the other system components.

TEST SYSTEM CONFIGURATION

An artist's concept of the test system configuration is shown in Figure 5-1. A major assumption made in preparing this test system layout is that the cable and containment pipe will be installed above ground. This raises the question as to whether or not such a system realistically simulates operational conditions for the containment pipe, which is normally installed underground. The obvious advantage to an aboveground installation is that inspection is greatly facilitated. To a large extent, the installation of the containment pipe is made more difficult in an aboveground installation, in that the supporting function of the soil is absent. It is believed that the advantage of simpler inspection outweighs the disadvantage of having to install more complex containment pipe supports.

As shown in Figure 5-1, it is recommended that a U-shaped configuration be adopted to include the installation of bends, a necessary element in any practical installation. This configuration also permits all exposed high-voltage components to be housed in one fenced area, which may be adjacent to the control room.

The recommended U-shaped configuration is approximately 1000 feet in length and houses three cable phases. Plan and elevation views of the test section are shown in Figures 5-2 and 5-3 respectively. The electrical components of the system are designed for a 500 kV, 3500 MVA system. Each of the three cable phases is terminated at two pothead terminations

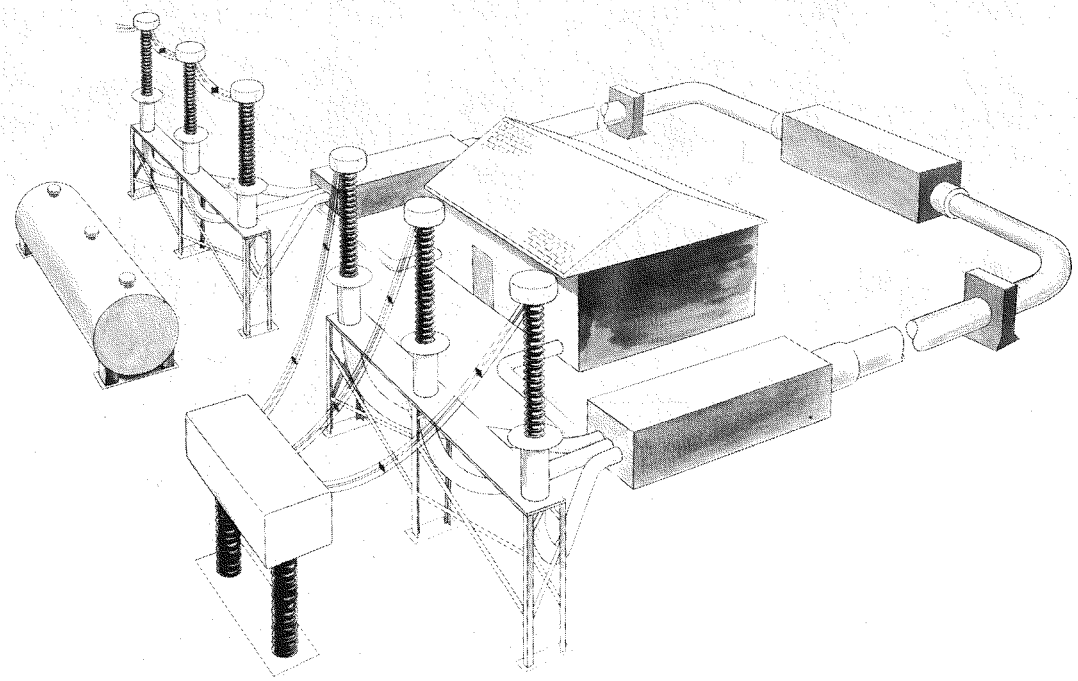

Figure 5-1. 1000-Foot, 500-kV, 3500 MVA Test System

which also provide a means of introducing and removing liquid nitrogen from the bore of the cable; a splice is included in each cable phase at the splice box, located at the far end of the U-shaped section. The cable envelope comprises foam-insulated FRP pipe sections, and the system is operated over a range of pressures (8 to 20 atmospheres) and over a range of temperatures (65 to 95 K).

TEST SYSTEM CAPABILITY

The test system should be designed to be capable of demonstrating the following electrical features:

- Application of rated voltage, 500 kV
- Circulation of rated current, 4040 amp
- Measurement of dissipation factor and corona level on all system components at 500 kV
- Qualification test at system BIL
- Measurement of conductor and shield ac losses

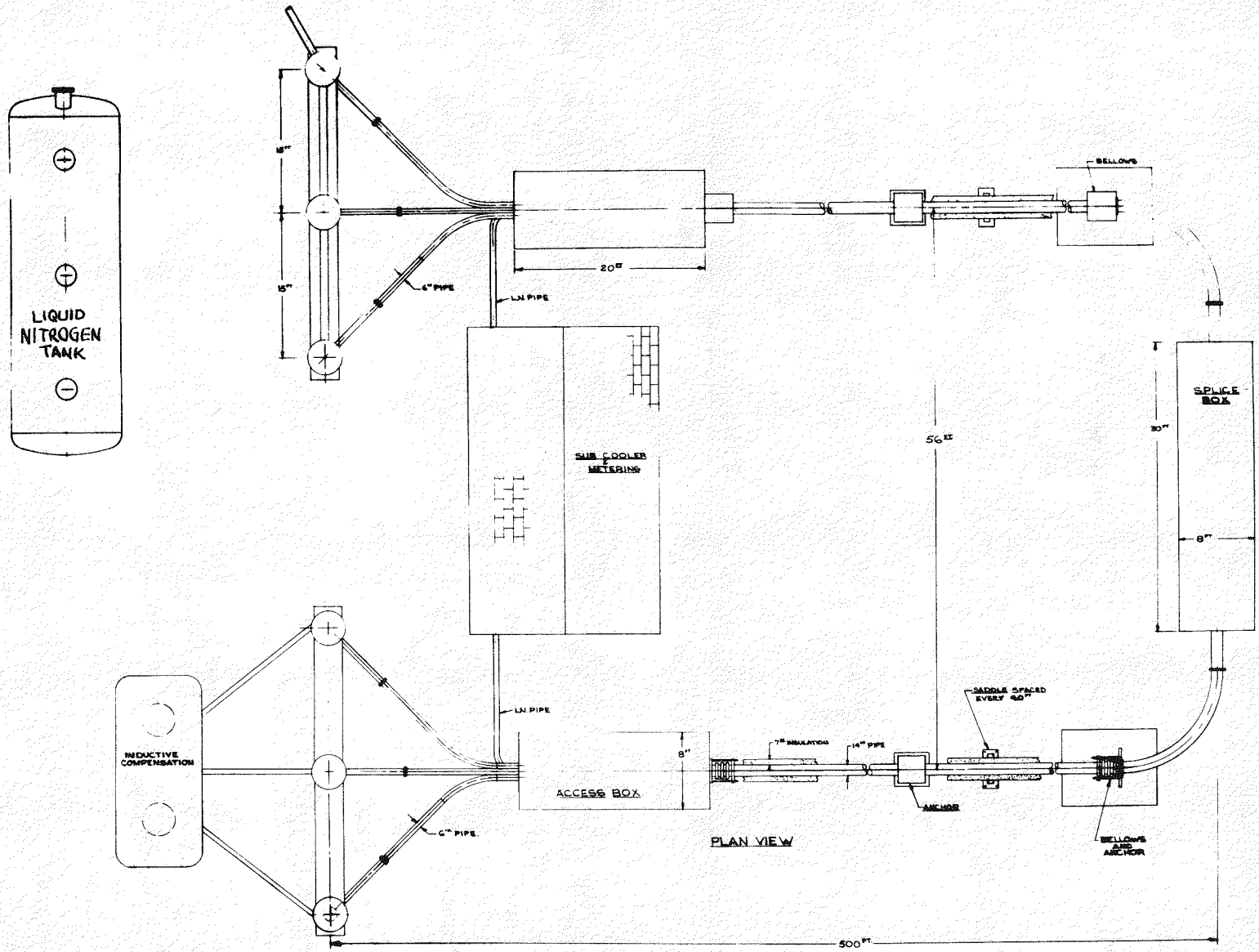

Figure 5-2. Plan of 500-kV, 3500 MVA 1000-Foot, Test Section

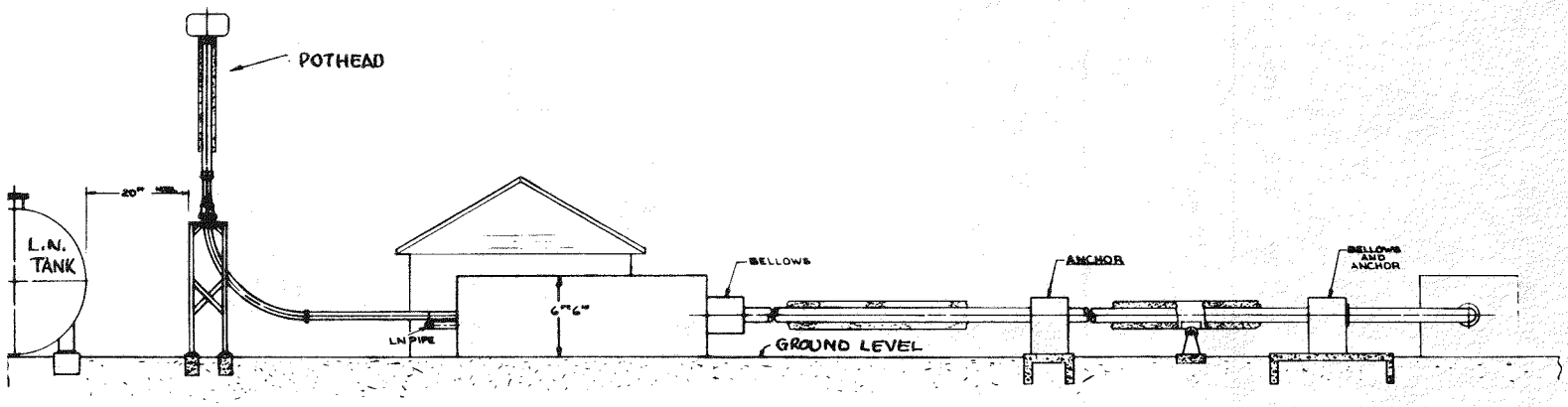

Figure 5-3. Elevation of 500 kV, 3500 MVA 1000-Foot Test Section

- Performance of the system under overvoltage and overcurrent conditions (approximately twice rated values)

From a mechanical standpoint, the system should be capable of demonstrating the following features:

- Ability to accommodate thermal contraction and expansion
- Measurement of thermal heat leak
- Measurement of liquid nitrogen pressure drop and temperature rise
- The effect of a simulated refrigerator failure

In the following sections, the recommended specifications of the system components, and illustrative designs for these components, are presented. However, it must be emphasized that complete component specifications cannot be prepared until after a test system design has been accomplished. The design of the 500 kV, 3500 MVA test system is outside the scope of this Phase III program.

CRYOGENIC CABLE

GENERAL SPECIFICATIONS

The cryogenic cable shall be suitable for installation in a pipe and shall be capable of operation at a 60 Hz system voltage of 500 kV. The cable is to be designed to accommodate the thermal contraction associated with operation in liquid nitrogen over a range of temperatures 65 to 95 K and over a range of pressures 8 to 20 atmospheres. The liquid nitrogen serves to cool the aluminum conductor, and acts as an impregnant for the electrical insulation. The cable shall be capable of withstanding a 1250 kV switching surge voltage ($200 \times 2000\,\mu$sec) and a 1550 kV impulse voltage (1.5×40 μsec) of either polarity. The hollow aluminum conductor must have an inside diameter of 1.5 inches, and an aluminum cross-sectional area of 3.6 in^2. The maximum strand diameter to be used in constructing the cable conductor is 0.060 inch. The individual strands are to be insulated and transposed. At rated voltage, the cable dissipation factor is to be less than 1500 μrads. Three cable sections of 1000 feet each are to be produced.

A recommended construction procedure and an illustrative cable design are presented below:

CABLE CONDUCTOR

The cable conductor is to be manufactured of stranded aluminum segments which are formed around a flexible former. The former is included to maintain the conductor segment configuration during manufacture and installation. The former should have a minimum inner diameter of 1.5 inches and a maximum outer diameter of 2.0 inches. The former may be manufactured from aluminum or stainless steel, and should be designed to provide uniform bending of the cable in conjunction with the cable conductor and insulation. Helical or perforated corrugated tube configurations are recommended for this former.

The cable conductor should be manufactured of EC grade aluminum, with a total cross-sectional aluminum area of 3.6 in^2. The number of segments and the number of strands per segment should be selected from the standpoint of uniform bending of the cable after manufacture. The maximum strand diameter is to be 0.060 inch, and each strand should be insulated with a conventional single coat of Formex. If the strands are compacted during the manufacture of the conductor segments, it must be ensured that the compacting operation does not destroy the insulating coat on the strands. Ideally, the strands should be perfectly transposed with respect to circumferentially directed magnetic fields, but a concentric strand configuration is also acceptable.

The conductor segments, individually protected with an insulating barrier, should be cabled around the former and served with an intercalated copper and carbon-black paper screen. This is followed by a single carbon-black tape such that the butt gap registers with the intercalated carbon-black tape. It is recommended that 0.005 × 1 inch copper tape, and 0.008 × 1 inch carbon-black paper tape be used for this purpose. The resistivity of the carbon-black paper tape should be close to 97 ohm-cm at 77 K.

Samples of the carbon-black tape selected for this purpose should be submitted to the contractor, prior to manufacture of the conductor, for qualification tests. These qualification tests will involve the measurement of dissipation factor on small dielectric samples impregnated with liquid nitrogen.

The conductor must be manufactured in continuous lengths that allow for the final manufacture of three continuous 1000-foot lengths of finished cable. In addition, at least three 100-foot lengths of finished cable must be provided for qualification tests.

CABLE INSULATION

High grade, conventional kraft paper insulation is to be used as the cable insulation material, with the following specifications:

- Type of pulp — Conventional kraft (CK)
- Water treatment — Deionized water
- Air resistance (maximum) — 3000 Gurley-sec
  (minimum) — 1500 Gurley-sec
- Paper density (maximum) — 0.81 gm/cc
  (minimum) — 0.85 gm/cc
- Thickness (nominal) — 0.005 and 0.0065 inches

The total insulation wall thickness shall be chosen on the basis of obtaining a maximum electric stress at the conductor surface of 430 V/mil for a system voltage of 500 kV. Tape tensions, tape widths and butt gap dimensions shall be chosen with a view to providing a cable with uniform bending capabilities, and high breakdown strength.

An outer screen of carbon-black paper and intercalated copper and carbon-black paper tape is to be applied over the cable insulation, in a similar manner to the inner screen, and two D-shaped polyethylene skid wires are to be applied over this outer screen.

It is recommended that the cable be taped in equilibrium with a controlled environment at a temperature of approximately 68 F and a relative humidity of 50 percent, to facilitate bending and installation in the field.

ILLUSTRATIVE CABLE DESIGN

As an example of an acceptable cable design, Figure 5-4 and the following information are presented:

- Former
  - Aluminum or stainless steel
  - Helically wound strip, 0.050×0.25 inch
  - Inside diameter, 1.5 inches
- Conductor
  - EC grade aluminum
  - Aluminum cross-sectional area, 3.6 in^2

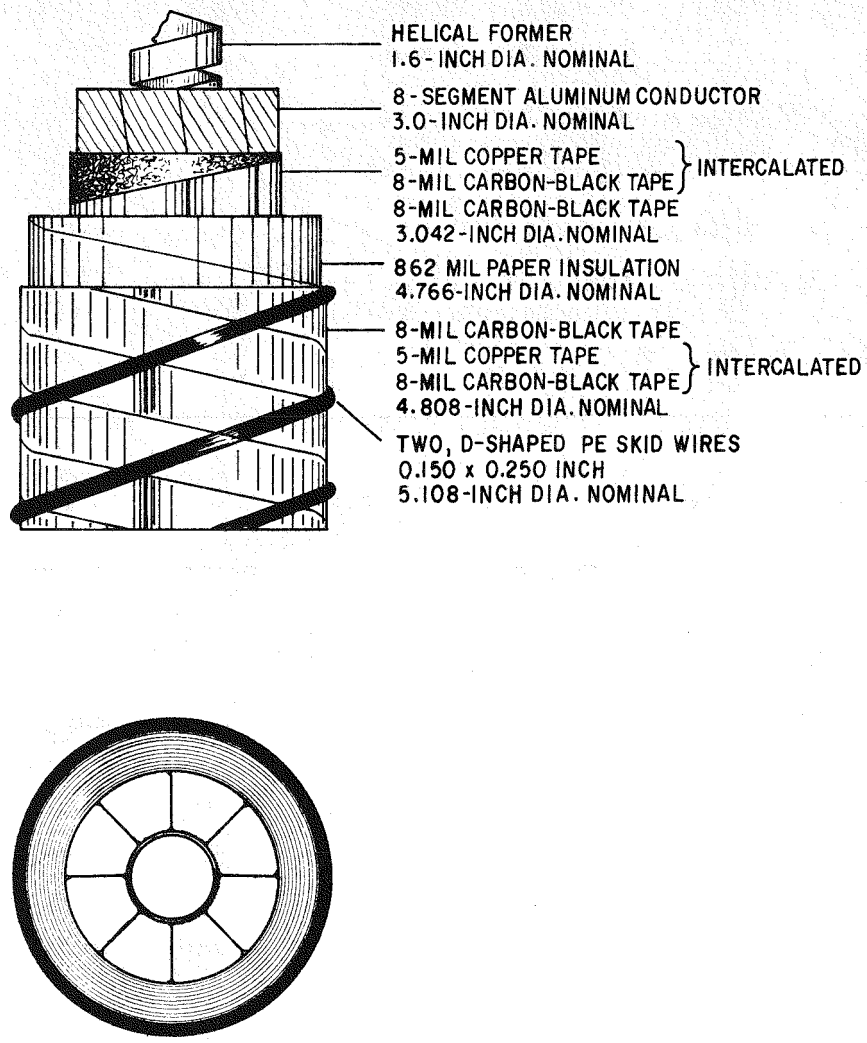

Figure 5-4. Illustrative Cryogenic Cable Design

  - 8 segments
  - 0.040-inch diameter strands, insulated

- Inner screen
  - Intercalated copper tape (0.005 × 1 inch) and carbon-black paper tape (0.008 × 1 inch). Carbon-black tape resistivity at 77 K, 97 ohm-cm.
  - One layer of carbon-black paper tape (0.008 × 1 inch)

- Insulation
  - Conventional kraft paper
  - Manufactured with deionized water
  - Air resistance, 1500 - 3000 Gurley-sec

- Density, 0.81 - 0.85 gm/cc
- Thickness, 0.005 and 0.0065 inch
- Moisture content, 5-7% by weight
- Tape widths, 1, 1 1/8, 1 1/4 inches
- Lay of tapes, see Table 1
- Total insulation wall thickness, 0.860 inch

- Outer Screen
  - One layer of carbon-black tape (0.008 × 1 inch)
  - Intercalated copper tape (0.005 × 1 inch) and carbon-black paper tape (0.008 × 1 inch). Carbon-black tape resistivity at 77 K, 97 ohm-cm

- Skid wires
  - Two D-shaped (0.150 × 0.250 inch) polyethylene skid wires

Table 5-1

CELLULOSE PAPER TAPING OPERATION

Taping Head	Number of Tapes	Tape Dimensions (inches)	Direction of Lay
1	6	1 × 0.005	LH
2	10	1 × 0.005	LH
3	10	1 × 0.005	LH
4	10	1 × 0.005	LH
5	10	1 × 0.005	RH
6	10	1 × 0.005	LH
7	10	1 × 0.005	RH
8	12	1 × 0.005	LH
9	12	1 1/8 × 0.005	RH
10	12	1 1/8 × 0.005	LH
11	12	1 1/8 × 0.0065	RH
12	12	1 1/8 × 0.0065	LH
13	10	1 1/4 × 0.0065	RH
14	8	1 1/4 × 0.0065	LH
15	5	1 1/4 × 0.0065	LH
16	7	1 1/4 × 0.0065	LH

CABLE ACCEPTANCE TESTS

Prior to the manufacture of the cable, the following materials shall be submitted to the contractor for qualification tests:

- Approximately 100 pounds each of the 0.005- and 0.0065-inch cellulose paper insulation will be submitted to the contractor in the form of 1-inch wide tapes. These materials will be used to manufacture small-scale cylindrical dielectric samples for the purposes of measuring the short-term ac breakdown strength and dissipation factor of each material impregnated with liquid nitrogen at 77 K, at a pressure of 80 psig.

- Approximately 20 pounds of the carbon-black paper tape will be submitted to the contractor for the purposes of measuring the effect of the carbon-black screen on the breakdown strength and dissipation factor of the samples described above.

During the manufacture of the cable sections, the following tests will be conducted:

- Approximately 100 feet of the manufactured conductor will be tested for strand-to-strand, and segment-segment shorts, at low voltage.

- At the start and finish of each cable section, a short length will be removed for the purposes of bend tests. Each of these sections will be subject to the following:

  - straightened from the reel
  - bent around a 14-foot diameter form
  - straightened
  - reverse bent around a 14-foot diameter form.

  Subsequent dissection of the cable insulation must show no excessive butt gap creases, tape buckles or tape damage. The cable must show no evidence of polygonization.

CABLE STORAGE

Following manufacture, it is recommended that the cable sections be stored on a reel in a controlled environment at 68 F and a relative humidity of 50 percent.

CRYOGENIC ENVELOPE

For an operational system, the cryogenic cable envelope diameter would be chosen in an iterative design process which involves trade-offs among many variables, including the desirable spacing between adjacent refrigerators. In the 1000-foot test system, the cable containment pipe need only be sized from the standpoint of dimensional clearances with respect to the three cable phases. On this basis, the inside diameter of the containment pipe needs to be approximately 13 inches. Although larger pipe diameters will be required for operational systems, the use of the 13-inch diameter pipe in the test system is expected to provide a meaningful demonstration of the expected performance of full-scale pipes.

GENERAL SPECIFICATIONS

The cryogenic envelope is used to contain the compressed liquid nitrogen coolant and the three cable phases.

A fiber reinforced plastic (FRP) pipe contains the low-temperature portion of the cable system. This FRP pipe is constructed in 40-foot long sections. The FRP pipe sections are attached to each other using adhesive bonded FRP/FRP pipe couplings. Similarly, the FRP pipe is attached to metallic system components by an FRP pipe/aluminum flange coupling. The three cryogenic cable phases are pulled through the pipe after the pipe joints are made up. Therefore, the interior pipe surface must be free of irregularities that may hinder the cable pulling process or damage the cable.

The FRP pressure pipe is surrounded by closed-cell foam thermal insulation. This thermal insulation can be applied to the FRP pipe sections at the factory. Pipe joints, however, must be insulated after assembly in the field.

The thermal insulation is covered by an outer envelope that protects the thermal insulation from air and moisture. In addition, the outer envelope must shield the environment from the electromagnetic fields generated by the cables.

The FRP pressure pipe, FRP/FRP pipe couplings, FRP/aluminum flange coupling and their joints must meet the following requirements:

- The envelope must withstand an axial force not to exceed 120,000 pounds at ambient temperature when the three cable phases are pulled through the FRP pressure pipe.
- The operating temperature range of the cryogenic envelope is 65 to 95 K. The envelope shall be capable of being cooled down a minimum of 20 times without damage to any of its components.

- The maximum expected temperature for the cryogenic envelope is 305 K, not operating.

- The maximum liquid nitrogen operating pressure will be 20 atmospheres absolute. The cryogenic envelope must be capable of containing liquid nitrogen at 30 atmospheres for short time intervals. The liquid nitrogen pressure will be lowered to 1 atmosphere absolute and raised to its operating level a maximum of fifty times during the operation of the test system.

- The permeation of air, nitrogen, and moisture through the FRP pressure pipe and outer envelope will be limited to a value such that the average heat flux to the liquid nitrogen from the environment will increase by not more than 15 percent in forty years.

- The design life for the cryogenic envelope components is forty years.

- The average heat flux to the liquid nitrogen from the environment through the thermal insulation and other penetrations shall not exceed an equivalent of 40 watts per meter of axial length of the cable system.

- The cryogenic envelope must withstand the axial forces due to thermal contraction during cooldown, and due to the pressure of the liquid acting on the expansion bellows assembly at the end of each straight run.

FRP PRESSURE PIPE

The pressure pipe for the three-phase cryogenic cable system shall be manufactured of fiber-reinforced plastic (FRP), in accordance with the following specifications:

Inside diameter	13 inches
Pipe section length	40 feet
Inner fluid	liquid nitrogen
Operating temperature range	65 to 95 K
Operating pressure range	0 to 20 atm. abs.
Test pressure at operating temperatures	30 atm. abs.
Successive cooldowns from ambient temperature	20
Successive pressurizations (at operating temperature) from ambient pressure	50
Design life	40 years

The ends of each pipe section are to be machined with a 1.5-degree external taper, approximately 10 inches long, to mate with the FRP/FRP couplings. FRP pipe and FRP couplings shall be cleaned with toluene or other suitable solvent to remove residual release agent applied to the winding mandrel. Pipe ends shall be wrapped in aluminum foil and protected from contamination and damage after machining.

Each FRP pipe section will have closed-cell urethane foam applied to its outer surface for thermal insulation. The foam insulation will meet the following specifications:

Apparent thermal conductivity	<0.15 MW/cm-^{o}K
Density	2 to 3 lb/ft^{3}
Compressive strength	25 psi (5% deflection)
Cell size	0.004 to 0.008-inch dia.
Minimum closed cell content	90% by volume
Minimum compressive modulus	700 psi

The thermal insulation may be applied in layers to prevent cracks in the foam, caused by differential thermal contraction during cooldown, from extending in a radial direction. The warmer (outer) portion of the foam insulation can be replaced with another type of insulation of the required rigidity and strength.

A thin cover of filament reinforced plastic shall be wound directly onto the outer surface of the thermal insulation. This outer cover shall permit the foam-insulated pressure pipe to be slid into the electromagnetic shield. The electromagnetic shield is an aluminum cylinder of 27-inch inner diameter and 3/16-inch wall thickness.

Prior to shipment, one end of each pressure pipe section shall be bonded to an FRP/FRP coupling. It is estimated that 24, 40-foot pipe sections will be required for the test system installation.

Experience with the manufacture and test of 8-inch diameter model FRP pressure pipe sections shows that the following materials specifications are expected to satisfy the above performance specifications:

Resin	Epon 826/Vandride 2/DMP-30 accelerator
Cure cycle	Gel stage at 50 to 60 C for 16 to 24 hours Post cure at 150 C for 16 hours

Reinforcement	Filament wound E-glass (Owens Corning Type 410AA675)
Glass content	72% by weight
Winding pattern*	o-xx-o-xx-.....o-xx
Wall thickness	7/16 inch
Foam thickness	6 inches
Average nitrogen permeation	less than 7×10^{-9} std $cm^3/cm^2/sec$

FRP/FRP PIPE COUPLINGS

The couplings between adjacent sections of FRP pressure pipe will also be made of fiber-reinforced plastic. These couplings will be tapered to mate with the tapered ends of the FRP pipe sections, and it is expected that each pipe section will be manufactured and shipped with an FRP/FRP coupling bonded to one of the ends.

Specifications for the FRP couplings are identical to those for the FRP pipe sections, except that the couplings will have an internal, rather than an external, taper and the dimensions of the coupling will be different, as presented below:

Coupling minimum inside diameter	13 inches
Coupling length	24 inches

The inside surface of both ends of the coupling are to be machined with a 1.5-degree taper, approximately 10 inches long, to mate with the FRP pressure pipe sections. The couplings can be manufactured from the same materials as the pressure pipe, with identical winding patterns, on a larger mandrel. Thermal insulation is not applied to the coupling before shipment to the installation site.

The adhesive joint between the coupling and the FRP pipe must also satisfy all the above-mentioned pressure, temperature and stress levels.

Prior to bonding an FRP pipe to an FRP coupling, the protective caps shall be removed and premachined surfaces shall be cleaned with acetone or MEK.** The surfaces shall then be lightly hand abraded using clean #120 grit paper. The adhesive shall then be applied to both mating surfaces and

---

* o represents a circumferential winding (88^o to 89^o)
x represents a helical winding (44^o to 46^o)
** Methyl ethyl ketone

the joint assembled with an axial force sufficient to produce a pressure of approximately 10 psi along the joint interface. The joint shall then be clamped using a jig to maintain this pressure and prevent motion during heat curing. Excess adhesive should be removed with acetone or MEK.

The adhesive recommended for this joint is Scotch Weld® #2216 B/A manufactured by the 3M Company. This adhesive is a modified epoxy produced for structural applications. Heating blankets shall be placed over the joint and the adhesive cured at 150 F for a one hour period. Thermocouple sensors shall be used to ensure that the proper curing temperature is achieved and to prevent heating the FRP pipe above 200 F.

Tests have been carried out on FRP/FRP joints of the required configuration using 8-inch diameter FRP pipes and FRP couplings. Fully satisfactory results have been obtained with the following joint:

Adhesive	#2216 B/A epoxy (3M Company)
Bond thickness	0.003 to 0.005 inch*
Cure	150 F for one hour

FRP PIPE/ALUMINUM FLANGE COUPLING

At certain locations, it will be necessary to join an FRP pipe section to metallic components. For example, an FRP/metal joint must be made where the pressure pipe joins the splice box.

The transition between FRP and metal is to be carried out by bonding an aluminum stub end to the end of an FRP section.

FRP pipe to aluminum flanges shall be made using adhesive bonded joints that are factory assembled using a machined scarf joint with a 2-degree taper, 2 1/2 inches long. The taper is machined so that the aluminum stub end is assembled over the FRP pipe.

Immediately prior to application of the adhesive (within two hours) the FRP surface shall be cleaned with acetone or MEK and then lightly hand abraded using clean #120 grit paper. The aluminum stub end shall be vapor degreased for five minutes in Perchloroethylene and then the joint surface shall be lightly vapor blasted (wet honed). The part shall then be rinsed in running distilled water and oven dried at 150 F for ten minutes.

---

* Obtained by glass mat shims distributed along the bond line
® Registered trademark of 3M Company

The adhesive shall be applied to the mating surfaces as well as to a 0.010-inch thick glass reinforcing mat ("Modiglass", Reichold Chemicals, Inc.) that is sandwiched in the joint. The mat shall be scarfed and applied to the FRP surface to form a continuous reinforcement layer. The aluminum flange is then assembled over the FRP with a slight rotary motion. An assembly fixture shall be used to apply sufficient axial force to maintain a bondline pressure of approximately 20 psi during curing. This fixture must also prevent relative movement of the FRP pipe and stub end during curing.

The adhesive recommended for this joint is TU-902, manufactured by the Amicon Corporation, Lexington, Massachusetts. This is a polyurethane adhesive that is cured at 176 F for two hours. Heating blankets shall be applied over the joint prior to application of heat. Thermocouple sensors shall be used to ensure that the proper curing temperature is achieved and to prevent heating the FRP pipe above 200 F.

The aluminum stub end is provided with a lap joint flange, which attaches to the metal component to which the FRP pipe section is being joined.

The FRP pipe/aluminum flange coupling must meet all specifications given above for the FRP pressure pipe. The coupling may be assembled as follows:

Stub end	14 inches, Flowline Corporation (6061-T6 aluminum)
Flange	14 inches, Flowline Corporation, lap joint flange or equivalent
Flange seal	Creavey Seal Company, AS400
Adhesive	Amicon Corporation, TU-902, Polyurethane adhesive
Bond thickness	0.001 to 0.005 inch
Curing cycle	176 F for 2 hours

EXPANSION JOINTS AND PIPE ANCHORS

The preparation of detailed specifications for metallic expansion joints, pipe supports and pipe anchors must await completion of design tasks to establish final dimensions of the cable, FRP pressure pipe and thermal insulation. Plans to place the 1000-foot test system above ground rather than to have it buried directly in the ground will place special requirements on pipe anchors and may require the use of pipe supports distributed along the cable run. Factors that must be considered when final specifications for the expansion joints and anchors are established are noted below.

Expansion Joints

Metallic expansion joints will be required at locations noted in Figures 5-2 and 5-3 to accommodate the axial contraction of the FRP pipe during cooling to operating temperature. This contraction will be approximately 1 1/2 inches for each 40-foot FRP pipe section. The bellows must be capable of extending this amount while tolerating any angular and lateral motions that are likely to occur because of pipe bowing and anchor settling.

The bellows must meet the same requirements at cryogenic temperature with respect to pressure and thermal cycling and leakage rates as described earlier for the FRP pipe. Because of the larger diameter of the bellows, it can add significant additional pressure thrust against pipe anchors unless this thrust is restrained by tie rods extending between flanges at each end of the bellows. Adjustable stops on the tie rods will permit installing the bellows at ambient temperature in a precompressed condition. After installation and before cooling, the stops will be readjusted to permit the bellows to lengthen, as the FRP pipe contracts. Stops can be positioned to ensure that a slight axial tension force remains in the FRP pipe after cooldown and pressurization, thereby avoiding an axial compression load on the pipe which would cause high buckling forces on pipe supports.

Expansion bellows must be provided with both internal and external sleeves to provide smooth surfaces to allow cable pulling and to prevent thermal insulation from entering the convolutions. Flanges shall be designed for bolted connections to the aluminum stub ends of adjacent FRP pressure pipes. Creavey type sealing rings shall be used at these joints.

Expansion joints may also be required at the splice box unless the metallic pipe bends prove sufficiently flexible to accommodate contractions of the metallic pressure pipe sections. Here again, detailed design is required to establish final requirements.

Anchors and Pipe Supports

As indicated in Figure 5-2, concrete anchors are required at several locations to properly support the cable test section in the proposed aboveground installation. These anchors must be designed to meet axial forces at proof pressure conditions as well as lateral forces that may result from pipe bowing during cooldown. In addition, the anchors must restrain the cryogenic envelope during pulling of the cable.

Pipe supports will be required at the free end of each bellows and possibly at several points along the cable run between anchors. These supports should maintain axial alignment of the cable pressure pipe but not restrain it from axial movement. Supports must be designed to prevent

significant additional heat leak and prevent damage to the thermal insulation and the electromagnetic shield.

Both the anchors and supports must provide a vapor tight enclosure for the thermal insulation at these locations.

Final design of the anchors will be possible after pressure pipe dimensions are established and the subsoil conditions are known for the specific site of this installation.

CRYOGENIC POTHEAD

GENERAL SPECIFICATIONS

Each end of the three-phase cable sections is terminated in a group of three potheads. Each pothead shall be suitable for terminating the cryogenic cable sections described earlier, and shall be capable of all-weather operation at a 60 Hz system rating of 500 kV, 3500 MVA. The pothead is to be designed to accommodate the thermal contractions associated with internal operation in liquid nitrogen over a temperature range 65 to 95 K and to restrain the cable conductor as it is cooled down from ambient temperature. The internal pothead operating pressure will be over the range 8 to 20 atmospheres. The pothead must also provide a means of introducing and removing liquid nitrogen from the bore of the cryogenic cable. The pothead pressure vessel specifications are the same as those described above for the FRP pressure pipe sections.

The pothead shall be capable of withstanding a 1250 kV switching surge voltage (200×2000 μsec) and a 1550 kV impulse voltage (1.5×40 μsec) of either polarity.

Thermal insulation and a conductor transition piece must be provided such that the total heat leak into the pothead is less than 1000 watts at a full load current of 4040 amps.

An illustrative pothead design is presented below.

ILLUSTRATIVE CRYOGENIC POTHEAD DESIGN

The cryogenic pothead configuration shown in Figure 5-5 has an overall length of approximately 15 feet and an overall diameter of 25 inches. The structural base for the pothead is supported above the pipe elbow that leads the cable into the pothead. The top flange of this pipe elbow is supported from the base plate by stainless steel bolts.

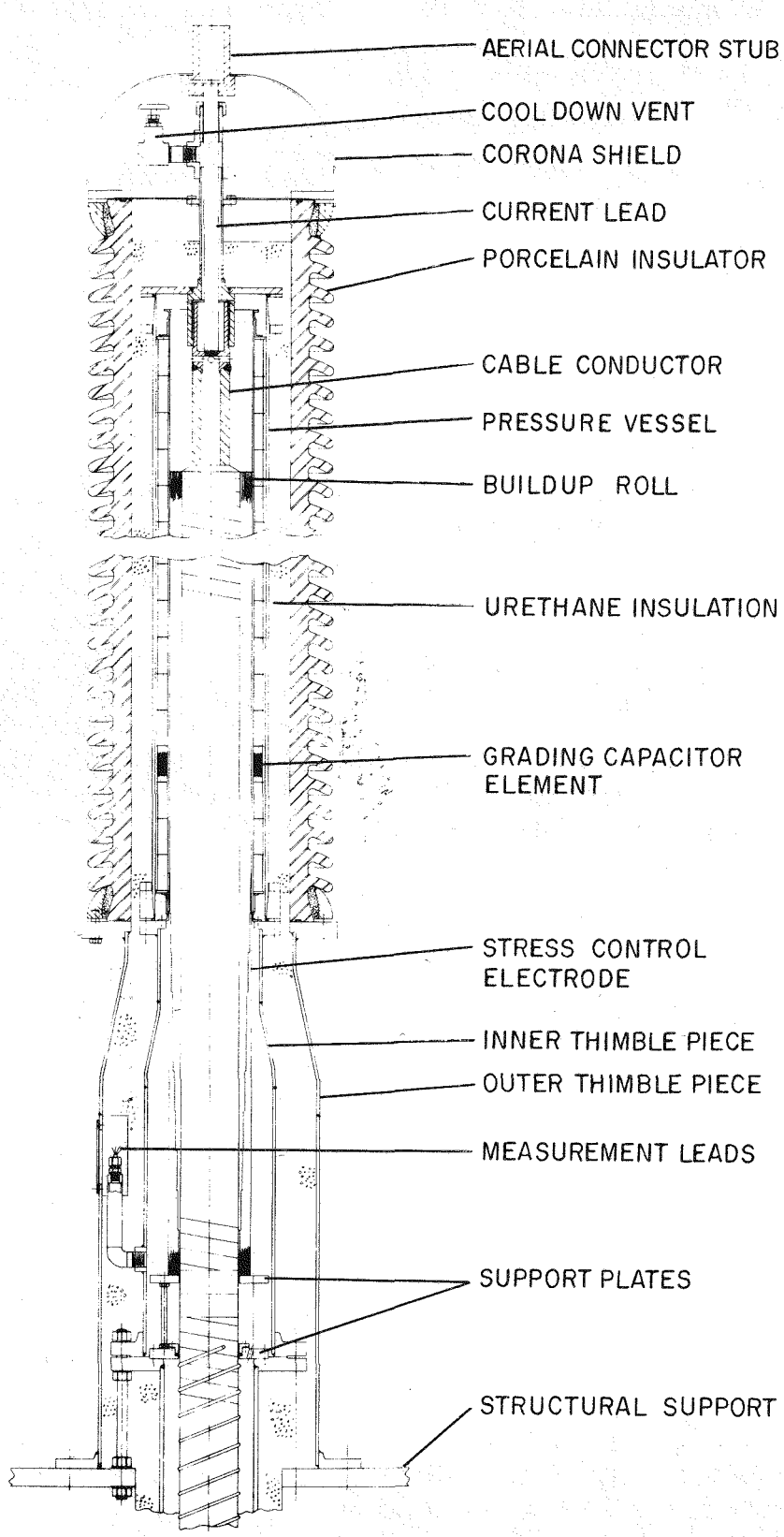

Figure 5-5. Illustrative Cryogenic Pothead Design

During assembly, the cable is cut to length and the outer shielding tapes are removed from the section of cable above the base plate. Cylindrical build-up rolls of cellulose paper insulation are applied in sections over the cable insulation. The edges of the build-up rolls are tapered such that crepe paper can be used to fill the spaces between adjacent rolls. The lower build-up roll contains a metallic ground shield which is contoured to form a log-log profile, and the lower end of this ground shield is lapped over the ground shield of the cable at a power factor gap.

Measurement lead connections are made to the two ground shields, and the inner and outer thimble pieces are installed over the lower section of the cable.

Series-connected cylindrical capacitors, mounted on an insulating support tube, are slid over the build-up rolls, and provide a means of longitudinal voltage grading along the build-up roll surface. The top capacitor is connected to the high-voltage terminal at the top of the pothead. A fiber-reinforced plastic (FRP) pressure vessel is mounted around the capacitor stack and contains the pressurized liquid nitrogen. Closed-cell foam thermal insulation surrounds the complete pothead and an outer porcelain shell provides weather protection. Liquid nitrogen flows up the bore of the cable, and is returned in a counterflow arrangement, between the capacitor stack and the pressure vessel.

COMPONENT RECOMMENDATIONS

The following recommendations are made with respect to the pothead components:

Thimble Pieces

Inner –	Material	6061-T6 aluminum, Schedule 40
	Length	36 inches
Low flange diameter (nominal)		10 inches, Flowline Corp., Part #FB-300
Upper flange diameter (nominal)		8 inches, Flowline Corp., Part #FB-300
	Reducer	10-inch to 8-inch dia., Flowline Corp., Part #R4-3003-F
Outer –	Material	6061-T6 aluminum, Schedule 40
	Length	36 inches

Lower flange diameter (nominal)	18 inches, Flowline Corp., Part #FB-150
Upper flange diameter (nominal)	14 inches, Flowline Corp., Part #FB-150
Reducer	18 to 14 inches, Flowline Corp., Part #124-3003-F
Foam Thermal Insulation	
Material	Urethane
Density	2 to 3 lb/ft^3
Closed cell content (minimum)	90%
Manufacturer	Atlas Insulation Company, Ayers, Massachusetts
Porcelain Shell	
Inside Diameter	14 inches
Length	140 inches
Configuration	Weatherproof skirts on the OD
Manufacturer	Locke Insulator Corp., N.Y.C.
Pressure Vessel	
Material	FRP pressure pipe section (See Cryogenic Envelope)
Inside diameter	9 inches
Length	132 inches
Capacitor Elements	
Inside diameter	6.8 inches
Outside diameter	8.6 inches
Length	3 inches
Number	38
Description	As used for 500 kV oil/paper pothead service
Build-up Rolls	
Cellulose paper	As described for cryogenic cable

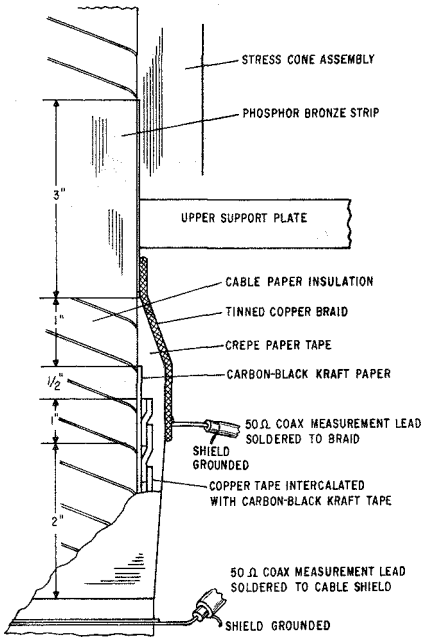

Figure 5-6. Cryogenic Pothead Power Factor Gap

RECOMMENDED STRESS LEVELS

On the basis of cryogenic pothead development experience gained to date, it is recommended that the stress levels within the cryogenic pothead be limited to the values shown below. The stress values (V/mil) are presented for 500 kV operation (290 kV line-to-neutral). The regions referred to below correspond to the regions shown in Figure 4-20 of Section 4, "Electrical Insulation Evaluation".

Region 1:	Axial stress between foils of adjacent capacitor foils	20
Region 2:	Radial stress between adjacent foils of one capacitor element	400
Region 3:	Radial stress in the liquid nitrogen annulus	250
Region 4:	Radial stress in support tube Axial stress in support tube	250 6
Region 5:	Radial stress at cable conductor surface	425
Region 6:	Radial stress at capacitor interface Axial stress at capacitor interface	45 9

POWER FACTOR GAP

The recommended configuration for the power factor gap between the outer screen of the cable and the ground shield of the lower build-up roll is shown in Figure 5-6. The power factor gap is located below the upper support plate shown in Figure 5-5. The carbon-black tape of the outer cable screen is terminated 1 inch below the support plate, and the copper tape of the outer cable screen is terminated 1.5 inches below the support plate. Creped kraft paper is taped around the end of the cable screen as shown in Figure 5-6. A total radial build of 0.030-inch creped paper is applied in a half-lapped configuration. The power factor gap is shielded by a layer of tinned copper braid, and this braid is electrically connected to a phosphor bronze strip surrounding the cable. This phosphor bronze strip makes contact with the ground shield of the lower build-up roll as the build-up roll is tightened around the cable insulation. Coaxial measurement leads are then connected to the shields, as shown in Figure 5-6, to complete the assembly.

CRYOGENIC CABLE SPLICE

GENERAL SPECIFICATIONS

Each of the three cable phases is to be spliced in the splice box located at the U-bend of the 1000-foot test system. Each splice shall be suitable for joining the cryogenic cable sections described earlier, and shall be capable of operation at a 60 Hz system voltage of 500 kV. The splices must be designed to operate in liquid nitrogen over a temperature range 65 to 95 K, and to restrain the cable conductor as it is cooled down from ambient temperature. The liquid nitrogen operating pressure will be over the range 8 to 20 atmospheres. The splice must also provide a means of maintaining the liquid nitrogen flow through the bore of one cable section to the bore of the adjoining cable section, and a means of joining the hollow-bore aluminum conductor of the cable sections, such that the joint can carry an operating current of 4040 amp.

An illustrative splice design is presented below.

ILLUSTRATIVE CRYOGENIC CABLE SPLICE DESIGN

The cryogenic cable splice configuration shown in Figure 5-7 has an overall length of approximately 124 inches and an overall diameter of approximately 5.5 inches.

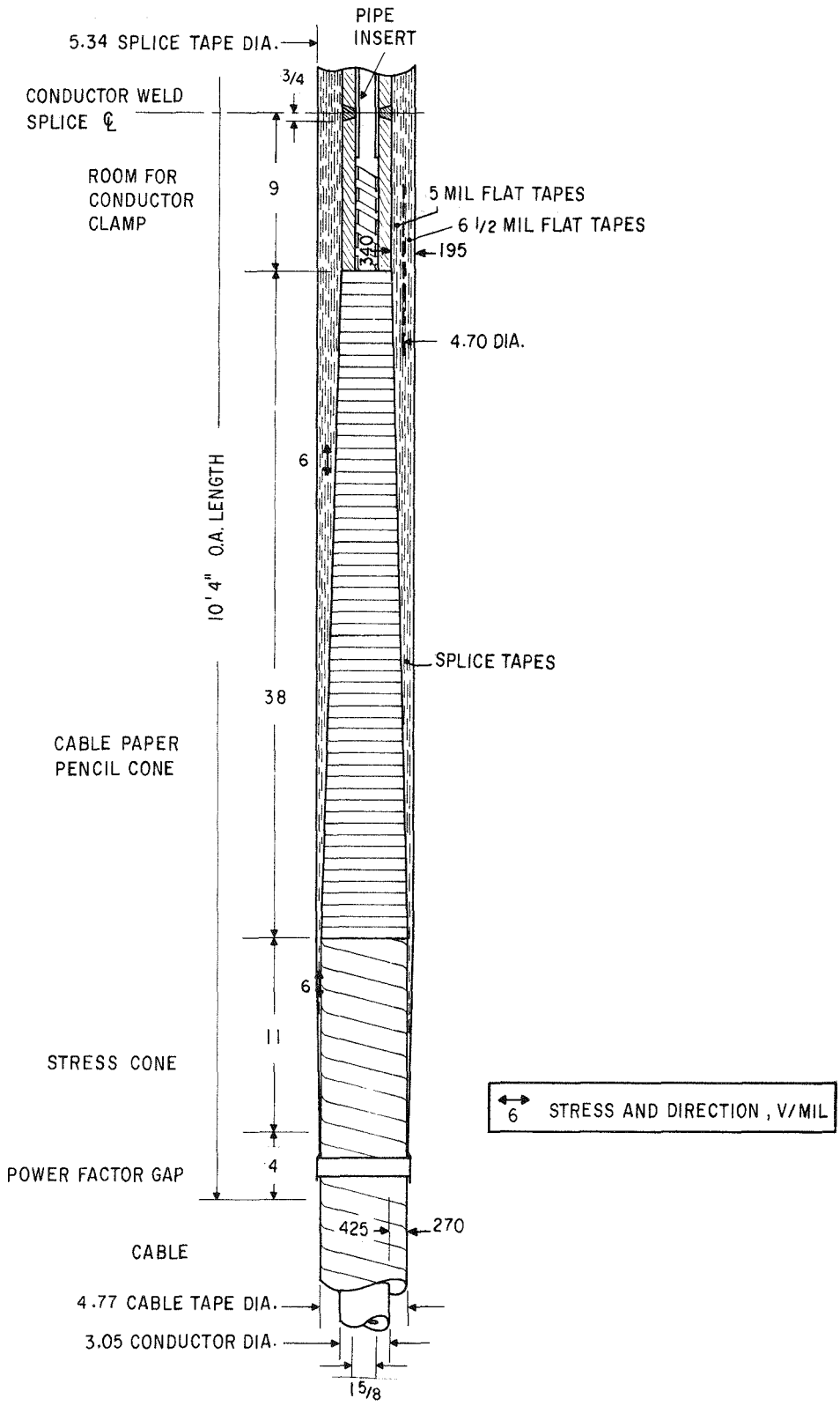

Figure 5-7. Cable Splice

CONDUCTOR JOINT

It is recommended that the adjacent conductors of the cable sections be welded to provide a reliable electrical and mechanical joint. To perform the welding operation, the cable insulation is removed from the cable for a distance of approximately 9 inches from the end of the cable conductor. A liner tube is inserted in the bore of the two conductors to provide support and alignment, and water-cooled clamps are applied to the cable conductor on either side of the weld region. The clamps are instrumented with thermocouples to ensure that the cable conductor is not heated above 70 C during the welding operation. After welding, the surface of the joint is smoothed with lead or other suitable conducting material, and the intercalated inner screen of copper and carbon-black tape is reapplied over the exposed conductor surface.

SPLICE TAPING

The cable tapes are first penciled back from the conductor joint to provide a transition between the machine-applied cable tapes and the hand-applied splice tapes. The slope of the penciled region is selected to limit the maximum value of the stress along the surface to less than 6 V/mil at rated voltage. Hand-applied cellulose paper tapes are then used to fill the region between the two penciled surfaces of the cable sections.

To reduce the stresses in the region of the hand-applied tapes, the diameter of the splice is designed to be greater than the diameter of the cable insulation, and at the two ends of the splice, the outside surface is profiled in a log-log configuration to maintain the axial stress constant in that region. The dimensions of the profiled region are shown in Figure 5-7.

OUTER SCREEN

A 1-inch wide copper band is applied over the cables at each end of the splice. A flat layer of carbon-black paper is taped over the surface of the splice with no butt gaps. Creped carbon-black tape is used over the profiled region of the splice to accommodate the surface contour. Finally, a copper braid is taped over the entire splice surface and is soldered in at least three locations circumferentially; at each location, the solder area runs for the whole length of the splice. At the ends, the copper braid is soldered to the two copper bands, as shown in Figure 5-8.

POWER FACTOR GAP

It is desirable to separate the splice shield and cable shields such that dissipation factor measurements can be made separately on each component. A recommended power factor gap configuration is shown in Figure 5-8.

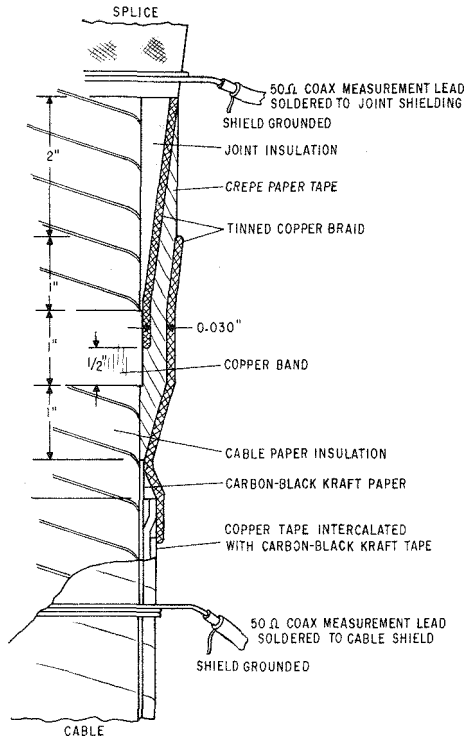

Figure 5-8. Power Factor Gap
-Cable Splice-

The outer screen of intercalated copper and carbon-black tapes on the cable is removed for a distance of 1.5 inches from the copper band applied around the ends of the splice. The carbon-black paper screen is removed for a distance of 1 inch. Creped cellulose paper is taped over the ends of the cable screen to provide a total radial build of 0.030 inch. The gap is then shielded by a layer of tinned copper braid which is electrically connected to the cable shield. Connection of the coaxial measurement lead completes the power factor gap assembly.

TEST FACILITY CAPABILITY

APPLICATION OF 60 HZ VOLTAGES

The test system is to be capable of long-term operation at a system voltage of 500 kV (290 kV line-to-neutral). Because the cable insulation is completely shielded, it is viable to energize all three cable phases from

a single-phase voltage source to stress the insulation. The system should also be capable of operation for significant periods of time at twice rated voltage; 580 kV line-to-neutral.

The high-voltage supply must be of sufficient rating to supply the charging current to the 3000 feet of cable, implying a rating of approximately 7.5 MVA at 290 kV, and 30 MVA at 580 kV. In addition, the voltage supply should be capable of applying a voltage to the test system without the introduction of switching surges, and must be adjustable such that the desired voltage levels can be maintained within one percent.

Measurements of dissipation factor and corona level will be made on each of the test system components at the different levels of test voltage. To permit the separate measurement of these values on each component, the outer screen of the cables will be sectionalized by power factor gaps.

APPLICATION OF IMPULSE VOLTAGES

The facilities at the site should include a suitable impulse generator. This equipment should be capable of applying 1250 kV switching surge voltages ($200 \times 2000\,\mu$sec) and 1550 kV impulse voltages ($1.5 \times 40\ \mu$sec) of either polarity to the test equipment. A minimum generator rating of 500 kJ is required.

For the purposes of impulse and switching surge tests, consideration must be given to removing the power factor gaps from the cable sections, splices and potheads.

CIRCULATION OF RATED CURRENT

The test system components are to be designed to be capable of long-term operation with circulating current flowing through the cable sections, potheads and splices. Since the measurement of the electrical losses in the system, including the losses in the electromagnetic shield of the cable envelope, is an important element in the test, it is necessary that the cable currents maintain 120 degree phase displacements.

To accomplish this, one set of three pothead terminations can be shorted, and the other set can be connected to a three-phase bank of capacitor elements that will compensate the series inductance of each of the cable phases. It is estimated that the rating of the three-phase capacitor bank will be 220 V, 6000 amp per phase. These capacitors should be insulated from ground, such that the potential on the capacitors can be raised to 580 kV above ground for combined rated voltage and rated current tests.

The current will be induced in each of the cable phases by means of current transformers mounted around the riser pipes of the three potheads. This arrangement is similar to that used for combined voltage and current tests on conventional oil-filled, pipe-type cable.

It is estimated that the rating of each of the current transformers mounted around the riser pipes will be 25 kVA at 6000 amp secondary current. If it is more convenient, two or more similar transformers may be located around the risers to provide the required rating of 25 kVA per phase. A three-phase supply is used to drive the current transformers, controlling the phase relationships between the phase currents and the magnitude of the phase currents.

A schematic layout of the electrical components described above is presented in Figure 5-9, and the estimated ratings of the reactive compensation components are presented below, for one of the three phases:

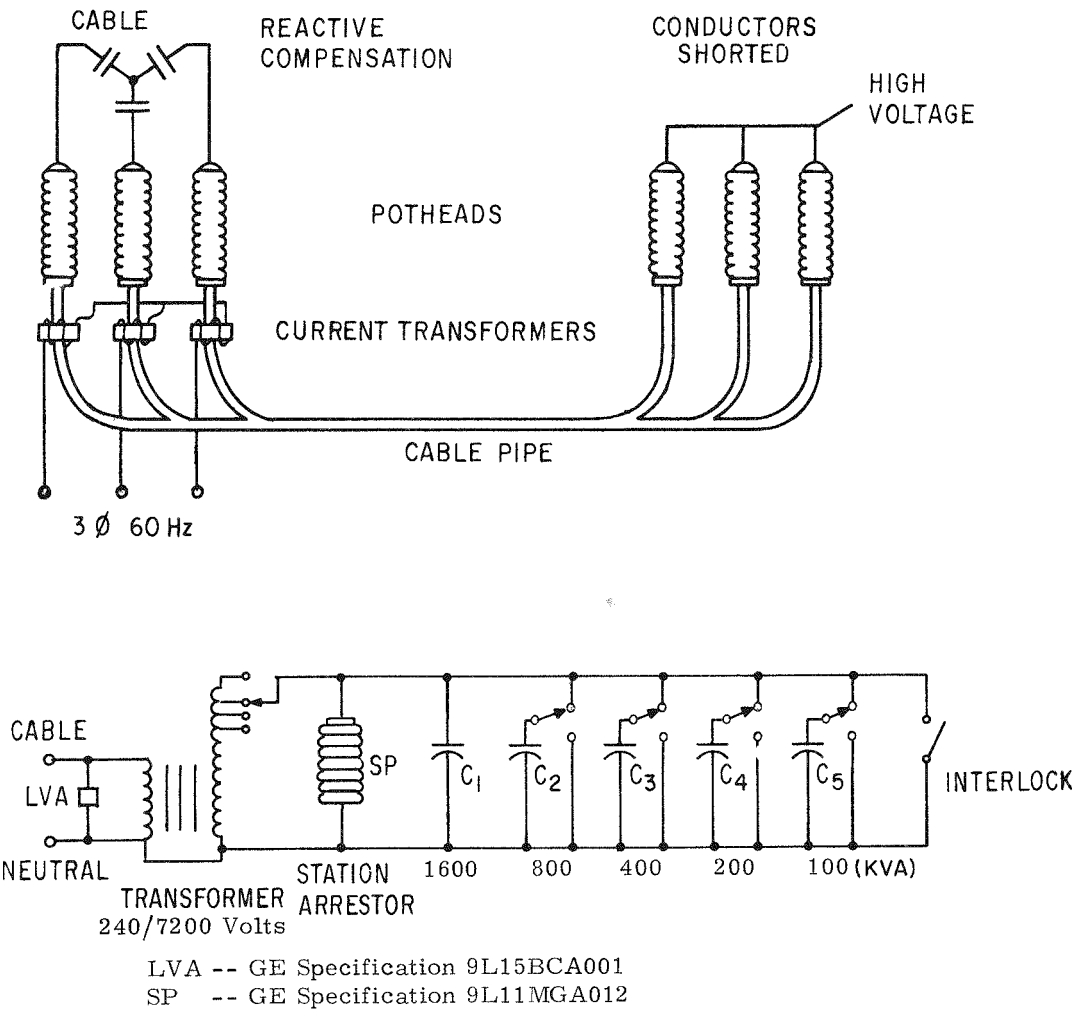

LVA -- GE Specification 9L15BCA001
SP -- GE Specification 9L11MGA012

Figure 5-9. Reactive Compensation Circuit

Single-Phase Transformer

Voltage rating	7200/240 V
Rating	1400 kVA
Floor space	9 × 9 feet
Height	7 feet
Weight	9600 lbs

Capacitor Bank

Voltage rating	7200 V
Total rating	3100 kVA
	- 15 units, 200 kVA
	- 1 unit, 100 kVA
Floor space	17 × 54 inches
Height	3 feet
Weight	1600 lbs

Lightning Arrestors

High voltage:	
Voltage rating	12 kV
Diameter	8.25 inches
Height	20.6 inches
Low voltage:	
Voltage rating	0.65 kV

Note: Each of the above components is required for each of the three cable phases.

LIQUID NITROGEN HANDLING

The cable tests are to be conducted at liquid nitrogen pressures ranging from 8 to 20 atmospheres and at liquid nitrogen temperatures ranging from 65 to 95 K. All metallic components such as aluminum piping, stainless steel expansion bellows and splice casings will be tested in accordance with appropriate piping and pressure vessel codes. FRP pipe and envelope sections will be inspected at the factory and subjected to low pressure leak testing at ambient temperatures.

The FRP piping portions of the liquid nitrogen flow system shown in Figure 5-10 will be subjected to one cooldown and a pressure test with liquid nitrogen to 30 atmospheres before the cable is installed. This cooldown will enable proper adjustment of bellows tie rod stops and inspection of joints for cold leaks. Blind flanges may be inserted in the piping system to enable testing of a few pipe sections at one time. As a final preoperational test, the completely assembled system will be tested to check out the instrumentation, liquid nitrogen circulation system and liquid nitrogen pressure and temperature control systems.

Liquid Nitrogen Circulation for the Cable

The liquid nitrogen used to cool the cable will be circulated by a centrifugal pump. This flow will pass through a heat exchanger to obtain the desired temperature of the input stream. Temperature control will be achieved by regulating the pressure and level of liquid nitrogen surrounding the heat exchanger tubes through which the cable stream is flowing. At least two pumps will be installed, with the requisite valving to permit pump maintenance while the system is in operation. The pump system will be required to circulate approximately 200 gpm. This flow must be maintained in the event that the primary pumping system fails or must be removed for maintenance.

A liquid nitrogen expansion tank will be provided to account for volume changes as the cable system undergoes temperature and pressure changes

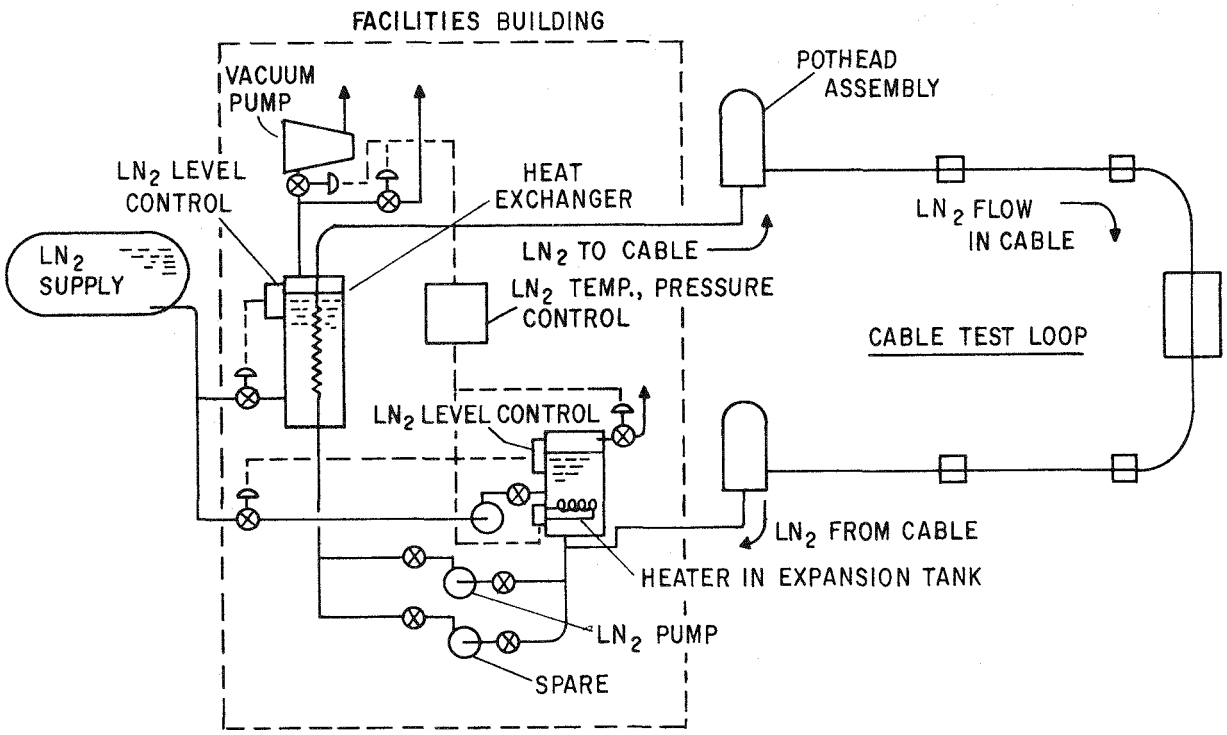

Figure 5-10. Liquid Nitrogen Flow Schematic

during testing. A liquid nitrogen level control and pump circuit will be provided to automatically maintain sufficient liquid nitrogen in the cable flow circuit regardless of the sequence of cable tests. Refilling with liquid nitrogen should not cause significant pressure or temperature fluctuations.

Heat Exchanger

The cable heat transferred to the liquid nitrogen stream will be removed by a heat exchanger located in the facilities building. Liquid nitrogen used to cool the heat exchanger will be provided from a storage tank or from a refrigerator. The heat exchanger will be designed for a total heat load of 100 kW although under normal test conditions, the steady state load is expected to be about 50 kW. The liquid nitrogen level on the cold side of the heat exchanger must also be regulated automatically. Whether this flow circuit will require a separate pump will depend upon final test system design and the selection of the type of liquid nitrogen supply system.

Instrumentation and Data Acquisition

The performance of the liquid nitrogen piping systems will be monitored continuously by sensors located in the facilities building, at the liquid nitrogen supply and along the cable envelope. The system will be designed to operate for extended periods with a minimum of supervision. Out-of-limit alarms will be provided to alert operators of equipment malfunctions or unusual operating conditions. Provision will be made for unattended data acquisition and recording. Real-time data display will be provided to aid in system checkout, cable cooldown and system operation.

Section 6

ELECTRICAL INSULATION AGING STUDY

SUMMARY OF RESULTS

A series of voltage endurance tests was run to obtain a first-cut evaluation of the aging characteristics of the cellulose paper which was selected for construction of the prototype cryogenic cables described in Section 4 of this report. The paper selected for these tests was not identical to the paper used in the cable, since the cable paper had not been manufactured at the time, but its physical characteristics were as close as possible to those chosen for the prototype cable paper. A comparison of the characteristics of the two types of cellulose paper is presented in Table 6-1 below.

Table 6-1

CHARACTERISTICS OF CELLULOSE PAPERS

Paper Used	Pulp	Thickness (mils)	Specific Gravity	Air Resistance (Gurley-sec)
Paper Used in Aging Tests	Modified kraft (high alpha)	4.12	0.84	2000
Paper Used in Prototype Cable	Conventional kraft	5.12	0.84	5100

The test samples were made by taping eight or nine layers of tape on a 1/2-inch diameter, stainless steel electrode. Two layers of carbon-black tape were applied to the rod to serve as the inner screen. The outer screen comprised one layer of butted carbon-black tape backed by copper foil. The butt gaps were 0.040 to 0.060 inch and 33 percent registration was used. The samples were terminated with a small stress cone under capacitively-graded terminations. This type of sample is described in Reference 4-6 as the standard "50 kV test sample". The samples were taped on a lathe with a tape-tensioning device attached to the toolpost; this procedure is also described in Reference 4-6. By taping the samples in this manner, it was anticipated that reasonable uniformity among samples would be obtained.

Automatic control of the voltage was not available during these tests. However, a voltage reference circuit was used, which compared the applied voltage with the reference voltages created by a ladder of zener diodes, spaced at 2.5 kV intervals. The voltage difference between the applied voltage and the voltage reference was recorded on a strip chart recorder, so that a true sample voltage history could be reconstructed at the end of the test. This true voltage history can then be used in the statistical analysis described below.

The test plan was to run a series of step-stress tests to determine the trend of the aging characteristic. These were followed by a series of constant-stress tests. Constant stress tests are preferred from the standpoint that the sample history is unambiguous, and that this exposure corresponds most closely to service conditions. In the actual execution of the tests, the constant voltage tests were terminated by a series of steps of increasing voltage to accelerate failure of the samples. This procedure was a matter of experimental convenience, to gather more data in a given elapsed time. The tests which were run are identified and summarized in Table 6-2 below. Further details of all the test histories are given later.

Table 6-2

TEST SERIES IDENTIFICATION

Test Number	Test Description
1	0.25 hour steps
2	1.0 hour steps
3	4.0 hour steps
4	41 kV constant voltage, no steps
5	38.5 kV constant voltage, 1974 hours plus steps (1.25 kV for approximately 100 hours)
6	42.6 kV constant voltage, 161 hours plus steps (1.25 kV for approximately 25 hours)

The test data were analyzed using a general purpose computer routine which fits the data to a Weibull distribution, using the inverse power law to relate life to stress. The curve fitting method is the method of maximum likelihood; this method allows the use of sample survival data as well as sample failure data in the analysis.

When the inverse power law is combined with the Weibull distribution, the resulting expression for the fraction of samples which survive to time t, under an applied stress E, is:

$$S(t) = \exp\left[-\left(\frac{E^n t}{C}\right)^{\beta}\right]$$

where $S(t)$ = fraction of samples surviving after time, t

E = electric stress (constant)

n = derived exponent

β = derived exponent

C = normalizing constant

The computer routine derives the three constants (n, β, and C) by means of maximum likelihood theory. This theory can handle data on samples that have survived to time t without failure, as well as samples that have failed. The results of this curve fit will be discussed here.

The inverse power law states that the following relationship holds between the applied stress and the time to failure:

$$E^n t = \text{const.}$$

or,

$$n \log E = \log (\text{const.}) - \log t$$

where n is the same exponent used in the above Weibull distribution. If this law is assumed to hold, and the sample aging is assumed to be independent of the actual aging history (independent of the order of application of different stresses, for example) an equivalent time can be computed for any sample that has been subjected to varying (i.e., step) stresses.

The equivalent time is computed for some base stress, and the equivalent time at any other stress is given by:

$$t_{equivalent} = t_{actual} \times \left[\frac{E_{actual}}{E_{base}}\right]^n$$

The total equivalent time is then the sum of the equivalent times at each stress level.

For purposes of visualizing the results, the equivalent time has been computed for each set of samples, using the stress corresponding to the initial applied voltage as the base stress. For the pure step-stress tests (1, 2, and 3), the base stress has been selected at the lowest level at which substantial failures occurred. These data have been plotted in Figure 6-1, a graph in which the coordinates are log stress (E) and log time (t). These coordinates linearize the Weibull relationship. Also plotted on the graph are the straight lines representing the Weibull relation for 10, 50, and 90 percent survival probabilities, calculated by using the constants derived from the curve fit analysis.

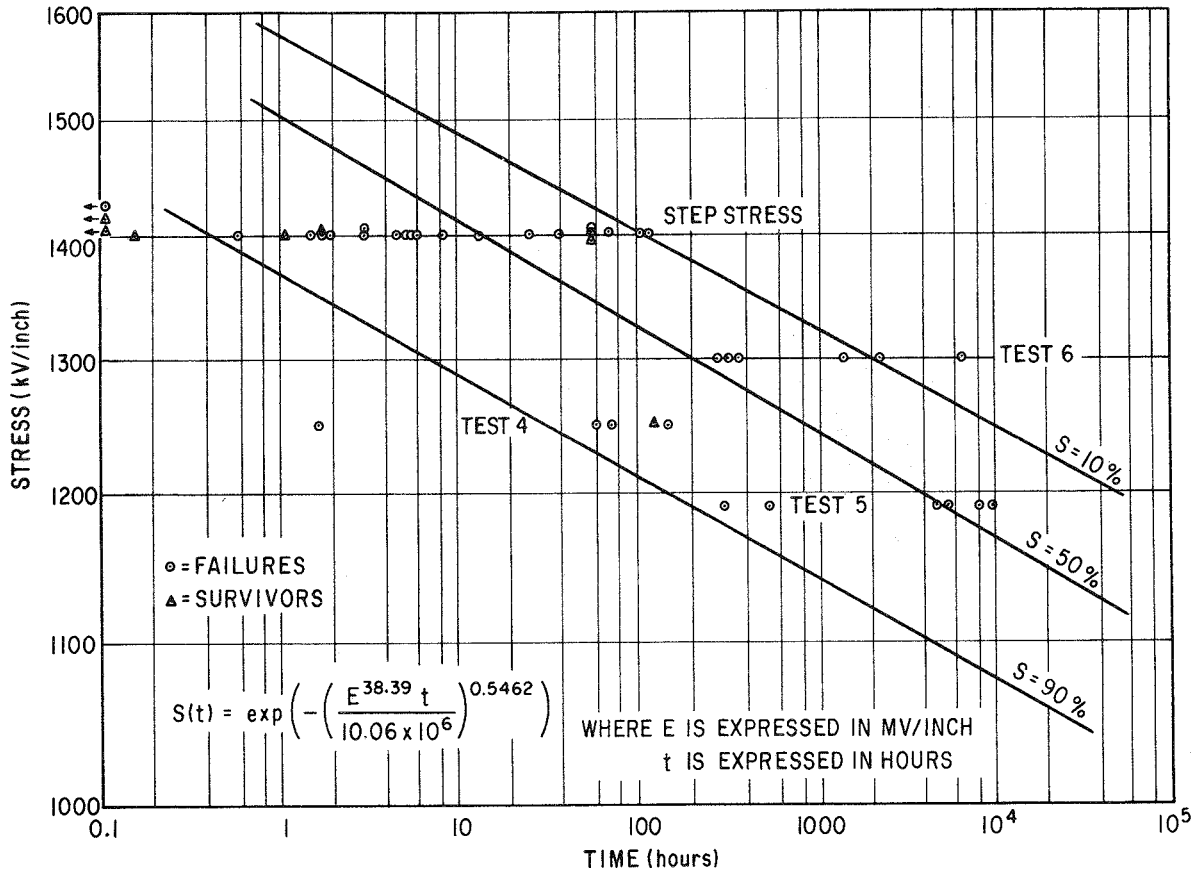

Figure 6-1. Aging Data For Liquid-Nitrogen-Impregnated Cellulose Paper

The results of the curve fit may be expressed in terms of a most likely value for three constants n, β, and C, and also in terms of the maximum and minimum values which could be predicted with 95 percent confidence. The values so derived from the present data are tabulated in Table 6-3. Also tabulated are data obtained on other materials in liquid nitrogen, which were derived during the Phase II Cryogenic Cable Program.

Table 6-3

MAXIMUM LIKELIHOOD FIT WEIBULL PARAMETERS

Material	Estimate			95% Confidence Limits					
				Lower			Upper		
	n	β	C	n	β	C	n	β	C
Cellulose Paper	38.390	0.54619	10.06 E6	29.479	0.39278	0.3854 E6	47.301	0.75952	262.5 E6
Polyethylene Paper (Tyvek)	19.022	0.81514	162	7.9	0.29	0.156	30.1	1.34	5.08 E6
Cellulose Polypropylene Laminate	9.698	0.99899	654	6.0	0.59	1.96	13.4	1.40	8.03 E5

Note: The constants in this table are dimensioned so that E is expressed in MV/inch and time in hours.

No intuitive importance can be attached to comparative values of the constant, C, since it is a normalizing constant only.

The test data for the polyethylene paper (Tyvek) and the cellulose-polypropylene laminate are described more fully in Reference 4-6. The polyethylene paper was post-calendered material, which was extensively tested during the Phase II program, while the laminate material was essentially capacitor paper, approximately one mil thick, which had shown very high short-term breakdown strength. This material was used in the aging comparison as a matter of convenience.

From examination of the graph in Figure 6-1, it is clear that there is considerable scatter in the data. What also appears likely is that the samples from Tests 4, 5, and 6 came from different populations. This hypothesis is indicated by the fact that the samples are clustered in different regions relative to the 50 percent survival line. This latter observation is a little difficult to rationalize, in view of the fact that considerable care had been taken to assure uniformity of samples. The general scatter in the data is reflected in the value for β, which is often called the Weibull shape parameter. β equal to one is a common value found for many populations, while β greater than one indicates smaller scatter and β less than one indicates larger scatter.

This test is very sensitive to errors in measurements of the voltage and the sample thickness, since both enter into the calculation of the stress. However, at the moment, no sources of systematic errors of either type are evident among separate tests. Another possibility, which does have systematic significance, is in the fact that the second two failures in Test 4 occurred coincidentally with the loss of pressure in the test vessel. A loss of pressure was connected with Test 5, although no sample failures were associated with it; in fact, the first two samples had already failed. In Test 6, the pressure was maintained at 80 psig throughout the test. The loss of pressure was manifested electrically in Tests 4 and 5 by a sub-

stantial increase in dissipation factor, which was confirmed by the physical observation of strong carbon deposition in the butt gaps adjacent to the inner and outer carbon-black screens.

It is also known that the breakdown strength of free liquid nitrogen increases by about 25 percent when the pressure is raised to a few atmospheres, although no such data exist on liquid-nitrogen-impregnated paper insulation. The hypothesis here is that operation at near-atmospheric pressure, for even a few hours, could cause accelerated aging even though the samples did not fail.

Despite the technical uncertainties of the data, the results to date are nearly unambiguous in indicating that the aging characteristics of liquid-nitrogen-cellulose paper insulation are very good. Using the Weibull relationship, one can calculate that the 99 percent survival time for these samples at an assumed cable design stress of 450 V/mil is 4.55×10^{16} hours, or 5.2×10^{12} years.

DETAILED ACCOUNT OF TEST HISTORY

STEP-STRESS TESTS

The first part of the program consisted of conducting tests in a step stress pattern on sets of six samples each in step sequences of 15 minutes, one hour, and four hours. Each set was tested to failure. The samples were subjected to progressively increasing, equal steps of voltage, all steps being of equal duration within each test. The initial voltage was 26 kV. For the first set of samples, the time step was 15 minutes, for the second set, one hour, and for the third set, four hours. The procedure is the same as that described in Reference 4-6.

Originally, it was hoped that the samples could be fused, so that each sample would be dropped off the bus as it failed, without interrupting the voltage. Initial trials with fuses showed, however, that they interrupted spontaneously without sample failure in seven out of twelve samples. Since the cause for this behavior could not be diagnosed, the high-voltage fuse approach was abandoned. The procedure was to allow sample failure to trip the transformer breaker; the failed sample was located and removed, and voltage was reapplied. During the fuse investigation, 18 data points were obtained for 15 minute steps, of which 10 were sample failures and seven were false fuse interruptions. The unfailed samples can be used to supplement the statistics on the failed samples in the maximum likelihood method of statistical analysis that is used. For a simplified impression of the results, the average breakdown stress for each time step sequence is shown in Table 6-4.

Table 6-4

COMPARATIVE SUMMARY OF STEP-STRESS TEST DATA

Step Duration	Present Test Cellulose		Polyethylene Paper		Polypropylene Cellulose Paper Laminate	
	Average Stress (V/mil)	Percent of 15 Min.	Average Stress (V/mil)	Percent of 15 Min.	Average Stress (V/mil)	Percent of 15 Min.
15 min.	1501	100	1354	100	1918	100
1 hour	1493	99	1337	99	1865	97
4 hours	1516	101	1282	95	1681	88
16 hours			1062	78	1310	68

Also shown in Table 6-4 are data taken from the Reference 4-6 final report pertaining to polyethylene paper and polypropylene/cellulose paper laminate tested in the same manner. The appearance of Table 6-4 indicates that the present cellulose paper has not experienced much time degradation in breakdown strength. That is, the average strength is substantially the same (within the experimental scatter) for the three time steps. The other two materials have shown a small degradation at the four-hour step.

Step-Stress Data

The step stress breakdown data for 15-minute, one hour, and four hour step sequences are shown in Tables 6-5, 6-6, and 6-7 (referred to as Test numbers 1, 2 and 3 respectively). Eleven calibrated voltage steps were used, the first being 26 kV, and the last, 51 kV.

The first two sets of samples for the 15 minute step sequence (Test number 1) were partly in the nature of trial runs in an attempt to diagnose the behavior of the fuses, which were used in the previous step-stress work and were known to fail in some cases when there was no bona fide sample failure. The system was instrumented to display the current decay through the sample on a fast response, digital storage oscilloscope, to detect any system transients which might be responsible for the false fuse interruptions. No clues to this behavior could be found; in all cases, the instrumentation gave identical information when the fuse opened. It was only when the samples were examined after the test that it could be determined whether they had failed or not. Among the twelve samples tested in this manner, seven showed no evidence of failure.

Table 6-5

DATA FROM TEST NUMBER 1: 15-MINUTE STEP-STRESS DATA
(STARTING STEP NO. 1: 26.0 kV)

Sample	Final Step	Final Voltage (kV)	Time in Final Step (min)	Stress (V/mil)	Survive/ Fail	Fuse (Yes/No)
26	11	51.0	35.5*	1597	F	N
33	11	51.0	35.5*	1597	F	N
9	11	51.0	66.1	1555	F	Y
31	11	51.0	10.3	1555	S	Y
12	11	51.0	8.9	1555	S	Y
2	11	51.0	2.3	1423	S	Y
6	11	51.0	2.1	1555	F	Y
28	11	51.0	2.0	1576	S	Y
7	11	51.0	0.5	1598	F	N
17	11	51.0	0.5	1620	F	N
29	10	48.5	15.0*	1499	F	Y
35	10	48.5	15.0*	1479	S	Y
14	9	46.0	11.0	1441	F	N
23	8	43.5	6.0	1326	S	Y
1	8	43.5	4.0	1213	S	Y
18	7	41.0	2.3	1345	F	Y
36	6	38.5	7.0	1206	F	N
37	6	38.5	15.0	1250	F**	Y

*Failed during increase in voltage to next step
**Failed at obvious wrinkle

To proceed expeditiously with the step-stress testing, it was decided at this point to abandon the fuse approach and to allow a failed sample to trip the transformer breaker. A detection circuit was installed to indicate which sample had failed, so that it could be removed from the bus and the voltage reapplied. This detection circuit was only partially effective; in many cases, more than one sample was indicated, and it was necessary to locate the actual failed sample by trial and error, removing one sample at a time and reapplying voltage. The results of this method were generally successful, however, and data were obtained for a third 15-minute step sequence, as well as for one-hour and four-hour sequences.

Table 6-6

DATA FROM TEST NUMBER 2: ONE-HOUR STEP-STRESS DATA
(STARTING STEP NO. 3: 31.0 kV)

Sample	Final Step	Final Voltage (kV)	Time in Final Step (min)	Stress (V/mil)	Survive/ Fail
5	11	51.0	1.0	1576	F
25	10	48.5	27.0	1498	F
22	10	48.5	18.0	1498	F
13	10	48.5	10.0	1471	F
38	9	46.0	60.0	1421	F
3	9	46.0	15.0	1441	S*

*Failure in termination

In Tables 6-5, 6-6, and 6-7, the samples are listed generally in the order of their failure voltages, with samples failing at the same step listed in order of the failure times. The entire set of 15-minute data is presented in Table 6-5, along with a notation as to whether a fuse was in place and whether the sample failed or not. Unfailed samples can be used as data points in the maximum likelihood method of analysis used in the data, although these points are not as powerful as failure points. It should also be noted that three of the samples survived more than 15 minutes at the highest calibrated step. In one case, the sample was left on voltage until it failed. The other two samples were left on voltage for 35.5 minutes, at which time an attempt was made to raise the voltage by an additional 2.5 kV step; the samples failed during the increase in voltage. These odd data points can be adequately handled in the analysis.

The data for the one-hour and four-hour steps (Tests number 2 and 3, respectively) shown in Tables 6-6 and 6-7 are straightforward and need no comment.

CONSTANT VOLTAGE TESTS

In the first of the constant voltage tests (Test number 4) five tape-wrapped cellulose paper samples were tested in liquid nitrogen at 41 kV. This test voltage corresponds to an electric stress of approximately 1250 V/mil; the precise stress depends on the final measurement of the sample insulation thickness. The first sample failed after 1.7 hours; the fifth sample was removed from test after 121 hours. The details of the sample failure times and the calculated stresses are shown in Table 6-8.

Table 6-7

DATA FROM TEST NUMBER 3: FOUR-HOUR STEP-STRESS DATA
(STARTING STEP NO. 3
31.0 kV, NO FUSES)

Sample	Final Step	Final Voltage (kV)	Time in Final Step (min)	Stress (V/mil)	Survive/ Fail
6	11	51.0	58.6	1576	F
15	11	51.0	22.4	1576	F
20	11	51.0	1.9	1620	F
19	10	48.5	106.3	1499	F
4	9	46.0	220.3	1403	F
8	9	46.0	164.0	1422	F

There is some question regarding the validity of the breakdown data on the third and fourth samples, since it is noted in Table 6-8 that the pressure had dropped when the samples failed. More correctly, it should be said that during a periodic inspection of the test it was observed that the transformer breaker had tripped, and the nitrogen pressure in the test vessel

Table 6-8

DATA FROM TEST NUMBER 4: TIME AT VOLTAGE TEST RESULTS

Sample	Time		Outside Diameter (inches)	Inside Diameter (inches)	E (V/mil)	Remarks
	Hours	Minutes				
4/32	1.70	102.0	0.582	0.512	1250	Normal failure
8/10	44.63	2677.9	0.576	0.509	1295	Normal failure
6/34	62.02	3721.5	0.582	0.512	1250	Pressure down
5/39	73.32	4399.3	0.582	0.512	1250	Pressure down
7/30	120.96	7257.9	0.582	0.512	1250	Removed/survived

had fallen to 0 psig. It is not known whether the loss of pressure was coincident with the breaker trip, although it is probable that the decrease in pressure was gradual, occurring over a period of an hour or more. Data obtained in an earlier phase of this program indicate that the breakdown strength of liquid nitrogen at a pressure of 0 psig is less than the breakdown strength at a pressure of 70 psig, the pressure maintained in these tests. Hence it is not unreasonable to assume that the loss of pressure initiated the sample failures. However, the fact that the fifth sample survived the drop in pressure without failure is contraindica-

tive, and it is possible that the third and fourth samples were close to failure at the time of the drop in pressure.

Although these test data are made suspect, to some extent, by the occurrence of the drop in pressure, the treatment of the third and fourth sample failures as legitimate data points will provide, if anything, a pessimistic result in predicting the aging characteristic of the electrical insulation.

It was stated earlier that the fifth sample was removed from test after 121 hours. It was decided to remove this sample because the measured dissipation factor had increased from 1720 microradians to about 4000 microradians, after the failure of samples three and four. At the time, it was suspected that the sample had been damaged by the previous failures, and after the accumulation of some additional hours at voltage it was removed from the line to preserve any evidence of damage. On inspection, the sample was found to be intact, but the outer layers of cellulose tape showed considerable carbon deposition in the butt gaps. This deposit is presumed to have come from the carbon-black screen. Deposits were also evident in the butt gaps at the inner electrode. The increased dissipation factor can be tentatively attributed to these carbon deposits.

Test number 5 consisted of a set of six samples which was put on test at 38.5 kV (1192 V/mil). They were operated at this level for a total of 1974 hours. During this initial period, two of the samples failed -- at 282 and 509 hours, respectively. After the accumulation of 1974 hours without further failures, it was decided to raise the voltage in small increments to cause the remaining samples to fail. The voltage was raised in steps of 1.25 kV, each step approximately 100 hours long. Four additional steps were required to fail the remaining four samples, the last sample failing part way into the step in which the nominal voltage was 43.5 kV (1347 V/mil).

Upon reexamination of the voltage variation recorded during that part of the test in which the voltage steps were applied, it was considered desirable to divide the applied voltage into 0.5 kV intervals and to read the time spent at each interval from the record. The results of this further analysis are shown in Table 6-9, with the pertinent sample dimensions.

One final observation about Test number 5 is appropriate. Some hours after the failure of the first two samples, a partial loss of pressure occurred. Although no sample failures were connected with this event, the measured dissipation factors of all the remaining samples showed a sharp increase, from about 1500 to 4000 microradians, in readings taken before and after the pressure loss. If carbon-black deposition is again the cause, the deposition is clearly connected with short-time exposure at low pressure rather than with time-at-voltage at the operating pressure of 70 psig. This occurrence is of minor concern with respect to the validity of the test

Table 6-9

DATA FROM TEST NUMBER 5: TIME AT VOLTAGE VERSUS VOLTAGE

Sample Number	I.D./O.D. (inches)	Applied Voltage (kV)								Total Time on Test (hours)
		38.5	39.75	41.3	42.4	42.9	43.4	43.9	44.9	
		Time at Voltage (hours)								
6(3)	0.509/0.578	1973.9	120.5	95.6	10.0	87.9	21.1	4.19	5.44	2318.6
8(6)	0.509/0.578	1973.9	120.5	95.6	10.0	87.9	11.0	3.39	--	2302.3
9(5)	0.509/0.578	1973.9	120.5	95.6	--	41.8	6	--	--	2237.8
5(2)	0.509/0.578	1973.9	120.5	95.6	--	33.2	--	--	--	2223.2
4(1)	0.509/0.578	509.2	--	--	--	--	--	--	--	509.2
7(4)	0.509/0.578	282.2	--	--	--	--	--	--	--	282.2

data, but may indicate that the use of carbon-black screens in cryogenic cable designs should be reconsidered.

The next test, Test 6, was performed to better define the breakdown stresses at the short-time end of the curve. In this test, six samples were subjected to a constant voltage of 42.6 kV, with the expectation that the mean failure time would be approximately 25 hours. After 161 hours without a failure it was decided to raise the voltage in steps to obtain failures. Four steps of 1.25 kV, each step approximately 25 hours long, were needed to fail the last sample. The summary of time at each step and the sample failures is given in Table 6-10. In this table, the nominal voltages are shown. A detailed examination of the voltage record has been made to determine the actual voltage pattern, but it did not deviate greatly from the nominal voltage pattern.

Table 6-10

DATA FROM TEST NUMBER 6: TIME AT VOLTAGE VERSUS VOLTAGE

Sample Number	I.D./O.D. (inches)	Applied Voltage (kV)					Total Time on Test (hours)
		42.6	44.1	45.3	46.7	48.1	
		Time at Voltage (hours)					
4(7)	0.509/0.578	161.4	25.6	19.4	7.9	--	214.3
5(8)	0.509/0.579	161.4	21.3	--	--	--	182.7
6(9)	0.509/0.578	161.4	25.6	19.4	32.6	17.2	256.2
7(10)	0.509/0.578	161.4	25.6	19.4	21.8	--	228.2
8(11)	0.509/0.581	161.4	25.6	19.4	11.3	--	217.7
9(12)	0.509/0.578	161.4	2.5	--	--	--	163.9

CONCLUSIONS

Despite the technical uncertainties of the data, the results to date are nearly unambiguous in indicating that the aging characteristics of liquid-nitrogen-cellulose paper insulation are very good. Using the Weibull relationship, one can calculate that the 99 percent survival time for these samples at an assumed cable design stress of 450 V/mil is 4.55×10^{16} hours, or 5.2×10^{12} years.

It is obviously unrealistic to attempt to draw conclusions from these limited data as to the precise life characteristic expected in a full-scale cryogenic cable using this insulation material. In fact, it is highly questionable whether it would ever be worthwhile to attempt to expand the data such that precise life characteristics could be derived. However, the data obtained and analyzed to date do provide a strong indication that the life characteristic of cryogenic insulation will be as good as, or better than, that of conventional oil/paper insulation.

Section 7

RECOMMENDED FUTURE WORK

CRYOGENIC ENVELOPE INVESTIGATION

In this program, the primary objectives of developing half-scale FRP pipe sections, FRP pipe/FRP pipe joints, and FRP pipe/metal flange joints to successfully pass a series of cryogenic qualification tests, have been accomplished. However, it is anticipated that a number of substantial technical challenges lie ahead in the development of full-scale envelope sections for cryogenic cable application.

In the Phase III program, the selection of adhesives and the design of adhesive bonded joints were primarily based on the results obtained from specific experimental investigations, rather than from detailed analytical studies. In this program, this approach was necessary in view of the lack of engineering data for the particular materials at low temperature, and the lack of a failure criterion for the FRP pressure pipe at low temperature.

Areas of future work that are recommended for consideration as part of the future development of full-scale envelope sections, and the associated joints, are discussed below:

- Meaningful design procedures and analyses for FRP pipe/metal flange joints will require a better understanding of the fracture properties of the adhesives at low temperature, and the influence of flaws on stress concentrations. Fatigue and creep property data at low temperature are also required for the adhesive systems as well as the FRP.

- Additional investigation of the performance of scarf joints, particularly the effects of longer lap lengths, is also expected to lead to the design of joints with higher strengths.

- A study of FRP pressure pipe manufacturing techniques is required to identify those techniques best suited to the manufacture of full-scale pipe sections, 40 feet in length. It will clearly be necessary to achieve a high degree of quality control during this manufacturing procedure.

- FRP pressure pipe manufacturing costs must also be estimated with a view to reducing manufacturing cost by selecting the "best" filament winding patterns. The selected patterns must also be consistent with requirements for good structural properties at low temperature.

ELECTRICAL INSULATION EVALUATION

The cable and pothead tests performed in this Phase III program have provided important information for the future development of these components. In general terms, it is believed that the selection of the specific cellulose paper used in the two prototype cable sections is the "best" candidate for near-future cable sections. Certainly, extensive insulation material development could be expected to provide an improved material, from the standpoint of reduced dissipation factor, but such a development effort is hardly warranted at this stage of development. In the future, it may be appropriate to initiate such a development, once the market potential of cryogenic cable systems has been established.

The experiences gained in this Phase III program clearly indicate that more attention must be given to the moisture content of the cable paper during manufacture and installation. This is not expected to provide a major problem, but it is necessary to decide whether the cable should be manufactured in a 50 percent relative humidity environment, to more closely match installation conditions, or whether the cable should be contained on hermetically sealed reels following manufacture.

Greater attention must also be given to the selection of a cable screen. Should carbon-black screens be used at all, and if so, what specifications are required for this material? It has been demonstrated that the high dissipation factor values measured in this series of cable tests can be attributed directly to the use of the duplex screen. Some limited study of this problem is recommended on small dielectric samples in liquid nitrogen.

Additional development work is also required in the area of the cryogenic potheads. This will probably require additional dielectric tests on small models to determine limiting stress values in specific pothead regions. However, in view of the experiences gained to date on this first series of pothead tests, it is believed that full-scale potheads can be designed and qualified for this application. In general terms, the mechanical and cryogenic performance of the pothead structures tested in this Phase III program proved to be completely satisfactory, and should be capable of extrapolation to full-scale.

TEST SYSTEM SPECIFICATIONS

In this report, the specifications of components for a 500 kV, 3500 MVA, 1000-foot test system are presented. It must be emphasized, however, that these specifications are based solely on the development work performed to date, and may require revision as further development is performed, and following the detailed design of the test system.

ELECTRICAL INSULATION AGING STUDY

The work performed to date provides a clear indication that the life characteristics of cellulose paper insulation impregnated with liquid nitrogen will be equal to or better than the characteristics of conventional insulation materials. A more detailed investigation to determine the precise life characteristic of cryogenic insulation materials with a view to predicting the anticipated life of a particular cable installation appears to be unwarranted.

Section 8

CABLE SYSTEM DESIGN STUDY

INTRODUCTION

PAST STUDIES

An initial cost estimate for possible configurations of a resistive cryogenic cable was performed in Phase I of the Cryogenic Cable Program. An important goal of that phase of the program, completed in 1971, was to screen the large number of possible cryogenic cable system designs, select a candidate for further design and development, and establish which areas of technology should be addressed in subsequent work. This was done through both technical and cost evaluations.

As a result of these evaluations, a configuration for a liquid nitrogen cooled cable system, using three flexible cables in a pipe insulated by evacuated multilayer thermal insulation, was selected in 1971. The study showed that an influential factor in the selection of a cable was the performance of the electrical insulation. Consequently, subsequent effort was directed at the development of an appropriate electrical insulation system. In addition, the Phase I study showed that the cryogenic envelope, based on evacuated multilayer insulation, and the installation of such a system would account for over one-half of the owner's cost. A major portion of the cost resulted from sophisticated techniques that must be utilized to achieve reliable assembly in the field.

PRESENT STUDY

In the present Phase III program, considerable attention has been paid to the development of FRP piping insulated with closed-cell foam as an alternative to the vacuum-insulated piping assumed in earlier studies. The foam-insulated FRP piping is expected to offer reduced system cost. But, it must be recognized that such a concept also affects previous considerations of manufacturing techniques, system losses, and sizing of the cable system components. In this section of the report, these considerations are revised in the light of the foam-insulated FRP piping concept.

In addition, it is desirable to estimate the dimensions and configurations of the components for full-scale operating systems so that future component development can address components of appropriate size.

This study was based on the configuration shown in Figure 3-1. The specific objectives of this study were to:

- Select the configuration, principal dimensions, and parameters of the cable system components (such as cables, piping, thermal insulation, and refrigerators).

- Evaluate the performance of the cable system in terms of system losses, refrigerator spacing, liquid nitrogen flow requirements, and thermal transient behavior.

- Prepare preliminary cost estimates for installed systems, based upon 20-mile transmission distances, to allow trade-offs to be made between competing cable system configurations.

In performing the system design study, the following principal features of the cryogenic cable system were maintained constant:

- Flexible cable configuration, for shipment on spools.

- Three cable phases in a single pressure pipe.

- Separate return pipe for the liquid nitrogen flow.

- Foam-insulated pressure pipe and return pipe.

The effects of varying the following parameters were investigated as part of this study:

- Single circuit capacity (nominal ratings of 2000, 3500, and 5000 MVA) at a nominal system voltage of 500 kV. However, consideration was given to a 345-kV system voltage for the lowest capacity, 2000 MVA.

- Liquid nitrogen inlet and outlet conditions (temperature and pressure).

- Dimensions of the pressure pipe, the return pipe, and the thermal insulation vapor barrier.

- Concepts for the FRP pressure pipe and the metal pressure pipe.

- Sensitivity analyses were performed for the physical parameters (such as, thermal conductivity of the electrical insulation, hydraulic friction factors, conductor space factor, and a-c/d-c loss ratios.

Throughout this study the intent was to impose limits on the component dimensions that reflect practical manufacturing, shipping, and cost limitations. Installation costs were based upon estimates prepared by Gibbs and Hill, Inc. as a subcontractor under this program.

COST DEFINITIONS

The following terminology is used throughout this section when comparing costs of the different systems. The "investment cost" has been based upon the cost of components and the installation of the complete system. Costs associated with purchase of land, construction of buildings, material transportation, sales taxes, system design engineering, and fuel escalation have been excluded.

The "owner's cost" is this investment cost plus the capitalized value of losses. These additional costs include charges associated with the added capital investment required to generate these losses plus the cost of the fuel. The costs for losses has been computed using $1000 per kilowatt. Since maintenance costs are likely to be similar for all of the systems, they were also excluded.

CABLE SYSTEMS CONSIDERATIONS

This section contains a number of general considerations involved in possible applications of a cryogenic cable to an electric power system. A cryogenic cable may be used as the sole means of transmission from a baseload generation site or used with conventional transmission in an interconnected network.

For either application, particular attention must be given to overload limitations of the cryogenic cable since they are quite different from those for existing underground cables. In conventional cables, considerable overloading can be tolerated for extended periods without risk of sudden failure in the electrical insulation. The overloads raise the temperature of the conductor and its insulation and cause gradual degradation of the insulating properties and a shortened life. The degree of damage depends upon the duration of the overload and the temperatures reached.

Conventional cables permit operation under overload conditions for extended periods of time. The resulting higher cable temperature shortens the cable's useful life, but does not otherwise jeopardize cable operation. This shortened life is caused by more rapid aging of the electrical insulation at a higher temperature. However, the overload capacity of a cryogenic cable is limited by the rapid failure of the electrical insulation when the saturation temperature of the liquid nitrogen is approached. To ensure reliable, long-term operation of the cable, the liquid nitrogen in the cable is maintained at a minimum of 10 K below the local saturation temperature. This is the basis for determining the maximum distance the liquid nitrogen travels along the cable before it must be returned to the refrigerator. This distance is referred to as the module length. Throughout this study, it has been assumed that this margin would not be reduced even though it is highly unlikely that any damage will occur to the cable insulation until the tempera-

ture approaches within a few degrees of the liquid nitrogen saturation temperature.

For cryogenic cables used in interconnected systems, it may be necessary to use phase angle regulators (PAR) to control the load carried by the cryogenic cable system and prevent overloads during the loss of other interconnected lines. Since such regulators are expensive and require considerable land area, it may prove more economical to install cables that are operated at loads below rated capacity provided this will allow the cable to absorb long-term overloads. Whether or not PAR's are required will depend upon how the cryogenic cable is applied in a specific system. They would not be needed if the cable is used for the exclusive transmission of power from a large generation site. The cost of PAR's has not been included in the cable system cost comparisons since this will depend upon details of the actual transmission system. A 600-MVA rated PAR costs about $2 million and requires about 2500 square feet of land area.

Specific details of an actual system will determine the minimum overload requirements of the cryogenic cable. This will depend upon:

- Short-term fault capability.
- Overloading during generator voltage swings after network load disturbances.
- Longer duration overloading (minutes to several hours) from loss of other transmission lines in the network, before load switching can occur and the system is rebalanced.
- Long-term overloading that may be required during major repairs that extend for many days. Such overloading capability could prevent dropping high efficiency generation.

Selection of the proper MVA capacity of a cryogenic cable installation will require a transmission planning study for a specific system that considers the cost and consequences of forced outages. Such a study should also include predictions of locations and magnitudes of future load growth.

For example, a 3000-MVA baseload plant served exclusively by cryogenic cables will require three cables each capable of 3000 MVA. Considering that such a plant is a $3 billion investment and each 1000-MVA unit may cost one-half million dollars a day for downtime, the installation of redundant cables to achieve a highly reliable system is warranted.

If one cable is serving the site, a second cable must be maintained in a standby (cold) condition for immediate use should the primary cable have to be removed from service. Because of the length of time required to repair a cryogenic cable, it will be necessary to start the cooldown of a third cable to have it in readiness should a second failure occur before repairs can be completed.

In an example illustrated in Figure 8-1, three 5000-MVA cables are shown serving a generation site of 5000-MVA capacity. Since two cables will be kept cold at all times, the possibility exists that these cables can share the system load. A thorough analysis of losses would be required to identify the most economical manner for operating such a system. The scope of this study did not include consideration of specific applications for the cryogenic cable in which questions raised by the above factors would have to be answered.

The overall system efficiency of a 5000-MVA cryogenic cable system for operation at partial capacity was estimated. This efficiency, shown for a 20-mile installation in Figure 8-2, will decrease from approximately 99 percent at rated capacity to 98.5 percent at 30 percent capacity. Partial capacity operation of 3500-MVA cables was also examined. Refrigeration requirements and system efficiency values for these situations are contained in Appendix I, "Computer Output Sheets," of this report.

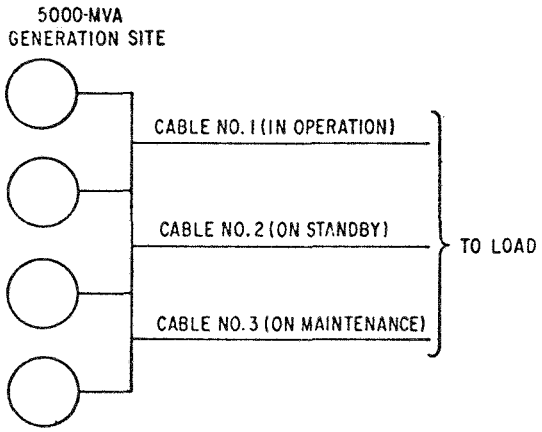

Figure 8-1.

Conceptual Cryogenic Cable System Serving a Major Generation Site

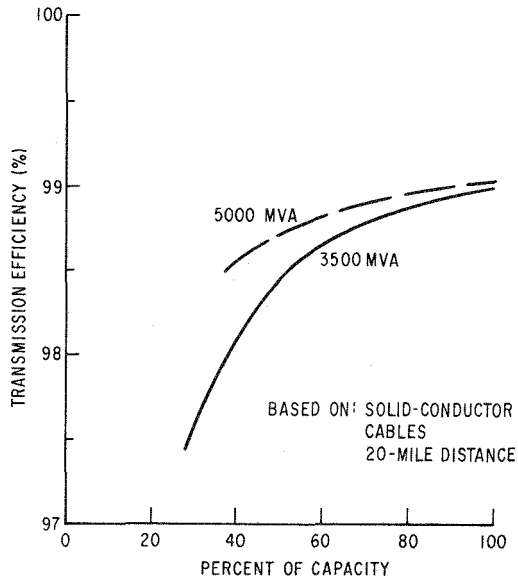

Figure 8-2.

System Efficiency Versus Percent of Rated Capacity

In an interconnected system, a comparison of operation at partial capacity versus the use of a phase shifter may indicate that operation at full rating is not the most economical method. Operation at part capacity would allow the system to pickup additional load during the loss of other lines. If PAR's are not needed for other reasons, operation at part capacity may prove less expensive than the use of a PAR to maintain rated loading.

Information summarizing the electrical and thermal performances of transmission systems based upon solid conductor cables is contained in Section 2, "Summary," and the following subsection, "Cable Design."

More detailed performance information, including the following, can be obtained from Appendix I for all of the concepts studied.

- System performance
- Conductor losses
- Dielectric losses
- Shield losses
- Thermal insulation loss
- Refrigeration capacity and input power
- Refrigeration station separation
- System efficiency

Appendix II, "Technical Data Sheets," of this report provides cable and piping dimensions as well as liquid nitrogen pressure and temperature conditions for each concept examined.

CABLE DESIGN

As a result of studies made during the 1971 Phase I portion of this program, aluminum was selected as the preferred conductor material. At cryogenic temperature, aluminum can exhibit an electrical conductivity equivalent to that of copper at a lower cost per unit volume. Cost comparisons remain the same as in 1971. Prices during the final week of 1976 for "primary" aluminum was 48 cents per pound and that for copper was 65 cents per pound. Sample cryogenic cables tested during Phase III were manufactured using electrical conductivity (EC) grade aluminum.

This same alloy, now designated as 1350, was selected for the system study following consideration of other alloys, such as 1100, 6101, and 6063, suggested by the Reynolds Aluminum Company. While high purity aluminum

would have lower resistivity values than the 1350 grade, its lower strength made it doubtful whether it could withstand the stresses of manufacture and installation.

The resistivity of the 1350 alloy was measured at 77 K using a 0.096-inch diameter wire. Its value of 0.31 $\mu\Omega$-cm compares favorably with a value of 0.28 that had been used earlier. The resistance ratio of the 1350 alloy measured at temperatures of 296 K and 77 K was determined to be 8.69. The resistivities for this and several other aluminums are shown in Figure 8-3 as a function of temperature within the range of interest.

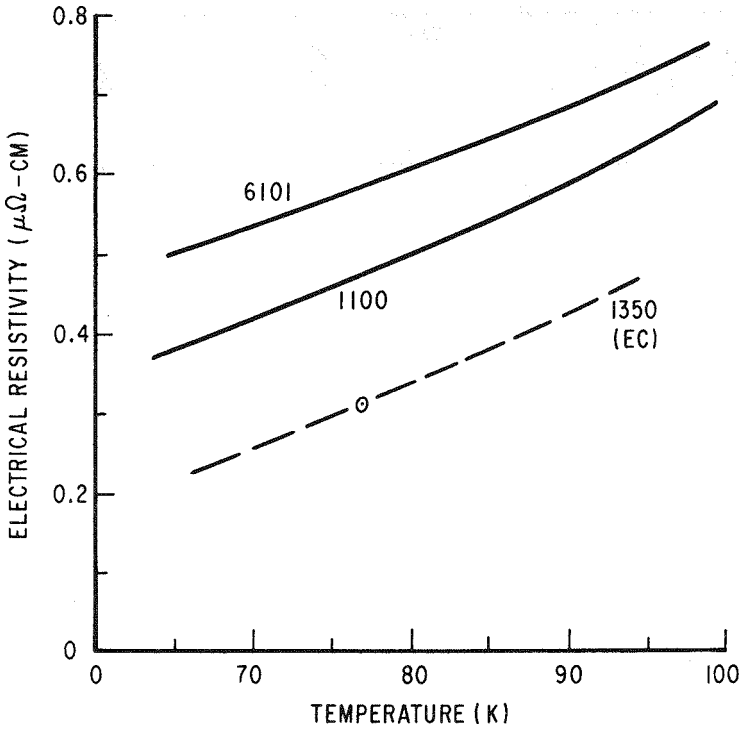

Figure 8-3. Resistivity of Aluminums for Cable Conductors

Conductor losses were computed for each cable system of interest in this study on the basis of a space factor of 0.75 and an ac/dc loss ratio of 1.25*. Losses predicted for a 3500-MVA, single-phase cable are shown in Figure 8-4 as a function of the conductor outside diameter. A family of curves is presented to also show how these losses are reduced as the cable bore is made smaller. Comparisons were made with solid conductor cables to evaluate which of the two constructions (hollow or solid conductors) would produce the lower owner's cost.

*This ratio was increased to 1.3 for the 2000-MVA, 345-kV solid-conductor case and decreased to 1.2 for the hollow-conductor cables.

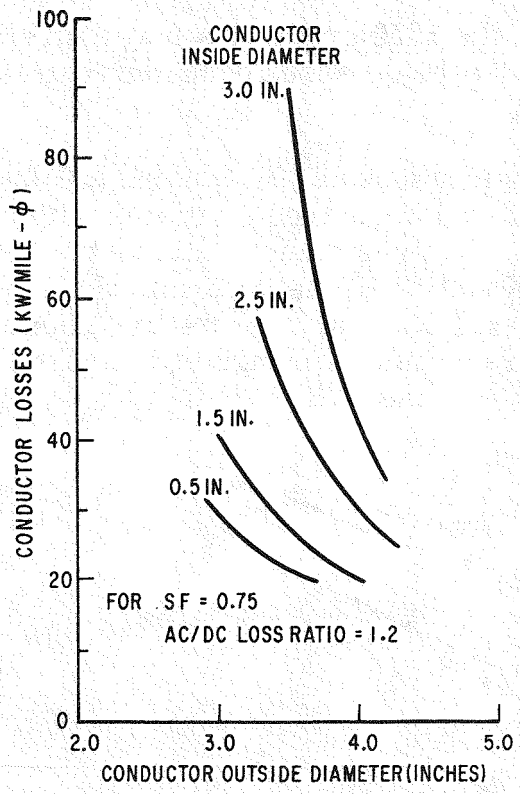

Figure 8-4.

Conductor Losses Estimated for 3500-MVA Cables

Cost analyses to determine owner's cost showed the power charges for system losses to be a major portion of the cost. For this reason the efficiency of the cable becomes important. As shown in Table 8-1, the power charge is over 25 percent of the total cost of a 20-mile long, 3500-MVA system. Cables for which these comparisons are made have a conductor outer diameter of 3.60 inches and a diameter over the skid wire of 5.78 inches. Cables of these diameters represent the largest that can be shipped by truck as an "oversize" load on a 14-foot diameter reel (Figure 8-5). Cables of larger diameter were not studied since their application to a 14-foot reel would require bending the cable to a radius that would exceed practical limits.

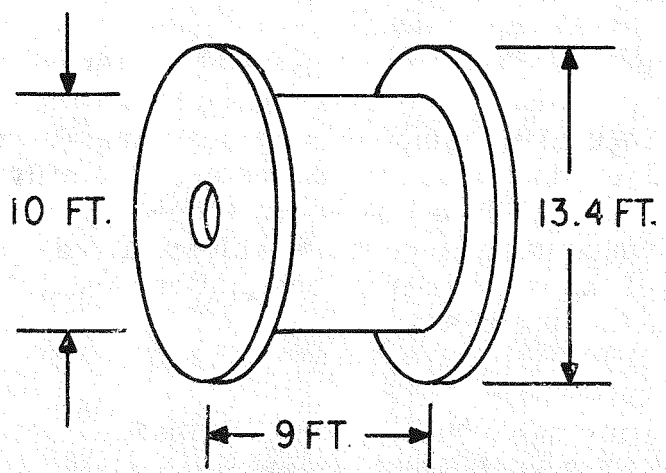

Figure 8-5.
Cable Shipping Reel

Table 8-1

POWER CHARGE FOR 500-KV CABLE SYSTEM LOSSES*
(Percent of Owner's Cost)

Cable Type	System Capacity		
	2000 MVA	3500 MVA	5000 MVA
Hollow-conductor Cable	26.2%	30.6%	34.5%
Solid-conductor Cable	20.8%	26.9%	31.0%

*Based on a 20-mile transmission distance.

Solid-conductor cables have lower conductor losses than hollow-conductor cables of the same outside diameter, which result in a lower power charge, as shown in Table 8-1. This is because the solid-conductor cable's higher cross-sectional area results in lower conductor losses. However, in contrast to the hollow-conductor cable that is simultaneously cooled from the outside and the bore, the solid-conductor cable can only be cooled from the outer surface.

While this study included consideration of cables of smaller conductor diameters, their higher losses led to higher owner's cost. For this reason further study of cables having conductor diameters less than 3.60 inches was dropped.

Analyses made of the thermal performance of both hollow- and solid-conductor cables showed that, for cables of the same conductor outside diameter, the solid-conductor cables could be cooled adequately and the refrigerators could be spaced farther apart. The "module" length is the distance the liquid nitrogen can travel along the cable before it must be refrigerated. This refrigeration distance, referred to as cable "module" length, is shown in Table 8-2 for the different MVA capacities and cable types. The slightly

Table 8-2

MODULE LENGTH FOR 500-KV CABLES
(5.78-inch diameter)

Cable Type	System Capacity		
	2000 MVA	3500 MVA	5000 MVA
Hollow-conductor Cable	10.6 miles	7.5 miles	4.9 miles
Solid-conductor Cable	13.2 miles	9.5 miles	6.3 miles

higher costs for the solid-conductor cables, as shown in Table 8-3, is more than compensated by the savings resulting from the lower conductor losses and the longer module lengths.

Table 8-3

ESTIMATED COST OF THREE-PHASE CABLES

Cable Type	System Capacity and Voltage			
	2000 MVA at 345 kV	2000 MVA at 500 kV	3500 MVA at 500 kV	5000 MVA at 500 kV
Solid-conductor Cable	$232/ft	$268/ft	$242/ft	$259/ft
Hollow-conductor Cable	$166/ft	$211/ft	$210/ft	$230/ft

The same type of cellulose paper insulation used to manufacture the test cables described in the section "Electrical Insulation Evaluation" (page 4-3) of this report was selected for this study. A dielectric constant of 2.0 and a loss tangent value of 1200 μrad was used in computing cable dielectric losses. A value of 0.0016 W/cm-K was used for the average thermal conductivity of the cellulose insulation (see Appendix III, "Thermal Conductivity of Liquid Nitrogen Impregnated Cellulose and Cellulose/Polypropylene Dielectric Materials," of this report).

The cellulose insulation thickness was based on a maximum voltage stress (at the conductor outer surface) of 400 volts per mil at rated voltage. Thus, thicknesses of approximately 0.9 inch and 0.6 inch were used for the studies based on the 500-kV and 345-kV cable systems, respectively. Figure 8-6 shows how the cellulose insulation thickness increases as the conductor diameter is reduced. The maximum outer diameter of 345-kV and 500-kV cables is shown in Figure 8-7 as a function of conductor diameter.

Conductor and dielectric losses from the three-phase cables contribute approximately 45 to 65 percent of the total losses for systems of 2000- to 5000-MVA rating. Dielectric losses are shown in Figure 8-8 as a function of conductor diameter. The major portion of the remaining losses is from heat transfer through the foam thermal insulation into the liquid nitrogen along the cable and along the liquid nitrogen return pipe. These losses have been included when comparing different cable designs by estimating a power charge that has been added to the investment cost of the cables, piping, terminals, and refrigeration system.

The costs for construction of the buildings housing the refrigerator and the liquid nitrogen pumps and the cost of land have been omitted from these comparisons. The system losses were charged at a rate of $1000 per kilo-

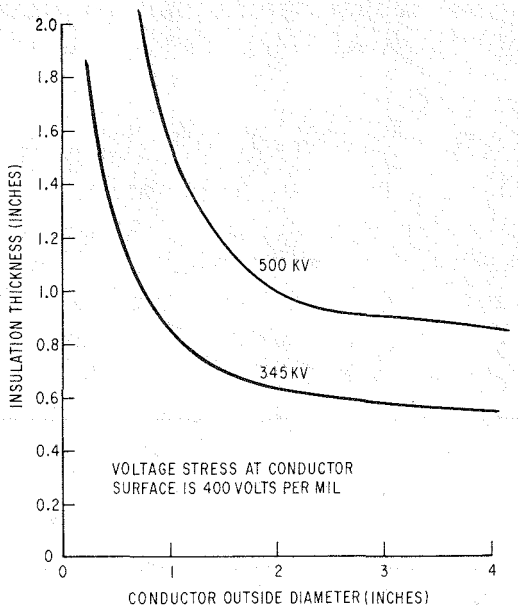

Figure 8-6.

Conductor Outside Diameter Versus Insulation Thickness

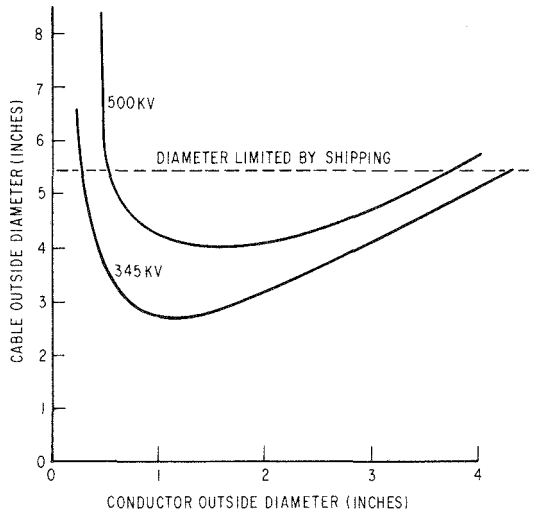

Figure 8-7.

Diameter of Cable Electrical Insulation Versus Conductor Diameter

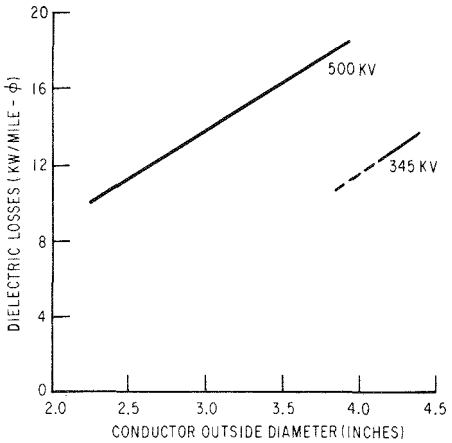

Figure 8-8.

Cable Dielectric Loss Versus Conductor Diameter

watt, to cover both capital and fuel costs.* Foam insulated pressure piping cost estimates do not include costs for electromagnetic shields since they may not be required in many installations.

CABLE DESIGN RECOMMENDATIONS

Solid-conductor rather than hollow-conductor cables are recommended for future development, since they result in lower owner's cost. Designs recommended for each system capacity are shown in cross section in Figures 8-9 through 8-11. Cable conductor outside diameters are the same for all three capacities listed in Table 8-4. This results in a maximum conductor cross-sectional area, and therefore lowest cable losses, within the maximum diameter of the cable that can be manufactured with existing cable stranding and taping machinery. An inner conductor, composed of eight segments of concentrically stranded wires, is surrounded by an outer conductor also made up of eight segments mutually insulated from each other. Estimates assume that noninsulated (bare) wire strands are used to form the conductor segments. Individual wire diameters are noted to be near 0.100 inch. This is done to minimize cable stranding cost. The number of wires that can be stranded into circular segments is restricted to 37, 61 or 91 wires. Final wire diameters are adjusted from 0.100 inch to achieve a high space factor and the maximum conductor area within the available space. Further details regarding tentative cable designs are contained in Table 8-4.

Table 8-4

500-KV SOLID-CONDUCTOR CABLE DESIGNS

Design Parameters	System Capacity		
	2000 MVA	3500 MVA	5000 MVA
Diameter Over Skid Wire, inches	5.78	5.78	5.78
Shield Outside Diameter, inches	5.48	5.48	5.48
Insulation Outside Diameter, inches	5.44	5.44	5.44
Conductor Screen Outside Diameter inches	3.64	3.64	3.64
Outer Conductor			
Diameter, inches	3.60	3.60	3.60
Number of Segments	8	8	8
Wires/Segment	61	91	91
Wire Diameter, inch	0.084	0.091	0.107
Inner Conductor			
Diameter, inches	3.00	2.50	2.00
Number of Segments	8	8	8
Wires/Segment	91	61	37
Wire Diameter, inch	0.106	0.108	0.110
Conductor Cross-sectional Area, square inches	9.2	9.2	9.2
Space Factor	0.89	0.90	0.92

*This rate represents today's cost of power and assumes no cost escalation.

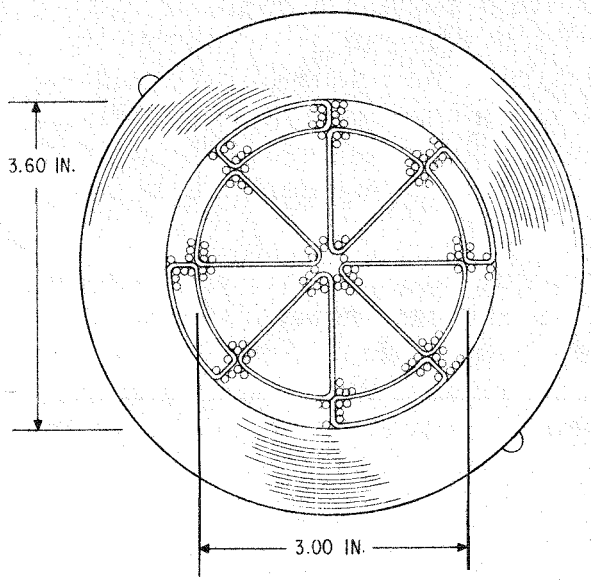

Figure 8-9.

Cross Section of 2000-MVA, 500-kV Solid-Conductor Cable

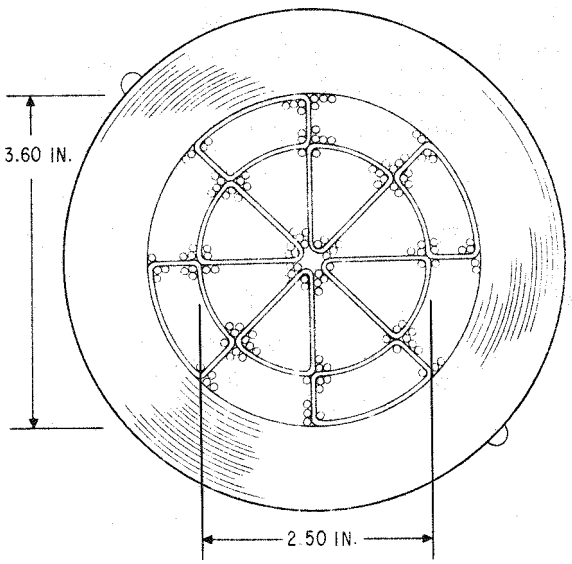

Figure 8-10.

Cross Section of 3500-MVA, 500-kV Solid-Conductor Cable

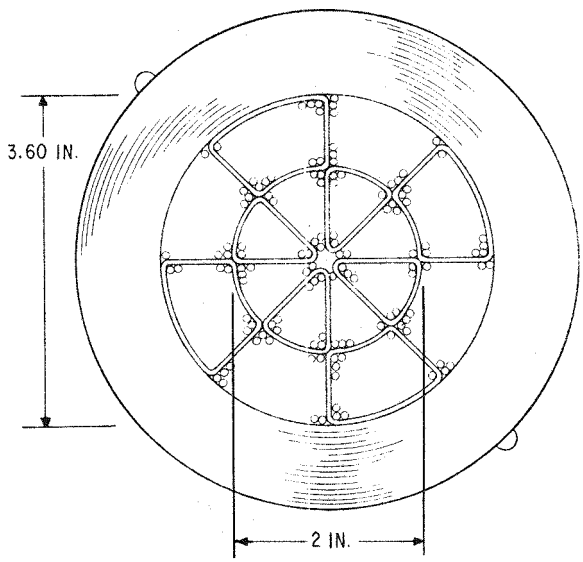

Figure 8-11.

Cross Section of 5000-MVA, 500-kV Solid-Conductor Cable

A significant advantage offered with the solid-conductor cables recommended for consideration in future phases of this program results from the fact that liquid nitrogen need not be removed from the center of the cable. Such removal is required for hollow-conductor cables when the transmission distance exceeds the module length (maximum distance between refrigerators). In that case, it is necessary to cool the liquid nitrogen in intermediate refrigeration stations.

Removal of liquid nitrogen from the center of hollow-conductor cables is complicated by the need to remove the liquid from the conductor that is at high voltage to the refrigerator that is at ground potential. For purposes of this study, it was assumed that potheads would be used at the ends of each module to remove liquid nitrogen from the hollow-conductor cables. Special cable splices rather than potheads might also be employed to provide this function. Such splices were examined in Phase I and are described in Section 3 of the May 1970 report.

Terminal costs of approximately $800,000 were estimated for a 3500-MVA, 20-mile system based on 500-kV, hollow-conductor cables, whereas with solid (no bore) cables this cost was estimated to be about $300,000. Schematic diagrams illustrating the differences in liquid nitrogen flow circuits resulting from these cable concepts are shown in Figures 8-12 and 8-13.

CABLE COST ESTIMATES

Cost estimates for cables have been prepared following procedures similar to those used for estimating conventional high-voltage cable costs. Every manufacturing operation has been reviewed and a cost attributed to each. Sales taxes and freight charges have been excluded. Among the items included are:

- Insulating Paper
  - Quality control
  - Acceptance testing
  - Slitting
- Manufacturing
  - Taping calculations
  - Setup trials
  - Production testing
- Other
  - Scrap for overruns and tails
  - Reel charges
  - Storage charges
  - Administration and general expenses
  - Profit of 15 percent before taxes

CABLE MANUFACTURING

Cables of the diameters recommended in this study are larger than have been manufactured in the United States to date. However, they have been designed with regard to manufacturing conditions and existing equipment

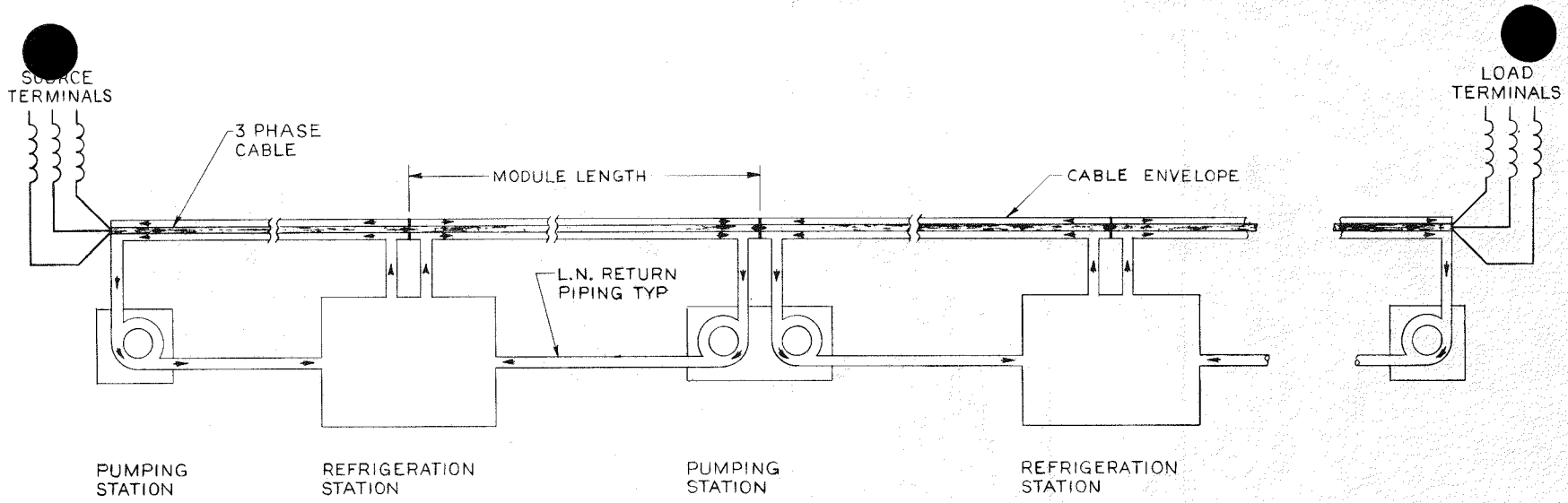

Figure 8-12.

Liquid Nitrogen Flow Circuit for Solid-Conductor Cables

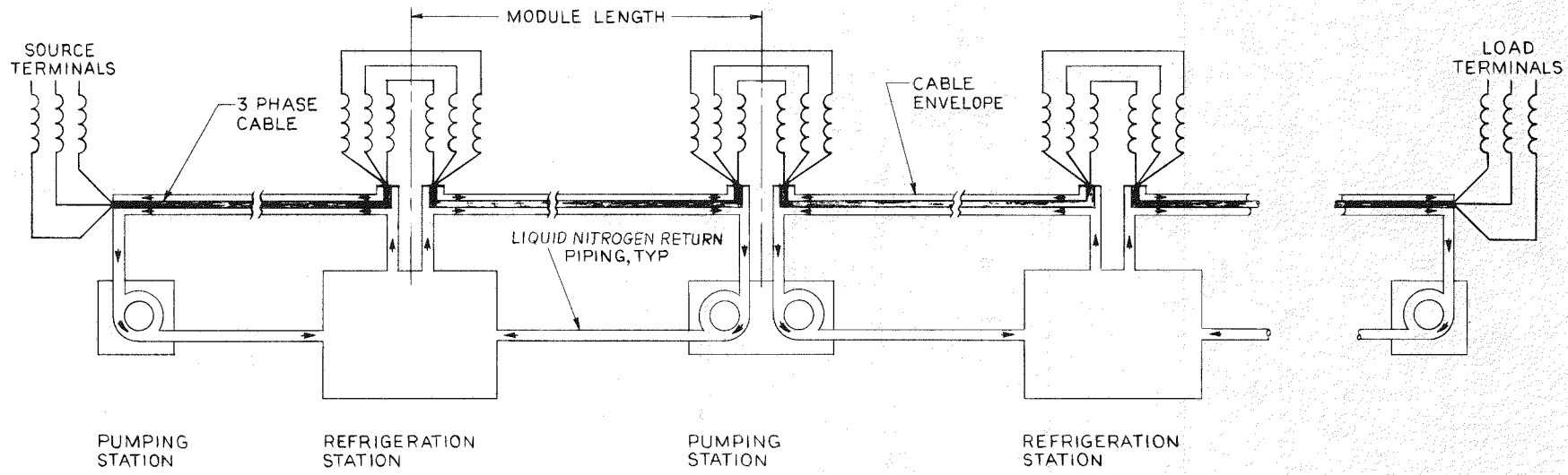

Figure 8-13.

Liquid Nitrogen Flow Circuit for Hollow-Conductor Cables

considerations. Insulating these larger cables will require the installation of approximately five additional taping heads to existing taping equipment. Each head must be capable of accommodating 12 tapes. The cost of these additional taping heads was not included when the cable selling prices were estimated. Additional heads will require an expenditure of approximately $1.5 million, an expense that would have a neglibible effect if significant lengths of cable are eventually produced with this facility.

Wire diameters and segment conductor constructions recommended in this study have been based upon limiting the number of wires per segment to 91 and the wire diameters to approximately 0.100 inch. This permits manufacture of the Milliken-type conductor segments, which are mutually insulated and concentrically stranded.

Conductor losses have been computed on the basis of wire diameters slightly smaller than shown in Table 8-4. A space factor of 0.75 was used in computing these losses. More detailed studies as well as some additional cable investigations will be required in the future to determine what restrictions on wire diameter are justified when considering trade-offs between conductor losses (particularly with regard to their a-c/d-c loss ratio) and manufacturing equipment constraints.

Because of the large cable diameters, the stiffness of the cable will increase to an extent that may require some increase in paper density. This would increase the dielectric loss slightly.

CABLE PRESSURE PIPING

A major objective of this study was to compare system performance and estimated owner's costs for FRP and metallic piping concepts. The use of metallic piping results in circulating current or shield losses that add to the refrigeration load, whereas FRP piping eliminates this loss in the low-temperature region. As shown in Table 8-5, shield losses in metallic piping can be 50 kW per mile or more. The variation of this loss as a function of low-temperature electrical resistivity for a specific pipe geometry is shown in Figure 8-14.

An investigation of metallic piping was centered on the use of aluminum piping or on an aluminum-lined, stainless-steel composite pipe. Electrical grade aluminums offer low resistivity values, but unfortunately they have low strength. However, an aluminum-lined, stainless-steel pressure pipe can achieve low circulating current losses and provide the strength required to withstand the high pressure. If the pressure pipe were to be made from tempered 1100 or 1350 alloys without benefit of the high strength stainless-steel outer pipe, the pipe wall thickness would be in the order of 1 inch. Use of a high-strength aluminum alloy, such as 6061-T6, is not practical because its resistivity is approximately five times higher. Comparisons of the properties and shield losses for several aluminums studied are shown in Table 8-5.

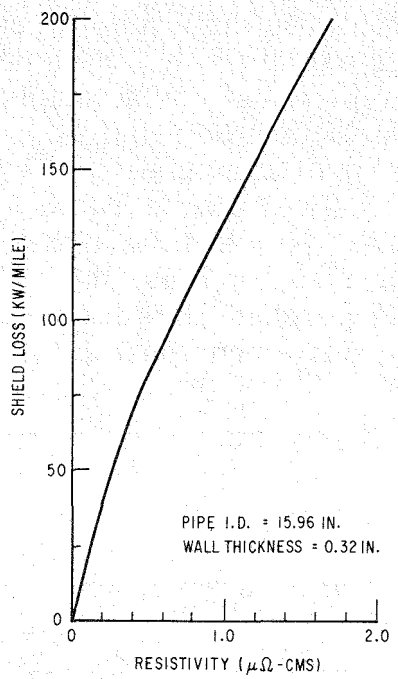

Figure 8-14.

Shield Losses Versus Pipe Resistivity (3500-MVA, 500-kV, metallic pressure pipe)

Table 8-5

SHIELD LOSSES IN ALUMINUM PRESSURE PIPE FOR 3500-MVA CABLE SYSTEM

Aluminum Alloy	Resistivity at 77 K ($\mu\Omega$-cm)	Shield Loss (kW/mile)	
		0.15- inch Wall Thickness	1.0-inch Wall Thickness
1350	0.31	81	53
1100	0.34	87	55
6061	1.68	330	129

Note: Pressure pipe inside diameter = 16.18 inches.

The 5.78-inch diameters of the solid-conductor cables recommended in this study require that the internal diameter of the containment pipe be 16.2 inches. This diameter provides the proper clearances to enable the cables to be drawn into the pipe without crossing one another and jamming. The ratio of the internal pipe diameter to the cable diameter is known as the "jam ratio" (Ref. 8-1). A ratio of 2.8 was used.

Cost analyses were made for 3500-MVA cable systems based upon FRP and metallic pressure piping having an inside diameter of 16.2 inches. The piping costs were selected to favor the metallic piping concept (Table 8-6). Sheath losses were computed for a 1350 aluminum alloy liner within a 9 percent nickel steel outer pipe. This low nickel alloy has been approved

for LNG service; but, because of its lower ductility in the liquid nitrogen temperature range, it has not been approved for use at 65 K. Nine percent nickel steel represents the lowest cost metallic pipe that could possibly be used. If not, more costly high nickel piping would then be required. Costs of $76 per foot for FRP pipe and $100 per foot for aluminum-lined, 9 percent nickel steel pipe were used in the cost analysis. As shown in Table 8-6, the price assumed for the metallic pipe is optimistic, whereas the higher of two estimates received for FRP pipe was used. Despite this bias, the owner's cost on a $/MVA-mile basis was shown to be 12 percent more for a 20-mile, 3500-MVA system based upon hollow-conductor cables enclosed in metallic piping (Table 8-7).

Table 8-6

PIPING COSTS
($/foot)

	FRP Piping Concept	Metallic Piping Concept	
		Aluminum Liner	9% Nickel Steel Jacket
Budgetary Estimates from Vendors	45 - 76	10 (excluding tooling)	155 - 270*
Cost Used in Analysis	76*		100**

*Based upon an order for 50,000 feet with tooling costs included.

**$100 per foot reflects the lowest budgetary estimate received for 9% nickel steel pipe, less tooling costs.

Table 8-7

OWNER'S COST ESTIMATES
3500-MVA HOLLOW-CONDUCTOR CABLE CONCEPTS*

	FRP Piping Concept ($ in Millions)	Metallic Piping Concept ($ in Millions)
Cable (three phase)	22.16	22.16
Piping and Fittings	15.57	17.17
Thermal Insulation	7.39	7.21
Refrigerator and Pumps	15.20	20.00
Cable End Terminals	0.77	0.92
Installation	41.21	41.21
Power Charge	45.07	56.44
Total	147.37	165.11
$/MVA/Mile	2105	2360

*Based upon a 20-mile installation.

FOAM THERMAL INSULATION

For purposes of this study, a foam thermal insulation having a density of 2.5 pounds per cubic foot and a thickness of 6 inches was used for all cable and liquid nitrogen return piping regardless of piping material. Thermal insulation losses computed for several insulation thicknesses as a function of pipe diameter are shown in Figure 8-15. Values of approximately 65 and 40 kW per mile were computed for 16-inch diameter pressure pipes and 8-inch liquid nitrogen return pipes, respectively. The costs for this insulation in 6-inch thickness are $41 and $27 per foot for 16-inch cable pipe and 8-inch return pipe, respectively. Additional cost information appears in Figure 8-16.

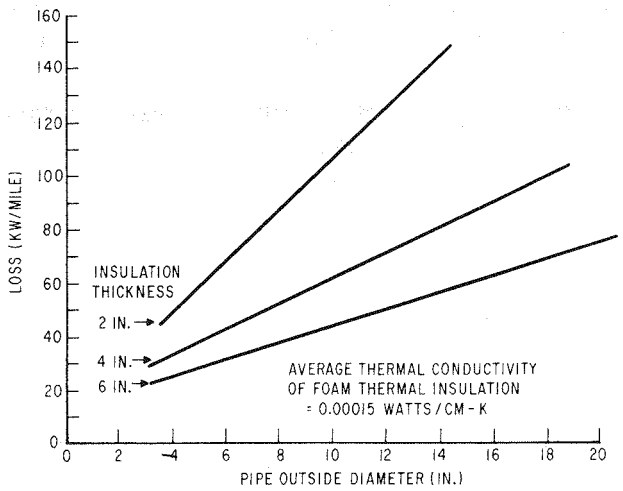

Figure 8-15. Thermal Insulation Loss Versus Pipe Diameter

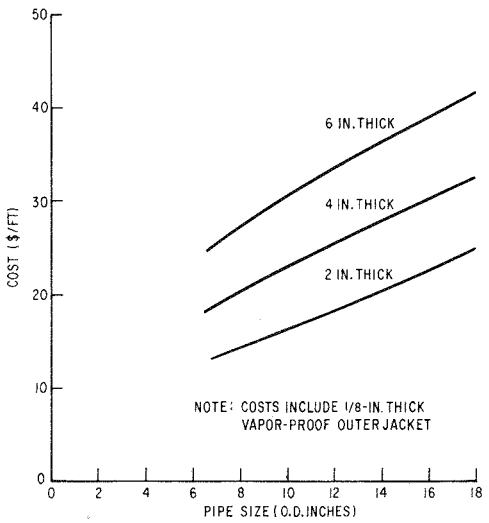

Figure 8-16. Estimated Cost of Foam Thermal Insulation

These cost estimates are based upon factory applied layers in which fiber-glass reinforcement is used at each 2 inches of foam thickness. The costs also include the application of a 1/8-inch thick layer of glass-reinforced polyester, vapor-proof protective layer applied over a cylindrically machined surface of the outer layer of the foam.

Transportation costs were not included in the above cost estimates for the polyurethane foam insulation. Since transportation costs may become significant, the possibility of providing an on-site facility for the application of the foam should be considered.

Foam insulation thicknesses of less than 6 inches could be used for the liquid nitrogen return piping without approaching thermal insulation loss values that would cause the liquid nitrogen to reach the saturation temperature. Detailed cost studies for a specific system would be necessary to identify optimum foam thicknesses, although at a charge of $1000 or more per kW for losses the thicker insulations are readily justified.

The thermal insulation thickness may be increased at locations where atmospheric water condensation on the outer surface of its vapor-proof jacket is not permissible.

The liquid nitrogen return pipe diameters, shown in Table 8-8, were computed on the basis that the pressure drop does not exceed six atmospheres. In all cases, a liquid nitrogen pump was used to repressurize the

Table 8-8

LIQUID NITROGEN RETURN PIPE DIAMETERS
BASED UPON 20-ATMOSPHERE INLET PRESSURE

(MVA) System Capacity	kV	Piping	Pipe Inside Diameter (inches)	
			Solid-conductor Cable	Hollow-conductor Cable
2000	500	FRP	8.25	8.6
2000	345	FRP	8.2	--
3500	500	FRP	8.5	8.5
5000	500	FRP	8.1	8.3
3500	500	Metal*	--	8.3

*Aluminum-lined stainless steel

return flow to 20 atmospheres before entering the return pipe. An examination of the possibility of returning the liquid nitrogen without this repressurization showed that the 5 K subcooling margin limit sought at the point where the liquid nitrogen returns to the refrigerator results in larger diameter piping and, therefore, a more expensive piping system. Liquid nitrogen return piping costs used in this study are shown in Table 8-9.

Table 8-9

ESTIMATED COSTS FOR LIQUID NITROGEN RETURN PIPING
($/foot)

Pipe Material	Liquid Nitrogen Return Pipe (8-in. i.d., 1/4-in. wall)
Glass-reinforced Epoxy	21
Aluminum, 6061 Alloy	11
Stainless Steel, Type-304	67

In the event that nitrogen boiling were to occur in this return line, the power transmitted along the cable would have to be reduced quickly to avoid the large pressure drop caused by two-phase flow in the liquid nitrogen flow circuit. Here again, a detailed study is required for each application, since for shorter module distances, such as occur with the 5000-MVA cases, the need for repressurization is doubtful. The final choice will depend upon economic factors as well as the desire to eliminate use of the repressurization pumps should the shorter distances make this technically feasible. With present pump technology, such pumps require major maintenance approximately every 14 weeks of continuous operation and must be replaced annually. Power charges for operation of such pumps is not a significant cost.

REFRIGERATION

The final report for the Phase I portion of this program, completed in 1971, describes the results of a study to define a refrigeration system for a 500-kV, 3500-MVA cryogenic cable. A 1000-kW (input) refrigerator was identified as a size of primary interest, and equipment sizes and costs were estimated on the basis of this refrigeration requirement. That study was based upon a liquid nitrogen return temperature of 89 K, whereas present studies indicate that this temperature will be somewhat higher. A further review and optimization of the neon refrigeration process will be required when specific site and cable capacity requirements are established.

The Phase I results, however, provided useful information for estimating installation costs for the refrigeration systems. More recent (1974) refrigerator cost information has been obtained from a survey (Ref. 8-2) of costs of low temperature refrigerators and liquefiers that cover a wide range of cooling capacities. The 1974 costs were escalated on the basis of a 7 percent annual increase to arrive at a 1976 cost.

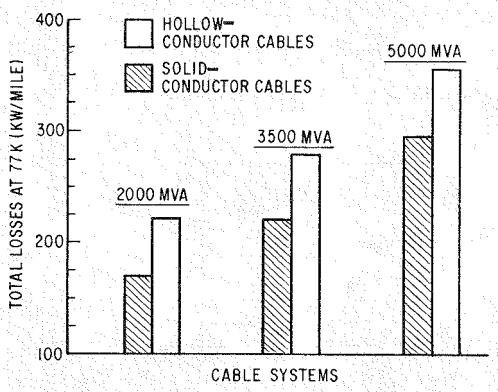

Figure 8-17.

Refrigeration Requirements for 500-kV Cable Systems

The refrigerator cost as a function of installed input power (P) in kW's was estimated: (1974) $ = 6000 $P^{0.7}$

Estimated costs for the refrigeration system on which the Phase III study has been based are shown in Figure 8-17 as a function of refrigeration load in kW/mile for module distances of 4 to 15 miles. Refrigeration requirements estimated for the different 500-kV systems are shown in Figure 8-18.

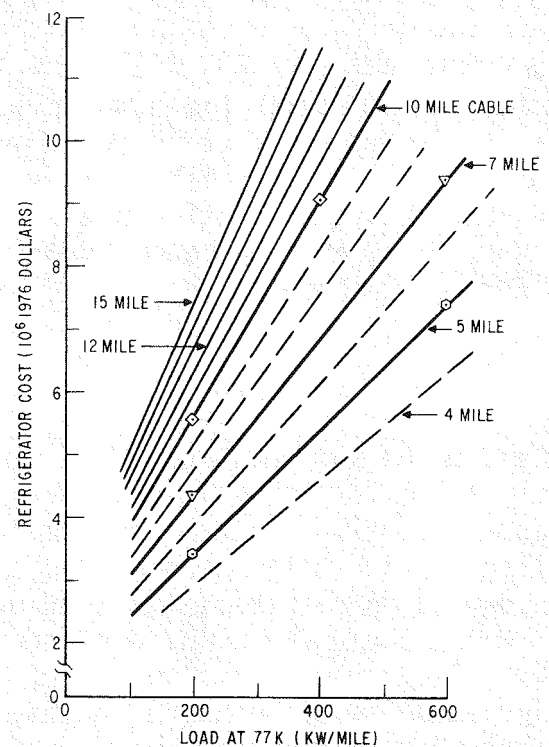

Figure 8-18.

Liquid Nitrogen Refrigerator System Costs (1976)

While it is beyond the scope of the Phase III effort, additional study is needed regarding the best techniques to handle the following:

- Changes in the volume of liquid nitrogen contained by the cable system. Temperature, pressure, and density variations result from changes in transmitted power.
- Storage of the pressurized liquid nitrogen that must be drained from a module length of the piping system before repairs can be made.
- Venting of liquid nitrogen required to avoid overpressurizing the piping system in the event of a prolonged refrigeration system failure.

The quantity of liquid nitrogen contained in a 3500-MVA cable is about 50,000 gallons per mile. Approximately 20 percent of this liquid would be evaporated if the operating pressure was gradually reduced to one atmosphere.

The general characteristics of pumps required for circulation of liquid nitrogen are contained in Table 8-10. Flow requirements computed for the different solid-conductor cable capacities involved in this study are shown below:

	Liquid Nitrogen Flow (lbs/s)
2000 MVA	
(345 kV)	70
(500 kV)	65
3500 MVA (500 kV)	80
5000 MVA (500 kV)	95

Table 8-10

GENERAL CHARACTERISTICS
OF LIQUID NITROGEN CIRCULATING PUMPS

Vertical, sealess, centrifugal
800 gpm at 460-foot head
3550 rpm
Input power: 90 kW
Efficiency: ~70 percent
Minimum continuous flow: ~100 gpm
Weight: 1300 pounds
Life: 1.1 years (10,000 hours)
Cold start: 5 seconds to full output
Cost: approximately $18,000 (uninstalled)

THERMAL ANALYSIS

STEADY-STATE ANALYSIS

A steady-state thermal analysis was developed for the hollow-conductor cable and modified for use with solid-conductor cables. A computer program was prepared for examination of hollow-conductor cable configurations based upon three cable conductors contained in a single pipe.

The analysis assumed no mixing of separate liquid nitrogen streams as flow occurs through the pressure pipe and through the cable bores. Pumping losses were neglected (although computed), since they were small in comparison to the three principal heat sources:

- Resistive losses in the cables.
- Alternating current dielectric losses in the cable insulation.
- Heat influx from the soil through the foam thermal insulation.

Other assumptions include:

- Specific heat, density, and viscosity of the liquid nitrogen coolant are not functions of the coolant temperatures or pressures.
- Resistive and dielectric losses are not functions of the coolant temperatures.
- Hydraulic friction factor is not a function of the coolant flow velocities.
- Thermal conductivities of the foam and dielectric materials are not functions of the coolant temperatures.
- Dissipation rates in the electromagnetic shield are not a function of the coolant temperatures.

The range of inlet and outlet conditions for the liquid nitrogen was dictated by its thermodynamic properties as shown in Figure 8-19. At pressures of 20 atmospheres, it can be a liquid only between 64 K and 115 K. The maximum temperature that the liquid nitrogen can reach has been limited to 10 K below the saturation temperature for the pressure at the cable exit. This has been referred to as a subcooling margin of 10 K, which ensures that no boiling can occur within the cable insulation. All results contained in this report are on the basis of this 10 K margin. Further details of the analysis are contained in Appendix IV, "Simplified Cable Thermal Analysis," of this report.

Computations to determine the liquid nitrogen return pipe diameters were performed separately, after the liquid nitrogen mass flow rate was computed for the cable.

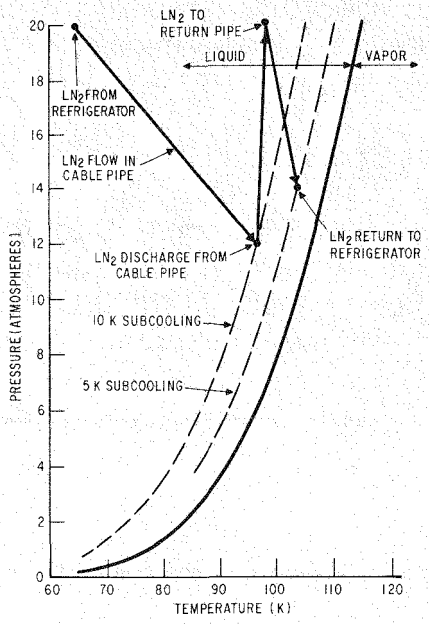

Figure 8-19.

Phase Diagram Showing Liquid Nitrogen Inlet and Outlet Conditions

THERMAL TRANSIENT AND COOLDOWN ANALYSES

Thermal transient analyses were made for a 3500-MVA, hollow-conductor cable system to obtain approximate estimates of the time required for cooling the cable from ambient temperature and to determine whether venting of nitrogen is required at intermediate points along the module length. It was assumed that cooldown would involve the flow of liquid nitrogen into the cable from a source located nearby. This liquid nitrogen could be supplied from a storage tank (expansion reservoir) required for cable operation. Over-the-road tankers could replenish the liquid nitrogen as required during cooldown. The refrigerators would not need to be placed in operation until cooldown had been completed.

A separate analysis was also made to evaluate the time that the cable could be operated under overload conditions. Results from each of the above analyses are summarized below.

Cable Cooldown Analysis

A "first order" analysis was made to estimate the length of time required to cool a 3500-MVA cable system having a module distance of 8.4 miles. The total time for such a cooldown depends on details of the process that are much more complicated than has been approximated in this analysis. On the basis of the assumptions made, the estimated cooldown time is judged to be somewhat longer than will actually occur. Appendix V, "System Cooldown Analysis," of this report contains the analysis and property values used. The conclusions reached from this work are summarized as follows:

- Nitrogen gas produced during cable cooldown is not Mach number flow limited (frictionally choked) when exhausting to atmospheric pressure.

- The time required to cool the cable to operating temperature has been estimated to be approximately one day, based upon an average flow of 50 pounds of liquid nitrogen per second.

Thermal Transient Behavior Under Overload Conditions

An approximate analysis was made for a 3500-MVA system to determine the thermal response of the cable to increases in internal heat generation produced by cable overloads. To simplify the analysis, the cooling of hollow-conductor cables from liquid nitrogen flow through the center of the cable was neglected. The major source of cooling occurs from liquid nitrogen flow along the outer surfaces of the cable. The information obtained from this analysis was:

- Thermal response of the cables to system overloads.
- Thermal response of the liquid nitrogen surrounding the cables to system overloads.

Results of this analysis, plotted in Figures 8-20 and 8-21, indicate that the cable will respond more rapidly to overload heating than the liquid nitrogen. The overload durations shown in Figure 8-21 have been based upon maintaining a 10 K margin between the conductor surface temperature and the saturation temperature of the liquid nitrogen. Additional overloading could be tolerated if this margin is reduced. Appendix VI, "Thermal Transient Analysis of Cable System Under Overload Conditions," of this report contains the analysis used to approximate the thermal transient behavior of the cable under overload conditions.

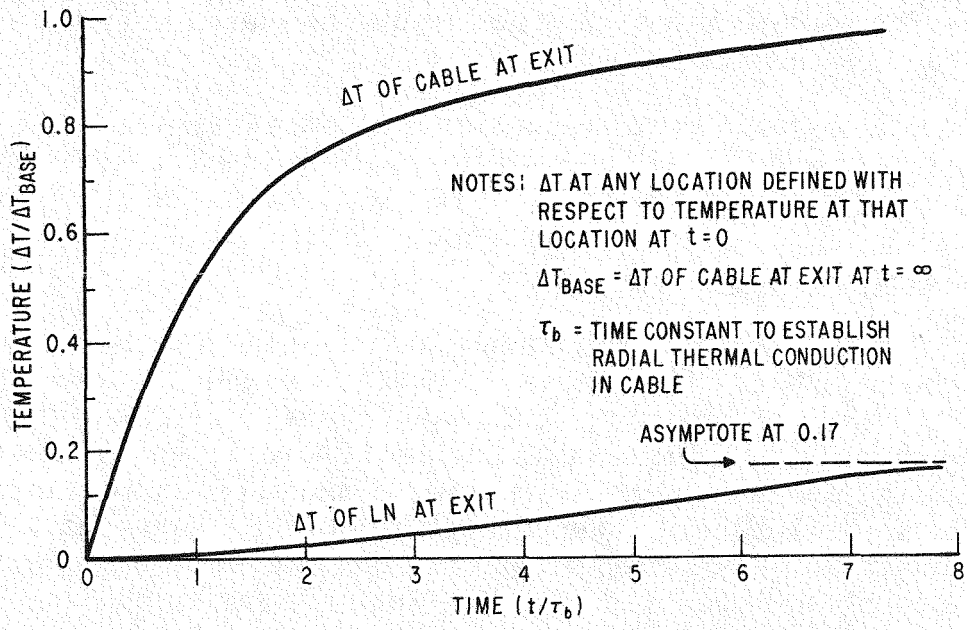

Figure 8-20. Response of Temperatures at Exit to Step Change in Cable Loading

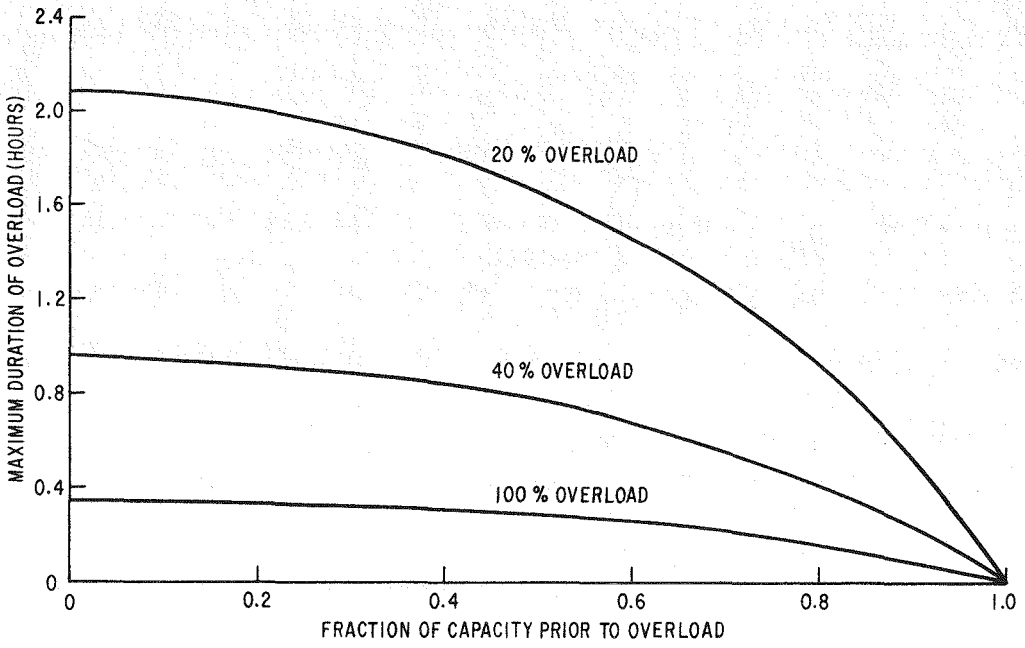

Figure 8-21. Overload Durations Estimated for 3500-MVA Cable Versus Fraction of Rated Capacity Prior to Application of Overload

The time constant for the cable was estimated to be about one hour compared to about nine hours for the bulk liquid nitrogen surrounding it. The maximum duration that an overload condition can be maintained is determined by the temperature of the liquid nitrogen-saturated electrical insulation at the conductor surface. This duration can be estimated from Figure 8-21 for different overloads as a function of the fraction of rated capacity the cable had been carrying prior to the overload. It is assumed that the cable would have reached thermal equilibrium prior to the overload. Approximately ten hours are required to reach this equilibrium.

To provide several examples, an overload of 20 percent above rated capacity can be maintained for about one hour provided the cable had been operated at 80 percent of capacity for some time prior to the overload. If the overload had been 100 percent above rated capacity, the duration would have been reduced to about 15 minutes.

CABLE SYSTEM MAINTENANCE

The cable should not require any significant maintenance, provided proper attention has been given to installation of the cable and piping. Particular care will be required to ensure that cable splicing and anchoring are done correctly. However, the refrigeration equipment and liquid nitrogen pumps will require periodic maintenance. Liquid nitrogen circulating pumps,

of modern sealless design, require major maintenance every 14 weeks when operated continuously. The useful life of such pumps is about one year.

In the event an electromagnetic shield is required to avoid cable interference with nearby communication circuits, it is likely that cathodic corrosion protection would be required for this shield. Such protection would require periodic inspection and possibly the replacement of electrodes installed intermittently along the cable.

REPAIR OF CABLES

If a cable should develop voltage arcing, the duration of the fault should be minimized with protective relaying to reduce cable damage and to prevent the possibility of damaging the FRP containment pipe. It is expected that fault currents in the order of 60,000 amperes could be interrupted in less than 15 cycles.

In the event of a cryogenic resistive cable failure, it is envisioned that repairs would be made by unsplicing all three conductors at the splices on each side of the fault and removing this complete section of cable. This repair will require the opening of two splice boxes and the removal of the three cables for a length of approximately 2,000 feet.

The common practice for repairing conventional underground cables is to add a short length of cable at the fault location regardless of the locations of the original splices. Whether or not this technique is used will depend upon each specific situation encountered. Construction of a large concrete splice box at the fault location may not prove feasible because of its size and cost.

The repair of a cryogenic cable will clearly require a number of weeks to complete, particularly when warmup and recooling times are included. If several cryogenic cables are placed in a common trench, it should be possible to safely reexcavate the cable trench to repair a three-phase cable while other cables remain energized. The steps involved in a cable repair are outlined below:

1. Fill expansion reservoir and ventdown damaged module.
2. Assemble repair crew equipment and new cable on job site.
3. Uncover splice boxes and remove thermal insulation around splices.
4. Untape original splices and remove damaged cable.
5. Install new cable section.
6. Complete splices.

7. Complete electrical tests and reapply thermal insulation.
8. Close splice box and start cooldown.
9. Complete cooldown and conduct final checkout.
10. Reenergize system.

REPAIR OF PIPING

The likelihood that a leak would develop in the liquid nitrogen piping system after the system has been subjected to initial cooldown and pressure testing at installation is expected to be very small. If a leak should develop in the cable pressure pipe after the cable has been installed, every effort should be made to make the repair without removing the cable.

Fiber-reinforced plastic piping that has developed a minor leak probably could not be repaired by the hand application of epoxy-saturated glass tape because of the low temperatures. However, it may be possible to make a temporary repair while the cable remains in service by the application of metallic clamshell-type clamps bolted around the FRP pipe. Materials such as indium, that remain soft at cryogenic temperature, can be employed to achieve a gasket-type seal. Use of special sealing rings or packings may also offer solutions to this repair problem. If the repair should require the removal of a section of pressure pipe, it would then be necessary to allow the system to warm up and then remove a section of the cable. Repairs to a single 40-foot length of pipe would very likely require the excavation of a major portion of the 250-foot trench section between the expansion joints. The piping must be exposed to permit the unbolting and removal of one expansion bellows. The damaged pipe length could then be cut from the remaining portions and removed. Ends of the remaining pipes would then have to be tapered and the surfaces prepared to enable reconnection to the new length. Removal of the expansion bellows would permit enough axial motion to allow the pipe ends to be inserted into the tapered couplings used for joining the pipe lengths. Adhesive bonding of FRP pipe joints would be done in the same manner as in the original installation.

In the case of liquid nitrogen return piping, it may be possible to make repairs without deenergizing the cable, provided the original installation included cryogenic valves and fittings at points along the return pipe to permit the installation of temporary piping to allow the return flow to be diverted around the damaged section.

In the event either the cable pressure pipe or the return pipe should be ruptured, it would be necessary to stop the liquid nitrogen flow to avoid flooding the cable trench and causing damage to nearby piping or building

structures. Such an event could cause considerable damage because of the brittle behavior of carbon steels at cryogenic temperatures. This could also produce a dangerous situation to people in the vicinity because a flow in the order of 700 gpm is used to cool the cables. A major advantage of using a solid-conductor cable rather than a hollow-conductor cable is that this permits the installation of valving that can immediately stop the loss of liquid nitrogen should this unlikely event occur.

In the event of accidental damage to the vapor-proof jacket or the foam thermal insulation, it is likely that repairs could be made without removing the cable from service. This possibility of damage could be minimized by a concrete or timber barrier placed near the top of the cable trench or by accurately identifying the cable location. Minor repairs could probably also be made to the electromagnetic shield without deenergizing the cable.

If a leak should occur in the vapor-proof jacket, air and water vapor condensation would occur in the foam structure and degrade the thermal insulation. Because the foam jacket would be "compartmented" every 250 feet or so, the full length of the cable insulation would not be subjected to this leak. If such a leak is not repaired, the frost and ice buildup could eventually cause the pipe to be damaged. Although repair techniques have not been investigated in detail to date, it is likely that such insulation repairs can be made without removing the cable from service. Resin-saturated glass tape could probably be applied by hand and heat-cured in place.

Heat flux thermopiles or other types of sensors to monitor heat flux or temperature in the insulation and aid in locating the damaged sections of piping would likely have been factory installed. Major repairs of the cable or its pressure pipe would require the cable to be removed from service and warmed to ambient temperature.

When specific installation sites are considered, the possibility of flooding should be considered to ensure that the buoyancy of the cable piping is resisted by the anchors at the expansion joints or by additional anchors.

CABLE SYSTEM COST ESTIMATES

Preliminary cost estimates were made for single-circuit, 3-phase, hollow- and solid-conductor cable concepts based upon foam-insulated piping. In addition, estimates were prepared for 3500-MVA system concepts using foam-insulated and evacuated, multilayer insulated, metallic piping.

Cost estimates for 20-mile transmission distances for the different cable capacities are summarized in Figures 8-22 and 8-23. The investment costs (components costs plus installation) and owner's cost (investment cost

plus costs associated with system losses) are shown separately in Figure 8-23. Table 8-11 provides a cost breakdown for a 3500-MVA, solid-conductor cable system having a module length of 9.5 miles. A cost breakdown for a 20-mile system of this same capacity is shown in Table 8-12. The costs for the 20-mile distance were determined using an average cost on a per mile basis obtained from the module estimate. This was done to enable comparisons of different systems even though module distances were different for each concept. Similar cost breakdown sheets for other system capacities are included in Appendix VII, "Cost Summary Sheets," and Appendix VIII, "20-Mile System Cost Estimate Sheets," of this report.

Figures 8-24, 8-25, and 8-26 contain pie-chart representations of the major costs for 20-mile systems, including the costs associated with system losses. These figures, for 2000-, 3500-, and 5000-MVA systems, respectively, were based upon cost estimates for solid-conductor cables and FRP piping with foam-thermal insulation.

The owner's costs for 500-kV systems are shown plotted in Figure 8-27 and tabulated in Table 8-13.

Cable costs are shown in Table 8-14 and in Figure 8-28. In all cases, the costs of solid-conductor cables are higher than the hollow-conductor cables of similar outer conductor diameter and capacity.

ASSUMPTIONS USED IN COST ESTIMATES

The cost estimates provided in this report must be considered preliminary and used only as a general guide in helping to direct future development tasks. These estimates are based upon a number of assumptions that are described below, but the following costs have been specifically excluded:

- Purchase of land
- Construction of buildings(1
- Transportation
- Sales taxes
- Maintenance
- Cable manufacturing equipment investment
- Fuel escalation
- Systems Design Engineering(2

1) Costs associated with the purchase and installation of services (power, water, etc.) to the refrigeration buildings are included in the installation costs.

2) Costs of engineering supervision required for installation have been included in the installation cost estimates.

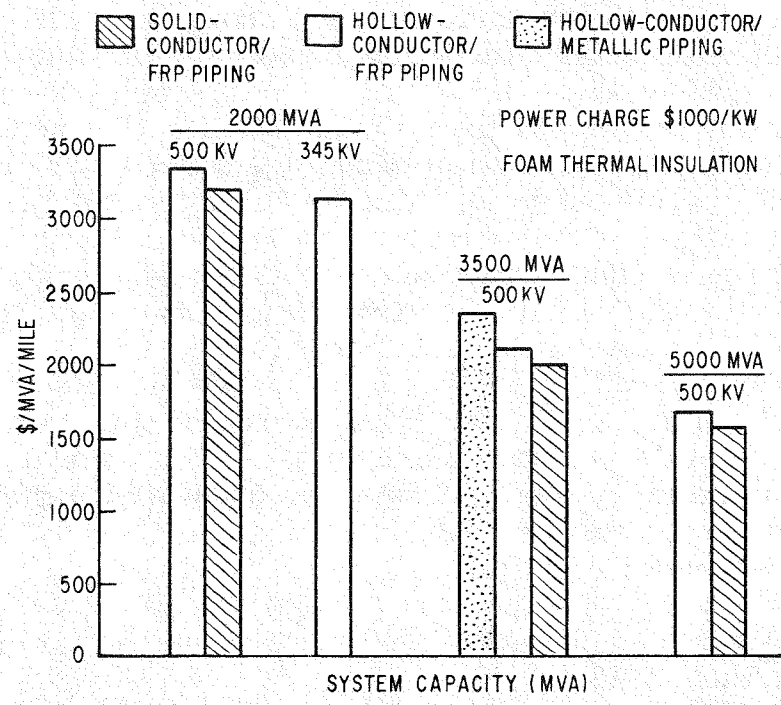

Figure 8-22. 20-Mile Owner's System Cost Estimates

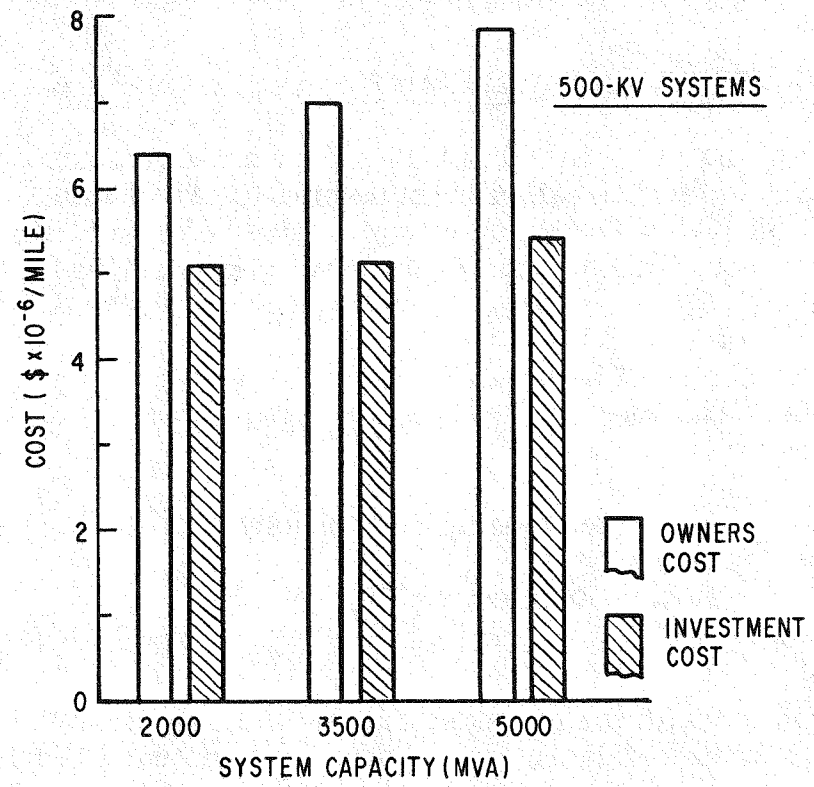

Figure 8-23. Cable System Costs Versus Transmission Capacity (Solid conductor)

Table 8-11

COST SUMMARY SHEET

Concept: 3500 MVA; 500 kV

Solid Cable; 9.5 Miles (Module length)

Components		Total Cost for Three-phase Module Length (Dollars in Millions)
Cable, $/three-phase ft	242.10	12.14
Pressure pipe, $/ft	76.00	3.81
Material	FRP	
Inside diameter, inches	16.2	
Return pipe, $/ft	21.50	1.08
Material	FRP	
Inside diameter, inches	8.5	
Foam thermal insulation and vapor jacket		
Pressure pipe, $/ft	41.00	2.06
Return pipe, $/ft	29.00	1.45
Terminal, 10^6/three-phase	0.143	0.29
Number of Terminals	2	
Refrigerator	16,470 Input KW	5.75
Expansion Joints, Fittings, and Miscellaneous, $/ft	50.00	2.51
Installation, 10^6/mile (Suburban)	2.06	19.57
Power Charge:	17,000 total losses (kW) @$1000.00/kW	17.00

Table 8-12

20-MILE SYSTEM COST ESTIMATE SHEET

Concept: 3500 MVA; 500 kV

Solid Cable; FRP Piping

	Dollars in Millions
Cable	25.56
Piping, Expansion Joints, and Miscellaneous	15.58
Foam Thermal Insulation for Cable Piping and Return Piping	7.39
Refrigerator and Liquid Nitrogen Repressurization Pumps	12.32
Terminals	0.29
Installation	41.20
Power Charge	35.79
Total Cost of Installed System for 20 Miles	138.13
Cost Per Mile	6.91

Actual Dollars/MVA-Mile 1.973

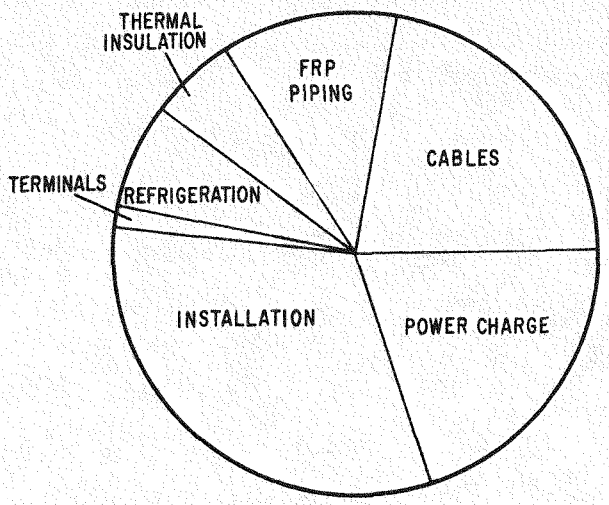

Figure 8-24.

Owner's Cost Breakdown for 2000-MVA Solid-Conductor Cable

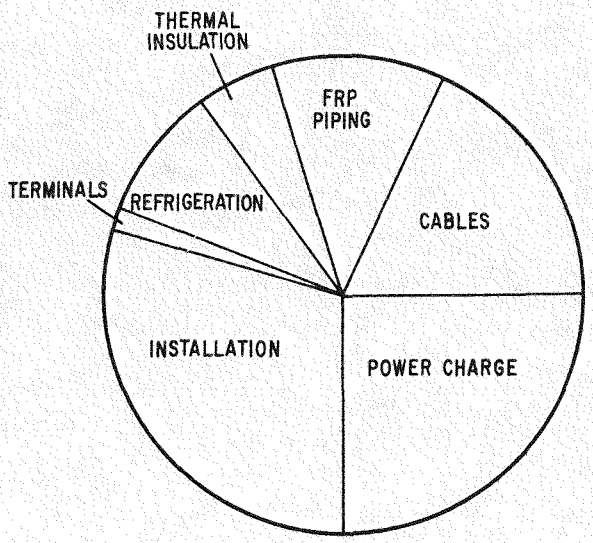

Figure 8-25.

Owner's Cost Breakdown for 3500-MVA, Solid-Conductor Cable

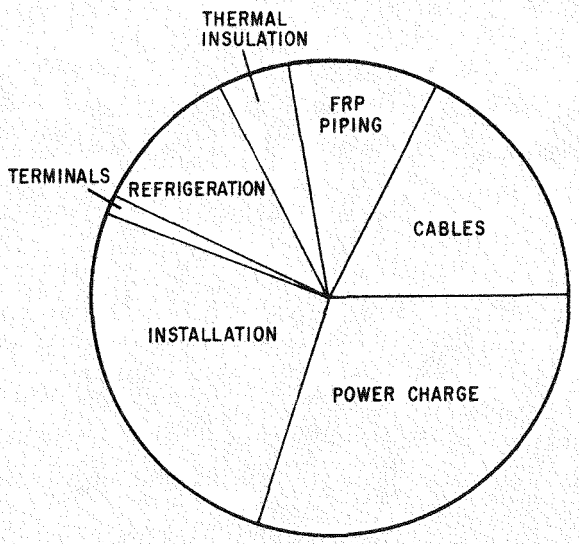

Figure 8-26.

Owner's Cost Breakdown for 5000-MVA, Solid-Conductor Cable

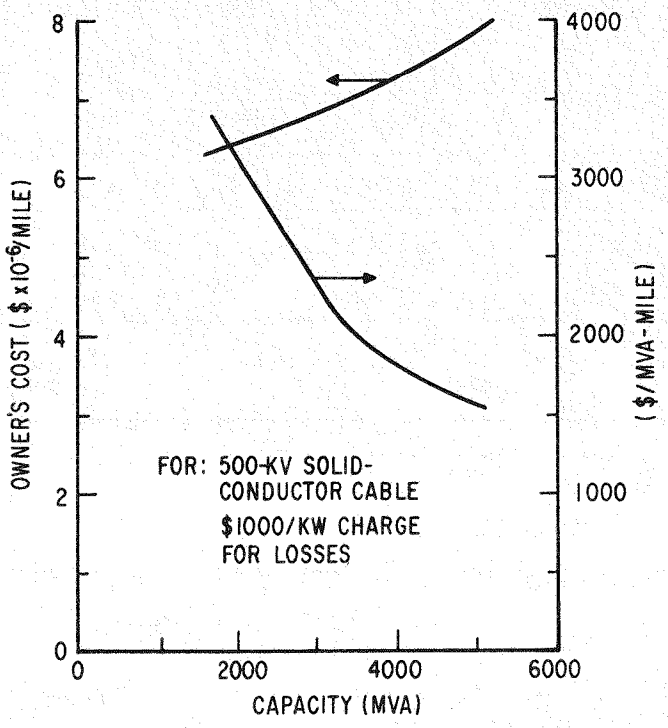

Figure 8-27.

Owner's Cost Versus Capacity for 20-Mile Transmission Distance

Table 8-13

ESTIMATED OWNER'S COSTS FOR 500-KV SYSTEMS

	2000 MVA	3500 MVA	5000 MVA
$ Million/Mile	6.43	6.91	7.84
$/MVA-Mile	3220	1973	1570

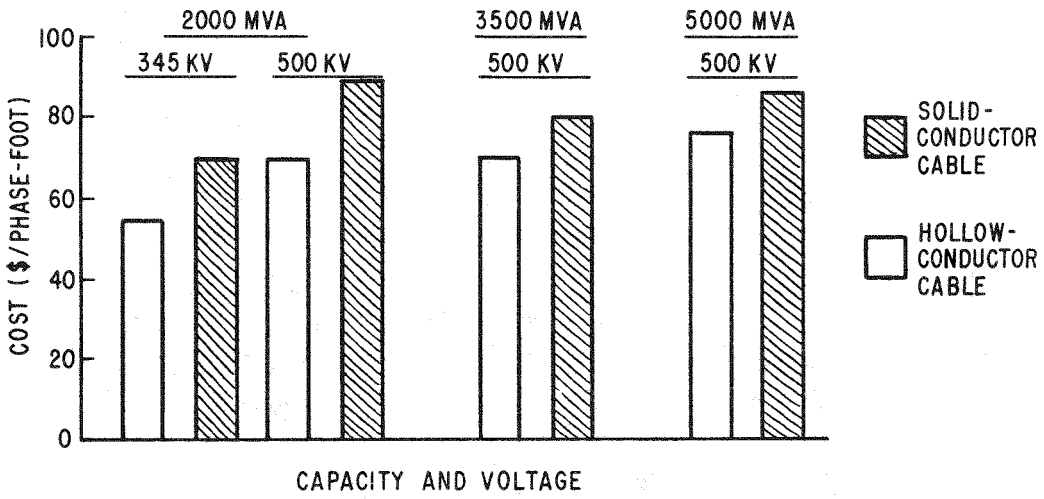

Figure 8-28. Cable Cost Estimate

Table 8-14

ESTIMATED COST OF THREE-PHASE CABLES

Cable Type	SYSTEM CAPACITY AND VOLTAGE			
	2000 MVA		3500 MVA	5000 MVA
	345 kV	500 kV	500 kV	500 kV
Solid Conductor Cable	232	268	242	259
Hollow Conductor Cable	166	211	210	230

Some of the major assumptions used in these costs estimates are:

- Thermal and electrical losses have been determined for each system, including losses in an electromagnetic shield. These shield losses, referred to as sheath losses in the cost summary sheets, were computed for metallic and FRP pressure piping concepts. The cost of the shield for the FRP pressure piping has not been included, because many installations will not require such a shield.

- The costs for system losses were based on continuous operation, whether at rated capacity or at partial capacity. The capitalized cost for these losses was charged at $1000 per kW. This charge includes a charge for plant investment and the cost of fuel necessary to supply these losses. This charge will differ depending upon the location and type of generation assumed. Fuel costs generally represent a large fraction of this cost.

- An installation cost of about $2 million per mile was used regardless of system concept, since the minor changes to trench widths and cable installation procedures were judged to produce an insignificant effect. Installation costs for foam-insulated metallic piping were estimated to be the same as for FRP piping.

- A cost of $50 per foot of transmission distance was used to cover the purchase of expansion joints, ground return cable, sealing rings, and other miscellaneous items.

- In all cases, a cost of $100,000 was added to the refrigeration cost to cover the purchase and installation of the repressurization pumps used to return liquid nitrogen to the refrigeration building. If cable installations should involve distances less than the module distance, such pumps may not be required.

- The installed cost of a 500-kV, three-phase pothead termination was assumed to be the same regardless of system capacity.

- Costs associated with equipment redundancy were not included, because the redundancy requirements will depend upon the details of specific applications.

- Special costs associated with installations involving changes in elevation as the buried cable follows the ground surface were neglected.

RELIABILITY CONSIDERATIONS

The reliability (and the related concept "availability") of a specific variant of a cryogenic cable system design is a system attribute just as is cost or efficiency. This study has considered the following types of cable concepts:

- Hollow-conductor cables contained in foam-insulated, FRP piping.

- Hollow-conductor cables contained in vacuum-insulated, metallic piping.

- Solid-conductor cables contained in foam-insulated, FRP piping. Analyses in this report show that this concept is the most desirable from the standpoint of cost and operation.

Reliability of the refrigeration system can be treated separately from that of the cable and its cryogenic envelope. Reliability of the refrigeration system can be independently chosen to achieve the desired degree of reliability by specifying redundant components.

COMPARISON OF CONCEPTS

Because of the lack of empirical data and operating experience from which failure rate or life characteristics for the cryogenic cable system can be developed, engineering judgement must be used to compare the three variants enumerated above.

Foam insulation represents a feasible technology that is attractive from the standpoint of long-term maintenance. On the other hand, vacuum insulation represents a concept that is dubious from the standpoint of maintenance of the vacuum, in an underground installation, over long periods of time. Therefore, from a reliability standpoint, foam insulation appears to be the preferred concept.

When a hollow-conductor cable transmission system containing several modules is installed, it is necessary to remove the liquid nitrogen from the cable bore (at high voltage) and deliver it to the refrigerator at ground potential. Specially designed splices, or potheads, must be used to perform this function at each refrigeration and pumping station. This equipment

represents an additional reliability burden on the system. Consequently, the cable system variant that uses solid-conductor cable is preferrable from a reliability standpoint.

The cable system using a solid-conductor cable contained in foam-insulated, FRP piping appears to be the most favorable choice from a reliability standpoint, if it is assumed that the FRP piping technology can be developed to the same degree that foam-insulated metallic piping exhibits today. Since this same system variant is also the most attractive from the standpoint of cost and operation, it represents the "best" overall alternative.

ESTABLISHMENT OF RELIABILITY CRITERIA

In order to specify redundancy for a power transmission system, it is necessary to have knowledge of the details of the overall system. Such a task is beyond the scope of this work, but the question of how reliability requirements affect the cryogenic cable installation can be discussed in general terms.

In future systems, availability and reliability criteria will probably be established in one of three ways:

- Numerical goals or specified requirements may be contractually established.
- Specific utility operating practices may be adhered to.
- Decisions may be reached using a formal framework of cost effectiveness analysis.

Because of the lack of operating data and because a specific application of the cable system is not called for, it is not useful at this point to discuss details of how the cryogenic cable can attain numerical reliability goals.

Current Utility Practice

Certain considerations in current utility practice would serve as strong determinants of the degree of system redundancy, even if outage or availability numerical goals were never formally stated. These considerations are discussed below.

Current Utility Practice -- Baseload Situation

In this situation, power generated at a distance is presumed as delivered to the load using buried cryogenic cable alone. It is anathema in utility practice for high capacity, low unit cost generating facilities to be unable to deliver power because of outages in the transmission network serving the

load. Therefore, typical practice is to design a system with sufficient redundancy such that the loss of two lines will not require the shedding of any load. Typically, for such systems (i.e., not interconnected with conventional transmission networks) it would be necessary to supply three paralleled 100 percent capacity cables within the trench. The scenario being planned for is one in which one cable is undergoing maintenance, during which period the second cable fails requiring the third cable to bear the load.

The cryogenic cable has the ability to perform without degradation at or below its rated capacity. It has been assumed here that at its rated capacity it is intolerant of overload situations. If operating at less than capacity, say 50 percent, it has a certain amount of overload capability; for example, it can run at 120 percent of rating for 1.6 hours and at 200 percent of rating for 0.4 hour. Relative efficiencies of transmission at fractional loadings, while not as good as at full capacity, are still quite close to this figure (Figure 8-2). A second observation to be made is that it takes several days to cool a cable from the ambient condition and place it in service. This is obviously not suitable for the near instantaneous system response required in time of failure. The overload capacity afforded also helps to protect against brief system transients.

Providing three three-phase circuits within a trench (Figure 8-29B) is more costly than supplying merely one (Figure 8-29A). The latter is the basic situation treated in the main body of the study. Certain material costs, such as for cable and for piping, increase as do certain key elements in the installation costs. Table 8-15 (which treats the impact on installation costs) and Table 8-16 (which treats the overall impact on cable system costs) attempt to evaluate these elements of increased costs. Table 8-16 has been prepared to compare owner's costs of a single 3500 MVA circuit with the costs of two different concepts in which cable redundancy is provided. Costs are shown in the center column for a concept in which three identical circuits are located in the same trench (Figure 8-29B). One circuit is to be fully energized while the second is maintained in a cold standby condition. Costs shown in the third column are based upon a concept using separate pressure pipes (Figures 8-29C) for each cable conductor. The additional two single-phase pipes are maintained in a cold standby condition. Trenching costs were assumed to be increased above those for the standard case by the amount of the additional cubic yards of excavation required and by the added width of pavement removal required. In brief, an additional $167 million cost is associated with a 20-mile long triplicated system. It is more than double the cost of a single-circuit, three-phase system (Figure 8-29A).

Another system possibility, opened up by the need for supplying redundancy to utility norms (again one line under maintenance and one line under repair causes no system load shedding), is placing single conductors within smaller diameter pipes, as shown in Figure 8-29C. Three single-phase circuits could carry the system three-phase load and another two single-

phase circuits (one of which at least would have to be held in a cooled down state) would be available to replace failures in any single-phase circuit. Increments in system costs for this variant are also found in Tables 8-15 and 8-16. For a 20-mile system, this variant would be roughly $145 million more expensive than the basic system studied. Note that this latter concept would presumably operate at rated load; therefore, it would have no load-sharing or load-growth potential.

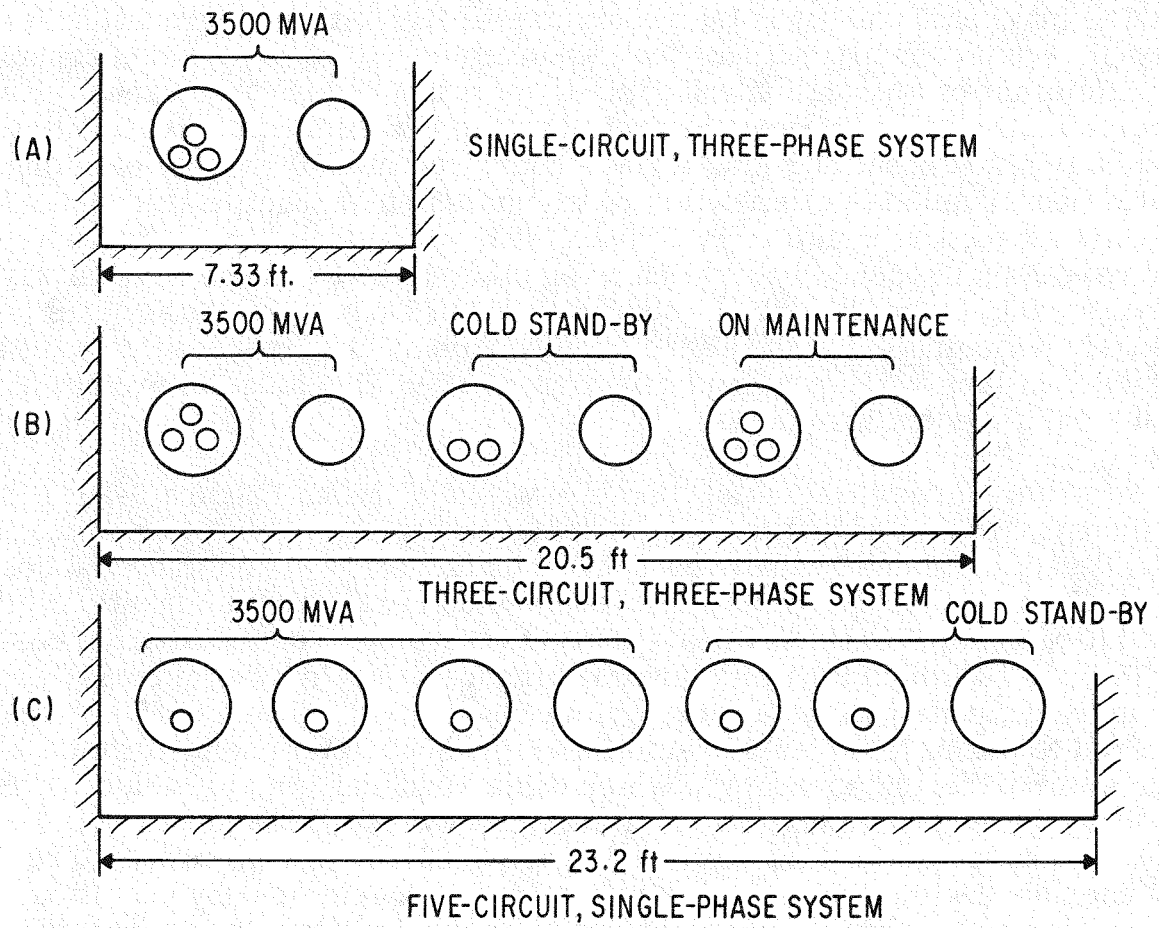

Figure 8-29. Conceptual Piping Configuration For a 3500 MVA System

Current Utility Practice -- Interconnected Load Situation

In this case, it is presumed that the utility has a capability in conventional transmission facilities to replace the loss of any two cryogenic cables (one lost to maintenance and one lost to failure). Conversely, the presumption holds that the cryogenic system in interaction with the system as a whole could replace any two conventional cables.

Conventional cables have the well-known ability to perform for extended periods under appreciable overload conditions (the price paid being an accelerated degradation of the cable insulation). However, as has been noted,

Table 8-15

PRELIMINARY INSTALLATION COST ESTIMATES FOR 10-MILE SYSTEMS[1]

	Single-circuit, Three-phase System	Three-circuit, Three-phase System	Five-circuit Single-phase System
Engineering	$ 1,300,000	$ 400,000	$ 500,000
Excavation and Backfill	4,550,000	3,947,000	4,824,000
Manholes and Anchors	774,000	1,548,000	976,000
FRP Piping	4,552,000	9,104,000	6,828,000
Cable Installation	1,618,000	3,236,000	3,236,000
Cable Utilities	349,000	100,000	100,000
Refrigeration Station Utilities	3,616,000	1,121,000	2,350,000
Testing and Pumping	376,000	758,000	564,000
	$ 17,135,000	$ 20,214,000[3]	$ 19,378,000[3]
		+17,135,000	+17,135,000
		37,349,000	36,513,000
	x 1.20[2]	x 1.20[2]	x 1.2[2]
	$ 20,562,000	$ 44,819,000	$ 43,816,000
	$ 2.06×10^6/mile	$ 4.48×10^6/mile	$ 4.38×10^6/mile

1) Based in part upon Gibbs and Hill installation cost estimate.
2) Contingency provision.
3) Incremental Cost

Table 8-16

CABLE SYSTEM COSTS

(For 20-mile System of 3500-MVA, 500-kV, Solid-conductor Cables)

(Dollars in Millions)	Single-circuit, Three-phase System	Three-circuit, Three-phase System	Five-circuit, Single-phase System
Cable	$ 25.56	$ 76.68	$ 42.60
FRP Piping, Expansion Joints, and Miscellaneous	15.58	46.74	38.95[1]
Foam Thermal Insulation for Cable and Return Piping	7.39	22.17	18.48
Refrigerator and Liquid Nitrogen Pumps[2]	12.32	16.14	20.33
Terminals	0.29	0.87	0.48
Installation	41.20	89.60	87.60
Power Charges	35.79	52.61	73.00
	$ 138.13	$ 304.81	$ 281.44
	($ 6.91/mile)	($ 15.24/mile)	($ 14.07/mile)

1) Single-conductor cable piping cost presumed to be one-half that of the single-circuit, three-phase case.
2) Additional equipment costs associated with interconnecting the refrigerator to the cables for the three-circuit, three-phase and five-circuit, single-phase concepts have been neglected.

cryogenic cable has no such overload capability; only if the cryogenic cable is deliberately kept at levels below rating in normal operation will it be able to compensate for the loss of other transmission equipment. Such a regime also permits brief operation at substantial overload, which can prove useful while system reconfiguration and rebalancing are under way. Of course, such planning and analyses must be carried out in the specific context of a given utility (its generating, transmitting, and load network and the nature of its linkages with adjacent utility grids).

Utility Practices -- Forecasted Growth

Utilities often base their decisions to install redundancy, operate at fractional capabilities, etc.in accordance with expected future growth in the loads served by the utility. The cryogenic cable system can be upgraded by the addition of refrigerators to shorten the module length. Growth considerations must be viewed in the context of a given utility and the anticipated nature of its load growth.

Summary

Utilities have developed a body of operating practices covering a loss of transmission capabilities in terms of the number of lines that can be lost without shedding load. System planning based on such considerations must consider alternate transmission links within the system and interconnections with other systems.

Realistic planning for cryogenic cable installations would also be subjected to evaluation by similar criteria in such planning. Considerations of future system growth play an intrinsic role in this planning process.

Cost-effectiveness Considerations

Failures of a cryogenic cable may cause loss of system function for up to approximately 28 days (see Table 8-17). Presuming an average loss of 20 days and predicated upon a lost-line cost of $0.02/kWh, this would result in a loss of $33.6 million per 20-day outage for a 20-mile long, 3500-MVA system.

It had been noted previously that the installation of three three-phase cables would require the expenditure of roughly an additional $167 million over the base case of nonredundant cable. A question of specific interest is: "Is the amount of additional expenditures ($167 million) warranted if it avoids a number of incidents, the average cost of which is $33.6 million per incident?" There are too many current uncertainties, especially in the achievable failure rate as well as in maintenance times and in present-worth factors, to answer this question at this time. But, the above costs give a general picture of the magnitude of the numbers involved in this trade-off.

The precise nature of the cryogenic cable refrigeration system will depend upon the design requirements of the system and the reliability/availability goals set for the total system. Therefore, it is currently impractical to suggest highly specific design details. In general, however, a refrigeration facility will be found in between two cable system modules (each 9.5 miles long in the case of the base system studied). This facility will contain three refrigerators, each rated to carry the total load of a single system module. One refrigerator will be dedicated to the left-hand module, one to the right hand, and the third will serve as an easily switchable spare that can stand in for either one of the other refrigerators in case of failure or maintenance. It will be necessary that the cold section of the third refrigerator be maintained at low temperature for rapid switchover. In addition, each refrigerator will contain within it appropriate internal subsystem redundancies, and a supply of essential spare modules will be on hand to expedite any repair process.

The refrigeration stations, spaced two modules apart from one another, will normally be unattended, whether in rural or suburban areas. Therefore, it is essential that the remote sensing of system states be possible and that automatic or commanded system switchover take place expeditiously in the case of failure.

At the end of each module, liquid nitrogen recirculation pumps will also be found. Since these continuously operating pumps have to be maintained every 14 weeks and replaced yearly, it is essential that a minimum of three 100-percent-capacity pumps be provided for each module to protect against the situation of pump failure while a pump is undergoing maintenance. The standby pumps must be cooled by a trickle flow of cold nitrogen to insure their near instantaneous availability in case of need.

The supply of electric power to the refrigeration station is no trivial matter; the base case (3500 MVA, 500 kV) will require about 35 MW of power into the refrigeration station serving any two modules. Such levels of power are normally never routinely available at typical suburban or rural locations. Therefore, it is planned to deliver such power through dedicated lines contained in the same trench with the cryogenic cables. It is essential that this power be capable of delivery from either end of the trench, in case interruption occurs anywhere along the power line.

A liquid nitrogen expansion tank is located in each module, which is useful for nitrogen storage when the cable is cooled from ambient temperature and covers fluctuating needs during brief system upsets. However, at the system requirement of roughly 700 gallons of liquid nitrogen per minute, this permits only some minor leeway in system switching and reconfiguration to restore refrigeration power. It is again obvious that power interruptions to the refrigerators for anything but brief periods of time will not be permissible. The liquid nitrogen pumps are also essential for system

Table 8-17

ESTIMATED MAINTENANCE TIMES
(In days)

	Replace Cable	Replace Pipe	Fix Pipe (In place)
Ventdown and Warmup	3	3	3
Assemble Crew, Equipment, and Cable	2	2	-
Uncover Splice Boxes	1	1	-
Remove Cable	2	2	-
Replace/Repair Damaged Piping	-	3	3
Install New Cable	1	1	-
Complete Splices	7	7	-
Electrical Tests (Thermal Insulation)	1	1	-
Close Splice Boxes and Start Cooldown	1	1	-
Complete Cooldown and Reenergize	7	7	7
Total	25	28	13(1

1) Temporary (clam shell) fix, if possible, would cause no cable function loss.

Summary of Criteria

The preceding discussion has attempted to illustrate ways in which levels of necessary redundancy may be decided. The specific requirement placed upon the ultimate cryogenic system designer and installer will obviously be strongly a function of utility practices and desires, as contractually expressed. The "cost-effectiveness" rationale, if the parameters involved in its analysis can be usefully estimated, can serve as an excellent bench mark against which system reliability and availability requirements can be measured and adjudicated.

REFRIGERATION SYSTEM--RELIABILITY CONSIDERATIONS

The refrigeration system (which includes, for convenience, the liquid nitrogen return pumps and the electric power supply to the refrigeration system) is effectively decoupled from the piping/cable network; that is, it can be independently driven to whatever levels of MTBF and system availability are considered appropriate. This is exemplified by the Phase I study on the reliability of cryogenic system refrigerators and by such papers as Reference 8-3.

functioning. Therefore, their power must also be capable of being supplied from either side of a power line break.

LIQUID NITROGEN RETURN LINES--RELIABILITY CONSIDERATIONS

Leakage in the liquid nitrogen return lines necessitating repair would involve shutdown of the cryogenic cable system if no provisions for redundancy were provided. As a minimum, two 100-percent-capacity return lines should be provided, each operating under normal circumstances at 50 percent of capacity (so that no time is lost cooling down a line upon need). In those system variants, previously discussed, where redundant cable-carrying piping is supplied, it might be possible to utilize one of the redundant cable pipes as a stand-in in the case of either failure of the cable pipe or of the liquid nitrogen return line. The engineering and operational consequences of this last possibility have not been explored.

SYNOPSIS

1. The most desirable piping/cable concept is that consisting of foam thermally insulated, FRP pressure piping containing solid-conductor cables.
2. The cable-carrying piping will require redundancy. The actual nature and amount of such redundancy will depend upon defined system need and detailed system analysis.
3. A redundant means of returning liquid nitrogen to the refrigeration module must be provided.
4. The refrigeration module can achieve any desired degree of reliability or availability by optimal incorporation of redundancy.
5. Liquid nitrogen repressurization pumps should be installed in triplicate for each module.
6. Electric power supply to the refrigerator and to the liquid nitrogen repressurization pumps must be capable of supply from two separate sources, as a minimum.

CONCLUSIONS

This Phase III system study has included consideration of a large number of electrical, thermal, hydraulic, and mechanical design parameters. A number of variations were examined to arrive at component and system configurations that have low system losses and owner's costs.

Although the cable diameters selected are larger than are now manufactured in the United States, it is still possible to use conventional stranding and taping machinery, and to ship the reeled cable by truck. Piping di-

ameters and lengths are within manufacturing and shipping constraints. Costs were based upon 40-foot long pipe sections and 2500-foot cable lengths.

The conclusions reached in this study have been based on the property values and system parameters indicated in Table 8-18. Available materials properties data at cryogenic temperatures were used for electrical conductors, electrical insulation, and thermal insulation. As noted under "Cable Design" on page 8-4, the ratio of a-c to d-c losses in the cable conductors was based on estimated values. This ratio is influenced by the strand-to-strand insulation, the degree of conductor strand transposition, and the compaction achieved in the cable segments. Cable contraction forces during cooling may also influence this ratio.

The liquid nitrogen temperature at the inlet to the cable was maintained at 65 K (1.9 K above the triple point temperature) throughout this study.

Losses for each of the systems examined in this study included electrical losses in the cable as well as those associated with heat transfer into the liquid nitrogen and its subsequent refrigeration.

Estimates of owner's costs were based upon 1976 component prices obtained from vendors on the basis of "budgetary" cost estimates for quantities required for a 10-mile long cable installation. Costs were not included for redundant refrigerators, because each installation will require thorough economic and reliability analyses to establish the trade-offs and redundancy needed to achieve specific forced outage limits.

The principal conclusions reached from this study are summarized below:

- A cable with a solid, rather than a hollow, conductor provides a more efficient and lower cost system. Greater operational simplicity is also possible.

- Depending upon the system transmission capacity (2000 to 5000 MVA), the module length can range from about 13 to 6 miles.

- The overall efficiencies that can be achieved for solid-conductor, 20-mile, 500-kV cable systems range from 98.7 percent for 2000-MVA to 99 percent for 5000-MVA (Figure 8-30).

- The use of foam-insulated, nonmetallic pressure piping results in a significantly lower owner's cost than is possible with foam-insulated metallic pressure piping or with multi-layer insulated (vacuum) metallic piping concepts (Table 8-19).

Table 8-18

VALUES FOR DESIGN PARAMETERS CONSTANT FOR ALL RATINGS

CABLE	
Conductor	
Material:	aluminum (1350)
Resistivity:	0.31 $\mu\Omega$-cm
Space factor:	0.75
A-c/d-c loss ratio:	Hollow conductors 1.20
	Solid conductors 1.25 (500 kV cables)
	Solid conductors 1.30 (345 kV cables)
Electrical Insulation	
Material:	cellulose paper
Thermal Conductivity:	0.0016 W/cm-°K
Maximum Voltage Stress:	400 V/mil
Dielectric constant:	2.0
Dielectric loss tangent:	1200 μrad
ELECTROMAGNETIC SHIELD	
Material:	aluminum (1100)
Resistivity (300 K):	2.8 $\mu\Omega$-cm
Wall thickness:	0.15 inch
Relative permeability:	1.0
CABLE PRESSURE PIPE	
Cable jam ratio:	2.8
Pipe wall thickness:	FRP 0.50 inch
	1100-H18 aluminum 0.85 inch
	6061-T6 aluminum 0.32 inch
Metallic pipe resistivity:	1100-H18 aluminum 0.34 $\mu\Omega$-cm
	6061-T6 aluminum 1.68 $\mu\Omega$-cm
	304L stainless steel 51.4 $\mu\Omega$-cm
Hydraulic friction factor:	0.06 (Darcy)
LIQUID NITROGEN	
To cable:	65 K, at 20 atmospheres
From cable:	97 K, at 12 atmospheres
Density:	0.814 g/cm^3
Minimum subcooling margin:	Leaving cable 10 K
	At liquid nitrogen return pipe discharge 5 K
Specific heat:	2.06 Joules/g-°K
SOIL IN CABLE TRENCH	
Surface temperature:	300 K
Thermal conductivity:	0.003 W/cm-°K
THERMAL INSULATION (POLYURETHANE FOAM)	
Thermal conductivity:	0.00015 W/cm-°K

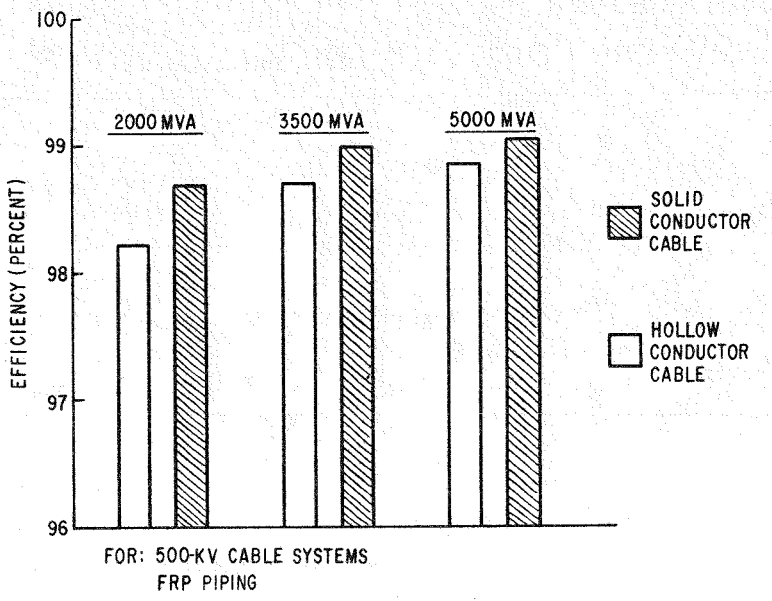

Figure 8-30.

Cable System Efficiency for 20-mile Installations

Table 8-19

COMPARISON OF PIPING CONCEPTS FOR 20-MILE, 3500-MVA SYSTEMS

	Owner's Cost in $ Million		
	Foam Insulated		Evacuated Multilayer Insulated Metallic Piping
	FRP Piping	Metallic Piping	
Cables	22.16	22.16	22.16
Piping	15.57	17.17	30.63
Thermal Insulation	7.39	7.21	0
Refrigerator	15.20	20.00	15.87
Terminals	0.77	0.92	0.92
Installation	41.21	41.21	53.56*
Power Charge	45.07	56.44	41.21
Total	147.37	165.11	164.35

*Note: This installation cost was assumed to be 30 percent more than for foam-insulated piping because of the added complexity associated with field welding, evacuation, and inspection required at the pipe joints. No detailed installation cost estimates were prepared for this concept.

- The cooldown of cables having lengths in the order of 10 miles appears technically feasible without requiring intermediate venting. Cooldown will take approximately one day.

- A separately insulated liquid nitrogen return pipe placed in the cable trench is recommended over concentric or other piping arrangements.

- Repressurization of the liquid nitrogen after removal from the cable is recommended before the liquid nitrogen is returned to the refrigerator.

- The investment cost of a cable system is essentially independent of the system capacity in the 2000- to 5000-MVA range. This cost has been estimated to be approximately $5 million per mile.

- The investment and owner's cost for a 2000-MVA cable system are slightly lower for a 345-kV cable system compared to a 500 kV cable system. However, at a capitalized cost of losses of $1000/kW, this advantage is small.

- The two major costs in a cryogenic cable installation are the installation cost and the charges associated with losses. These two items account for more than one-half of the total owner's cost. Piping and cable costs are next in importance, whereas refrigeration and terminal costs are much smaller.

- Estimated owner's cost on a dollar per MVA mile basis for 2000 -, 3500-, and 5000-MVA systems are $3220, $1973, and $1570, respectively.

- 500-kV cable systems ranging from 2000-MVA to 5000-MVA differ only in module length and refrigerator rating. The addition of refrigeration stations provides a means of increasing rated capacity to accommodate future load growth.

Number on Form	Description
1	MVA rating of the three-phase cable circuit.
2	Line-to-line rms kilovolt rating of the cable circuit.
3	"Solid" refers to solid-conductor cables cooled from the outer surface. "Hollow" refers to hollow-conductor cables cooled from the cable bore as well as from the outside.
4	Computer run number assigned.
5	Material assumed for both the cable pressure piping and the liquid nitrogen return piping.
6	The maximum distance liquid nitrogen can flow along the cable before it must be returned to the refrigerator.
7	Total conductor losses (including a-c losses) per phase (7A for three-phases).
8	Dielectric losses in the cable insulation per phase (8A for three-phases).
9	Circulating current losses in the metallic pressure piping (not applicable to FRP piping concepts).
10	Heat input from the surrounding soil to the liquid nitrogen within the cable pressure piping.
11	Heat input from the surrounding soil to the liquid nitrogen within the return piping.
12	The total of all cable and piping losses to the liquid nitrogen streams. Pumping losses are neglected.
13	Refrigerator input power required to maintain cooling with the three-phase cable circuit operating continuously at rated capacity. Input power has been assumed to be 7.8 watts per watt at low temperature.

Appendix I

COMPUTER OUTPUT SHEETS

Results from the steady-state thermal analysis for each cable concept examined in this study are summarized on separate pages in this appendix. These pages give the magnitude of the major losses for each concept on a module basis. Included here are the refrigeration requirement, the refrigeration spacing distance, and the estimated system efficiency for a 20-mile distance.

Performance values are also presented for 3500- and 5000-MVA systems for operation at capacities below the rated capacity.

An explanation of the parameters listed on the computer output sheets follows. The numbers referred to relate to the sample form shown below.

COMPUTER OUTPUT SHEET

Concept: (1) MVA; (2) kV; (3) Cable

Run No. (4); (5) Piping

Module length: (6) Miles

Cable Losses

Resistive/phase (7) x 3 = (7A) kW/mile

Dielectric/phase (8) x 3 = (8A) kW/mile

Sheath (Metallic piping only) (9) kW/mile

Heat Leak

Pressure pipe (10) kW/mile

Liquid nitrogen return (11) kW/mile

Total Losses at Low Temperature (12) kW/mile

Refrigerator Input = (12) x 7.8 x (6) miles/module = (13) kW/module

Sheath Losses = (14) kW/mile x (6) miles/module = (14) kW/module

Total Losses (15) kW/module

Total Losses (16) kW/mile

Transmission efficiency for 20-mile system (17) %

14	Circulating current losses in an electromagnetic shield surrounding the foam thermal insulation used with the cable pressure piping (not applicable for metallic pressure piping).
15	Total transmission losses for a three-phase circuit operated continuously at rated capacity (1) and other conditions included on this form. These losses are for a transmission distance of module length (6).
16	Total transmission losses on a per mile basis for the module length (6) shown.
17	Overall transmission efficiency for a 20-mile transmission distance based on the losses per mile shown in (16).

COMPUTER OUTPUT SHEET

Concept: 2000 MVA; 345 kV; Solid Cable

Run No. --- ; FRP Piping

Module length: 12.5 Miles

Cable Losses

Resistive/phase	11.28	× 3 = 33.84	kW/mile
Dielectric/phase	13.12	× 3 = 39.36	kW/mile
Sheath(1		0	kW/mile
Heat Leak			
Pressure pipe		57.7	kW/mile
Liquid nitrogen return		40.0	kW/mile
Total Losses at Low Temperature		170.9	kW/mile

Refrigerator Input = 170.9 × 7.8 × 12.5 miles/module = 16,663 kW/module

Sheath Losses(2 = 38.0 kW/mile × 12.5 miles/module = 475 kW/module

Total Losses 17,138 kW/module

Total Losses 1,371 kW/mile

Transmission efficiency for 20-mile system 98.63 %

1) Metallic piping
2) FRP piping

COMPUTER OUTPUT SHEET

Concept: 2000 MVA; 500 kV; Solid Cable

Run No. --- ; FRP Piping

Module length: 13.2 Miles

Cable Losses

Resistive/phase	7.12	× 3 = 21.36	kW/mile
Dielectric/phase	16.85	× 3 = 50.55	kW/mile
Sheath(1		0	kW/mile
Heat Leak			
Pressure pipe		57.7	kW/mile
Liquid nitrogen return		40.0	kW/mile
Total Losses at Low Temperature		169.5	kW/mile

Refrigerator Input = 169.5 × 7.8 × 13.2 miles/module = 17,450 kW/module

Sheath Losses(2 = 18.0 kW/mile × 13.2 miles/module = 238 kW/module

Total Losses 17,690 kW/module

Total Losses 1,340 kW/mile

Transmission efficiency for 20-mile system 98.66 %

1) Metallic piping
2) FRP piping

COMPUTER OUTPUT SHEET

Concept: 3500 MVA; 500 kV; Solid Cable

Run No. --- ; FRP Piping

Module length: 9.5 Miles

Cable Losses

Resistive/phase	22.5	x 3 =	67.5	kW/mile
Dielectric/phase	16.85	x 3 =	50.6	kW/mile
Sheath(1			0	kW/mile
Heat Leak				
Pressure pipe			63.2	kW/mile
Liquid nitrogen return			41.0	kW/mile
Total Losses at Low Temperature			222.0	kW/mile

Refrigerator Input = 222.0 x 7.8 x 9.5 miles/module = 16,470 kW/module

Sheath Losses(2 = 55.0 kW/mile x 9.5 miles/module = 520 kW/module

Total Losses 17,000 kW/module

Total Losses 1,790 kW/mile

Transmission efficiency for 20-mile system 98.98 %

1) Metallic piping
2) FRP piping

COMPUTER OUTPUT SHEET

Concept: 3500/3150* MVA; 500 kV; Solid Cable

Run No. --- ; FRP Piping

Module length: 9.5 Miles

Cable Losses

Resistive/phase	18.23	x 3 =	54.68	kW/mile
Dielectric/phase	16.85	x 3 =	50.6	kW/mile
Sheath(1			0	kW/mile
Heat Leak				
Pressure pipe			63.2	kW/mile
Liquid nitrogen return			41.0	kW/mile
Total Losses at Low Temperature			209.5	kW/mile

Refrigerator Input = 209.5 x 7.8 x 9.5 miles/module = 15,524 kW/module

Sheath Losses(2 = 44.0 kW/mile x 9.5 miles/module = 418 kW/module

Total Losses 15,942 kW/module

Total Losses 1,678 kW/mile

Transmission efficiency for 20-mile system 98.93 %

1) Metallic piping
2) FRP piping
*Capacity transmitted

COMPUTER OUTPUT SHEET

Concept: 3500/2450* MVA; 500 kV; Solid Cable

Run No. --- ; FRP Piping

Module length: 9.5 Miles

Cable Losses

Resistive/phase	11.03	x 3 = 33.08	kW/mile
Dielectric/phase	16.85	x 3 = 50.6	kW/mile
Sheath(1		0	kW/mile
Heat Leak			
Pressure pipe		63.2	kW/mile
Liquid nitrogen return		41.0	kW/mile
Total Losses at Low Temperature		187.88	kW/mile

Refrigerator Input = 187.88 x 7.8 x 9.5 miles/module = 13,922 kW/module

Sheath Losses(2 = 26.0 kW/mile x 9.5 miles/module = 247 kW/module

Total Losses 14,169 kW/module

Total Losses 1,491 kW/mile

Transmission efficiency for 20-mile system 98.78 %

1) Metallic piping
2) FRP piping
*Capacity transmitted

COMPUTER OUTPUT SHEET

Concept: 3500/1750* MVA; 500 kV; Solid Cable

Run No. --- ; FRP Piping

Module length: 9.5 Miles

Cable Losses

Resistive/phase	5.625	x 3 = 16.88	kW/mile
Dielectric/phase	16.85	x 3 = 50.6	kW/mile
Sheath(1		0	kW/mile
Heat Leak			
Pressure pipe		63.2	kW/mile
Liquid nitrogen return		41.0	kW/mile
Total Losses at Low Temperature		171.7	kW/mile

Refrigerator Input = 171.7 x 7.8 x 9.5 miles/module = 12,722 kW/module

Sheath Losses(2 =15.0(Est) kW/mile x 9.5 miles/module = 143 kW/module

Total Losses 12,865 kW/module

Total Losses 1,345 kW/mile

Transmission efficiency for 20-mile system 98.45 %

1) Metallic piping
2) FRP piping
*Capacity transmitted

COMPUTER OUTPUT SHEET

Concept: 3500/1000* MVA; 500 kV; Solid Cable

Run No. --- ; FRP Piping

Module length: 9.5 Miles

Cable Losses

Resistive/phase	1.84	× 3 =	5.51	kW/mile
Dielectric/phase	16.85	× 3 =	50.6	kW/mile
Sheath(1			0	kW/mile
Heat Leak				
Pressure pipe			63.2	kW/mile
Liquid nitrogen return			41.0	kW/mile
Total Losses at Low Temperature			160.31	kW/mile

Refrigerator Input = 160.31 × 7.8 × 9.5 miles/module = 11,879 kW/module

Sheath Losses(2 = 8.0 (Est) kW/mile × 9.9 miles/module = 76 kW/module

Total Losses 11,955 kW/module

Total Losses 1,258 kW/mile

Transmission efficiency for 20-mile system 97.48 %

1) Metallic piping
2) FRP piping
*Capacity transmitted

COMPUTER OUTPUT SHEET

Concept: 5000 MVA; 500 kV; Solid Cable

Run No. --- ; FRP Piping

Module length: 6.3 Miles

Cable Losses

Resistive/phase	45.0	× 3 =	135.0	kW/mile
Dielectric/phase	16.85	× 3 =	50.6	kW/mile
Sheath(1			0	kW/mile
Heat Leak				
Pressure pipe			71.4	kW/mile
Liquid nitrogen return			39.5	kW/mile
Total Losses at Low Temperature			297.0	kW/mile

Refrigerator Input = 297.0 × 7.8 × 6.3 miles/module = 14,590 kW/module

Sheath Losses(2 = 113.0 kW/mile × 6.3 miles/module = 712 kW/module

Total Losses 15,300 kW/module

Total Losses 2,430 kW/mile

Transmission efficiency for 20-mile system 99.03 %

1) Metallic piping
2) FRP piping

COMPUTER OUTPUT SHEET

Concept: 5000/2000* MVA; 500 kV; Solid Cable

Run No. --- ; FRP Piping

Module length: 6.3 Miles

Cable Losses

Resistive/phase	7.12	x 3 = 21.36	kW/mile
Dielectric/phase	16.85	x 3 = 50.6	kW/mile
Sheath(1		0	kW/mile
Heat Leak			
Pressure pipe		71.4	kW/mile
Liquid nitrogen return		39.5	kW/mile
Total Losses at Low Temperature		182.9	kW/mile

Refrigerator Input = 182.9 x 7.8 x 6.3 miles/module = 8,988 kW/module

Sheath Losses(2 = 18.0 kW/mile x 6.3 miles/module = 113 kW/module

Total Losses 9,101 kW/module

Total Losses 1,445 kW/mile

Transmission efficiency for 20-mile system 98.56 %

1) Metallic piping
2) FRP piping
*Capacity transmitted

COMPUTER OUTPUT SHEET

Concept: 2000 MVA; 500 kV; Hollow Cable

Run No. 250012 ; FRP Piping

Module length: 10.6 Miles

Cable Losses

Resistive/phase	24.5	x 3 = 73.5	kW/mile
Dielectric/phase	16.85	x 3 = 50.6	kW/mile
Sheath(1		0	kW/mile
Heat Leak			
Pressure pipe		57.7	kW/mile
Liquid nitrogen return		41.0	kW/mile
Total Losses at Low Temperature		223.0	kW/mile

Refrigerator Input = 223.0 x 7.8 x 10.6 miles/module = 18,420 kW/module

Sheath Losses(2 = 18.0 kW/mile x 10.6 miles/module = 191 kW/module

Total Losses 18,600 kW/module

Total Losses 1,760 kW/mile

Transmission efficiency for 20-mile system 98.24 %

1) Metallic piping
2) FRP piping

COMPUTER OUTPUT SHEET

Concept: 3500 MVA; 500 kV; Hollow Cable

Run No. 350008 ; FRP Piping

Module length: 7.5 Miles

Cable Losses

Resistive/phase	42.0	x 3 =	126.0	kW/mile
Dielectric/phase	16.85	x 3 =	50.6	kW/mile
Sheath(1			0	kW/mile
Heat Leak				
Pressure pipe			63.2	kW/mile
Liquid nitrogen return			42.0	kW/mile
Total Losses at Low Temperature			282.0	kW/mile

Refrigerator Input = 282.0 x 7.8 x 7.5 miles/module = 16,485 kW/module

Sheath Losses(2 = 55.0 kW/mile x 7.5 miles/module = 413 kW/module

Total Losses 16,898 kW/module

Total Losses 2,250 kW/mile

Transmission efficiency for 20-mile system 98.71 %

1) Metallic piping
2) FRP piping

COMPUTER OUTPUT SHEET

Concept: 3500 MVA; 500 kV; Hollow Cable

Run No. 350100 ; Metallic Piping (Foam Insulation)

Module length: 6.3 Miles

Cable Losses

Resistive/phase	42.0	x 3 =	126.0	kW/mile
Dielectric/phase	16.85	x 3 =	50.6	kW/mile
Sheath(1			81.0	kW/mile
Heat Leak				
Pressure pipe			63.2	kW/mile
Liquid nitrogen return			41.0	kW/mile
Total Losses at Low Temperature			362.0	kW/mile

Refrigerator Input = 362.0 x 7.8 x 6.3 miles/module = 17,780 kW/module

Sheath Losses(2 = 0 kW/mile x --- miles/module = 0 kW/module

Total Losses 17,780 kW/module

Total Losses 2,820 kW/mile

Transmission efficiency for 20-mile system 98.39 %

1) Metallic piping
2) FRP piping

COMPUTER OUTPUT SHEET

Concept: 3500 MVA; 500 kV: Hollow Cable

Run No. 350100 : Metallic Piping (Evacuated Multilayer Insulated)

Module length: 6.3 Miles

Cable Losses

Resistive/phase	42.0 × 3 =	126.0	kW/mile
Dielectric/phase	16.85 × 3 =	50.6	kW/mile
Sheath(1		81.0	kW/mile
Heat Leak			
Pressure pipe		4.0*	kW/mile
Liquid nitrogen return		2.6*	kW/mile
Total Losses at Low Temperature		264.2	kW/mile

Refrigerator Input = 264.2 × 7.8 × 6.3 miles/module = 12,982 kW/module

Sheath Losses(2 = 0 kW/mile × --- miles/module = 0 kW/module

Total Losses 12,982 kW/module

Total Losses 2,060 kW/mile

Transmission efficiency for 20-mile system 98.82 %

1) Metallic piping
2) FRP piping
*The Cryenco Division of Cryogenic Technology, Inc. has estimated this loss could be reduced approximately 25 percent by design modifications, but at higher piping cost.

COMPUTER OUTPUT SHEET

Concept: 5000 MVA; 500 kV: Hollow Cable

Run No. 500011 ; FRP Piping

Module length: 4.9 Miles

Cable Losses

Resistive/phase	64.0 × 3 =	192.0	kW/mile
Dielectric/phase	16.85 × 3 =	50.6	kW/mile
Sheath(1		0	kW/mile
Heat Leak			
Pressure pipe		71.4	kW/mile
Liquid nitrogen return		41.0	kW/mile
Total Losses at Low Temperature		355.0	kW/mile

Refrigerator Input = 355.0 × 7.8 × 4.9 miles/module = 13,570 kW/module

Sheath Losses(2 = 113.0 kW/mile × 4.9 miles/module = 554 kW/module

Total Losses 14,120 kW/module

Total Losses 2,880 kW/mile

Transmission efficiency for 20 mile system 98.85 %

1) Metallic piping
2) FRP piping

Appendix II

TECHNICAL DATA SHEETS

This appendix contains data sheets that contain dimensional information for cables and piping, as well as for liquid nitrogen conditions on which the results from this study are based. A separate sheet is used for each transmission capacity, operating voltage, and cable and piping concept examined.

TECHNICAL DATA SHEET

Concept: 2000 MVA; 345 kV; Solid Cable
Run No. _____; FRP Piping

Cable	
Conductor bore, inches	---
Conductor outside diameter, inches	4.26
Insulation outside diameter, inches	5.44
Inlet pressure, atmospheres	20
Δ Pressure, atmospheres	8
Inlet temperature, °K	65
Liquid nitrogen Δ temperature, °K	32
Conductor resistivity, μΩ-cm	0.31
Insulation thermal conductivity, W/cm-°K	0.0016
Pressure Pipe	
Inside diameter, inches	16.18
Outside diameter, inches	17.18
Liquid Nitrogen Return	
Inside diameter, inches	8.2
Outside diameter, inches	8.8
Exit pressure, atmospheres	14
Flow rate, lbs/s	66.16
Shield	
Inside diameter, inches	29.18
Wall thickness, inch	0.15
Resistivity, uΩ-cm	2.8
Foam Thickness	
Pressure pipe, inches	6
Liquid nitrogen return pipe, inches	6

TECHNICAL DATA SHEET

Concept: 2000 MVA; 500 kV; Solid Cable
Run No. _____; FRP Piping

Cable	
Conductor bore, inches	---
Conductor outside diameter, inches	3.60
Insulation outside diameter, inches	5.44
Inlet pressure, atmospheres	20
Δ Pressure, atmospheres	8
Inlet temperature, °K	65
Liquid nitrogen Δ temperature, °K	32
Conductor resistivity, μΩ-cm	0.31
Insulation thermal conductivity, W/cm-°K	0.0016
Pressure Pipe	
Inside diameter, inches	16.18
Outside diameter, inches	17.18
Liquid Nitrogen Return	
Inside diameter, inches	8.25
Outside diameter, inches	8.8
Exit pressure, atmospheres	14
Flow rate, lbs/s	64.19
Shield	
Inside diameter, inches	29.18
Wall thickness, inch	0.15
Resistivity, uΩ-cm	2.8
Foam Thickness	
Pressure pipe, inches	6
Liquid nitrogen return pipe, inches	6

TECHNICAL DATA SHEET

Concept: 3500 MVA; 500 kV; Solid Cable
Run No. _____; FRP Piping

Cable	
Conductor bore, inches	---
Conductor outside diameter, inches	3.60
Insulation outside diameter, inches	5.44
Inlet pressure, atmospheres	20
Δ Pressure, atmospheres	8
Inlet temperature, °K	65
Liquid nitrogen Δ temperature, °K	32
Conductor resistivity, μΩ-cm	0.31
Insulation thermal conductivity, W/cm-°K	0.0016
Pressure Pipe	
Inside diameter, inches	16.18
Outside diameter, inches	17.18
Liquid Nitrogen Return	
Inside diameter, inches	8.5
Outside diameter, inches	9.1
Exit pressure, atmospheres	14
Flow rate, lbs/s	75.71
Shield	
Inside diameter, inches	29.18
Wall thickness, inch	0.15
Resistivity, μΩ-cm	2.8
Foam Thickness	
Pressure pipe, inches	6
Liquid nitrogen return pipe, inches	6

TECHNICAL DATA SHEET

Concept: 5000 MVA; 500 kV; Solid Cable
Run No. _____; FRP Piping

Cable	
Conductor bore, inches	---
Conductor outside diameter, inches	3.60
Insulation outside diameter, inches	5.44
Inlet pressure, atmospheres	20
Δ Pressure, atmospheres	8
Inlet temperature, °K	65
Liquid nitrogen Δ temperature, °K	32
Conductor resistivity, μΩ-cm	0.31
Insulation thermal conductivity, W/cm-°K	0.0016
Pressure Pipe	
Inside diameter, inches	16.18
Outside diameter, inches	17.18
Liquid Nitrogen Return	
Inside diameter, inches	8.1
Outside diameter, inches	8.7
Exit pressure, atmospheres	14
Flow rate, lbs/s	92.9
Shield	
Inside diameter, inches	29.18
Wall thickness, inch	0.15
Resistivity, μΩ-cm	2.8
Foam Thickness	
Pressure pipe, inches	6
Liquid nitrogen return pipe, inches	6

TECHNICAL DATA SHEET

Concept: 2000 MVA; 500 kV; Hollow Cable
Run No. 250012 ; FRP Piping

Cable	
Conductor bore, inches	3.00
Conductor outside diameter, inches	3.60
Insulation outside diameter, inches	5.44
Inlet pressure, atmospheres	20
Δ Pressure, atmospheres	8
Inlet temperature, °K	65
Liquid nitrogen Δ temperature, °K	32
Conductor resistivity, μΩ-cm	0.31
Insulation thermal conductivity, W/cm-°K	0.0016
Pressure Pipe	
Inside diameter, inches	16.18
Outside diameter, inches	17.18
Liquid Nitrogen Return	
Inside diameter, inches	8.6
Outside diameter, inches	9.2
Exit pressure, atmospheres	14
Flow rate, lbs/s	79.6
Shield	
Inside diameter, inches	29.18
Wall thickness, inch	0.15
Resistivity, uΩ-cm	2.8
Foam Thickness	
Pressure pipe, inches	6
Liquid nitrogen return pipe, inches	6

TECHNICAL DATA SHEET

Concept: 3500 MVA; 500 kV; Hollow Cable
Run No. 350008 ; FRP Piping

Cable	
Conductor bore, inches	2.50
Conductor outside diameter, inches	3.60
Insulation outside diameter, inches	5.44
Inlet pressure, atmospheres	20
Δ Pressure, atmospheres	8
Inlet temperature, °K	65
Liquid nitrogen Δ temperature, °K	32
Conductor resistivity, μΩ-cm	0.31
Insulation thermal conductivity, W/cm-°K	0.0016
Pressure Pipe	
Inside diameter, inches	16.18
Outside diameter, inches	17.18
Liquid Nitrogen Return	
Inside diameter, inches	8.5
Outside diameter, inches	9.1
Exit pressure, atmospheres	14
Flow rate, lbs/s	90.8
Shield	
Inside diameter, inches	29.18
Wall thickness, inch	0.15
Resistivity, uΩ-cm	2.8
Foam Thickness	
Pressure pipe, inches	6
Liquid nitrogen return pipe, inches	6

TECHNICAL DATA SHEET

Concept: 3500 MVA; 500 kV; Hollow Cable
Run No. 350100 ; Metallic Piping (Foam Insulation)

Cable	
Conductor bore, inches	2.50
Conductor outside diameter, inches	3.60
Insulation outside diameter, inches	5.44
Inlet pressure, atmospheres	20
Δ Pressure, atmospheres	8
Inlet temperature, °K	65
Liquid nitrogen Δ temperature, °K	32
Conductor resistivity, μΩ-cm	0.31
Insulation thermal conductivity, W/cm-°K	0.0016
Pressure Pipe	
Inside diameter, inches	16.18
Outside diameter, inches	17.18
Liquid Nitrogen Return	
Inside diameter, inches	8.3
Outside diameter, inches	8.9
Exit pressure, atmospheres	14
Flow rate, lbs/s	98.7
Shield	
Inside diameter, inches	16.18
Wall thickness, inch	0.15
Resistivity, μΩ-cm	0.31
Foam Thickness	
Pressure pipe, inches	6
Liquid nitrogen return pipe, inches	6

TECHNICAL DATA SHEET

Concept: 3500 MVA; 500 kV; Hollow Cable
Run No. _____ ; Metallic Piping,
(Evacuated Multilayer Insulated)

Cable	
Conductor bore, inches	2.50
Conductor outside diameter, inches	3.60
Insulation outside diameter, inches	5.44
Inlet pressure, atmospheres	20
Δ Pressure, atmospheres	8
Inlet temperature, °K	65
Liquid nitrogen Δ temperature, °K	32
Conductor resistivity, μΩ-cm	0.31
Insulation thermal conductivity, W/cm-°K	0.0016
Pressure Pipe	
Inside diameter, inches	16.18
Outside diameter, inches	----
Liquid Nitrogen Return	
Inside diameter, inches	8.3
Outside diameter, inches	----
Exit pressure, atmospheres	14
Flow rate, lbs/s	Not Computed
Shield	
Inside diameter, inches	16.18
Wall thickness, inch	0.15
Resistivity, μΩ-cm	0.31
Foam Thickness	
Pressure pipe, inches	Not Used
Liquid nitrogen return pipe, inches	Not Used

TECHNICAL DATA SHEET

Concept: 5000 MVA; 500 kV; Hollow Cable
Run No. 500011 ; FRP Piping

Cable	
Conductor bore, inches	2.00
Conductor outside diameter, inches	3.60
Insulation outside diameter, inches	5.44
Inlet pressure, atmospheres	20
Δ Pressure, atmospheres	8
Inlet temperature, °K	65
Liquid nitrogen Δ temperature, °K	32
Conductor resistivity, μΩ-cm	0.31
Insulation thermal conductivity, W/cm-°K	0.0016
Pressure Pipe	
Inside diameter, inches	16.18
Outside diameter, inches	17.18
Liquid Nitrogen Return	
Inside diameter, inches	8.3
Outside diameter, inches	8.9
Exit pressure, atmospheres	14
Flow rate, lbs/s	108.8
Shield	
Inside diameter, inches	29.18
Wall thickness, inch	0.15
Resistivity, μΩ-cm	2.8
Foam Thickness	
Pressure pipe, inches	6
Liquid nitrogen return pipe, inches	6

Appendix III

THERMAL CONDUCTIVITY OF LIQUID NITROGEN IMPREGNATED, CELLULOSE AND CELLULOSE/POLYPROPYLENE DIELECTRIC MATERIALS

INTRODUCTION

As part of the General Electric funded development of low-temperature dielectrics, Prof. P. Thullen of the Massachusetts Institute of Technology performed measurements of the effective thermal conductivity of liquid nitrogen impregnated, cellulose paper dielectric over a range of pressures from 14.7 to 400 psia. Experiments were carried out on two separate samples of cellulose paper, using liquid nitrogen and gaseous helium as the impregnant, at pressures up to 400 psia and temperatures up to 135 K. The measurements are summarized in this appendix.

PRIOR WORK

Prior work of a similar nature is outlined in the thesis of Parisi (Ref. III-1). The apparatus of Parisi has been reproduced and improved for these tests.

Preliminary estimates of the thermal conductivity of liquid nitrogen impregnated cellulose papers will be found in the report of Norris (Ref. III-2). Experimental data reported herein fall within the range anticipated by Norris. The experimental data are in the high region of his estimates.

Discussions of the equivalent thermal conductivity of packed particles in a fluid at rest, a related topic, will be found in Jakob (Ref. III-3) and McAdams (Ref. III-4). Unfortunately, these authors give little useful insight into the problem at hand.

SAMPLE

Sheet wrapped, cylindrical test samples were chosen for these experiments. This also proved to be a suitable geometry for the design of the surrounding pressure vessel and general ease of construction.

FACILITIES

Work was carried out at the Cryogenic Engineering Laboratory of the Massachusetts Institute of Technology. Normal laboratory instruments, equipment, and procedures were used. A general overview of the experimental facility is shown in Figure III-1. Mechanical work was done by members of the technical staff under the supervision of Dr. P. Thullen.

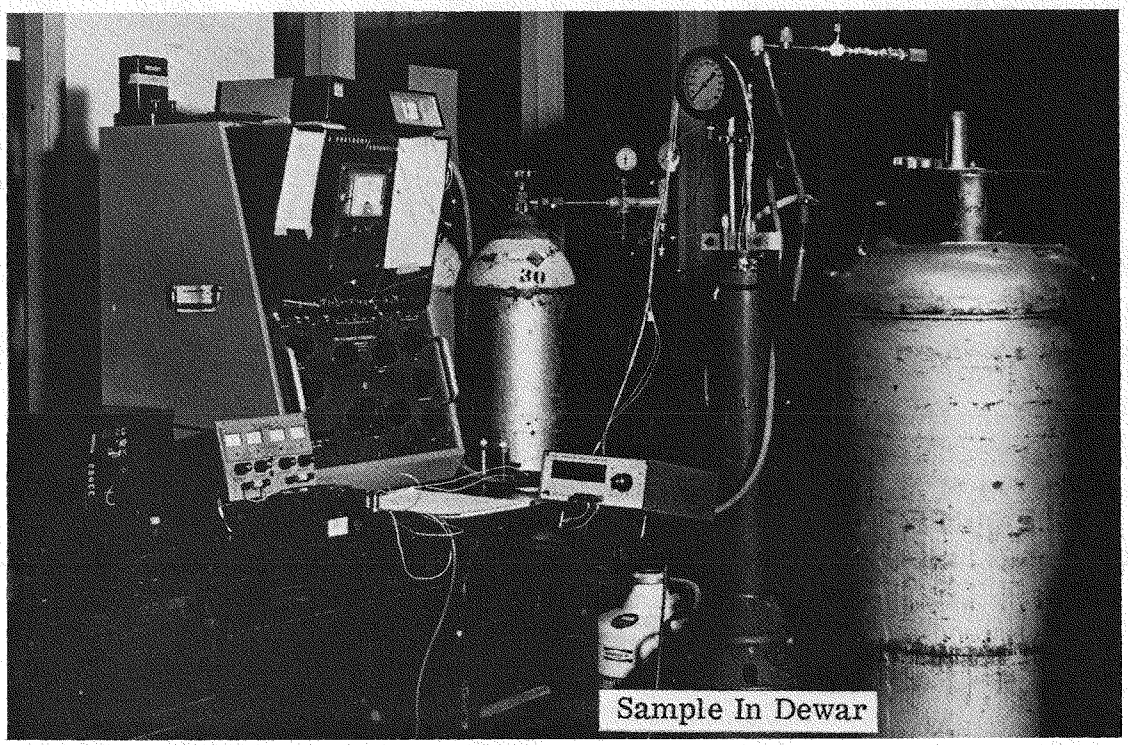

Figure III-1. Overall View of Experiment

DATA REDUCTION

Measurements of temperature difference as a function of heat input were made under the various conditions described. They were mathematically reduced to provide values of local effective (not average) thermal conductivity as a function of temperature. This allows direct comparison of the data with the known values of nitrogen and helium conductivity.

RESULTS

The thermal conductivity of the papers tested, when impregnated with liquid nitrogen, was constant at an approximate average value of 1.5 mW/cm/deg K (actual values will be found on page III-13). This value appears to be influenced by natural convection or some other undetermined phenomenon that may be a result of the design of the experiment. The conductivity was not found to be influenced by pressure, temperature, or moisture content of the paper over the ranges tested. Behavior in the presence of gaseous helium as an impregnant was also recorded and differed markedly from that found with liquid nitrogen present. Helium data are presented on Page III-13.

DESIGN OF THE EXPERIMENT

Cylindrical sample configurations for thermal conductivity tests have been in use for many years. Jakob (Ref. III-5) gives an interesting historical ac-

count and indicates that the first application to solids was reported in 1905 and to liquids in 1888. Because of this, estimates of the performance of such experiments and guidelines for their design have appeared in the literature.

A cross-section drawing of the experimental sample is shown in Figure III-2. Photographs of the components are shown in Figures III-3 and III-4. Proceeding from the centerline, the sample consists of:

1. Phenolic heater support rod.
2. Spiral constantan heater.
3. Apiezon-grease-filled gap.
4. Inner stainless-steel pressure tube.
5. Cellulose paper sample.
6. Outer stainless-steel pressure tube.

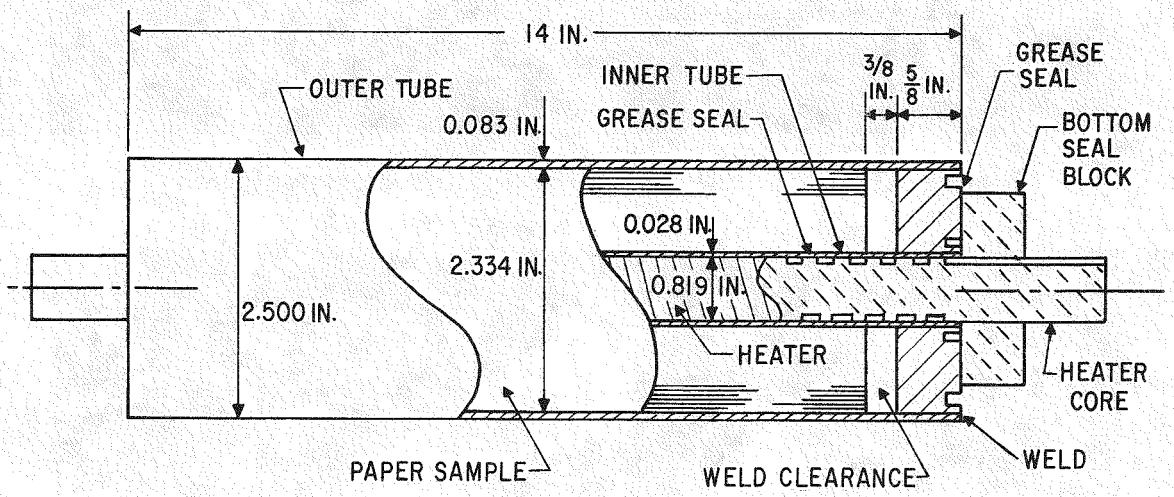

Figure III-2. Cross Section Through Test Sample

End caps are welded to the two stainless-steel pressure vessel walls. The paper ends are 3/8 inch from the caps to prevent damage during welding. Temperatures are measured with copper-constantan thermocouples. Succeeding paragraphs give details of these components.

PRESSURE VESSEL

At the time of Parisi's work, it was decided that the sample itself would be encapsulated in a welded pressure vessel to avoid building a pressurizable nitrogen dewar. Wall thicknesses of this vessel were kept small by maintaining

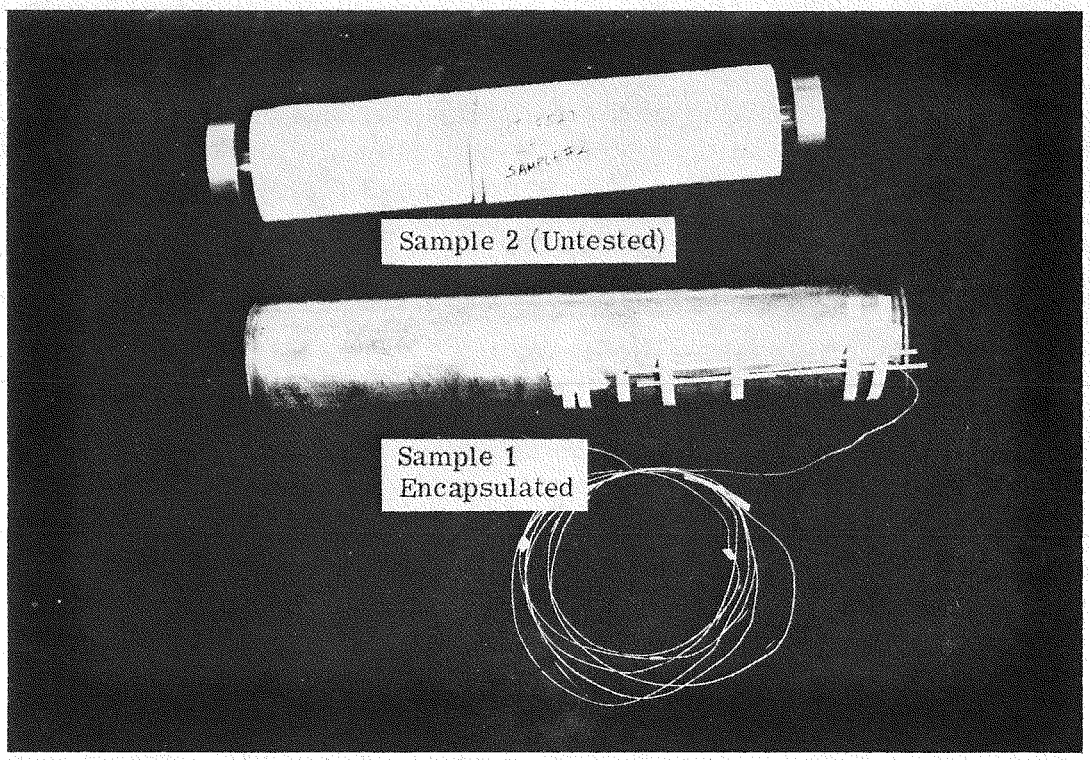

Figure III-3. Sample Before and After Encapsulation

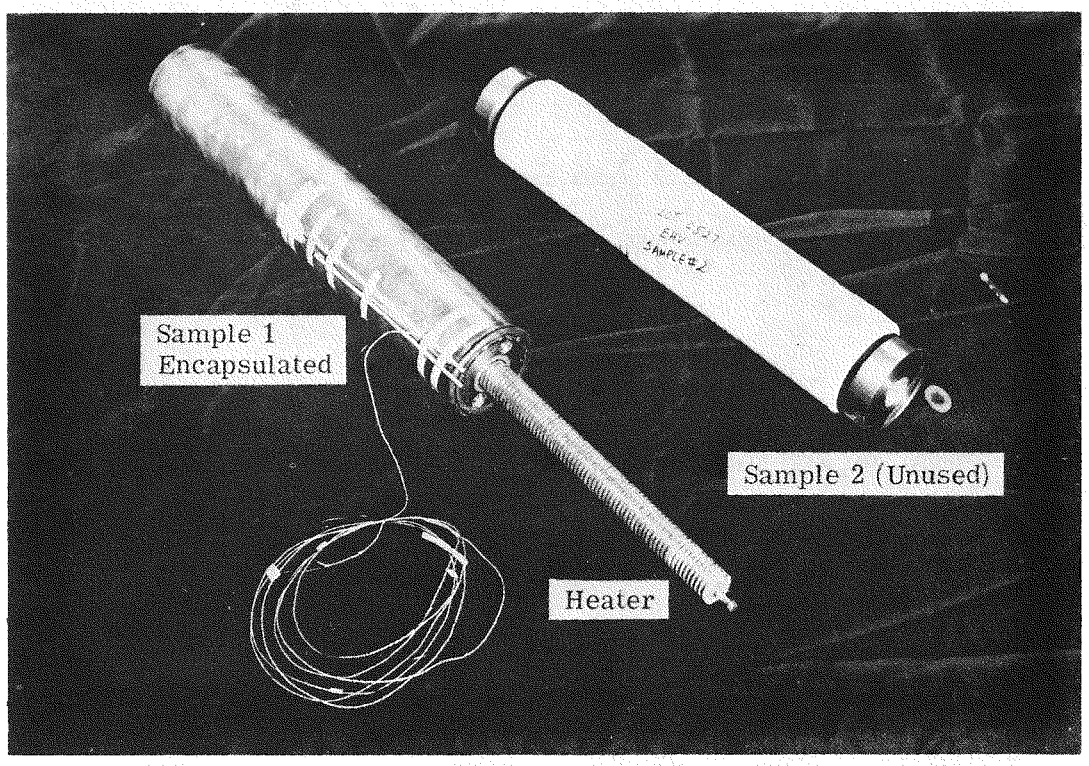

Figure III-4. Sample Showing End Penetrations and Heater

a relatively small sample diameter. The length was chosen to be 10 to 15 times the heater diameter to minimize end effects. Welded joints were chosen for integrity, strength, and convenience. Pipe penetrations at the end caps used standard pipe threads sealed with Teflon tape. All of the pressure vessel parts (including fill and vent tubes) were type 304 stainless steel. The vessel was designed along guidelines furnished by the A. S. M. E. code for unfired pressure vessels; it was not pressure tested before use, since a suitable factor of safety was included in its design.

SAMPLE

Dielectric samples were prepared at the General Electric Company on inner stainless-steel tubes. The paper samples were 12 inches in width, with a one-inch empty length on each end of the stainless-steel tube for cap and weld clearance. The outside diameter was considerably oversize, and paper was removed to provide a snug fit in the outer pressure vessel tube. The samples were stored at normal room conditions before assembly and testing, and were at a moisture content consistent with normal summer conditions in Boston. End caps were TIG welded at each tube junction. The tube walls were cooled following each weld, and no evidence could be found of damage to the paper.

HEATER

The heater, a self-contained unit, was used for each test. It consisted of rectangular constantan wire (0.060 inch by 0.018 inch) wound on a phenolic core. The winding pitch was eight per inch. The top of the heater wire was 0.014 inch below the top of the spiral groove to provide electrical insulation and clearance for thermocouple wires. Electrical taps were separated by a distance of 14 inches. The resistance of the heater was roughly 10.5 ohms at all temperatures. Four electrical leads were attached, and current and voltage were measured for each data point.

The clearance space between the constantan wire and the inner pressure vessel tube was filled with Apiezon M or N grease which has a thermal conductivity of 1 to 2 mW/cm/deg K between 100 and 200 K as measured by Ashworth and Loomer (Ref. III-6). During assembly, the grease was heated and liquefied to allow it to flow, displace gas pockets, and attain good thermal contact with the heater, the phenolic rod, and the tube wall.

THERMOCOUPLES

Copper constantan thermocouples were used to measure temperature. All of the leads were brought to room temperature. Adequate heat sinking was provided in the cold space to prevent heat conduction down the wires to the experiment. The constantan wires were interconnected at room temperature, and only temperature differences were recorded. The Omega thermo-

couple tables (Ref. III-7) were used to convert thermocouple voltages to temperature differences.

The inner thermocouple was brought to the midpoint of the heater by way of a small axial slot milled in the phenolic above the top of the heater wire for this purpose, as shown in Figure III-5. The junction was placed in a small radial hole in the phenolic to provide electrical insulation. The slot and hole were well greased before assembly. This construction causes the thermocouple to indicate the temperature at some radial location between the heater and the inside of the sample. It is also influenced, to some degree, by axial conduction. Due to the length of the thermocouple and the good conductivity of the grease, these effects are thought to be negligible. The temperature of the thermocouple is assumed to be the temperature of the inner sample wall.

The outer thermocouple was attached to the outer pressure vessel wall of sample 1 and simply immersed in the liquid nitrogen bath for sample 3.

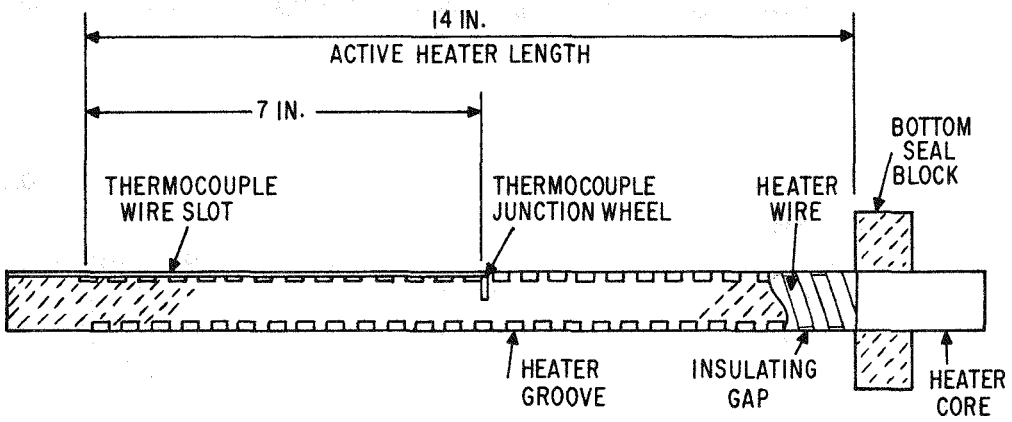

Figure III-5. Cross Section of Heater

PRESSURE SOURCES

The system was pressurized to 23 psig by a standard 160 liter liquid nitrogen dewar. Higher pressures were obtained with a regulated cylinder of prepurified nitrogen gas. Pressures were measured with a calibrated bourdon tube gage. Two pressure lines were connected to the sample. One was used as a working line, and the other was kept free as an emergency discharge. Pressure levels were maintained through the action of the regulator, the relief valves, and a manually controlled throttle.

Some tests were run with helium gas as the impregnant. In preparation for these tests, the system was brought to room temperature, evacuated, and refilled with helium gas. Gas pressure was maintained at 12.5 psig for these tests. The system was then cooled to nitrogen temperature.

NITROGEN DEWAR

A 25 liter, large mouth, spherical nitrogen dewar was used to contain the nitrogen for these tests. During testing, the dewar neck was kept full of liquid to prevent heat leaks from ambient temperatures into the sample space.

INSTRUMENTS

Instrumentation was provided to measure:

- Thermocouple emf.
- Sample pressure.
- Heater voltage.
- Heater current.

In each case, the instrument represented the best equipment available in the laboratory.

Thermocouple emf was measured with a Leeds and Northrup K-3 potentiometer. The standard cell emf was checked with a Hewlet Packard 3460A digital voltmeter.

Heater voltage was measured with a Keathly digital voltmeter. This meter agreed with the K-3 potentiometer to 1 part in 1000.

Heater current was measured by a Weston Model 1 ammeter. This is a deArsenval meter calibrated in 1973, traceable to the NBS. It agreed with the Keathly voltmeter to 1 part in 1000 when placed in series with a standard ohm.

Pressures were measured with a bourdon tube gage. The gage was calibrated with a dead-weight tester.

Heater power was supplied by a transistor power supply acting as a current source.

DATA REDUCTION

Data reduction is based upon an integration of Fourier's law of heat conduction of the following form:

$$\int_{T_i}^{T_o} k\,dt = \frac{q}{2\pi\ell} \ln \frac{r_o}{r_i} \qquad \text{(III-1)}$$

where: q = total heat supplied by the heater.

ℓ = heater length (14 inches).

r_i = inside radius of the sample (0.4375 inch).

r_o = outside radius of the sample (1.155 inches).

K = thermal conductivity.

T_o, T_i = outside and inside temperature of the sample.

T = general temperature.

In general, the heat flux could be represented by one of the following equations with constants determined by least-squares:

$$q = a_0(\Delta T) \tag{III-2}$$

or

$$q = a_1(\Delta T) + a_2(\Delta T)^2 \tag{III-3}$$

where: ΔT = temperature above 77.4 K.

a_0, a_1, a_2 = constants from least square data fit.

The thermal conductivity is then found by differentiation of Equations III-2 and III-3 and multiplication by the proper geometric constants:

$$k = \frac{\ln \frac{r_o}{r_i}}{2\pi\ell}(a_0) \tag{III-4}$$

$$k = \frac{\ln \frac{r_o}{r_i}}{2\pi\ell}(a_1 + a_2(\Delta T)) \tag{III-5}$$

Equation III-4 represents liquid nitrogen data, and Equation III-5 represents helium gas data.

Axial heat conduction causes the experimental values of conductivity to be higher than the actual value. This problem has been treated by Van Rinsum as reported by Jakob (Ref. III-5). Axial conduction errors are caused by the presence of:

- The phenolic heater support.
- The heater wire.
- The thermocouple wires, principally the copper wire.
- The stainless-steel pressure tube.

Assuming the length from the midpoint of the sample (the thermocouple location) to the ends to be 6.5 inches and the end temperature to be 77.4 K, the error in the temperature difference (ΔT) was found to be roughly 0.5 percent.

This implies that the final conductivity data have a systematic error of 0.5 percent, which was not considered in the data reduction because of its small magnitude.

A systematic error was also introduced by spurious voltages in the thermocouple circuit. These voltages can be attributed to temperature gradients along the wires and strain hardening of the wire during installation. Wire from a single source was used to keep such signals at a minimum. In general, they represent an error in emf of -4.5 to +1.5 μV at zero heat flux. Viewed another way, these errors imply an infinite thermal conductivity by indicating zero temperature difference at finite values of heat flux. A three μV error signal corresponds to a temperature error of about 0.2 K, so these spurious signals have greater importance at low heat fluxes. Since they remained more or less constant for each experimental setup, an approximate correction was made in the thermocouple emf during data reduction.

EXPERIMENTAL PROCEDURE

All reasonable care was exercised to assure consistency of the data taking. The same instruments were used for all of the tests. The nitrogen dewar was kept filled so that the measurements were not affected by the liquid level. The electrical instruments were checked against one another and found to be consistent to within 1 part in 1000.

The sample was cooled to nitrogen temperature slowly to reduce the effects of differential thermal contraction on its components. During cooldown, nitrogen gas at 23 psig was supplied to the sample from the liquid nitrogen storage dewar. A positive gas pressure was maintained continuously while the sample was at liquid nitrogen temperature to prevent contamination by atmospheric air. The sample was allowed a day to come to thermal equilibrium when cooled from room temperature.

Basic operations were similar for both the liquid nitrogen and the helium gas tests.

LIQUID NITROGEN TESTS

During these tests, the sample was pressurized to test pressure from a supply bottle of prepurified nitrogen gas. Very little high pressure gas was required once the sample was filled with liquid by condensation from the nitrogen storage dewar. This made pressure regulation a difficult task.

Thermal conductivity of the dielectric impregnated with liquid nitrogen was not found to be a function of pressure, so precise values of pressure were not maintained. This made data gathering easier, since the pressure tended to drift more than the other measured quantities and a great deal of attention was required to keep it constant. The pressure was always kept

well above the saturation pressure at the highest temperature within the sample so that boiling could not occur.

A constant heat input was maintained during each test run by supplying the heater from a current source. In general, temperatures were observed and recorded until a steady state had been reached. This required about one hour. Some tests were continued over a longer period for convenience. In all cases, the temperatures appeared to have reached steady state after one hour. A plot of temperature versus time for a typical experiment is shown in Figure III-6.

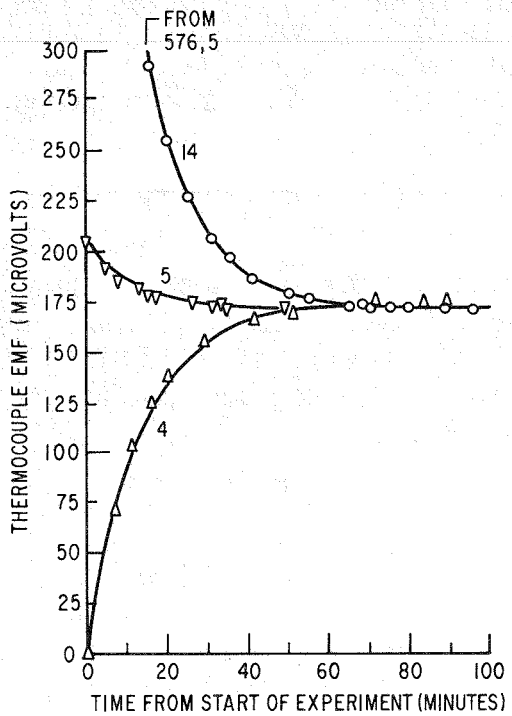

Figure III-6.

Thermocouple EMF with Time for Three Tests with Fixed Heater Current (Numbers refer to Table III-1).

HELIUM GAS TESTS

Following completion of the liquid nitrogen tests, the sample was warmed to room temperature and pumped to remove the remaining nitrogen gas. The sample was then pressurized with helium gas and recooled. This operation was performed without disturbing the sample by allowing the nitrogen dewar to run dry and warm up.

Some water was removed from the sample during the pumping process. To determine the effect of the water removal, a retest with liquid nitrogen was made on sample 1 following the helium gas tests. No effect was observed.

The test procedure was identical to that with liquid nitrogen impregnation.

RESULTS

These tests indicate that the effective conductivity of nitrogen-impregnated paper is constant over the range of temperatures investigated. When helium gas is used as the impregnant, the conductivity rises with temperature at about the same rate as the conductivity of helium gas alone. In both cases, the effective conductivity is greater than that of the impregnant alone. In the case of liquid nitrogen, it appears that the values obtained were influenced by natural convection.

Actual data, as recorded, are listed in Tables III-1 and III-2 and plotted in Figures III-7 and III-8. Values of conductivity were deduced from a least square curve fit as explained on page III- and are shown as a function of temperature in Figure III-9.

Table III-1

TEST DATA - SAMPLE 1

Test Number	Date (1975)	Fluid	Pressure (psig)	Thermocouple emf(1 (microvolts)	Heater Current (amperes)	Heater Voltage (volts)
1(2	9/5	N_2	50	196.5	0.600	6.21
2(2	9/5	N_2	150	408.5	0.800	8.26
3(2	9/5	N_2	150	306.0	0.700	7.25
4	9/9	N_2	180	174.2	0.600	6.24
5	9/9	N_2	195	173.0	0.600	6.23
6	9/9	N_2	170	320.0	0.800	8.27
7	9/9	N_2	250	525.0	1.000	10.35
8	9/10	N_2	23	73.0	0.400	4.13
9	9/10	N_2	23	-7.5	0.200	2.07
10	9/10	N_2	23	38.0	0.300	3.10
11	9/10	N_2	23	15.2	0.200	2.06
12	9/11	N_2	23	-4.5	0	0
13	9/11	N_2	400	785.5	1.200	12.45
14	9/11	N_2	400	172.0	0.600	6.22
15	9/22	N_2	12	110.0	0.400	4.14
16	9/22	He	12	255.0	0.600	6.23
17	9/22	He	12	458.1	0.800	8.27
18	9/25	He	12	724.5	1.000	10.35
19	9/25	He	12	1063.7	1.200	12.44
20	9/26	He	12	886.0	1.100	11.40
21	9/26	He	12	582.0	0.900	9.32
22	9/26	He	12	346.5	0.700	7.25
23	9/26	He	12	174.1	0.500	5.17
24	9/27	N_2	350	173.3	0.600	6.22

Notes: 1) A correction for zero point error must be made by adding 4.5 uV to the indicated values, before temperature differences can be calculated.
2) Early data point taken before grease was melted to improve thermal conductance. Not used to determine conductivity.

Table III-2

TEST DATA - SAMPLE 3

Test Number	Date (1975)	Fluid	Pressure (psig)	Thermocouple emf (microvolts)	Heater Current (amperes)	Heater Voltage (volts)
1	10/31	N_2	175	137.0	0.502	5.23
2	11/3	N_2	190-140	270.7	0.700	7.29
3	11/3	N_2	195	457.1	0.900	9.36
4	11/3	N_2	357	712.2	1.100	11.48
5	11/3	N_2	50-100	51.4	0.303	3.16
4a	11/3	N_2	315	709.8	1.100	11.46
6	11/5	N_2	245	567.6	0.991	10.32
7	11/5	N_2	260	362.9	0.811	8.44
8	11/6	N_2	105	190.5	0.595	6.17
9	11/6	N_2	195	85.6	0.400	4.16
10	11/12	He	12.5	161.5	0.491	5.09
11	11/13	He	12.5	323.5	0.695	7.20
12	11/13	He	12.5	697.0	1.000	10.37
13	11/13	He	12.5	489.6	0.851	8.83
14	11/15	He	12.5	253.9	0.619	6.41
15	11/15	He	12.5	988.5	1.198	12.44

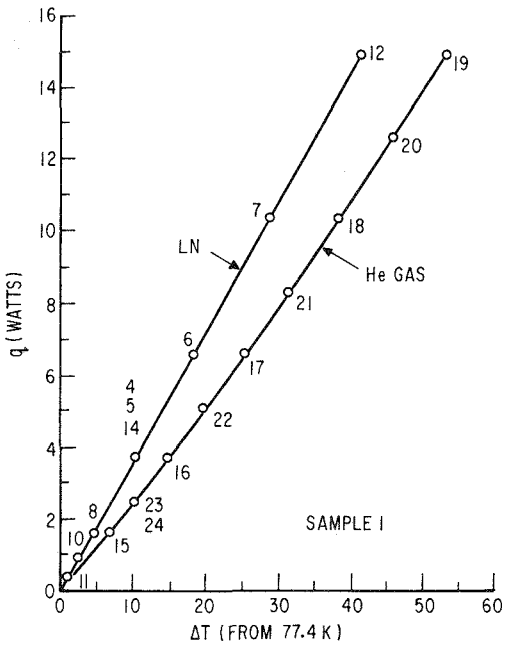

Figure III-7. Sample 1 Data (Numbers refer to Table III-1)

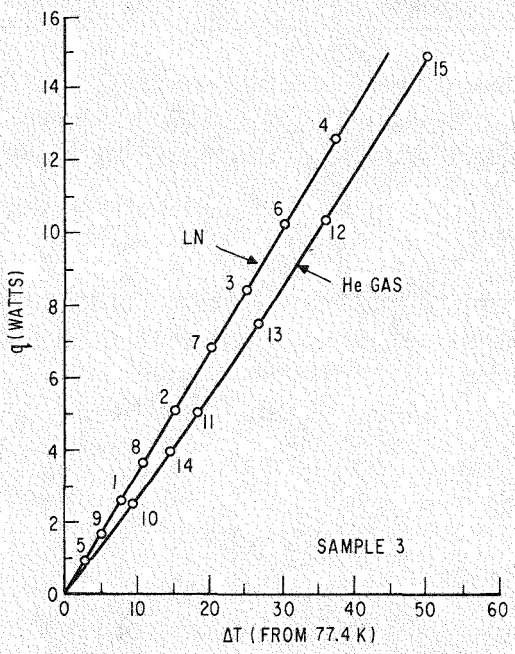

Figure III-8. Sample 3 Data (Numbers refer to Table III-2)

Curve	Sample	Fluid	Paper
1	1	LN_2	Cellulose
2	3	LN_2	Cellulose and polypropylene
3	3	He	Cellulose and polypropylene
4	1	He	Cellulose
5	Ref. III-8	LN_2	None
6	Ref. III-8	He	None

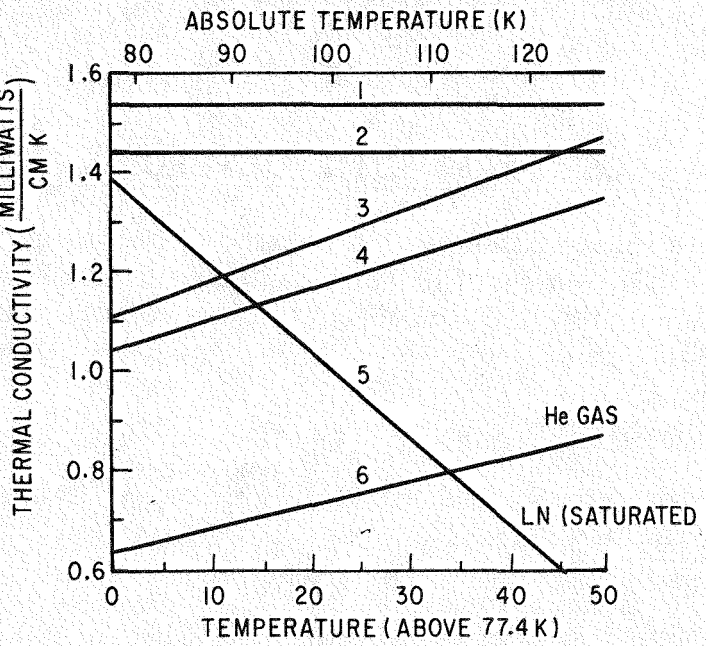

Figure III-9. Comparison of Thermal Conductivities

SAMPLE 1 -- CELLULOSE PAPER

Sample 1 was cellulose paper, lot 6527, EHV, supplied by the General Electric Company. Data from all of the tests on sample 1 are listed in Table III-1. The results are shown graphically in Figure III-7.

Nitrogen Tests -- Sample 1

When the sample is impregnated with liquid nitrogen, the relation between heat flux and temperature, as determined by a least squares fit, is:

$$q = 354.9\ (\Delta T) \text{ milliwatts} \qquad \text{(III-6)}$$

the resulting effective thermal conductivity is:

$$k = 1.542\ \frac{mw}{cm^{\circ}K} \qquad \text{(III-7)}$$

No effect of nitrogen impregnant pressure was observed as shown by tests 4, 5, 14, and 24, which were run at the same heat flux and various pressures. No effect of moisture (water) content was found as shown by tests 14 and 24, which were run at the same heat flux before and after removal of approximately 15 cc of water.

Helium Tests -- Sample 1

When sample 1 is impregnated with helium gas, the heat flux and conductivity relationships are:

$$q = 240.8\ (\Delta T) + 0.7041\ (\Delta T)^2 \text{ milliwatts} \qquad \text{(III-8)}$$

$$k = 1.046 + 0.006118\ (\Delta T)\ \frac{mw}{cm^{\circ}K} \qquad \text{(III-9)}$$

SAMPLE 3 -- CELLULOSE PAPER WITH POLYPROPYLENE

Sample 3 was cellulose paper with a coating of polypropylene on one side, as supplied by the General Electric Company. Data from all of the tests on sample 3 are listed in Table III-2, and the results are shown graphically in Figure III-8.

Nitrogen Tests -- Sample 3

When sample 3 is impregnated with liquid nitrogen, the heat flux and conductivity relationships are:

$$q = 331.4\ (\Delta T) \text{ milliwatts} \qquad \text{(III-10)}$$

$$k = 1.440\ \frac{mw}{cm^{\circ}K} \qquad \text{(III-11)}$$

Helium Tests -- Sample 3

When sample 3 is impregnated with helium gas, the heat flux and conductivity relationships are:

$$q = 255.6\ (\Delta T) + 0.8330\ (\Delta T)^2 \text{ milliwatts} \qquad \text{(III-12)}$$

$$k = 1.111 + 0.007239\ (\Delta T)\ \frac{mw}{cm\,^{\circ}K} \qquad \text{(III-13)}$$

DISCUSSION

Figure III-9 shows a comparison of the conductivities of samples 1 and 3 with the conductivities of helium gas and saturated liquid nitrogen. Several conclusions can be drawn:

- The conductivity of the liquid-nitrogen-impregnated samples is not temperature dependent even though the conductivity of the saturated liquid is strongly temperature dependent.
- The conductivity of the helium-gas-impregnated samples has about the same temperature dependence as helium gas.
- The conductivity of the plastic-coated paper is lower than that of uncoated paper in the presence of liquid nitrogen and higher in the presence of helium gas.
- The conductivity of the nitrogen-impregnated sample does not equal the conductivity of the helium-impregnated sample at the point at which the conductivities of helium and nitrogen are equal.

These conclusions indicate the importance of other properties in addition to impregnant conductivity in determining the average overall conductivity. This is particularly evident in the case of the nitrogen-impregnated samples.

Natural convection, caused by a radial temperature gradient and an axial body force field acting on a slightly compressible fluid, may account for the apparent contradictions in the results. Fluid could be made to flow axially in the spiral passage formed when the paper is wrapped on the central core. The pressure head which induces the flow could be caused by the density difference between light fluid at the warm center wall and heavy fluid at the cold outer wall. Energy could be transferred by the net enthalpy flux associated with the fluid circulation. Fluid friction would limit the flow. The rate of heat transfer for such a model is:

$$q = \left(\frac{Ad^2}{64}\right)(g)\ (\Delta T)^2 \left(\frac{\rho C_p \beta}{\nu}\right) \qquad \text{(III-14)}$$

where: Ad^2 = geometric constant.

g = acceleration of gravity.

ΔT = temperature difference inducing flow.

$\frac{\rho C_p \beta}{\nu}$ = fluid properties.

when laminar flow is assumed. For each sample tested, all of the parameters are fixed except the fluid properties and the temperature difference. The fluid properties of nitrogen and helium vary greatly as shown in Table III-3. It is shown that, under equivalent conditions, liquid nitrogen has four orders of magnitude more ability to transport heat by natural convection than helium gas. If natural convection is altering the results, it is likely to have a much more severe effect in the case of liquid nitrogen.

Table III-3

FLUID PROPERTIES

	Helium	Nitrogen
Temperature, K	80	80
Phase	Gas	Liquid
Pressure, atmosphere	1.0	1.0
ρ, gm/cm^3	5.08×10^{-4}	8×10^{-1}
C_p, Joules/gm/°K	5.2	2.05
β, 1/°K	1.25×10^{-2}	2×10^{-3}
μ, poise	85×10^{-6}	1.4×10^{-3}
$\frac{\rho^2 C_p \beta}{\mu}$	2×10^{-4}	1.9

The simple model indicates that the natural convection effects should vary as the square of the tests temperature difference. This is not evident in the experimental data. Insufficient information is available to judge the effects of sample geometry.

RECOMMENDATIONS

The data obtained in this experiment show unexpected trends. The zero ΔT data (left hand intercepts in Figure III-9) are likely to be uninfluenced by convection if it exists. This suggestion is also made by Jakob. In addition, the nitrogen data should probably decrease with increasing temperature so that it intersects the appropriate helium data at 111.5 K. To establish the effect of convection and obtain more accurate data, it is recommended that:

- The experiment should be rerun with its axis in the horizontal position, or one end of the sample should be sealed with epoxy or grease to prevent net circulation of the fluid.
- Natural convection should be as important with helium gas, at 400 psig, as an impregnate as with liquid nitrogen. Testing should be made over a range of helium pressures to determine the effects of natural convection.

Appendix IV

SIMPLIFIED CABLE THERMAL ANALYSIS

CABLE COOLING

Three principal heat sources act as loads upon the liquid nitrogen coolant:

- Heat leak through the foam insulation, Q_F.*
- Resistive losses in the conductor, Q_R.
- Alternating-current dielectric losses in the electrical insulation, Q_D.

Viscous losses also exist in the coolant flow, but these are small by comparison and are therefore ignored in this analysis.

Figure IV-1 is a sectioned view of the cables and the cable envelope, showing the distribution of these losses between the bore and the interstitial coolant streams. In the figure:

Q_F = external heat leak, W/cm.

Q_I = portion of resistive and dielectric losses transferred to the interstitial fluid from each cable, W/cm.

Q_B = portion of resistive and dielectric losses transferred to the bore fluid from each cable phase, W/cm.

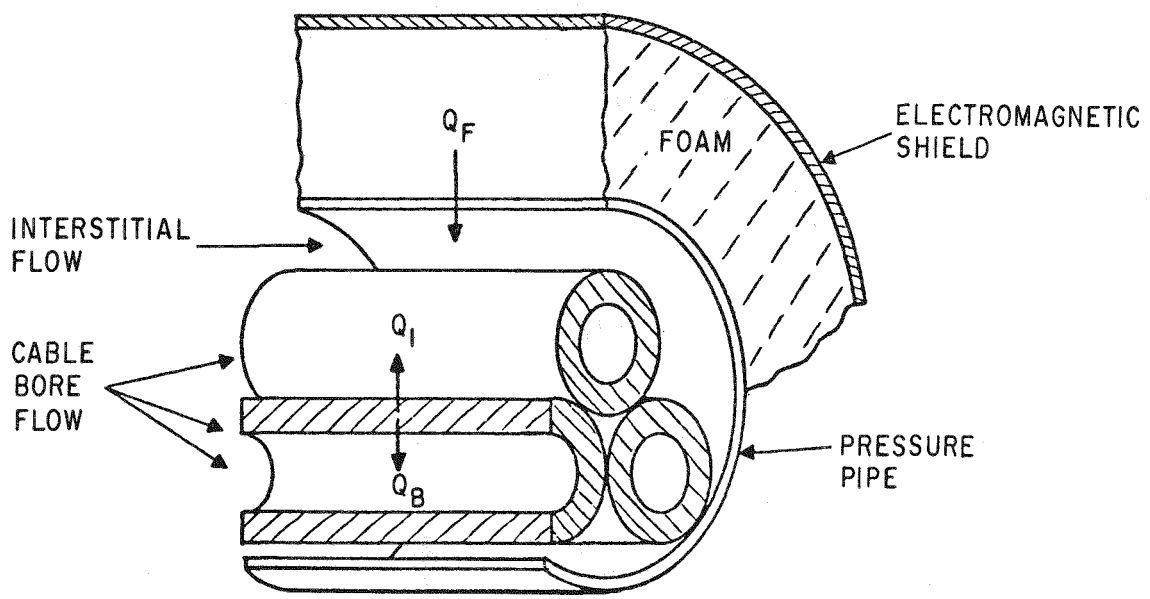

Figure IV-1. Cable System Segment

*Units are W/unit length of the cable and the envelope.

The sum of Q_I and Q_B must be exactly equal to the total electrical dissipation rate:

$$Q_I + Q_B = Q_D + Q_R \qquad \text{(IV-1)}$$

If the total coolant flow rate is W and a fraction, X, of this flows in the bore stream, then conservation of energy applied to the two streams yields:

$$\text{(Bore)}\ WXC_p \frac{dT_B}{dz} = 3Q_B \qquad \text{(IV-2)}$$

$$\text{(Interstitial)}\ (1 - X)\ WC_p \frac{dT_I}{dz} = Q_F + 3Q_I \qquad \text{(IV-3)}$$

where: W = total coolant flow rate, g/s.

X = fraction of W flowing in the three bore tubes.

C_p = specific heat of coolant, J/g/°K.

T_B = temperature of bore fluid, °K.

T_I = temperature of interstitial fluid, °K.

z = distance measured from system inlet, cm.

To solve these equations for the system temperature profiles, further information pertaining to quantities Q_B, Q_F, and Q_I is required. These quantities are not constants but depend upon the values of T_B and T_I. Using appropriate assumptions (summarized below), it can be shown that these heat flows have the forms:

$$Q_F = \xi + \omega T_I \qquad \text{(IV-4)}$$

$$Q_I = \gamma + \delta\,(T_B - T_I) \qquad \text{(IV-5)}$$

$$Q_B = \alpha + \beta\,(T_B - T_I) \qquad \text{(IV-6)}$$

where α, β, γ, δ, ω, and ξ are constants that depend upon the system dimensions and thermal properties; they are summarized below. Substitution of Equations IV-4 through IV-6 into Equations IV-2 and IV-3 yields:

$$\frac{dT_B}{dz} = A + BT_B - BT_I \qquad \text{(IV-7)}$$

$$\frac{dT_I}{dz} = C + DT_I + ET_B \qquad \text{(IV-8)}$$

where:

$$A = \frac{\alpha}{XWC_p}$$ (W is defined in Equation IV-16).

$$B = \frac{\beta}{XWC_p}$$

$$C = \frac{\xi + \gamma}{(1-X)WC_p}$$

$$D = \frac{\varphi + \delta}{(1 - X)WC_p}$$

$$E = \frac{\delta}{(1 - X)WC_p}$$

Differentiating Equation IV-7 and combining with Equation IV-8 to eliminate T_I yields,

$$\frac{d^2T_B}{dz^2} + P\frac{dT_B}{dz} + S\,T_B = R \qquad \text{(IV-9)}$$

where: $P = -B - D$

$S = B(D + E)$

$R = -B \cdot C - D \cdot A$

This equation gives the following solutions for the temperatures of the two streams at any distance, z, from the inlet:

$$T_B = C_1 e^{m_1 z} + C_2 e^{m_2 z} + \frac{R}{S} \qquad \text{(IV-10)}$$

$$T_I = C_1 e^{m_1 z}\left(1 - \frac{m_1}{B}\right) + C_2 e^{m_2 z}\left(1 - \frac{m_2}{B}\right) + \frac{A}{B} + \frac{R}{S} \qquad \text{(IV-11)}$$

where: $m_1 = \frac{-P}{2} + \sqrt{\frac{P^2}{4} - S}$

$m_2 = \frac{-P}{2} - \sqrt{\frac{P^2}{4} - S}$

$C_1 = \frac{m_2\left(T_0 - \frac{R}{S}\right) - A}{m_2 - m_1}$

$C_2 = \frac{-m_1\left(T_0 - \frac{R}{S}\right) + A}{m_2 - m_1}$

T_0 = inlet temperature (z = 0) of both streams, °K.

When L, the cable length, is substituted into Equations IV-10 and IV-11 these equations give the exit temperatures of the two streams. If it is desirable to proceed in the reverse direction (i.e., specify the exit temperatures and compute the cable length), it is necessary to solve these relations by trial and error for the appropriate L. Newton's trial and error scheme has been used in the computations for this report.

Although it has not been mentioned, the pressure drop is also specified in these calculations. It appears in the expression for the mass flow rate, W, which is derived below.

MASS FLOW RATE AND DISTRIBUTION

The pressure drop in the bore flow is given by:

$$\Delta P_B = \frac{\rho V^2_B}{2} \left(\frac{L}{D_B}\right) f_B, \text{ dynes/cm}^2 \qquad \text{(IV-12)}$$

where: ρ = mass density of coolant, g/cm^3.

V_B = velocity of coolant in bore, cm/s.

L = length of cable, cm.

D_B = hydraulic diameter of bore = $4A_B/P_B$, cm.

f_B = hydraulic friction factor in bore.

A_B = area of bore flow = $3\pi r_1^2$, cm^2.

P_I = perimeter of bore flow = $6\pi r_1$, cm.

All dimensions refer to Figures IV-2 and IV-3.

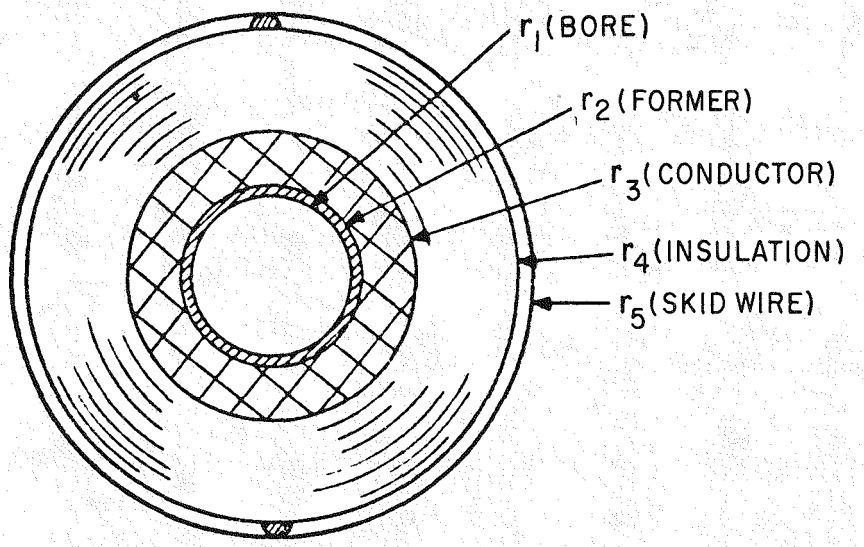

Figure IV-2. Cable Section

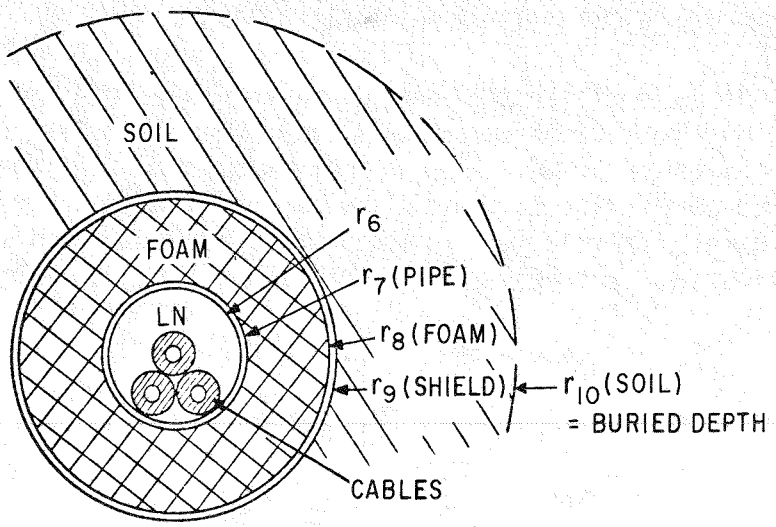

Figure IV-3. Cable Envelope Section

Similarly, for the interstitial flow:

$$\Delta P_I = \rho \frac{V_I^2}{2} \frac{L}{D_I} f_I, \text{ dynes/cm}^2 \qquad \text{(IV-13)}$$

where: $D_I = 4A_I/P_I$ = hydraulic diameter of interstitial space, cm.

f_I = hydraulic friction factor.

$A_I = \pi(r_6^2 - 3r_5^2)$, cm^2

$P_I = 2\pi(r_6 + 3r_5)$, cm

If the two pressure drops are set equal to ΔP, then Equations IV-12 and IV-13 can be solved for the flow rate, noting that:

$$V_I = \frac{(1 - X)W}{A_I \rho} \qquad \text{(IV-14)}$$

and, by continuity:

$$V_B = \frac{XW}{A_B \rho} \qquad \text{(IV-15)}$$

Thus:

$$W = \frac{\Delta P}{f_B} \frac{2\rho}{X^2} \left(\frac{D_B}{L}\right) A^2_B, \text{ g/s} \qquad \text{(IV-16)}$$

and the flow split is given by:

$$X = \left[1 + \frac{f_B}{f_I} \cdot \frac{D_I}{D_B} \cdot \left(\frac{A_I}{A_B}\right)\right]^{-1} \qquad \text{(IV-17)}$$

HEAT EXCHANGE THROUGH ELECTRICAL INSULATION

Distribution of the dielectric and resistive losses (Q_D and Q_R) between the interstitial and bore fluid streams (Q_I and Q_B) is controlled by heat conduction in the electrical insulation. If a one-dimensional radial model is used to describe conduction in the dielectric material and the dielectric losses are uniformly distributed throughout the volume of this material, then the following equations give the distribution of the heat load:

$$Q_B = \alpha + \beta \cdot (T_B - T_I) \qquad \text{(IV-18)}$$

$$Q_I = \gamma + \delta\,(T_B - T_I) \qquad \text{(IV-19)}$$

where: $\alpha = Q_R + Q_D \left[\dfrac{1}{2 \ln (r_4/r_3)} - \dfrac{r^2_3}{r^2_4 - r^2_3}\right]$, W/cm.

$\beta = \dfrac{-2\pi K_D}{\ln (r_4/r_3)}$, W/cm/°K

$\gamma = -Q_D \left[\dfrac{1}{2 \ln (r_4/r_3)} - \dfrac{r^2_4}{r^2_4 - r^2_3}\right]$, W/cm.

$\delta = -\beta$, W/cm/°K.

Q_R = resistive losses per unit length of cable, W/cm.

Q_D = dielectric losses per unit length of cable, W/cm.

K_D = thermal conductivity of dielectric material, W/cm/°K.

HEAT LEAK THROUGH FOAM ENVELOPE

If a one-dimensional radial model is used to describe heat conduction in the foam and the soil and the soil is presumed to surround the envelope in a cylinder that has a fixed temperature, T_E, at radius r_{10}, then the heat leak is given by:

$$Q_F = \xi + \varphi\, T_I \qquad \text{(IV-20)}$$

where: $\xi = \dfrac{\epsilon}{\epsilon + \sigma}\ [Q_S + \sigma T_E]$, W/cm.

$\varphi = \dfrac{-\sigma\epsilon}{\epsilon + \sigma}$, W/cm/°K

Q_S = shield dissipation rate per unit length of cable, W/cm

$\epsilon = \dfrac{2\pi\, K_F}{\ln (r_8/r_7)}$, W/cm°K.

$$\sigma = \frac{2\pi K_E}{\ln (r_{10} r_9)}, \text{ W/cm/°K}$$

K_F = mean thermal conductivity of foam between 300 K and 77 K, W/cm/°K.

K_E = thermal conductivity of soil, W/cm/°K.

T_E = soil temperature at radius r_{10}, °K.

Appendix V

SYSTEM COOLDOWN ANALYSIS

The objective of this analysis was to obtain a first order approximation of the cooling of a 3500-MVA cryogenic cable system based upon use of an FRP pressure pipe 8.4 miles in length. The information sought was to determine:

- Whether the cable and the pressure pipe can be cooled from 300 to 77 K without having to provide intermediate vents along the pressure pipe.
- Approximate time required for cooldown.

PROPERTIES OF THE SYSTEM

CABLE AND LINE PROPERTIES

Pressure pipe length: L = 8.4 miles ≅ 44,000 feet
Initial state: 300 K = 540 R; 20 Atmospheres = 294 psi
Fluid friction factor: 0.06 (Darcy)
D_h: hydraulic diameter = 5.2 inches = 0.44 feet
A: flow area = 132 square inches = 0.92 square feet
Cable: aluminum conductor 14.6 lbs/ft
cellulose insulation 15.2 lbs/ft
FRP pipe: 21 lbs/ft

PROPERTIES OF THE FLOW

$M_1 = 0.0109$
$M_2 = 0.217$
$T_2 = 535$ R = 297 K
$c_1 = 1160$ ft/s
$c_2 = 1150$ ft/s
$V_1 = 12.6$ ft/s
$V_2 = 250$ ft/s
$\dot{m} = 16.5$ lbs/s

If it is assumed the flow is frictionally choked and adiabatic from an initial state at 300 K, the initial Mach number, M, is given by

$$4f\frac{L}{D} = \frac{1-M^2}{kM^2} + \frac{k+1}{2k}\ln\left(\frac{(k+1)M^2}{2\left(1+\frac{k-1}{2}M^2\right)}\right) \qquad \text{(V-1)}$$

for: $k = 1.4,\ 4f\,(L/D) = 6000$

$$8401 = \frac{1}{M^2} + 1.2 \ln \left(\frac{1.2M^2}{1+0.2M^2} \right) \qquad \text{(V-2)}$$

$$M = 0.0109 \qquad \text{(V-3)}$$

To achieve a Mach number of 1.0, the exit pressure, P', at the vent becomes:

$$P' = M \sqrt{\frac{2\left(1+\frac{k-1}{2}m^2\right)}{k+1}}\, P \qquad \text{(V-4)}$$

for: $M = 0.0109$; $P = 20$ atmospheres

$$P' = 0.199 \text{ atmosphere} \qquad \text{(V-5)}$$

Since the pressure pipe will be vented to atmospheric pressure, the flow will not be frictionally choked.

Integration of Equation V-1 between flow inlet state 1 and exit state 2 yields:

$$\frac{4fL}{D} = \frac{1}{k}\left(\frac{1}{M_1^2} - \frac{1}{M_2^2} + \frac{k+1}{2} \ln \left(\frac{\left(1+\frac{k-1}{2}M_2^2\right)}{\left(1+\frac{k-1}{2}M_1^2\right)} \frac{M_1^2}{M_2^2} \right) \right) \qquad \text{(V-6)}$$

for: $4f\,(L/D) = 6000$, $k = 1.4$

$$8400 = \frac{1}{M_1^2} - \frac{1}{M_2^2} + 1.2 \ln \left(\left(\frac{1+0.2M_2^2}{1+0.2M_1^2} \right) \left(\frac{M_1}{M_2} \right)^2 \right) \qquad \text{(V-7)}$$

Assume flow continues past states 1 and 2 to the sonic condition. Equation V-4 holds between either state 1 or state 2 and the sonic condition.

Therefore:

$$\frac{P_2}{P_1} = \sqrt{\frac{1+0.2M_1^2}{1+0.2M_2^2}}\, \frac{M_1}{M_2} \qquad \text{(V-8)}$$

Iterative solution of Equations V-7 and V-8 for $(P_2/P_1) = 20$ gives

$$M_1 = 0.0109$$

$$M_2 = 0.217$$

Flow resistance of the line ($\Delta P/\dot{m}$) will be a decreasing function of time, as average temperature decreases, average density increases, and average flow velocity for a given $\dot{m}$ decreases. This will make it possible to maintain or increase this flow rate through the transient.

FLOW PROPAGATION VELOCITY

To compute the propagation velocity, simple one-dimensional models will be used.

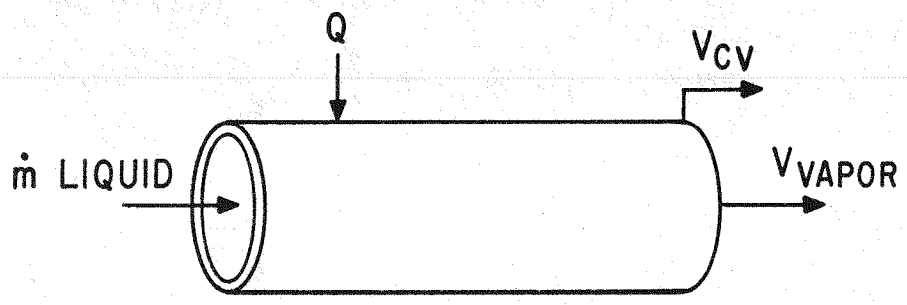

Consider a control volume encompassing a portion of the line extending from the inlet to a point in the warm vapor just ahead of the advancing cold front. The energy equation for this control volume yields:

$$Q - \frac{dE}{dt} = \rho_v A(V_v - V_{cv})h_v - \dot{m}_l h_l - \frac{H_p}{L} V_{cv} \qquad (V\text{-}9)$$

where H_p is evaluated at the warm condition.

It is presumed that the temperature front propagates without changing shape and the region behind this front has constant properties at liquid temperature.

$$\frac{dE}{dt} = \left(\rho_l A \; V_l + \frac{E_p}{L}\right) V_{cv} \qquad (V\text{-}10)$$

for E_p at cold conditions.

An estimate of Q can now be made by presuming that the temperature front is of rather limited length and neglecting the heat transfer along this length with respect to heat transfer to the much larger isothermal region behind the front. The length of the isothermal section is approximately:

$$L = \int_0^t V_{cv}\, dt \qquad (V\text{-}11)$$

If q is the steady-state heat transfer per unit length, then:

$$Q = q\left[\int_0^t V_{cv}\, dt\right] \qquad \text{(V-12)}$$

With these assumptions, the rate of accumulation of mass in the control volume is simply the liquid density times the rate of change of the volume. So from continuity:

$$\dot{m}_l = A\left(\rho_v V_v + (\rho_l - \rho_v) V_{cv}\right) \qquad \text{(V-13)}$$

Substituting and rearranging Equations V-10 through V-13 yield:

$$q\left[\int_0^t V_{cv}\, dt\right] + A(\rho_v(h_v - h_l) + \rho_l (h_l - v_l)) + \left(\frac{h_p - E_p}{L}\right) V_{cv} = \dot{m}_v(h_v - h_l) \qquad \text{(V-14)}$$

At t=o, the integral on the left is zero, and the initial velocity of propagation of the temperature front, V_{cvo}, becomes:

$$V_{cvo} = \frac{V_v}{\left(1 + \frac{\rho_l}{\rho_v (h_v - h_l)} + \frac{\Sigma \rho_p (h_p - e_p)}{\rho_v (h_v - h_l)} \frac{A_p}{A}\right)} \qquad \text{(V-15)}$$

From Equation V-14, the time constant of the system is:

$$\tau = \frac{A(\rho_v(h_v - h_l) + p_l) + \Sigma A_p \rho_p (h_p - e_p)}{q} \qquad \text{(V-16)}$$

The velocity of propagation, given constant V_v, is:

$$V_{cv} = V_{cvo}\, e^{-t/\tau} \qquad \text{(V-17)}$$

To approximate $\Sigma A_p \rho_p h_p$ (300 K) - e_p (77 K)):

1. Ignore the difference between h_p and e_p: $e_p \cong h_p$.
2. Evaluate $\Sigma A_p \rho_p h_p$ (300 K) using available data for this.
3. Determine the enthalpy ratio for aluminum h_{Al} (77 K)/h_{Al} (300 K) by Debye law using θ_d = 390 K.
4. Assume other enthalpies scales like h_{Al}.

$$\Sigma A_p \rho_p (h_p(300\,K) - e_p(77K)) \cong \left(1 - \frac{h_{Al}(77\,K)}{h_{Al}(300\,K)}\right) \Sigma A_p \rho_p h_p (300\,K) \qquad \text{(V-18)}$$

$$V_{cvo} = \frac{12.6 \text{ ft/s}}{\left(1 + \frac{4.26 \times 10^6 \text{ J/ft}}{2.5 \times 10^5 \text{ J/ft}}\right)} = 0.7 \text{ ft/s} = 0.48 \text{ mph} \qquad \text{(V-19)}$$

From equation IV-13:

$$\dot{m}_l = 16.5 \text{ lbs/s} + 44.2 \frac{\text{lbs}}{\text{ft}} \quad V_{cv}$$

$$= (16.5 + 31\, e^{-t/\tau_o}) \text{ lbs/s} \qquad \text{(V-20)}$$

$$\dot{m}_l (t=o) = 47 \text{ lbs/s}$$

Equation V-20 shows $\dot{m}_l$ to be a decreasing function of time. This arises because $\dot{m}_v$ was selected to be a constant. With constant pumping power, it should be possible to maintain $\dot{m}_l$ constant at the initial value. Of course, this assumption gives the same initial velocity, V_{cvo}, with a time constant for decay of the propagation changed to:

$$\tau = \frac{A\rho_l(h_v - V_l) + \Sigma A_p \rho_p (h_p - e_p)}{q} \qquad \text{(V-21)}$$

$$\tau = 166 \text{ hours} \qquad \text{(V-22)}$$

From Equation V-17, the time to cool a length L is give by

$$t = -\tau \ln\left(1 - \frac{L}{V_{cvo}\tau}\right) \qquad \text{(V-23)}$$

For the time constant of Equation V-22, the cooldown time given by Equation V-23 is

$$t = 18.5 \text{ hours}$$

The quantity of liquid nitrogen required for cooldown:

$$M = \int_o^t \dot{m}_l \, dt$$

$$\cong 3.2 \times 10^6 \text{ lbs}$$

The total time for cooldown depends on details of the process which are much more complicated than a simple first order equation. More detailed pressure drop calculations could be introduced without dropping the simple "temperature front" notion, permitting treatment of mass flow as a dependent variable determined by the state of the line and by the applied ΔP. Such a solution would indicate a shorter cooldown time.

Appendix VI

THERMAL TRANSIENT ANALYSIS OF CABLE SYSTEM UNDER OVERLOAD CONDITIONS

The objective of this analysis is to determine the thermal response of the cable to changes in internal heat generation caused by changes in power levels being transmitted by the cable. A one-dimensional model used for this analysis is shown in Figure VI-1. The results from this analysis are to be added to those obtained from the steady-state analysis described in Appendix IV of this report.

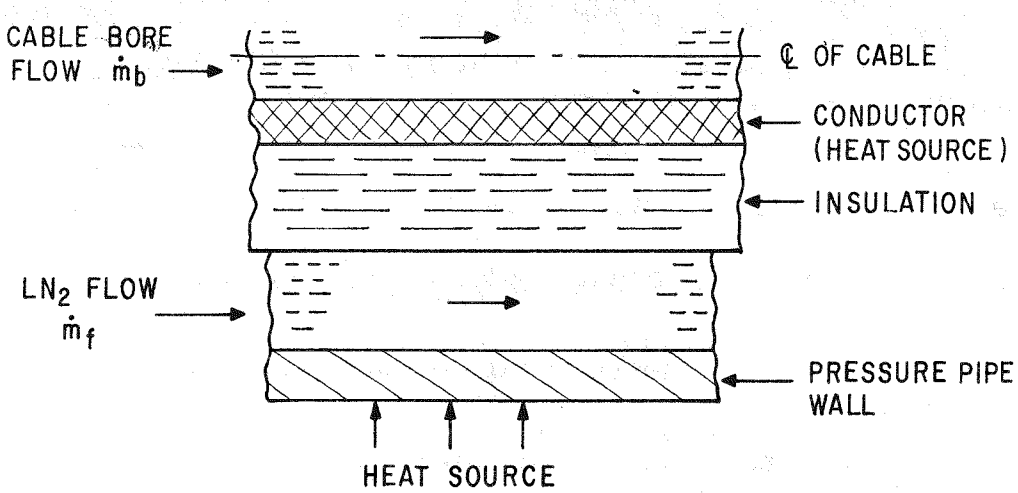

Figure VI-1. One-dimensional Model of Cable and Liquid Nitrogen Flow Streams

The following assumptions have been used in this analysis:

- The conductor is assumed to be in thermal equilibrium with fluid "b", flowing in the cable bore.
- The pipe wall is in thermal equilibrium with fluid "f" flowing on the outside of the cable.
- The electrical insulation can be represented by assigning part of its heat capacity to the material at temperature T_b and the remainder to the material at temperature T_f. These two thermal capacitances are separated by a thermal conductance, U, per unit length.

These assumptions allow the heat generated per unit volume to be replaced by heat per unit length.

The differential equations of the system then become:

$$\dot{q} - U(\Delta T_b - \Delta T_f) = h_b \frac{\partial \Delta T_b}{\partial X} + e_b \frac{\partial \Delta T_b}{\partial t} \qquad \text{(VI-1)}$$

$$U(\Delta T_b - \Delta T_f) = h_f \frac{\partial \Delta T_f}{\partial X} + e_f \frac{\partial \Delta T_f}{\partial t} \qquad \text{(VI-2)}$$

for: $\dot{q} = (x, t)$ = increment of heat generation per unit length.

e_b = change in thermal energy in material at temperature T_b per unit, ΔT.

e_f = change in thermal energy in material at temperature T_a per unit, ΔT.

$\dot{h}_b = \dot{m}_b C_{pb}$.

$\dot{h}_f = \dot{m}_f C_{pf}$.

U = thermal conductance per unit length $q_{ba} = U(T_b - T_a)$.

ΔT_b and ΔT_f are measured from the values at t=0 and appropriate X.

Because the liquid nitrogen flow through the cable bore does not contribute significantly to the steady-state cooling of the cable, its flow will be neglected.

The equations below are normalized by defining terms as follows:

$c = \frac{h_f}{e_f}$ = characteristic velocity for second equation.

$\tau_f = \frac{L}{c}$ = time for temperature transient to traverse the pipe.

$\tau_b = \frac{U}{e_b}$ = thermal time constant for bore material.

$x = \frac{X}{L} \frac{\tau_f}{\tau_b} = \frac{X}{c\tau_b}$ = dimensionless length.

We can redefine dependent variables to be

$$\Delta T_f \text{ and } \Delta T_{bf} = \Delta T_b - \Delta T_f .$$

The equations then are:

$$\frac{\partial \Delta T_{bf}}{\partial t} + \tau_b \Delta T_{bf} = \frac{\dot{q}}{e_b} - \frac{\partial \Delta T_f}{\partial t} \qquad \text{(VI-3)}$$

$$\frac{\partial \Delta T_f}{\partial t} + c \frac{\partial \Delta T_f}{\partial x} = \frac{U}{e_f} \Delta T_{bf} \qquad \text{(VI-4)}$$

Defining terms:

$\Delta\theta = \frac{\Delta T}{\Delta T_b}$ (dimensionless temperature)

$\tau = \frac{t}{\tau_b}$ (dimensionless time)

$$\Delta\theta_{bf_o} = \frac{\dot{q}\,\frac{\tau_b}{e_b}}{\Delta T_o}$$

$$R = e_b/e_f$$

reduces Equations VI-3 and VI-4 to:

$$\frac{\partial \Delta\theta_{bf}}{\partial \tau} + \Delta\theta_{bf} = \frac{1}{x_{max}R+1} - \frac{\partial \Delta\theta_f}{\partial \tau} \qquad \text{(VI-5)}$$

$$\frac{\partial \Delta\theta_f}{\partial \tau} + \frac{\partial \Delta\theta_f}{\partial x} = R\ \Delta\theta_{bf} \qquad \text{(VI-6)}$$

If the last term in Equation VI-5 is neglected, Equation VI-5 can be solved independently of Equation VI-6, which in turn simplifies solution of Equation VI-6.

The initial conditions of the system are

$$\Delta\theta_{bf} = \Delta\theta_f = 0 \text{ at } \tau = 0 \qquad \text{(VI-7)}$$

The boundary condition is

$$\Delta\theta_f = 0 \text{ at } x = 0 \qquad \text{(VI-8)}$$

The solution to Equation VI-5 under these conditions is

$$\Delta\theta_{bf} = \frac{1}{x_{max}R+1}(1-e^{-\tau}) \qquad \text{(VI-9)}$$

The complete solution to Equation VI-6 is

$$\Delta\theta_f = \frac{R}{x_{max}R+1}\ (x+e^{-\tau}(1-e^{x})) \quad , \text{ for } x < \tau \qquad \text{(VI-10)}$$

$$\Delta\theta_f = \frac{R}{x_{max}R+1}\ (\tau+e^{-\tau}-1) \quad , \text{ for } x > \tau \qquad \text{(VI-11)}$$

From this the magnitude of the neglected term can be computed.

$$\frac{\partial \Delta\theta_f}{\partial \tau} = \frac{R}{x_{max}R+1} + e^{-\tau}(e^{x}-1) \quad , \text{ for } x < \tau \qquad \text{(VI-12)}$$

$$\frac{\partial \Delta\theta_f}{\partial \tau} = \frac{R}{x_{max}R+1}\ 1-e^{-\tau} \quad , \text{ for } x > \tau \qquad \text{(VI-13)}$$

For $x<\tau$, the maximum occurs at $x = \tau$, and that maximum is always the same as the value for $x>\tau$, so

$$\left(\frac{\partial \Delta\theta_f}{\partial \tau}\right)_{max} = \frac{R}{x_{max}^{R+1}} (1-e^{-\tau})$$

We see that the approximation reduces to the assumption

$$R(1-e^{-\tau}) << 1$$

Numerically $R = 0.028$ for the system in question, so the approximate solution is quite satisfactory in this case.

The results plotted in Figure 8-20 represent the following values:

$R = 0.028$

$\tau_b = 1.16$ hours

$\tau_f = 8.73$ hours

$c = 1.4$ ft/s

$x = x_{max} = 7.5$

The hottest spot in the cable is always the bore at x_{max}. Because the pressure is also lowest at this point, this is the location of the lowest subcooling margin. Therefore, the bore temperature of x_{max} is the value which will first reach its limit during transient overload conditions.

The above analysis may be used to predict the maximum time for which a transient overload may be applied without causing the bore temperature at x_{max} to exceed its design value.

Suppose that the condition $\Delta\theta_b = 1$ at $x = x_{max}$ and $\tau = \infty$ corresponds to rated conditions. If the conductor heating is a fraction, Q, of the rated value, the corresponding steady-state temperature at x_{max} is $\Delta\theta_b = Q$, leaving a temperature margin $1 - \Delta\theta_b = 1 - Q$ for transient overloads. If the conductor heating during the overload interval is an amount Q_o, the maximum permissible overload time is that time for which

$$(Q_o - Q)\,\Delta\theta_b(x_{max}, \tau) = 1 - Q \qquad \text{(VI-14)}$$

Figure 8-21 is a representation of the solution to Equation VI-14. The basic square-law dependence of conductor heating on line loading is accounted for in the derivation of Figure 8-21.

NOMENCLATURE

A = cross-section area

D_h = hydraulic diameter

E = internal energy

H_p = enthalpy of solid material of cable

L = length

M = Mach number, also total mass of refrigerant

Θ_d = Debye temperature

P = pressure

Q = heat transfer

T = temperature

V = velocity

c = sonic velocity

f = friction factor

h = specific enthalpy

k = specific heat ratio c_p/c_v

$\dot{m}$ = mass flow rate

q = heat transfer per unit length

t = time

ρ = density

τ = time constant

Subscripts

Al = aluminum

cv = control volume

l = liquid

p = solid components of cable system

v = vapor

Appendix VII

COST SUMMARY SHEETS

This appendix contains a summary of component, installation, and power charge costs associated with each cable system concept studied. All costs are given for the specific module distance computed to be the maximum possible distance within the design restraints. Further information relating to the component costs is provided under "Cable System Cost Estimates" on page 8-42 of this report. Installation costs were obtained for FRP piping concepts from Reference 8-4.

COST SUMMARY SHEET

Concept: 2000 MVA; 345 kV

Solid Cable; 12.5 Miles (Module length)

Components	Total Cost for Three-phase Module Length (Dollars in Millions)
Cable, $/three-phase ft 231.75	15.30
Pressure pipe, $/ft 76.00	5.02
Material FRP	
Inside diameter, inches 16.2	
Return pipe, $/ft 21.00	1.39
Material FRP	
Inside diameter, inches 8.2	
Foam thermal insulation and vapor jacket	
Pressure pipe, $/ft 41.00	2.71
Return pipe, $/ft 27.50	1.82
Terminal, 10^6/three-phase 0.11	0.22
Number of Terminals 2	
Refrigerator 17,138 Input KW	5.95
Expansion Joints, Fittings, and Miscellaneous, $/ft 50.00	3.30
Installation, 10^6/mile (Suburban) 2.06	25.75
Power Charge: 17,138 total losses (kW) @$1000.00/kW	17.14

COST SUMMARY SHEET

Concept: 2000 MVA; 500 kV

Solid Cable; 13.2 Miles (Module length)

Components	Total Cost for Three-phase Module Length (Dollars in Millions)
Cable, $/three-phase ft 268.20	18.69
Pressure pipe, $/ft 76.00	5.30
Material FRP	
Inside diameter, inches 16.2	
Return pipe, $/ft 21.00	1.46
Material FRP	
Inside diameter, inches 8.25	
Foam thermal insulation and vapor jacket	
Pressure pipe, $/ft 41.00	2.86
Return pipe, $/ft 27.50	1.92
Terminal, 10^6/three-phase 0.143	0.29
Number of Terminals 2	
Refrigerator 17,450 Input KW	6.05
Expansion Joints, Fittings, and Miscellaneous, $/ft 50.00	3.48
Installation, 10^6/mile (Suburban) 2.06	27.19
Power Charge: 17,690 total losses (kW) @$1000.00/kW	17.69

COST SUMMARY SHEET

Concept: 3500 MVA; 500 kV

Solid Cable; 9.5 Miles (Module length)

Components		Total Cost for Three-phase Module Length (Dollars in Millions)
Cable, $/three-phase ft	242.10	12.14
Pressure pipe, $/ft	76.00	3.81
Material	FRP	
Inside diameter, inches	16.2	
Return pipe, $/ft	21.50	1.08
Material	FRP	
Inside diameter, inches	8.5	
Foam thermal insulation and vapor jacket		
Pressure pipe, $/ft	41.00	2.06
Return pipe, $/ft	29.00	1.45
Terminal, 10^6/three-phase	0.143	0.29
Number of Terminals	2	
Refrigerator	16,470 Input KW	5.75
Expansion Joints, Fittings, and Miscellaneous, $/ft	50.00	2.51
Installation, 10^6/mile (Suburban)	2.06	19.57
Power Charge:	17,000 total losses (kW) @$1000.00/kW	17.00

COST SUMMARY SHEET

Concept: 5000 MVA; 500 kV

Solid Cable; 6.3 Miles (Module length)

Components		Total Cost for Three-phase Module Length (Dollars in Millions)
Cable, $/three-phase ft	258.90	8.61
Pressure pipe, $/ft	76.00	2.53
Material	FRP	
Inside diameter, inches	16.2	
Return pipe, $/ft	20.50	0.68
Material	FRP	
Inside diameter, inches	8.1	
Foam thermal insulation and vapor jacket		
Pressure pipe, $/ft	41.00	1.36
Return pipe, $/ft	27.00	0.90
Terminal, 10^6/three-phase	0.143	0.29
Number of Terminals	2	
Refrigerator	14,590 Input KW	5.15
Expansion Joints, Fittings, and Miscellaneous, $/ft	50.00	1.66
Installation, 10^6/mile (Suburban)	2.06	12.98
Power Charge:	15,300 total losses (kW) @$1000.00/kW	15.30

COST SUMMARY SHEET

Concept: 2000 MVA; 500 kV

Hollow Cable; 10.6 Miles (Module length)

Components	Total Cost for Three-phase Module Length (Dollars in Millions)
Cable, $/three-phase ft 210.75	11.80
Pressure pipe, $/ft 76.00	4.25
Material FRP	
Inside diameter, inches 16.2	
Return pipe, $/ft 22.00	1.23
Material FRP	
Inside diameter, inches 8.6	
Foam thermal insulation and vapor jacket	
Pressure pipe, $/ft 41.00	2.29
Return pipe, $/ft 28.00	1.57
Terminal, 10^6/three-phase 0.143	0.29
Number of Terminals 2	
Refrigerator 18,420 Input KW	6.20
Expansion Joints, Fittings, and Miscellaneous, $/ft 50.00	2.80
Installation, 10^6/mile (Suburban) 2.06	21.84
Power Charge: 18,600 total losses (kW) @$1000.00/kW	18.60

COST SUMMARY SHEET

Concept: 3500 MVA; 500 kV

Hollow Cable; 6.3 Miles (Module length)

Components	Total Cost for Three-phase Module Length (Dollars in Millions)
Cable, $/three-phase ft 210.00	6.99
Pressure pipe, $/ft 100.00	3.33
Material Metal	
Inside diameter, inches 16.2	
Return pipe, $/ft 12.50	0.42
Material Metal	
Inside diameter, inches	
Foam thermal insulation and vapor jacket	
Pressure pipe, $/ft 41.00	1.36
Return pipe, $/ft 27.50	0.91
Terminal, 10^6/three-phase 0.143	0.29
Number of Terminals 2	
Refrigerator 17,780 Input KW	6.20
Expansion Joints, Fittings, and Miscellaneous, $/ft 50.00	1.66
Installation, 10^6/mile (Suburban) 2.06	12.98
Power Charge: 17,780 total losses (kW) @$1000.00/kW	17.78

COST SUMMARY SHEET

Concept: 3500 MVA; 500 kV

Hollow Cable; 7.5 Miles (Module length)

Components		Total Cost for Three-phase Module Length (Dollars in Millions)
Cable, $/three-phase ft	210.00	8.31
Pressure pipe, $/ft	76.00	3.01
Material	FRP	
Inside diameter, inches	16.2	
Return pipe, $/ft	21.50	0.85
Material	FRP	
Inside diameter, inches	8.5	
Foam thermal insulation and vapor jacket		
Pressure pipe, $/ft	41.00	1.62
Return pipe, $/ft	29.00	1.15
Terminal, 10^6/three-phase	0.143	0.29
Number of Terminals	2	
Refrigerator	16,490 Input KW	5.60
Expansion Joints, Fittings, and Miscellaneous, $/ft	50.00	1.98
Installation, 10^6/mile (Suburban)	2.06	15.50
Power Charge:	16,900 total losses (kW) @$1000.00/kW	16.90

COST SUMMARY SHEET

Concept: 5000 MVA; 500 kV

Hollow Cable; 4.9 Miles (Module length)

Components		Total Cost for Three-phase Module Length (Dollars in Millions)
Cable, $/three-phase ft	229.50	5.94
Pressure pipe, $/ft	76.00	1.97
Material	FRP	
Inside diameter, inches	16.2	
Return pipe, $/ft	21.50	0.56
Material	FRP	
Inside diameter, inches	8.3	
Foam thermal insulation and vapor jacket		
Pressure pipe, $/ft	41.00	1.06
Return pipe, $/ft	28.50	0.74
Terminal, 10^6/three-phase	0.143	0.29
Number of Terminals	2	
Refrigerator	13,570 Input KW	4.80
Expansion Joints, Fittings, and Miscellaneous, $/ft	50.00	1.29
Installation, 10^6/mile (Suburban)	2.06	10.09
Power Charge:	14,120 total losses (kW) @$1000.00/kW	14.12

COST SUMMARY SHEET

Concept: 3500 MVA; 500 kV

Hollow (Evacuated Multilayer Insulated) Cable; 6.3 Miles (Module length)

Components	Total Cost for Three-phase Module Length (Dollars in Millions)
Cable, $/three-phase ft 210.00	6.99
Pressure pipe, $/ft (1) 200.00	6.65
Material Metallic	
Inside diameter, inches 16.2	
Return pipe, $/ft 60.00 (2)	2.00
Material Metal	
Inside diameter, inches 8.3	
Foam thermal insulation and vapor jacket	
Pressure pipe, $/ft Not used	---
Return pipe, $/ft Not used	---
Terminal, 10^6/three-phase 0.143	0.29
Number of Terminals 2	
Refrigerator 12, 982 Input KW	4.90
Expansion Joints, (3) Fittings and Miscellaneous, $/ft 30.00	1.00
Installation, 10^6/mile (Suburban) (4) 1.3 x 2.06	16.87
Power Charge: 12,980 total losses (kW) @$1000.00/kW	12.98

1) Estimates from two vendors ranged from $190/ft to $230/ft for superinsulated metallic piping. No aluminum liner was included.

2) Same cost ratio applied as for 16 inch pipe.

3) Piping contains an inner and outer expansion joint.

4) Increased 30 percent over FRP piping.

Appendix VIII

20—MILE SYSTEM COST ESTIMATE SHEETS

Cost estimates were prepared for a transmission distance of 20 miles. The average cost on a per mile basis obtained for components for the module distances were used to extend the transmission distances to 20 miles. Cost summary sheets contained in this appendix provide estimates for the total system cost per mile as well as for an MVA mile.

20-MILE SYSTEM COST ESTIMATE SHEET

Concept: 2000 MVA; 345 kV

Solid Cable; FRP Piping

	Dollars in Millions
Cable	24.48
Piping, Expansion Joints, and Miscellaneous	15.54
Foam Thermal Insulation for Cable Piping and Return Piping	7.25
Refrigerator and Liquid Nitrogen Repressurization Pumps	9.68
Terminals	0.22
Installation	41.20
Power Charge	27.42
Total Cost of Installed System for 20 Miles	125.8
Cost Per Mile	6.30

Actual Dollars/MVA-Mile 3,147

20-MILE SYSTEM COST ESTIMATE SHEET

Concept: 2000 MVA; 500 kV

Solid Cable; FRP Piping

	Dollars in Millions
Cable	28.32
Piping, Expansion Joints, and Miscellaneous	15.52
Foam Thermal Insulation for Cable Piping and Return Piping	7.24
Refrigerator and Liquid Nitrogen Repressurization Pumps	9.32
Terminals	0.29
Installation	41.20
Power Charge	26.80
Total Cost of Installed System for 20 Miles	128.69
Cost Per Mile	6.43

Actual Dollars/MVA-Mile 3,217

20-MILE SYSTEM COST ESTIMATE SHEET

Concept: 3500 MVA; 500 kV

Solid Cable; FRP Piping

	Dollars in Millions
Cable	25.56
Piping, Expansion Joints, and Miscellaneous	15.58
Foam Thermal Insulation for Cable Piping and Return Piping	7.39
Refrigerator and Liquid Nitrogen Repressurization Pumps	12.32
Terminals	0.29
Installation	41.20
Power Charge	35.79
Total Cost of Installed System for 20 Miles	138.13
Cost Per Mile	6.91

Actual Dollars/MVA-Mile 1,973

20-MILE SYSTEM COST ESTIMATE SHEET

Concept: 5000 MVA; 500 kV

Solid Cable; FRP Piping

	Dollars in Millions
Cable	27.33
Piping, Expansion Joints, and Miscellaneous	15.46
Foam Thermal Insulation for Cable Piping and Return Piping	7.17
Refrigerator and Liquid Nitrogen Repressurization Pumps	16.67
Terminals	0.29
Installation	41.20
Power Charge	48.57
Total Cost of Installed System for 20 Miles	156.69
Cost Per Mile	7.84

Actual Dollars/MVA-Mile 1,567

20-MILE SYSTEM COST ESTIMATE SHEET

Concept: 5000/2000[1] MVA. 500 kV

Solid Cable; FRP Piping

	Dollars in Millions
Cable	27.33
Piping, Expansion Joints, and Miscellaneous	15.46
Foam Thermal Insulation for Cable Piping and Return Piping	7.17
Refrigerator and Liquid Nitrogen Repressurization Pumps	9.32[2]
Terminals	0.29
Installation	41.20
Power Charge	28.90
Total Cost of Installed System for 20 Miles	129.67
Cost Per Mile	6.48

Actual Dollars/MVA-Mile 3,242

1) Capacity transmitted
2) Refrigerator sized for 2000 MVA system

20-MILE SYSTEM COST ESTIMATE SHEET

Concept: 5000/2000[1] MVA; 500 kV

Solid Cable; FRP Piping

	Dollars in Millions
Cable	27.33
Piping, Expansion Joints, and Miscellaneous	15.46
Foam Thermal Insulation for Cable Piping and Return Piping	7.17
Refrigerator and Liquid Nitrogen Repressurization Pumps	16.67[2]
Terminals	0.29
Installation	41.20
Power Charge	28.90
Total Cost of Installed System for 20 Miles	137.02
Cost Per Mile	6.85

Actual Dollars/MVA-Mile 3,426

1) Capacity transmitted
2) Refrigerator sized for 5000 MVA

20-MILE SYSTEM COST ESTIMATE SHEET

Concept: 2000 MVA; 500 kV

Hollow Cable; FRP Piping

	Dollars in Millions
Cable	22.26
Piping, Expansion Joints, and Miscellaneous	15.62
Foam Thermal Insulation for Cable Piping and Return Piping	7.28
Refrigerator and Liquid Nitrogen Repressurization Pumps	11.89
Terminals	0.55
Installation	41.20
Power Charge	35.09
Total Cost of Installed System for 20 Miles	133.9
Cost Per Mile	6.70

Actual Dollars/MVA-Mile 3,348

20-MILE SYSTEM COST ESTIMATE SHEET

Concept: 3500 MVA; 500 kV

Hollow Cable; FRP Piping

	Dollars in Millions
Cable	22.16
Piping, Expansion Joints, and Miscellaneous	15.57
Foam Thermal Insulation for Cable Piping and Return Piping	7.39
Refrigerator and Liquid Nitrogen Repressurization Pumps	15.20
Terminals	0.77
Installation	41.20
Power Charge	45.07
Total Cost of Installed System for 20 Miles	147.37
Cost Per Mile	7.37

Actual Dollars/MVA-Mile 2,107

20-MILE SYSTEM COST ESTIMATE SHEET

Concept: 5000 MVA; 500 kV

Hollow Cable; FRP Piping

	Dollars in Millions
Cable	24.24
Piping, Expansion Joints, and Miscellaneous	15.59
Foam Thermal Insulation for Cable Piping and Return Piping	7.35
Refrigerator and Liquid Nitrogen Repressurization Pumps	20.0
Terminals	1.18
Installation	41.20
Power Charge	57.63
Total Cost of Installed System for 20 Miles	167.19
Cost Per Mile	8.36

Actual Dollars/MVA-Mile 1,672

20-MILE SYSTEM COST ESTIMATE SHEET

Concept: 3500 MVA; 500 kV

Hollow Cable; Metallic Piping

	Dollars in Millions
Cable	22.16
Piping, Expansion Joints, and Miscellaneous	17.17
Foam Thermal Insulation for Cable Piping and Return Piping	7.21
Refrigerator and Liquid Nitrogen Repressurization Pumps	20.0
Terminals	0.92
Installation	41.20
Power Charge	56.44
Total Cost of Installed System for 20 Miles	165.10
Cost Per Mile	8.26

Actual Dollars/MVA-Mile 2,360

20-MILE SYSTEM COST ESTIMATE SHEET

Concept: 3500 MVA; 500 kV

Hollow Cable; Metallic (Evacuated Multilayer Insulated)

	Dollars in Millions
Cable	22.16
Piping, Expansion Joints, and Miscellaneous	30.63
Foam Thermal Insulation for Cable Piping and Return Piping	0
Refrigerator and Liquid Nitrogen Repressurization Pumps	15.87
Terminals	0.92
Installation	41.20
Power Charge	53.56
Total Cost of Installed System for 20 Miles	164.34
Cost Per Mile	8.22

Actual Dollars/MVA-Mile 2,350

Appendix IX

REFERENCES

4-1 Whitehead, J.B., "The Dielectric Strength and Life of Impregnated-paper Insulation - I," Transactions of the American Institute of Electrical Engineers, Vol. 59, 1940, pp. 715-720.

4-2 Whitehead, J.B., "Radial and Tangential Stresses in Impregnated-paper Insulation," Transactions of the American Institute of Electrical Engineers, Vol. 70, Part I: Communication and Electronics, 1951, pp. 56-63.

4-3 Atkinson, R.W., and DelMar, W.A. "Discussion Contributions on Reference 2," Transactions of the American Institute of Electrical Engineers, Vol. 50, 1940, pp. 1085, 1088-1089.

4-4 Cloke, P., and Khandelwal, K.K., "The Variation at Constant Density of the Dielectric Breakdown of Paper with Air Resistance," Transactions of the American Institute of Electrical Engineers, Vol. 71, Part I: Communication and Electronics, 1952, pp. 309-314.

4-5 Whitehead, J.B., "The Dielectric Strength and Life of Impregnated-paper Insulation - II," Transactions of the American Institute of Electrical Engineers, Vol. 59, 1940, pp. 660-663.

4-6 General Electric Company, Resistive Cryogenic Cable, Phase II, Final Report, Report No. SRD-74-042, Edison Electric Institute Contract No. 14-01-0001-1483, Schenectady, N.Y., April 17, 1974.

4-7 Association of Edison Illuminating Companies, Specifications for Impregnated-paper Insulated Cable -- High Pressure Type, Specification No. AEIC NO2-73, 3rd ed., New York, N.Y., 1973.

8-1 Edison Electric Institute, Underground Systems Reference Book, EEI Publication No. 55-16, New York, N.Y., 1957, p. 3-14.

8-2 Strobridge, T.R., Cryogenic Refrigerators--An Updated Survey, Technical Note TN-655, National Bureau of Standards, Washington, D.C., June, 1974.

8-3 Kadi, F.J., and Longsworth, R.C., Optimization of Helium Refrigerators for Superconducting Power Transmission Lines in Terms of Cost and Reliability, Paper No. 76-WA/PID-16, Americal Society of Mechanical Engineers, New York, N.Y., 1976.

8-4 Gibbs & Hill, Inc., Construction Procedures and Costs for the Installation of a Resistive Cryogenic Cable System, Final Report, Contract No. E (49-18)-2104, U.S. Energy Research and Development Administration and Electric Power Research Institute, June 1976.

III-1. Parisi, J.P., Thermal Conductivity of Liquid Nitrogen Impregnated Electrical Insulation, Master of Science Thesis, Department of Mechanical Engineering, Massachusetts Institute of Technology, September 1974.

III-2. Norris, R.H., Thermal Conductivity of Solid Dielectric Materials at Cryogenic Materials -- A Review of the Values, Scope, and Limitations of Available Data, work performed under EEI Project RP 78-6, private communication from A. Rios.

III-3. Jakob, M., "Measurement of the Equivalent Thermal Conductivity of Packed Particles in Fluid at Rest," Heat Transfer, Vol. II, John Wiley & Sons, New York, N.Y., 1957.

III-4. McAdams, W.M., "Conductivity of Stagnant Packed Beds," Heat Transmission, McGraw-Hill, New York, N.Y., 1954, p. 290.

III-5. Jakob, M., "Cylindric Arrangements for Thermal-conductivity Tests" (Section 9-2) and "Determination of the Thermal Conductivity of an Insulating Material in Hollow-cylinder Form, Considering the Axial Heat Loss in the Cylindric Heating Element" (Section 12-3), Heat Transfer, Vol. 1, John Wiley & Sons, New York, N.Y., 1949, pp. 149-151 and 246-250.

III-6. Ashworth, T., and Loomer, J.E., "Thermal Conductivity of Nylons and Apiezon Greases," Advances in Cryogenic Engineering, Vol. 18, 1973, pp. 271-279.

III-7. Omega Engineering, Inc., The Omega Temperature Measurement Handbook, Stamford, Conn., 1974.

III-8. Johnson, V.J., Compendium of the Properties of Materials at Low Temperatures, Phase 1, Part 1: Properties of Fluids, National Technical Information Service, U.S. Department of Commerce, 1960.

Appendix X

BIBLIOGRAPHY

SECTION 3

FRP MATERIALS

Ashton, J.E., Halpin, J.C., and Petit, P.H., Primer on Composite Materials: Analysis, Technomic Publishing Company, Stanford, Conn., 1969.

Garg, S.K., Svalbonas, V., and Gurtman, G.A., Analysis of Structural Composite Materials, M. Dekker, Inc., New York, N.Y., 1973.

Hahn, H.T., and Pagano, H.J., "Curing Stresses in Composite Laminates," Composite Materials, Vol. 9, January 1975, p. 91.

Hanson, M.P., Static and Dynamic Fatigue Behavior of Glass Filament-wound Pressure Vessels at Ambient and Cryogenic Temperatures, paper presented at 1970 Cryogenic Engineering Conference, Boulder, Colo., June 1970.

Kasen, M.B., "Mechanical and Thermal Properties of Filamentary Reinforced Structural Composites at Cryogenic Temperatures," Cryogenics, Vol. 15, June 1975.

National Aeronautics and Space Administration, Isometric Scan Method for Ultrasonic Evaluation of Composite Panels, NASA Technical Brief B75-10014, Washington, D.C., 1975.

Nielsen, Mechanical Properties of Polymers and Composites, Vol. 1, M. Dekker, Inc., New York, N.Y., 1974.

Parrish, M., and Brown, N., "Environmental Effects on the Tensile Deformation of Polymers at Low Temperatures," Journal of Macromolecular Science - Physics, B8(3-4), 1973, pp. 655-672.

Rabinowitz, S., and Beardmore, P., "Craze Formation and Fracture in Glassy Polymers," CRC Critical Reviews in Macromolecular Science, January 1972.

Sih, G.C., and Chen, E.P., "Fracture Mechanics of Plastic-Fiber Composites," Engineering Fracture Mechanics, Vol. 6, 1974, pp. 343-359.

Soffer, L.M., and Molho, R., "Mechanical Properties of Epoxy Resins and Glass/Epoxy Composites at Cryogenic Temperatures," Cryogenic Properties of Polymers (T.T. Serafini and J.L. Koenig, eds), M. Dekker, Inc. New York, N.Y., 1968.

Young, R.E., History and Potential of Filament Winding, paper presented at the 13th Annual Meeting of the Reinforced Plastics Division of the Society of the Plastics Industry, Inc., New York, N.Y., 1958.

STRUCTURAL ADHESIVES AND JOINT DESIGNS

Bolger, J.C., "Structural Adhesives for Metal Bonding," Treatise on Adhesion and Adhesives, Vol. 3, M. Dekker, Inc., New York, N.Y., 1973.

DasGupta, S., and Sharma, S.P., "Stresses in an Adhesive Lap Joint," The American Society of Mechanical Engineers Publication, New York, N.Y., December 1975.

Hertz, J., "Epoxy-Nylon Adhesives for Low-temperature Applications," Advances in Cryogenic Engineering, Vol. 7, 1961, pp. 336-342.

Miska, K.H., "Which Low-temperature Adhesive is Best for You," Materials Engineering, May 1975.

Pascuzzi, B., and Hill, J.R., "Structural Adhesives for Cryogenic Applications," Adhesives Age, March 1965.

Raphael, C., "Variable-Adhesive Bonded Joints," Applied Polymer Symposia, No. 3, 1966, pp. 99-108.

Renton, W.J., and Vinson, J.R., "The Efficient Design of Adhesive Bonded Joints," Journal of Adhesion, Vol. 7, 1975, pp. 175-193.

Roseland, L.M., "Structural Adhesives and Composite Materials," Machine Design, March 17, 1966, p. 190.

Roseland, L.M., Adhesives for Cryogenic Applications, NASA-Case Conference on the Properties of Polymers at Cryogenic Temperatures (T.T. Serafini and J.L. Koenig, eds) M. Dekker, New York, N.Y., 1968.

Smith, M.B., and Susman, S.E., "Development of Adhesives for Very Low Temperature Applications," Advances in Cryogenic Engineering, Vol. 8, 1963, pp. 300-305.

FOAM INSULATION

Arvidson, J.M., Durcholz, R.L., and Reed, R.P., "Compressive Properties of Polyurethane and Polystyrene Foams from 76 to 300 K," Advances in Cryogenic Engineering, Vol. 18, 1973.

Hayes, R.G., "Cellular Plastics for Cryogenic Insulation," Cryogenic Technology, July/August 1972, p. 127.

Hayes, R.G., "Development of Urethane Foams for LNG Insulation," Advances in Cryogenic Engineering, Vol. 20, 1975.

"Single Layer Application for LNG Pipe Insulation," Cryogenic and Industrial Gases; September/October 1973, p. 21.

SECTION 8

CABLE SYSTEM DESIGN

Billinton, R., and Lee, S.Y. "Unavailability Analysis of an Underwater Cable System," IEEE Transactions on Power Apparatus and Systems, Vol. PAS-96, No. 1, January/February 1977.

Clark, A.F., Childs, G.E., and Wallace, G.H., "Electrical Resistivity of Some Engineering Alloys at Low Temperatures," Cryogenics, August 1970.

Coulter, D.M., LNG-Crude Oil Slurry Cryogenic Pipelines, Paper 76-WA/PID-8, American Society of Mechanical Engineers, New York, N.Y., 1976.

Flieder, W.G., Loria, J.C., and Smith, W.J., "Bowing of Cryogenic Pipelines," Journal of Applied Mechanics, September 1961, pp. 409-416.

King, C.R., Williamson Jr., K.D., and Soree, W., Development of Large Fiberglass Reinforced Plastic Dewars for Superconducting Magnets at 4K, Paper 76-WA/PID-11, American Society of Mechanical Engineers, New York, N.Y., 1976.

Marshall, S.P., and Brandt, J.L., "The 1974 Installed Cost of Corrosion Resistant Piping," Chemical Engineering, October 28, 1974, pp. 94-103.

"Reliable Cooling for Superconductors Now Feasible," Electrical World, January 1, 1977, pp. 39-40.

Steward, W.G., Smith, R.V., and Brennan, J.A., "Cooldown Transients in Cryogenic Transfer Lines," Advances in Cryogenic Engineering, Vol. 15, 1970, pp. 354-363.

Voth, R.O., and Hord, J., "Economics of Cryocables," International Journal of Hydrogen Energy, Vol. 1, 1976, pp. 271-289.

Werdy, B.M., and Rigby, S.J., Loading Capability of Liquid Nitrogen Cooled Underground Cables, paper presented at IEEE 1976 Underground Transmission and Distribution Conference, Atlantic City, N.J., 1976.